INSTITUTE OF GENETIC MEDICINE

NEWCASTLE UNIVERSITY

Vangl2 as a key regulator of cell behaviour within the developing cardiac outflow tract: elaborating specific roles in second heart field and neural crest cells

VIPUL SHARMA

Submitted in accordance with the requirement for the degree of Doctor of Philosophy

April 2014

Supervisors: Prof. DEBORAH HENDERSON

Dr. BILL CHAUDHRY

Abstract

Vangl2 is a key member of the multi-protein planar cell polarity (PCP) pathway. Previous studies using the loop-tail (*Lp*) mouse, which carries a mutation in the *Vangl2* gene, have shown that PCP is required for normal development of the cardiac outflow tract. The main cell types involved in development of the outflow tract are neural crest cells (NCC) and cells derived from the second heart field (SHF). The PCP pathway plays important roles in polarisation of cells within tissues and in directional cell movements. I hypothesised that PCP signalling is required for efficient movement of progenitor cells into the developing heart and that an abnormality in these processes is sufficient to cause common outflow tract defects.

Whilst loss of *Vangl2* in NCC has no affect on outflow tract development, deletion of *Vangl2* from SHF cells (using *Vangl2*^{flox} crossed with *Isl1-Cre* mice) recapitulates the shortened outflow tract and malalignment defects seen in *Lp* mice. The cellular distribution of Vangl2 changes as SHF cells pass from a progenitor state, still expressing Isl1 protein, to differentiated myocardium. When Vangl2 is lost from the cells derived from the SHF, the cells within the distal walls of the outflow tract show altered localisation of polarised molecules such as β-catenin, fibronectin and laminin, as well as PCP proteins including Dvl2 and Celsr1, suggesting disrupted cellular polarity. The expression of PKCζ and E-cadherin is also altered in the distal outflow tract walls of *Vangl2*$^{flox/flox}$*;Isl1-Cre* embryos, supporting the idea that Vangl2 may regulate the polarity of this tissue. Together, these studies suggest that Vangl2 plays a role in imparting polarity on SHF cells as they contribute to the outflow and that this is important for its lengthening. Confirmation of the importance of the PCP pathway in regulating the polarity of the cells in the distal outflow tract, and its importance for outflow tract development, was obtained by examining upstream components (Wnt5a and Ror2) and downstream targets (Rac1 and ROCK) of the pathway, showing outflow defects and a similar expression pattern of polarised molecules.

To my daddy, Vijay Sharma

my mummy, Poonam Sharma

my sister, Pearly Sharma

and all the mice which were sacrificed for this study.

ACKNOWLEDGEMENT

Any assignment puts to litmus test of an individual's knowledge, credibility or experience and thus sole efforts of an individual are not sufficient to accomplish the desired work. Successful completion of a project involves interest and efforts of many people and so this becomes obligatory on my part to record thanks to them.

Therefore, first of all I would like to thank my supervisors **Prof Deborah Henderson** and **Dr Bill Chaudhry**, for their guidance, help and constant encouragement throughout this training. Working under them was an enriching experience.

Next in equivalence, I would like to thank **Dr Helen Phillips** for the encouragement and her constant interest in the activities of my project right from its inception. Without her, this project and thesis would not have been possible.

I am thankful to **Dr Amy-Leigh Johnson**, for always being there, saving me from lab accidents, rescuing me, answering to every little query (science related and not related!). In addition I would like to extend my thanks to all members of Hanger lab, past and present, for practical tips, discussion and entertainment in the lab.

I am grateful to a long list of my friends within the Institute of Genetic Medicine for their support and the amazing times we had in lab, in office and at outings. **Dave**, **Paul** and **Dr Gavin Richardson** for the laughy chats, **Alberto**, **Rebecca** and **Kate** for the cake moments! **Dr Ann Marie Hynes** for the endnote support, **Dr Simon Bamforth** for primer designing and the **FGU staff** for all the help with mice.

I would also like to thank all my **friends in India** and **USA** for showing absolutely no enthusiasm in my work, never being interested in my work and whenever I tried to tell them, calling my work gross! You all made me more proud of my work!

Finally, I would like to thank my **parents** and my **sister**, who always believed in me, even when I didn't, who always think I'm the best. Their constant support and belief is what that made this thesis possible.

Table of Contents

List of Abbreviations

Abbreviations	Expanded Form
A	Apical
ABP	Apical-basolateral polarity
AJ	Adherens junction
APC	Adenomatosis polypsis coli
ASD	Atrial septal defect
αSMA	Alpha smooth muscle actin
AVSD	Atrio-ventricular septal defect
B	Basal
BHF	British Heart Foundation
BMP	Bone morphogenetic protein
Ca	Calcium
CAT	Common arterial trunk
cDNA	Complementary deoxyribose nucleic acid
CE	Convergent Extension
CHD	Congenital heart defects
CK1α	Casein kinase 1α
CNCC	Cardiac neural crest cell
Crc	Circle-tail
CRD	Cystein rich domain
CRN	Craniorachischisis
CVD	Cardiovascular defects
Cx43	Connexin 43
Daam	Dishevelled associated activator of morphogenesis
DAB	3,3’-diaminobenzidine
ddH_2O	Double distilled water
DEPC	Diethyl pyrocarbonate

Dgo	Deigo
DNA	Deoxyribose nucleic acid
dNTP	Deoxyribonucleotide triphosphate
DORV	Double outlet right ventricle
Ds	Dachsous
DSAA	Double sided aortic arch
Dvl	Dishevelled
E	Embryonic day
EDTA	Ethylenediaminetetraacedic acid
EMT	Epithelial to mesenchymal transition
ES cells	Embryonic stem cells
ET-1	Endothelin-1
ETA	Endothelin receptor A
eYFP	Enhanced yellow fluorescent protein
FCS	Fetal calf serum
Fgf	Fibroblast growth factor
FHF	First heart field
Fiji	Fiji is just ImageJ
Fj	Four-jointed
Floxed	Flanked with loxP sites
FLP	Flippase
Fmi	Flamingo
FRT	FLP recognition target
Ft	Fat
Fz	Frizzled
GAPDH	Glyceraldehyde 3-phosphate dehydrogenase
GFP	Green fluorescent protein
GSK3β	Glycogen synthase kinase 3β

gt	Gene trap
GTPase	Guanosine triphostase
Hand1	Heart and neural crest derived 1
Hand2	Heart and neural crest derived 2
H&E	Hematoxylin and eosin
H_2O_2	Hydrogen peroxide
HCl	Hydrochloric acid
Isl1	Islet1
IVS	Interventricular septum
JNK	c-jun terminal kinase
KDa	Kilo Dalton
LA	Left atria
Lp	Loop-tail
Lrp	Lipoprotein related protein
LV	Left ventricle
Mesp	Mesoderm progenitor
mg	Milligram
$MgCl_2$	Magnesium chloride
µl	Microlitre
ml	Millilitre
mRNA	Messenger RNA
Msx	Msh homeobox
MTOC	Microtubule organising centre
n	Number of embryos
N	Asparagine
NCC	Neural crest cell
NeoR	Neomycin
NFAT	Nuclear factor associated with T-cells

Nkx2.5	NK2 homeobox 5
NTD	Neural tube defect
OFT	Outflow tract
P	Postnatal day
PBS	Phosphate buffer saline
PCP	Planar cell polarity
PCR	Polymerase chain reaction
PDE	Phosphodiesterase
PDGF	Platelet derived growth factor
PFA	Paraformaldehyde
PGK	3-phosphoglycerate kinase
Pk	Prickle
PKCζ	Protein kinase C zeta
PLC	Phospholipase C
PNC	Posterior notochord cell
PT	Pulmonary trunk
PTK7	Protein tyrosine kinase 7
RA	Right atria
RAR	Retinoic acid receptor
RNA	Ribose nucleic acid
ROCK	Rho kinase
ROCKDN	ROCK dominant negative
RPM	Rotations per minute
RRESA	Retroesophageal subclavian artery
RT-PCR	Reverse transciptase PCR
RTK	Receptor tyrosine kinase
RV	Right ventricle
S	Serine

S-phase	*Synthesis phase*
SDS	Sodium dodecyl sulphate
SHF	Second heart field
Shh	Sonic hedgehog
Stan	Starry night
Stbm	Strabismus
T	Thymus
TAE	Tris acetic acid EDTA
TBS	Tris buffered saline
TBST	TBS with Tween 20
TBS-Tx	TBS with Triton X100
Tbx	T box
TJ	Tight junction
TK	Tyrosine kinase
UV	Ultra violet
V	Volts
Vang	Vang gogh
VSD	Ventricular septal defect
WT	Wild type

List of Figures

List of Tables

Chapter 1

Introduction

The project aims to establish the importance of cell polarity in embryonic heart development, looking at *Vangl2*, a core planar cell polarity gene, the role it plays and the cell type/s which require Vangl2 during this process.

1.1 Congenital heart defects

Congenital heart defects (CHD) are the commonest form of abnormalities seen in newborn babies, affecting 1 in 145 live births (BHF). In the past, genetic studies of families with multiple affected individuals have provided insights into the genetic basis of several CHD, such as atrial septal defect or patent ductus atrieosis (Schott *et al.*, 1998; Satoda *et al.*, 2000). To pinpoint the genesis of CHD it is important to understand the embryological processes during heart development and how dysregulation at any step on its own or in combination may lead to CHD. Although the major cause of CHD can be attributed to the genetic contribution, there have been reports that genetic predisposition of an individual can interact with the environment and cause CHD (Jenkins *et al.*, 2007). For instance, exposure to angiotensin-converting-enzyme inhibitors at prenatal stage can increase the risk of developing congenital malformations including those related to heart (Cooper *et al.*, 2006). However, the environmental factors are more of the risk factors and to comprehend the mechanism underlying CHD it is crucial to understand the developmental genetics of heart.

Medical care has increased and developed immensely and there have been tremendous advances in diagnosis and treatment of CHD, however knowledge about the causes of CHD is limited, although cardiovascular genetics is rapidly expanding. Determining the possible causes will help in understanding the pathobiological basis of these problems and define disease risk, which will lead to prevention.

There are a lot of defects which can be classified under CHD, but to make it easy to understand, CHD can be divided into 3 main categories – Cyanotic heart disease, Left sided obstruction defects, and septation defects (Bruneau, 2008). Cyanotic heart diseases are those in which the baby looks blue because of mixing of deoxygenated and oxygenated blood. In left sided obstruction defects, there is an obstruction or defect in the left side of the heart and septation defects involve any defect in different septums present in heart like ventricular septum, atrial septum or atrioventricular septum. Different defects under these categories are summarized in figure 1.1. In these, defects of cardiac valves and their associated structures (25-30% of all defects) (Armstrong and Bischoff, 2004), septation defects and outflow tract defects are of prime concern because of the relative high occurrence (Bruneau, 2008).

Hence, a major goal for the biomedical profession is to design preventive measures that can be taken in the pre-conceptual period and this is an area of active research. Over the years, greater insights have been provided into the development of the cardiovascular system with the genes and signalling cascades involved in cardiovascular defects, although, there is still a lot to be understood. Therefore, it is necessary to fully understand normal development in order to unravel the aetiology of congenital cardiovascular defects and to develop therapies.

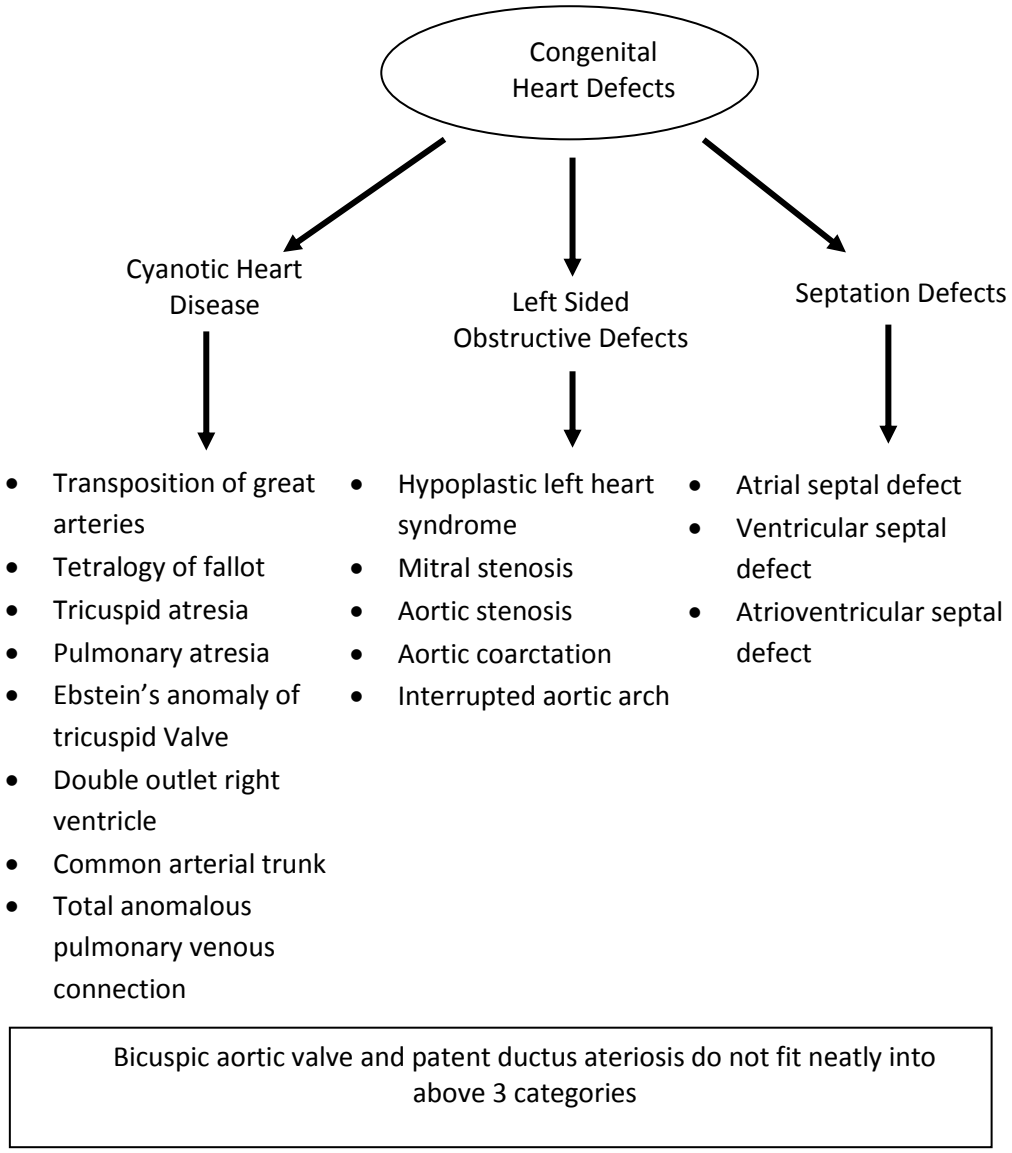

Figure 1.1: Classification of different congenital heart defects. Adapted from (Bruneau, 2008).

1.2 Mouse as a model for human disease

A number of factors are considered while decided a suitable animal model. Mammals have similar physiology and anatomy to humans which may make them more suitable for research purposes but it is also noteworthy that there is surprising degree of functional conservation in basic cell-biological processes between invertebrates and mammals suggesting that flies and worms can be used as a model to understand disruptions in these conserved cellular processes at a genetic and molecular level (Lieschke and Currie, 2007). Despite this, invertebrates lack many structures and organs, for example lack of heart sepatation and cannot be used to study cardiac sepatation defects.

"Its life cycle is man's life cycle in miniature." (Little, 1937), this comparison of similarity between physiology of mouse and human was done in Life magazine, but still holds relevance as now we know that mice and humans share ~99% of their genes (Waterston *et al.,* 2002). They also share common inherited diseases (both Mendelian and polygenic) including diabetes, atherosclerosis, heart disease, cancer, glaucoma, anaemia, hypertension, obesity, osteoporosis, bleeding disorders, asthma and neurological disorders (Peters *et al.,* 2007). Although other mammals also share physiology and disease inheritance, mice are preferred as a model because they are small and easily grow in lab setting, are cost effective to maintain, have a short life cycle and reproduce quickly producing large litters so show results quickly.

However, of more significance is the amount of information, resource, experimental technology and approaches which are present today for mouse genetics. Vast understanding of mouse genetics and complete sequencing of its genome makes it relatively easy to manipulate genes in controlled conditions. By manipulating different genes, researches can study the functions of these genes.

Therefore, mouse is a good and efficient model for studying human disease because they closely recapitulate human conditions and phenotype when associated gene is mutated. But there is a difference between being similar and being the same, so although mouse is a good model, intrinsic differences between mouse and human physiology, such as faster heart beat, shorter gestation period,

etc need to be carefully considered while doing interpretations and associating them with humans.

1.3 Embryonic heart development

Heart development in the developing embryo is a complex process and requires multiple cell types, signals, genes, transcription factors to work in coordination and any aberration at any step may lead to CHD. It is very important to understand normal heart development and then look at how any mutated gene leads to variation from that normal process.

1.3.1 Basic heart development

The heart is the first organ to start functioning in vertebrate embryos as it is required for providing oxygen and nutrients to the developing embryo. Whilst working, the heart starts from a linear muscular tube, undergoes a series of lengthening and looping steps and is transformed into a 4-chamber pump (Buckingham *et al.*, 2005).

During early embryogenesis, an embryonic structure called the primitive streak gives rise to cardiac progenitor cells and these progenitor cells migrate at about embryonic day (E) 6.5 in order to form two groups of cells in the lateral region of the embryo. By E 7.5 these cells come to lie under the head folds to form crescent shaped endocardial heart tube in the precephalic region (Tam *et al.*, 1997; Zaffran and Frasch, 2002) (figure 1.2a). As a result of lateral body folding, the developing heart in the splanchnic mesoderm is moved in medial direction and comes to lie in front of the foregut. The two heart tubes move towards each other and fuse at the midline to form the early cardiac tube at E8 (figure 1.2b) (DeRuiter *et al.*, 1992). The significance of fusion is that at this point differentiated myocardial cells are observed and the tube begins to beat (Kramer and Yost, 2002). The cardiac progenitor cells present at the cardiac crescent, which give rise to the linear heart tube are called first heart field cells (FHF). The fused tube is surrounded by cardiac jelly, which is surrounded by a myocardial mantle. This is

the future heart and is positioned in front of the foregut and is attached to the posterior body wall by a dorsal mesocardium (figure 1.2b), which disappears and will only be attached at the inflow and outflow of the heart. At this point the heart tube can be divided into different parts of the future heart. Starting from the posterior pole, the heart tube has the inflow region, which receives blood from the veins, and has fused atria and ventricle over it, and finally the outflow tract which goes to the aortic sac which distributes blood into pharyngeal arches (figure 1.2c). In order to form the mature heart, this linear heart tube needs to expand, which occurs by two ways: cell proliferation and addition of additional extra-cardiac cells. Lineage labelling experiments in chick and mice have shown the addition of progenitor cells derived from pharyngeal mesoderm through the outflow and inflow regions of the linear heart tube, and this population of cells is known as second heart field cells (SHF) (Mjaatvedt *et al.*, 2001; Waldo *et al.*, 2001; Buckingham *et al.*, 2005; Moorman *et al.*, 2007). Blood from aortic sac goes to the aortic arches. Subsequent to this, looping of the heart tube to the right is observed to form the basic shape of the heart (at E 8.5) (figure 1.2d,e). Two loops are formed, bulbo-ventricular loop and atrio-ventricular loop. Bulbo-ventricular loop forms between bulbus cordis and primitive ventricle and goes forward ventrally and caudally. Atrio-ventricular loop goes posteriorly and cephalically so atria are posteriorly located and ventricle located anteriorly and by E 10.5 well defined chambers are seen in the heart (Brand, 2003) (figure 1.2f). However, the heart tube is still unseptated at this stage. The outflow tract is the region of the heart tube from the right ventricle to the aortic sac where the pharyngeal arch arteries originate; it is divided into distal and proximal regions. This single vessel divides to form two outflow vessels – the aorta and pulmonary trunk. The septum between the pulmonary trunk and the aorta develops in a spiral fashion, where pulmonary trunk comes from the right ventricle and aorta from the left ventricle. Aortico-pulmonary septum also contributes to the interventricular septum when it interacts with the muscular interventricular septum and the endocardial tissue to form the membranous interventricular septum. Development and septation of outflow tract is explained in more detail in the next section (1.3.2).

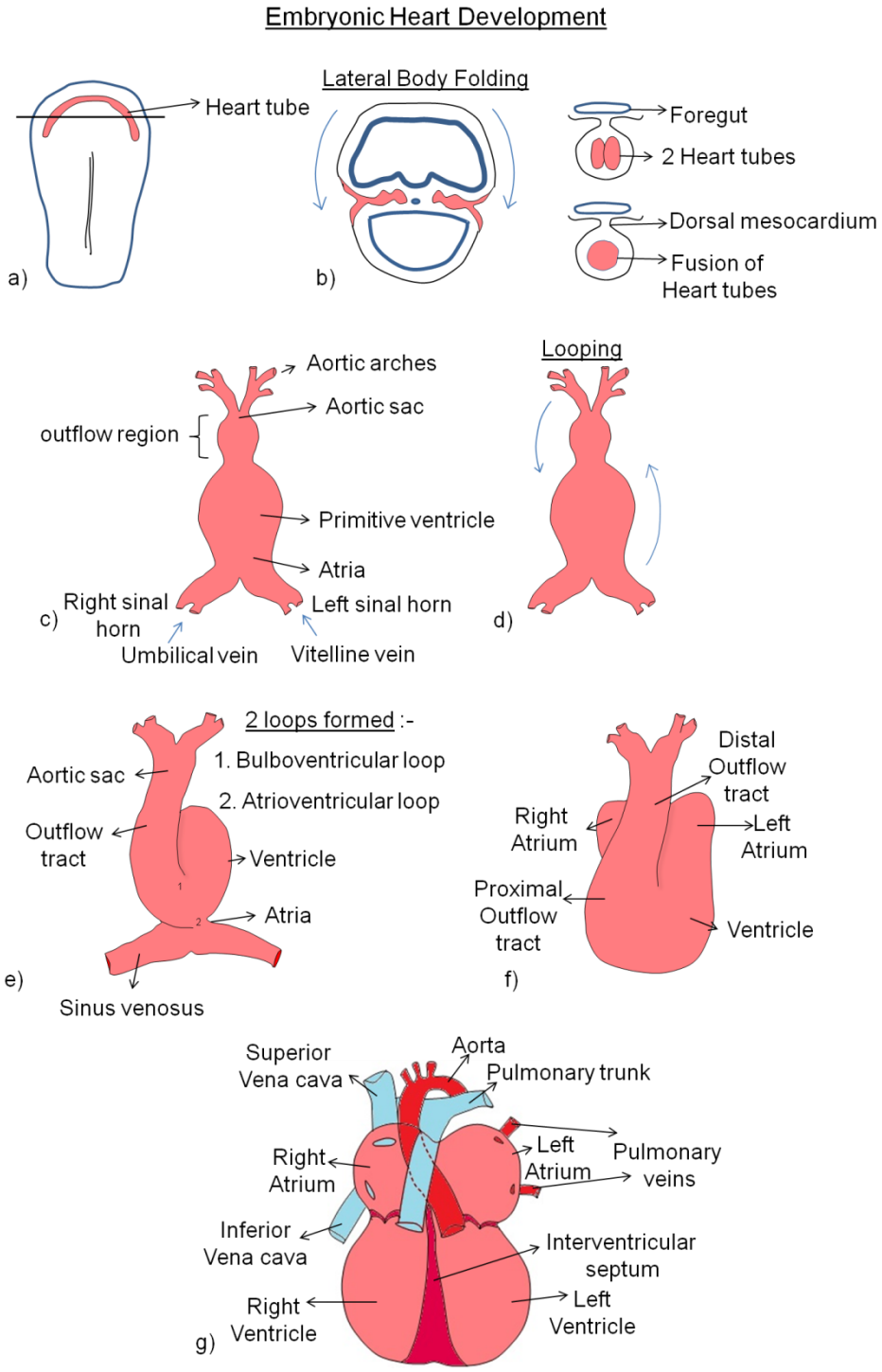

Figure 1.2: Overview of cardiac development

Different stages of embryonic heart development, starting from cardiac crescent at E7.5 (a), lateral body folding leading fusion of heart tubes (b) giving a linear heart tube at E8.0 (c). The heart tube undergoes looping by E8.5 (d) and forms the basic heart shape without any septations by E10.5 (e,f). Septation takes place between atria and ventricles along with outflow tract septation giving a 4-chambered fully functional heart at E14.5 (g). E-embryonic day. Adapted from (Marino, 2005).

The aortic arches connect the outflow region of the heart with the developing dorsal aorta. By E11.0 pharyngeal arch arteries are formed and start remodelling to form aortic arch. There are in total 5 pharyngeal arch arteries, which appear sequentially and never at the same time. First and 2nd aortic arches degenerate and have very little contribution to the great vessels. Distal 3rd aortic arch along with dorsal aorta form the internal carotid artery and the proximal 3rd aortic arch along with ventral aorta between 3rd and 4th arches contribute to the right common carotid artery (figure 1.3) (Hiruma and Nakajima, 2002). A new vessel is developed at the junction of common and internal carotid called the external carotid artery. The distal ventral aorta degenerates. Fourth aortic arch has different fates at different sites. On the left side the 4th aortic arch contribute to the arch of the aorta and the right side contribute to the subclavian artery (Hiruma and Nakajima, 2002). Dorsal aorta between 3rd and 4th arches degenerate, however the ventral part remains on the right side and connects the aorta to the subclavian and the common carotid (figure 1.3). Fifth aortic arch never really appears and hence does not contribute. The proximal portion of 6th aortic arch contributes to the pulmonary arteries. The right portion of 6th aortic arch degenerates along with the rest of the descending aorta on the right and the left side of the 6th arch forms the ductus arteriosus (figure 1.3), which closes after birth (Hiruma and Nakajima, 2002). The inflow region of the heart deals with the development of the major veins. There is common cardinal vein which empties blood in the heart into the sinus venosus. These common cardinal vein receive blood from the anterior cardinal and the posterior cardinal veins. By E14.5 atrial and ventricle septation also occurs to form distinct right and left atrial and ventricular chambers, connected to the pulmonary trunk and aorta respectively (Figure 1.2g) forming a fully developed heart with outermost layer formed from epicardial progenitor cells (Buckingham *et al.*, 2005).

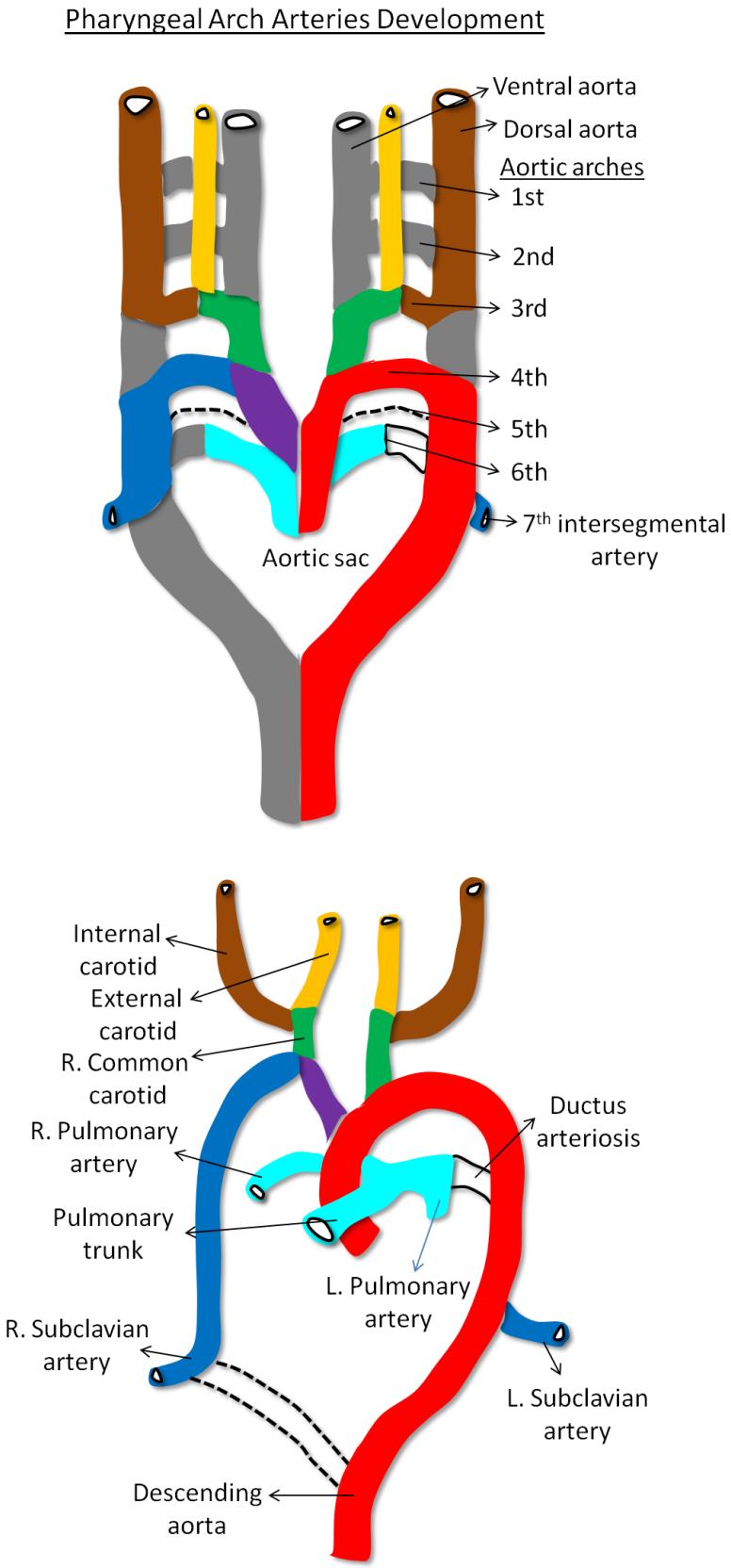

Figure 1.3: Overview of arch arteries development

The fate of aortic arches, dorsal and ventral aorta. Adapted from (Marino, 2005)

1.3.2 Outflow tract development

Outflow tract morphogenesis involves multiple cell types and signalling pathways making it complex and prone to anomalies. Outflow tract is formed from SHF, which are cardiac progenitor cells present in the pharyngeal mesoderm. SHF progressively add myocardium during the elongation of the heart tube (Kelly and Buckingham, 2002; Buckingham *et al.*, 2005). As compared to the FHF, which give rise to the early heart tube, SHF show high level of proliferation and differentiation delay and continue adding to the heart tube through the inflow and outflow region. This addition of myocardium is essential for elongation of the heart tube before it starts to septate, which is regulated by NCC. After looping, outflow tract has a dog-leg bend which divides it into distal and proximal portions. Cardiac jelly is present in the lumen of the primary heart tube and this jelly concentrates itself into pairs of facing cushions lining the outflow tract, continuous through the proximal and distal regions (Anderson *et al.*, 2003).

NCC migrates from the neural tube through the caudal pharyngeal arches into the outflow tract. By E10.5 in mouse embryos, there is already invasion of cells from the NCC into the distal region of the outflow tract (Hutson and Kirby, 2007). They migrate to a circular ring like structure of nerves and ganglia surrounding the pharynx, known as circumpharyngeal ridge and then enter pharyngeal arches 3, 4 and 6 (Kuratani and Kirby, 1991). NCC surround the endothelial cells which form the arch arteries and helps in their patterning (Kuratani and Kirby, 1992). At this stage the wedge of tissue is visible in the dorsal wall of the aortic sac that, which is called as the transient aortico-pulmonary septum (Anderson *et al.*, 2003). By E11.5, there is a rapid increase in the number of NCC, as a consequence of their continuous migration into the outflow cushions and proliferation of cells already in the cushions (Hutson and Kirby, 2007), packing the distal outflow cushions and the dorsal wall of the aortic sac (figure 1.4c). Due to the increased number of NCCs the dorsal wall of the aortic sac comes in contact with the most distal regions of the expanded outflow cushions (figure 1.4d,e) and fuses, along with the fusion of the two cushions with each other, initiating outflow septation and separating the systemic and pulmonary circulations (figure 1.4f) (Anderson *et al.*, 2003). Thus, the fusion of the cushions divides the distal part of the outflow

vessel into the aorta and pulmonary trunk, and with the aorto-pulmonary septum connects the developing aortic channel to the artery of the fourth pharyngeal arch. Fusion of these cushions with the posterior mesenchyme connects the pulmonary trunk to the artery of the sixth pharyngeal arch. Once septation is initiated by the fusion of the dorsal wall of the aortic sac with the distal outflow tract cushions, it proceeds in a distal to proximal direction (De La Cruz *et al.*, 1977; Waldo *et al.*, 1998). As the cusion fusion reaches till the point of dog-leg bend, they take a characteristic whorl (Anderson *et al.*, 2003) (figure 1.4f). As the most proximal part of the cushions fuse, muscular tissue is added to the most proximal region, and this process is known as myocardialisation. The fusion of cushions and muscularisation continues and completes the separation between the aorta and the pulmonary trunk (Van Den Hoff *et al.*, 1999; Kruithof *et al.*, 2003). Right ventricle initially holds the whole outflow tract, but fusion of the cushions separates the aorta and pulmonary trunk and this septum joins the wall of right ventricle pushing the aorta to the left ventricle, and leaving the pulmonary trunk exiting from the right ventricle (figure 1.4g).

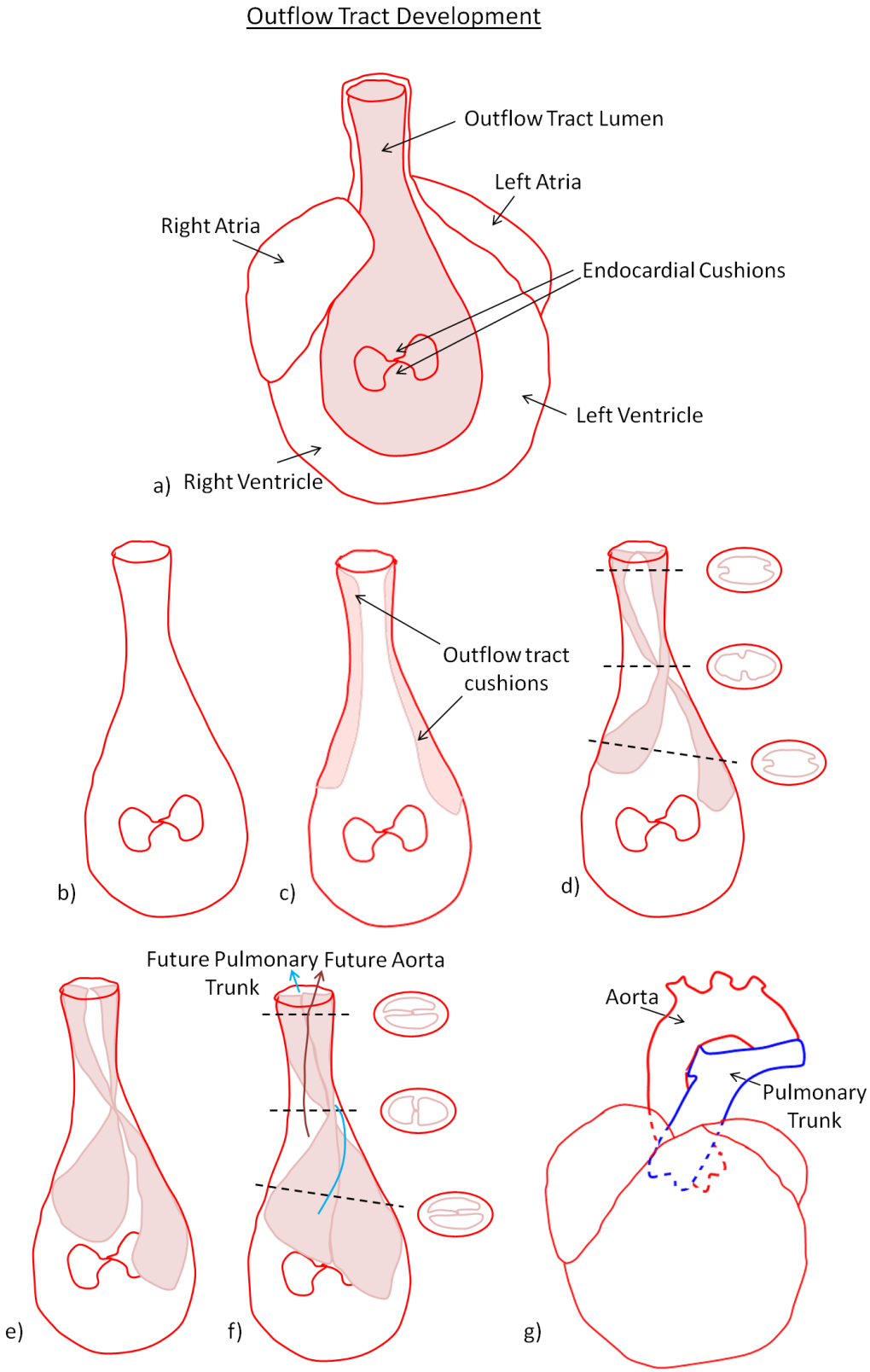

Figure 1.4: Outflow tract development

Different stages from initiation to completion of septum between the aorta and pulmonary trunk.

1.4 Outflow tract congenital heart defects

The outflow tract is susceptible to cardiac abnormalities accounting for 30% of all congenital heart defects (Srivastava and Olson, 2000; Bruneau, 2008). The reason for outflow tract being highly susceptible is that it requires the normal development and proliferation of multiple cell types, like SHF (abnormality leads to elongation defect), NCC (abnormality leads to septation defect), myocardium (abnormality leads to alignment defect), and endocardium (abnormality leads to cushion defect) (Kirby, 2007). NCC and SHF cells involved in the outflow tract development work in coordination and NCC regulates proliferation of SHF cells (Waldo *et al.*, 2005a). Disruption in either of the two, SHF or NCC, contributes to a spectrum of outflow tract defects in humans and animal developmental models (Moon, 2008). As SHF cells are contributing to the myocardium of the lengthening heart tube (figure 1.5a), impairment of SHF leads to failure of heart tube elongation resulting in disruption of outflow tract rotation and modelling leading to alignment defects (Abu-Issa and Kirby, 2007) like double outlet right ventricle, transposition of great arteries, over-riding aorta (figure 1.5b). Complete loss of SHF leads to loss of outflow tract. As NCC contribute to the septation of outflow tract (figure 1.5a), loss or reduction of NCC leads to septation defects like common arterial trunk and double outlet right ventricle (figure 1.5b). Abnormalities in NCC can indirectly affect SHF, resulting in a composite septation and alignment defect (Hutson and Kirby, 2003). Hence, during outflow tract morphogenesis it is crucial that these different cell lineages are tightly controlled and regulated so that cells proliferate, move and differentiate at the correct time at the correct location.

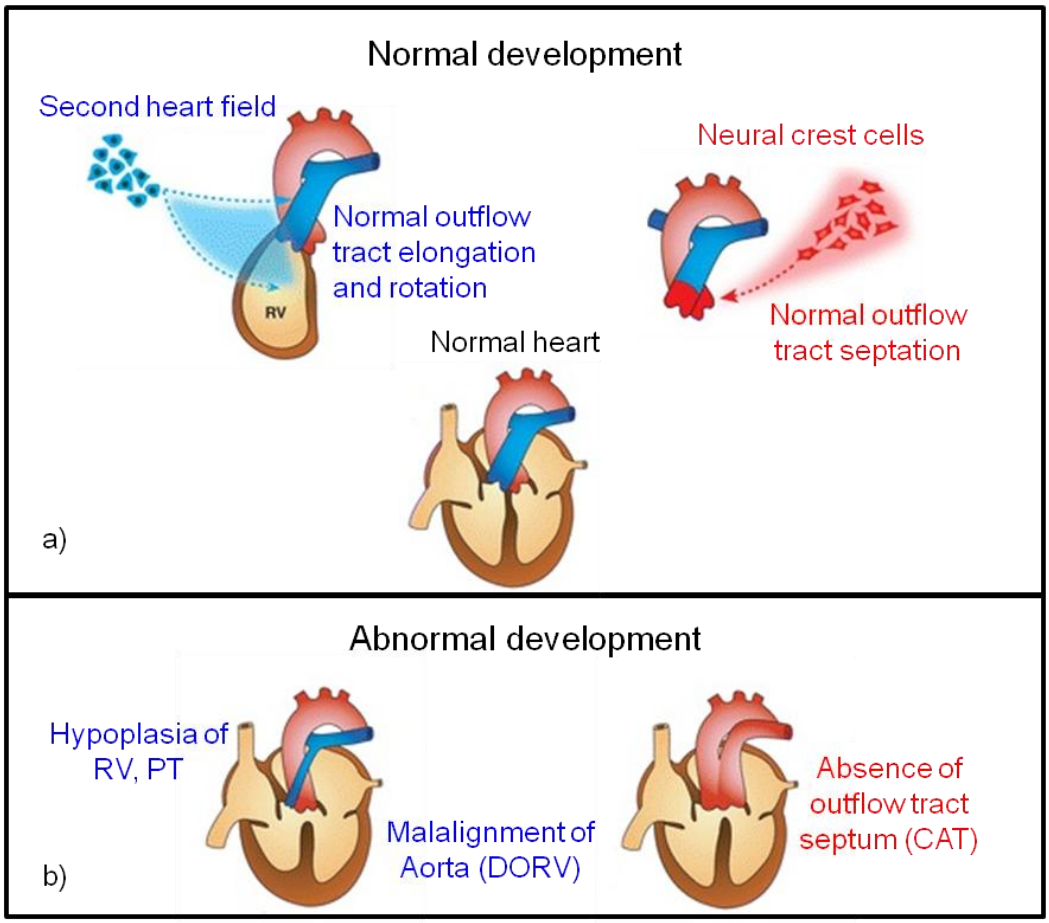

Figure 1.5: Different cellular contributions to the heart development

a) Contribution of extra cardiac cells to different regions of the heart. SHF contributes to the addition of myocardium and NCC helps in outflow tract septation. b) Abnormalities in SHF and NCC leading to defects like hypoplasia of right ventricle and outflow tract, malalignment of aorta and left ventricle leading to double outlet right ventricle and absence of outflow tract septum resulting in common arterial trunk. RV-right ventricle, PT- pulmonary trunk, DORV-double outlet right ventricle, CAT-common arterial trunk. Modified and reprinted by permission from Springer publishers: Anatomical Science International (Yamagishi *et al.*, 2009), copyrights (2009).

1.4.1 Neural crest cells

NCC are multipotent, migrating progenitor cells which originate from the neural tube and migrate to different regions of the body and differentiate into diverse cell types including melanocytes, smooth muscle cells, craniofacial connective tissue, cartilage, glia etc, reviewed in (Huang and Saint-Jeannet, 2004). They originate at the border of neural plate and non-neural ectoderm. During neurulation, the borders of the neural plate, known as neural folds, come together to fuse and form the neural tube. After the closure of the neural tube, neural crest cells delaminate and migrate towards different directions, reviewed in (Huang and Saint-Jeannet, 2004). All this happens under a genetic network of signals, transcription factors and genes.

NCC can be divided into 4 categories based on their rostro-caudal location where they originate in the neural tube and their final destination (figure 1.6) – cranial, trunk, vagal and sacral, and cadiac NCC (Le Douarin, 1982; Gilbert, 2000).

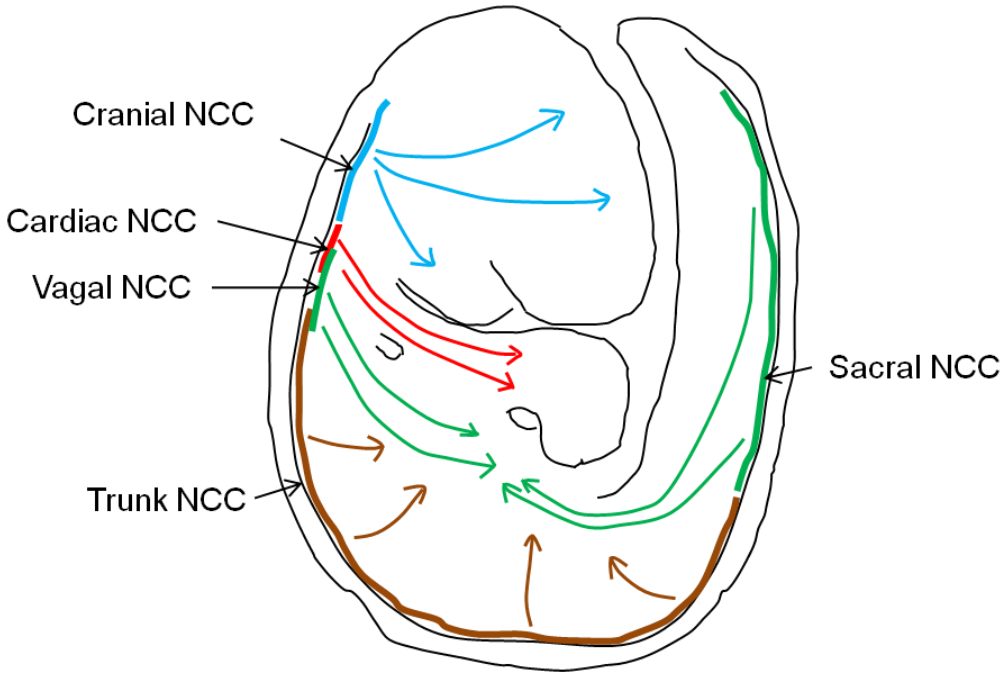

Figure 1.6: Different types of NCC

Cranial, cardiac, vagal and trunk NCC and their migration pattern in the developing embryo. Adapted from (Le Douarin, 1982; Gilbert, 2000)

Extensive work done on chick and mice have showed ablation of NCC leads to outflow tract abnormalities and a particular section of NCC are essential for outflow tract septation and aortic arch development, and these are categorized as cardiac neural crest cells (CNCC) (Kirby and Waldo, 1990; Kirby and Creazzo, 1995; Kirby and Waldo, 1995).

1.4.1.1 NCC in heart development

There are different molecular pathways which control initial induction, migration, proliferation, differentiation and apoptosis of NCC. Under the influence of signalling molecules like Wnt, fibroblast growth factor (Fgf) and bone morphogenetic protein (BMP), initial induction of NCC occurs and this leads to migration of these cells towards the heart (Kuratani and Kirby, 1992; Kirby and Hutson, 2010). The exact signalling cascade is unknown but it is known that intermediate BMP signalling is required, as low and high levels prevent cells from migrating (Kirby and Hutson, 2010).

Following induction, NCC migrate towards the cirumpharyngeal region which is just above the pharyngeal arches (Kirby, 1987; Kuratani and Kirby, 1991; Gilbert, 2000). They lose cell-cell contact and interact with extracellular matrix which helps in their migration (Kuratani and Kirby, 1992; Kirby and Hutson, 2010). The cells which lead the migration have a polygonal shape, have a longer filopodia and proliferate more than the trailing cells (Kirby and Hutson, 2010). The cells which are in the middle also have protrusions which aide in interaction with leading and trailing cells and also receiving extracellular signals from various growth and transcription factors (Kirby and Hutson, 2010). Wnt signalling has two signalling pathways, one which required β-catenin known as canonical Wnt pathway and one which is β-catenin independent, known as non-canonical Wnt pathway (Gessert and Kühl, 2010). Both pathways are important for NCC as canonical Wnt pathway is important for cell cycle regulation of NCC and their migration (Gessert and Kühl, 2010). Lower levels of β-catenin lowers NCC proliferation and downregulates Lrp6, which is a Wnt coreceptor and leads to reduction of NCC resulting in cardiac defects (Brault *et al.*, 2001; Gessert and

Kühl, 2010). However, once the cells have reached their destination, non-canonical Wnt pathway takes over and is responsible for NCC differentiation and outflow tract development (Gessert and Kühl, 2010). Non-canonical Wnt pathway is antagonistic to canonical Wnt pathway, therefore it is important the non-canonical Wnt pathway takes over once the cells no longer need to migrate and proliferate at a higher rate. Apart from differentiation, non-canonical Wnt signalling also regulates migration of NCC in *Xenopus* (De Calisto *et al.*, 2005), however this is still to be established in mammals.

Once these cells reach the circumpharyngeal region, they enter the pharyngeal arches 3, 4 and 6 (Kirby, 1987; Kuratani and Kirby, 1991; Gilbert, 2000) and through them pass in to the outflow tract (figure 1.7). They help in formation of connective tissue in the arches and smooth muscle cells and aortopulmonary septum in the outflow. Wnt5a acts as a ligand for activation of non-canonical Wnt signalling pathway and its loss in mice results is unseptated outflow tract resulting in common arterial trunk suggesting important role in NCC (Schleiffarth *et al.*, 2007). CNCC ablation in both chick and mice leads to defects in the heart outflow and pharyngeal patterning, however they are not required for the initial formation of the arch arteries, but play a significant role in their patterning. Notch signalling is also required for differentiation of NCC into smooth muscle cells and disruption can lead to aortic arch branching defects and pulmonary stenosis along with defects in smooth muscle cells development in the 6^{th} arch artery in mice (Niessen and Karsan, 2008). In humans such mutation often leads to calcification of aortic valve and bicuspid aortic valve (Garg *et al.*, 2005).

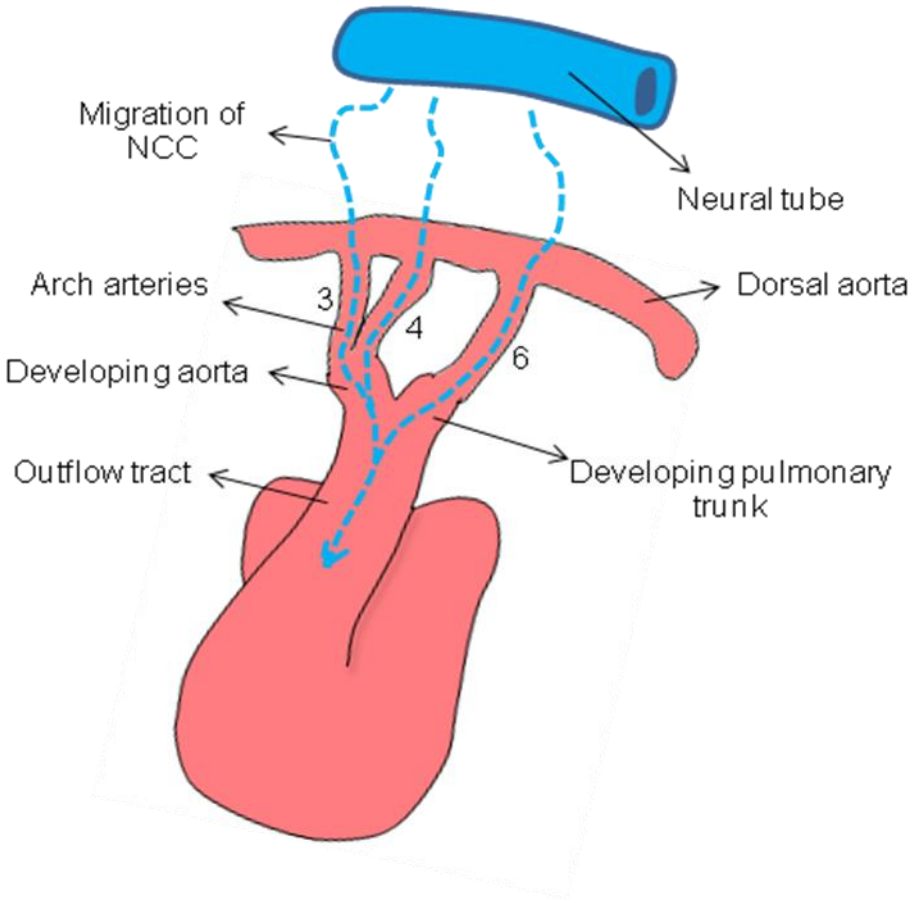

Figure 1.7: NCC migration into outflow tract

Contribution and migration of NCC during heart development from their origin in neural tube to the outflow tract through pharyngeal arches. Adapted from (Kirby, 2007).

Endothelin signalling plays a role in aortic arch patterning influencing the NCC. Mutation in Endothelin-1 (ET-1) signalling pathway leads to arch patterning defects (Kurihara *et al.*, 1995) and Endothelin A (ETA) which is a receptor of ET-1 is expressed in NCC in the pharyngeal arches. The ETA null cells are excluded from the walls of the aortic arch which suggests that NCC which surround the endothelial cells in the arch arteries require ETA to interact with the endothelium of the aortic arch arteries (Yanagisawa *et al.*, 1998; Clouthier *et al.*, 2003). Apart from these, Notch, BMP, and GATA transcription factors also play important roles in NCC migration and differentiation and any disruption in this complex leads to cardiac defects.

1.4.1.2 Phenotype arising from ablation of NCC genes

Ablation of NCC in associated with outflow tract defects, aortic arch defects, craniofacial skeletal abnormalities, pigmentation defects and defects in pharyngeal derivatives including thymus, parathyroids and thyroids (Leatherbury and Kirby, 1996). Human defects with similar phenotype, associated with NCC are also known, for example DiGeorge Syndrome which has cardiac-craniofacial-pharyngeal defects, Waardenburg Syndrome with craniofacial-pigmentation defects, CHARGE association;Goldberg-Sprintzen having cardiac-craniofacial defects, and ABCD Syndrome which has pigmentation defects. Although all these syndromes have different combinations and variability of defects, but they all are associated with NCC (Creazzo *et al.*, 1998).

Majority of work on NCC and understanding their role has been carried out in quail-chicken chimeras, where cardiac neural crest cells were surgically removed prior to their migration and were replaced by quail-NCC or quail-chicken chimeras, which showed developmental defects like common arterial trunk, ventricular septal defects and abnormal patterning of pharyngeal arch arteries, apart from non-cardiac phenotype like absence or hypoplastic thymus, thyroid and parathyroids (Le Lievre and Le Douarin, 1975; Kirby *et al.*, 1983; Phillips *et al.*, 1987; Waldo *et al.*, 1998). Although work in chick has given in-depth explaination of NCC's role in cardiac morphogenesis, there are differences

between cardiac development in chicken and mouse. Therefore, similar work has been done on mouse models. Splotch and Patch are two naturally occurring mouse mutants for NCC and their cardiac phenotype is similar to the defective cardiac phenotype observed in chick embryos, but these mouse mutants have severe non-cardiac defects as well along with cardiac defects (Auerbach, 1954; Franz, 1989; Morrison-Graham *et al.*, 1992; Epstein, 1996; Conway *et al.*, 1997a; Conway *et al.*, 1997b; Conway *et al.*, 1997c).

Splotch mouse have mutation in transcription factor gene, *Pax3* (Goulding *et al.*, 1993) and embryos with this mutation die in utero. Apart from outflow tract abnormalities, they also have neural tube closure defect along with defects in limb musculature (Auerbach, 1954; Franz and Kothary, 1993). This implies *Pax3* is essential for NCC migration and can be used as marker for NCC (Conway *et al.*, 1997b). These mutant mice have common arterial trunk, alignment defect of outflow tract like double outlet right ventricle, aortic arch patterning defect, absent thymus, thyroid and parathyroids, spina bifida and pigmentation abnormalities. Pax3 is expressed in dorsal neural tube and early migrating NCC but expression is reduced when they reach the pharyngeal arch region and outflow tract. Cre-lox technology used to look at Pax3 expression in normal and splotch mice showed that there is decrease of migration on NCC in the arch arteries and outflow tract (Epstein *et al.*, 2000; Kwang *et al.*, 2002), and these splotch mutants have up-regulation of Msx2, which is downstream target of Pax3. *Msx2* loss of function mutation rescues cardiac defects in splotch mice (Kwang *et al.*, 2002).

The Patch mouse has mutation (deletion) in the α-subunit of the platelet-derived growth factor (PDGF) receptor, which is important for NCC interaction with extracellular matrix which assists in their proliferation, survival and migration. This receptor is expressed in more cell types as compared to Pax3 and therefore the phenotype is more severe than Splotch mutants (Smith *et al.*, 1991; Price *et al.*, 2001).

NCC express Cx43, which is a gap junction protein and plays a role in intracellular channels (Reaume *et al.*, 1995; Lo *et al.*, 1999). Cx43 is required for

NCC migration as *Cx43* null embryos show reduced directionality and speed of NCC while they are migrating (Huang *et al.*, 1998). Lo et al used a portion of Cx43 promoter and used it to drive LacZ expression to mark NCC and look at the migration and involvement in cardiac development (Lo, 1997). All subtypes of retinoic acid receptors (RAR) are expressed in NCC and *RAR αβ2* and *αγ* homozygous double knockout mice also have outflow tract and aortic arch defects associated with NCC (Rowe *et al.*, 1994). Use of Cre-lox technology has further enhanced the ability to track NCC and understand their role in embryonic development. Most commonly used promoter which drive Cre recombinase expression for NCC are *Wnt1-Cre, Pax3-Cre*, *PO-Cre* and *PlexinA2-Cre* (Lee *et al.*, 1996; Jiang *et al.*, 2000; Brown *et al.*, 2001). Although there are slight differences in these models with respect to NCC labelling, but they all confirm major migration patterns and contributions of NCC in mice as seen in chick. The *Wnt1-Cre* transgenic mice have been widely used to study NCC lineage in context of their migration and fate, because *Wnt1* gene is highly expressed in the dorsal neural tube prior to NCC migration (Hutson and Kirby, 2007; Lewis *et al.*, 2013).

1.4.2 The Second Heart Field

During early developmental stages of the embryo, the heart tube elongates by the addition of myocardium from progenitor cells that lie outside the heart. These mesodermal progenitor cells are called the SHF and reside in the anterior pharynx during the period when the heart tube is forming and as it lengthens (from E8.5-E10.5) these cells migrate into the poles of the heart after formation of the linear heart tube. Therefore SHF cells are the progenitor cells situated in splanchnic pharyngeal mesoderm which migrate into the developing heart and facilitate maximal extension of the heart tube.

Addition to the developing heart after formation of the linear heart tube was first suggested by studies done during the 1960s and 1970s (Stalsberg and DeHaan, 1969; De La Cruz *et al.*, 1977; Viragh and Challice, 1977), however it was only confirmed in 2001, where three separate studies on chick and mouse revealed the

origin of these extracardiac cellular additions (Kelly *et al.*, 2001; Mjaatvedt *et al.*, 2001; Waldo *et al.*, 2001).

Mjaatvedt et al (2001) showed the source of myocardial cells that contribute to the lengthening of the outflow tract using chick as model. By labelling cells in the undifferentiated mesoderm surrounding the aortic sac and present anterior/cranial to the heart tube using Mitotracker or replication-deficient adenovirus which express β-gal, they observed destination of these cells in the distal and proximal regions of the outflow tract and named them anterior heart-forming field (Mjaatvedt *et al.*, 2001). Waldo et al (2001) identified a similar source of myocardial cells by using quail-chick chimeras and mitotracker dye concluding the presence of these cells in proximal outflow tract and their contribution to heart development (Waldo *et al.*, 2001). This work on chick was supported by work on mice by Kelly et al (2001). Using *Fgf10-nLacZ* reporter mouse they showed that right ventricle and outflow tract myocardium are added from both pharyngeal arch core and splanchnic mesoderm. As the myocardial cells are added to the heart tube, there is downregulation of *Fgf10* and *LacZ*, however β-galactosidase protein was still present in the cells, showing that these cells had their origin from Fgf10 expressing cells residing in the pharynx (Kelly *et al.*, 2001). These cells were given the name second heart field cells.

Cardiac progenitor cells are divided into 2 types, and categorized on the basis of the function and fate, FHF and SHF. The SHF is distinguished from the FHF, which forms the linear heart tube, by the persistent expression of transcription factors such as *Isl1* and *Tbx1* and the growth factors *Fgf8* and *Fgf10*, whereas they are expressed in the FHF only transiently (Thompson *et al.*, 1985; Bartelings and Gittenberger-de Groot, 1989; Kelly *et al.*, 2001). Both FHF and SHF have expression of these genes, however FHF down-regulate *Isl1* and *Fgf8* expression as they differentiate and there is a prolonged expression of *Isl1* and *Fgf8* in SHF which helps in its elevated proliferation and delay in differentiation (Park *et al.*, 2006; Prall *et al.*, 2007).

The FHF contributes to the formation of left ventricle, portions of right ventricle and inflow region of the heart whereas the SHF contributes to the formation of

outflow tract, right ventricle, and also to the inflow region (Kelly and Buckingham, 2002; Buckingham *et al.*, 2005) (figure 1.8), as shown by many genetic tracing experiments extensively done on avian and mouse models (Kelly *et al.*, 2001; Mjaatvedt *et al.*, 2001; Waldo *et al.*, 2001; Cai *et al.*, 2003; Zaffran *et al.*, 2004; Verzi *et al.*, 2005; Tirosh-Finkel *et al.*, 2006; Rana *et al.*, 2007; Guo *et al.*, 2011; Kelly, 2012). Hence outflow tract is exclusively from the SHF. Work on human embryos is in initial stages but supports previous work on mice, showing *Isl1* positive SHF cells contributing to the outflow tract (Sizarov *et al.*, 2012; Yang *et al.*, 2013). Apart from the myocardial contribution to the heart, SHF are also shown to contribute to the endocardium of the right ventricle and proximal outflow tract, and smooth muscle in the outflow tract (Moretti *et al.*, 2006). Therefore, once inside the heart, SHF gives rise to myocardial, endocardial and smooth muscle cells (Laugwitz *et al.*, 2005; Moretti *et al.*, 2006). Cell labelling in chick showed that these SHF derived smooth muscle cells are at the proximal outflow tract and present between smooth muscle derived from NCC (distally) and myocardium of the outflow tract (proximally). Another study in chick shows the difference of position of SHF cells leads to different fate. Labelled SHF cells were traced revealing that right side of SHF cells are found in left side of spiralling outflow tract and generate smooth muscle cells of aorta and coronary stems (Waldo *et al.*, 2005b; Sun *et al.*, 2007), while the cells present at the left side contribute to smooth muscles cells of pulmonary trunk. During outflow tract formation, maximal extension of the outflow tract is required for the proper alignment of the base of the aorta with the left ventricle during aorto-pulmonary septation (Sugishita *et al.*, 2004; Rochais *et al.*, 2009b). Disturbances in the SHF during early stages of their movement into the heart tube leads to many congenital heart defects ranging from failure of heart tube extension to alignment defects, including double outlet right ventricle, overriding aorta, suggesting that early SHF myocardial addition is essential for outflow tract elongation and alignment. When SHF are ablated at later stages, outflow tract alignment is normal; however coronary artery defects are present (Ward *et al.*, 2005). Hence time of SHF movement and addition in the heart tube is crucial with respect to outflow tract development. SHF which enter the heart tube from

the inflow region contribute to portions of atria, atrial septum and myocardium of the venous pole (Kelly, 2012).

The targeted disruption of a number of genes within the SHF, including *Isl1*, *Fgf8*, *Tbx1*, and *Tbx20*, gives rise to outflow tract malformations in mice, reviewed in (Watanabe *et al.*, 2010). Furthermore, human patients with outflow tract malformations have been shown to have potentially disease causing polymorphisms in SHF genes, including *Tbx1* and *Isl1* (Gruber *et al.*, 2010), indicating a developmentally conserved role for the SHF during cardiac development.

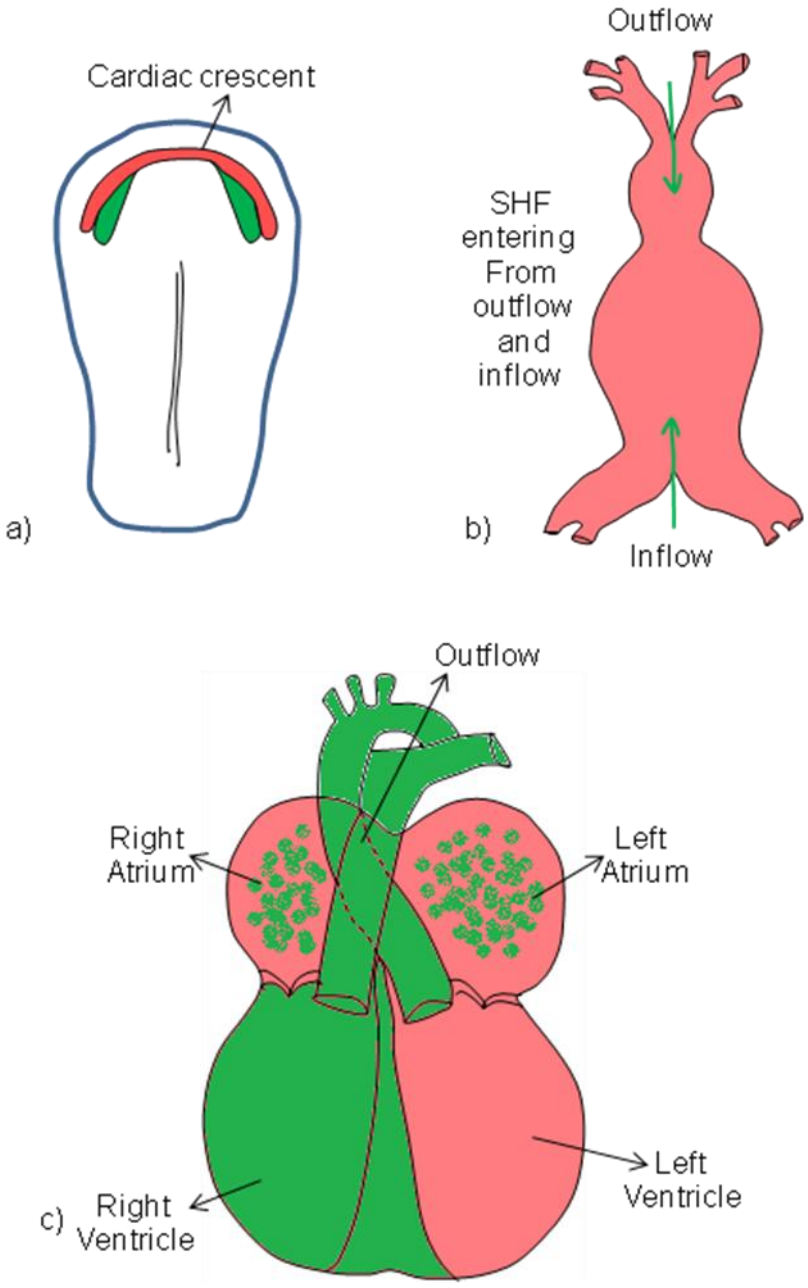

Figure 1.8: Contribution of SHF in heart development

SHF contribution (shown in green) to outflow tract, right ventricle, parts of right and left atria, and FHF contribution (shown in red) to left ventricle, right and left atria. Adapted from (Buckingham *et al.*, 2005).

1.4.2.1 Signalling involved in SHF during heart development

SHF cells originate in the splanchnic mesoderm and the mesodermal core of the pharyngeal arches. Signals necessary for the development, proliferation, movement and differentiation of SHF in the developing heart are likely to originate from interactions between the genes and signals which are present in this region and the neighbouring ectodermal and endodermal layers of the arches, including Fgf, BMP, canonical and non-canonical Wnt signalling (Evans *et al.*, 2010), apart from the interactions with the other cell types which populate these tissues.

Heart development starts with the expression and activation of transcription regulator Mesp1, which activates cardiac transcription factors, including *Isl1*, *Tbx5*, *Nkx2.5*, *Mef2c*, *Gata4* and *Baf60c* (Bruneau, 2002; Van Weerd *et al.*, 2011; Miquerol and Kelly, 2013). Transcription factor Isl1 is a target of Wnt signalling and plays a central role in SHF development with regulating signalling pathway ligands and receptor gene expression (Cai *et al.*, 2003; Lin *et al.*, 2007). Study on ES cells show that Isl1, along with Mesp1 plays a role during cardiac specification (Kwon *et al.*, 2009; Bondue *et al.*, 2011). Interrupted *Isl1* expression in embryos leads to disorganisation in SHF deployment at both inflow and outflow region of the heart tube, resulting in shortened outflow tract (Cai *et al.*, 2003). Cells which express *Isl1* do not differentiate and continue to proliferate (Cai *et al.*, 2003). These cells are present in the pharyngeal mesoderm are isolated at dorsal pericardial wall and enter from both poles contributing in heart tube elongation. Work on chick and mice show high proliferative rate in this region (Van Den Berg *et al.*, 2009; de Boer *et al.*, 2012). This proliferation is regulated by Sonic hedgehog (Shh) and Fgf signalling with Fgf3, Fgf8 and Fgf10 as ligands (Ilagan *et al.*, 2006; Park *et al.*, 2008; Dyer and Kirby, 2009; Watanabe *et al.*, 2010; Urness *et al.*, 2011). Of these Fgf8 has the major driving effect for proliferation, with important contributions from Fgf3 and Fgf10 as Fgf8 is critical for heart tube elongation and *Fgf10* null embryos show normal SHF deployment but when deleted along with *Fgf8* show increased severity in cardiac defects (Ilagan *et al.*, 2006; Park *et al.*, 2006; Park *et al.*, 2008; Watanabe *et al.*, 2010; Urness *et al.*, 2011; Francou *et al.*, 2013). This Fgf ligand expression in the dorsal

pericardial wall is regulated by Notch and Wnt/β-catenin signalling (figure 1.9) (Cohen *et al.*, 2007; High *et al.*, 2009; Klaus *et al.*, 2012). This proliferation is maintained with the help of Shh signalling through transcription factor Tbx5, which is a positive regulator for SHF proliferation (Goddeeris *et al.*, 2007; Dyer and Kirby, 2009) (figure 1.9). T-box transcription factor Tbx1 regulates Fgf signal response (figure 1.9) (Cai *et al.*, 2003; Baldini, 2005; Aggarwal *et al.*, 2006) with Six1 and Eya1 playing intermediate roles (Guo *et al.*, 2011). Notch signalling which is upstream of Wnt/β-catenin signalling has a target gene *Hes1*, which is also expressed in the dorsal pericardial wall and is important for proliferation (Rochais *et al.*, 2009a). Fgf8 expression in SHF cells is regulated by Notch signalling, through Jag1 ligand (figure 1.9) (High *et al.*, 2009).

While SHF are proliferating, their survival and check on apoptosis is also important and bHLH transcription factor Hand2 plays a role in this process (Tsuchihashi *et al.*, 2011). Retinoic acid signalling also plays a role in SHF maintenance in dorsal pericardial wall (Li *et al.*, 2010). As SHF approach the distal heart tube, they are exposed to BMP and non-canonical Wnt signalling (figure 1.9). These both are involved in differentiation of SHF. However, proliferation needs to be regulated and balance between proliferation driving Fgf signalling and differentiation driving BMP signalling is influenced by NCC present in the pharyngeal region (Kelly, 2012). NCC act as a brake to Fgf signalling and hence on over-proliferation of SHF after the heart tube is optimally elongated (Yelbuz *et al.*, 2002; Hutson *et al.*, 2006). This is achieved by BMP signalling, through BMP induced transcription factor encoding genes *Msx1* and *Msx2* in NCC (figure 1.9) (Tirosh-Finkel *et al.*, 2010). These Msx1 and Msx2 are also required for expression of Hand2 and survival of SHF (Chen *et al.*, 2007). Apart from regulating proliferative effects of Fgf signalling, BMP also modulates proliferative effect of Hedgehog signalling (Dyer *et al.*, 2010), and promotes differentiation of *Isl1* expressing cells through transcriptional activation of microRNA 17-92, which targets SHF transcripts, *Isl1* and *Tbx1* (Yang *et al.*, 2006; Wang *et al.*, 2010).

Transcription factors, Nkx2.5, Tbx20, Mef2c, Gata4 play important role in SHF cell differentiation (Waldo *et al.*, 2001; Francou *et al.*, 2013). In the absence of

Nkx2.5, BMP signalling is elevated which down regulates SHF proliferation (Prall *et al.*, 2007; Barth *et al.*, 2010) and favours its differentiation. In the absence of T-box transcription factors, BMP signalling is down regulated which increase the proliferation of SHF cells by elevated Fgf signalling (Mesbah *et al.*, 2012). *Tbx1*, which is a candidate gene for DiGeorge Syndrome is associated with craniofacial and cardiovascular defects and is known to prevent SHF cells differentiation (Baldini, 2005). *Tbx1* is regulated by canonical Wnt signalling and hedgehog signalling and promotes Fgf ligand expression and have antagonistic effect of differentiation by negatively influencing BMP and retinoic acid signalling (figure 1.9) (Garg *et al.*, 2001; Vitelli *et al.*, 2002b; Hu *et al.*, 2004; Roberts *et al.*, 2005; Fulcoli *et al.*, 2009; Huh and Ornitz, 2010). Embryos lacking *Tbx1* have premature activation of differentiation markers and over expression of *Tbx1* inhibit differentiation of SHF cells (Chen *et al.*, 2009). *Tbx1* controls several SHF markers, like Fgf8 and Fgf 10. In *Tbx1* null mice there is decreased expression of both Fgf 8 and Fgf10 (Vitelli *et al.*, 2002b; Xu *et al.*, 2004). Fgf8, as mentioned before, is necessary for SHF proliferation and survival and is regulated by *Tbx1* through an auto regulatory mechanism involving *Foxc2* (Brown *et al.*, 2004; Hu *et al.*, 2004) and it is suggested Fgf10 also controls SHF proliferation under the regulation of *Tbx1* (Xu *et al.*, 2004). However Fgf10 expression is down regulated in Fgf8 deficient embryos (Frank *et al.*, 2002) indicating its downstream position. Transcription factors Foxa2, Foxc2, and Foxc1 regulate *Tbx1* activation in pharyngeal endoderm in SHF in a dosage dependent manner under the influence of Shh signalling (figure 1.9) (Yamagishi *et al.*, 2003; Maeda *et al.*, 2006). *Foxc1* and *Foxc2*, along with *Foxf1* also regulate Isl1 (figure 1.9), together with Gata4 (Kang *et al.*, 2009). Other SHF markers, *Mef2c* and *Foxh1* also contribute to SHF signalling in the developing heart. *Foxh1* lies upstream of *Mef2c* and along with *Nkx2.5* directs its expression in the SHF (figure 1.9) (von Both *et al.*, 2004). *Mef2c* expression in SHF is also regulated by *Isl1* and *Gata4* (Dodou *et al.*, 2004). Tbx20 is also involved in activation of Mef2c by physically interacting with Isl1 (Takeuchi *et al.*, 2005).

Cre-labelling experiments have helped in refinement of SHF model and their function, in particular *Isl1-cre* and *Mef2cAHF-Cre*. *Isl1-Cre* allele is expressed in

cells giving rise to outflow tract, right ventricle and portions of atria (Cai *et al.*, 2003) and *Mef2cAHF-Cre* in outflow tract, right ventricle, interventriular septum and atrial septum (Verzi *et al.*, 2005). *Isl1* expression contributes to the differentiation, by the activation of *Mef2c* expression (Dodou *et al.*, 2004), which is required to initiate myogenic differentiation (Chen *et al.*, 2009; Fulcoli *et al.*, 2009; Pane *et al.*, 2012). This is negatively regulated by Wnt/β-catenin signalling, which favours proliferation by regulating Fgf signalling (Cohen *et al.*, 2012). However, Wnt/β-catenin signalling is inhibited by non-canonical Wnt/PCP signalling (Cohen *et al.*, 2012), which favours differentiation. *Tbx1* targets *Wnt5a*, which is a ligand for non-canonical Wnt signalling (Chen *et al.*, 2012). Mutations in non-canonical Wnt signalling ligands, *Wnt5a* and *Wnt11* leads to outflow tract defects revealing their roles in its development (Schleiffarth *et al.*, 2007; Zhou *et al.*, 2007a). *Wnt5a* is expressed in SHF cells and *Wnt5a-/-* embryos have common arterial trunk along with abnormal NCC invasion (Schleiffarth *et al.*, 2007). *Wnt11-/-* embryos have shortened outflow tract (Zhou *et al.*, 2007a) suggesting role of non-canonical Wnt signalling pathway in addition of SHF to the outflow tract. *Tbx1* is pro-proliferation and non-canonical Wnt signalling is pro-differentiation suggesting a feedback regulation between the two. Therefore it can be stated that time specific gene expression and signalling intervention are required for regulating SHF in developing heart, starting from proliferation and migration in the outflow tract and then differentiating into cardiomyocytes. Summary of signalling pathways involved in regulating SHF is shown in figure 1.9.

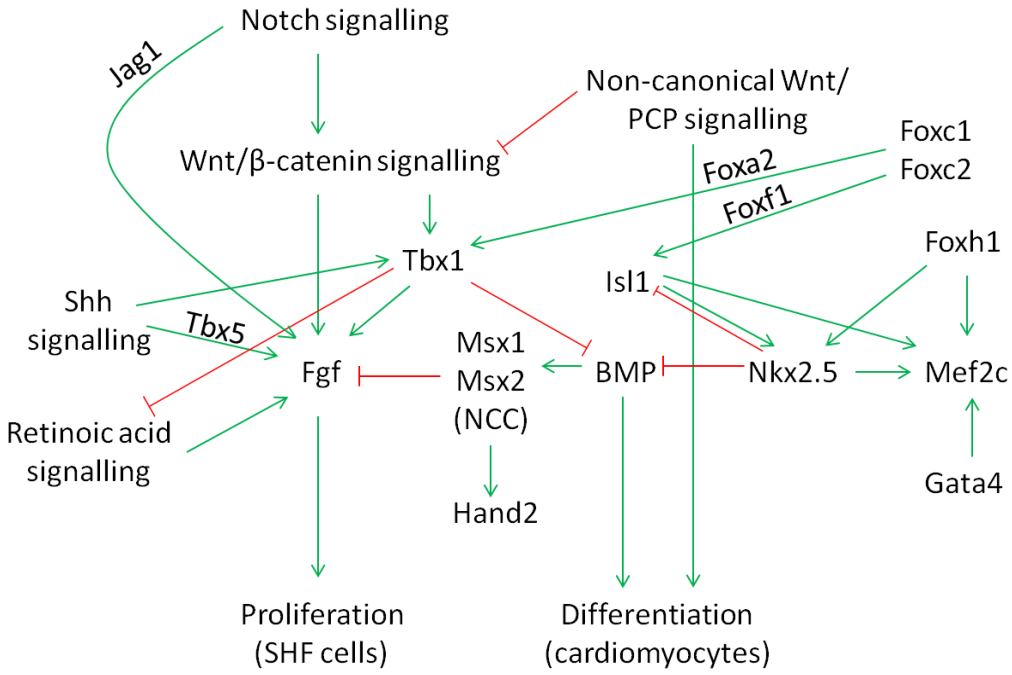

Figure 1.9: Signalling pathways regulating SHF

1.4.2.2 Phenotype arising from ablation of SHF genes

Absence or reduction of SHF specific genes leads to spectrum of cardiovascular defects. *Isl1* expression labels the largest proportion of SHF and its absence results in failure of heart looping and complete absence of the outflow tract, right ventricle and parts of atria (Cai *et al.*, 2003). *Isl1* ablation results in embryonic death by E10.5 and large contribution of Isl1 expressing cells in heart are determined by outflow tract, right ventricle and atrial defects seen in Isl1 ablated embryos (Cai *et al.*, 2003). Loss of other SHF genes which are less broad as compared to *Isl1*, like *Mef2c* and *Foxh1* results in less severe but related phenotypes like abnormal looping, shortened outflow tract and right ventricle abnormalities (Lin *et al.*, 1997; von Both *et al.*, 2004). SHF specific *Mef2c* contribution is more restricted, with contributions to outflow tract, right ventricle and ventricular septum (Verzi *et al.*, 2005). Like *Mef2c*, *Foxh1* also contributes to the right ventricle and outflow tract with similar phenotype of *Mef2c-/-* and *Foxh1-/-* embryos (Lin *et al.*, 1997; Lin *et al.*, 1998; Bi *et al.*, 1999).

Mice which have *Tbx1* mutation die in-utero displaying features of DiGeorge syndrome, like common arterial trunk and defects in aortic arch arteries (Jerome and Papaioannou, 2001; Lindsay *et al.*, 2001; Vitelli *et al.*, 2002a). *Cre* labelling experiments have shown *Tbx1* expression in SHF which contribute to inferior and lateral walls of outflow tract and to myocardium at the base of pulmonary trunk (Maeda *et al.*, 2006; Huynh *et al.*, 2007). Ablation in myocardium at the base of the pulmonary trunk is the prime cause of outflow tract alignments defects like overriding aorta, tetralogy of fallot, pulmonary hypoplasia and ventricular septal defect (Di Felice and Zummo, 2009; Van Praagh, 2009). There is reduced contribution of cells in the outflow tract in *Tbx1-/-* mice and Tbx1 regulates SHF cell proliferation (Xu *et al.*, 2004). *Tbx1-/-* embryos have common arterial trunk (Vitelli *et al.*, 2002a) which is associated with NCC as they form the septum between pulmonary trunk and aorta, however abnormally aligned outflow tract in these embryos is associated with SHF ablation. When *Tbx1* was specifically deleted from mesoderm, similar phenotype of *Tbx1-/-* mice was observed and restoration of mesodermal *Tbx1* expression gives normal outflow tract, however can only rescue partial pharyngeal arch artery development, and has no effect on non-SHF regions and derivatives like thymus, NCC migration (Zhang *et al.*, 2006). *Fgf8* hypomorphic mouse also have alignment defects such as double outlet right ventricle and ventricular septal defect (Abu-Issa *et al.*, 2002), which arise from SHF disturbance.

At the venous pole, SHF contributes to atrial myocardium which results in atrial and atrioventricular septal structures, and defects in SHF developments results in atrial and atrioventricular septal defects (Snarr *et al.*, 2007; Galli *et al.*, 2008). Therefore SHF ablation studies demonstrate how reduced SHF contribution or aberrations in SHF during heart development generate major form of congenital heart anomalies and these findings should be taken into account while studying other mutants with SHF abnormalities.

1.4.3 CNCC interaction with SHF

As mentioned in the section 1.4.2.1, NCC acts as a brake for SHF proliferation. The over-proliferation of SHF is due to excessive Fgf8 signalling in the caudal pharynx and increased expression of Fgf target genes resulting in SHF proliferation rather than their migration and differentiation into myocardium. This is normally buffered by the presence of NCC (Hutson *et al.*, 2006). SHF adds myocardium and helps in elongation of the outflow tract, aiding in alignment with the ventricles. Absence of NCC primarily leads to failure of division of the outflow tract. However, NCC deficiency also results in cardiac alignment defects as a consequence of its effect on the SHF; the SHF cells proliferate abnormally instead of migrating into the outflow tract and differentiating into myocardium (Waldo *et al.*, 2005a). Thus, the absence of NCC results in the over proliferation of SHF cells, disturbing the balance between proliferation and differentiation and resulting in abnormal myocardial bulges at the junction of myocardium and aortic sac (Waldo *et al.*, 2005a).

This close interaction between NCC and SHF cells is also suggestive from the overlapping phenotype in their ablations. Abnormal cardiac looping is observed in the absence of CNCC which is due to a lack of myocardium in the outflow tract. Direct or indirect perturbations in NCC or SHF can lead to a spectrum of outflow tract defects like common arterial trunk, overriding aorta, double outlet right ventricle and ventricular septal defects.

Thus, both SHF and NCC are essential for normal cardiac outflow morphogenesis, which forms the basis for this project.

1.5 Wnt Signalling Pathway

In the previous sections it was discussed that Wnt signalling plays a role in SHF and NCC during heart development. The Wnt signalling pathway is a group of signalling pathways which involve proteins that pass signals from outside the cell to inside and induce gene expression. These signals can be autocrine or paracrine, and lead to various cellular functions such as patterning of the body axis, cell fate specification, cell proliferation and cell migration. They are of very important clinical relevance because of their involvement in development and disease, including cancer and type-2 diabetes (Logan and Nusse, 2004; Komiya and Habas, 2008).

Discovery of Wnt signalling was initiated by Roel Nusse and Harold Vamus research on oncogenic retrovirus which lead to the identification of a proto-oncogene in mice, which is called *integration1* (*int1*) (Nusse *et al.*, 1984; Nusse and Varmus, 2012). This *int1* had high degree of conservation across different species and it was found out that int1 is the mammalian homologue of a gene discovered in *Drosophila*, known as *Wingless* (*Wg*) (Cabrera *et al.*, 1987; Rijsewijk *et al.*, 1987; Nusse and Varmus, 2012). Apart from mutants lacking wings, mutation in *Wg* gene also caused segmentation defects. A number of segment polarity gene mutations in *Drosophila* have been traced back in components of Wnt signalling pathway (Nusslein-Volhard and Wieschaus, 1980; Nüsslein-Volhard *et al.*, 1984), suggesting role of *int1* in Wnt signalling pathway during embryonic development (Klaus and Birchmeier, 2008). To identify more genes related to *int1* and *Wg*, a new gene nomenclature was given to the *int/wingless* family and it came to be known as Wnt (Wg + int) standing for wingless related integration site (Nusse and Varmus, 2012).

The Wnt proteins are a diverse family of glycoproteins but have conserved cystein rich residues which undergo palmitoylation which helps in binding these Wnt proteins to their receptors on plasma membrane through covalent attachments of fatty acids (Logan and Nusse, 2004).

The Wnt signalling pathway can be classified as 3 types, canonical Wnt pathway, non-canonical Wnt/PCP pathway and non-canonical Wnt/Ca^{2+} pathway. The

difference between canonical and non-canonical is their dependence on β-catenin (Rao and Kühl, 2010). The canonical Wnt pathway is β-catenin dependent and requires it to regulate gene transcription. Non-canonical Wnt pathways are β-catenin independent. Non-canonical Wnt/PCP pathway is required for cellular polarity and cytoskeleton arrangement and Wnt/Ca^{2+} pathway regulate calcium inside the cell. The basic foundation of all 3 pathways is the same as they share upstream proteins. The signalling starts when a Wnt protein binds to the N-terminal of cystein rich extracellular domain of Frizzled (Fz) (Rao and Kühl, 2010). This can be facilitated by other co-receptors like low density lipoprotein related protein 5/6 (LRP5/6), which is required in the canonical Wnt pathway (He *et al.*, 2004), and Ryk and Ror2, which are involved in non-canonical Wnt pathways (Lu *et al.*, 2004a; Nishita *et al.*, 2006; Komiya and Habas, 2008; Gao *et al.*, 2011; Andre *et al.*, 2012). After this binding, signal is transduced to cytoplasmic Dishevelled (Dvl) which binds to Fz. Dvl has 3 conserved domains, amino terminal DIX domain, central PDZ domain and carboxy terminal DEP domain. These domains are important as their different combinations leads to these 3 different pathways (Habas and Dawid, 2005).

1. Canonical Wnt/β-catenin Pathway – This pathway regulates cell proliferation during heart development and is β-catenin dependent, where β-catenin acts as a transcriptional activator. Wnt protein binds to Fz and activates it in the presence of LRP5/6 coreceptor which leads to binding of Dvl to Fz. Dvl is phosphorylated leading to translocation of β-catenin to the nucleus where it binds to the DNA and assists in transcription of target genes along with other transcription factors (figure 10) (Logan and Nusse, 2004; Komiya and Habas, 2008).

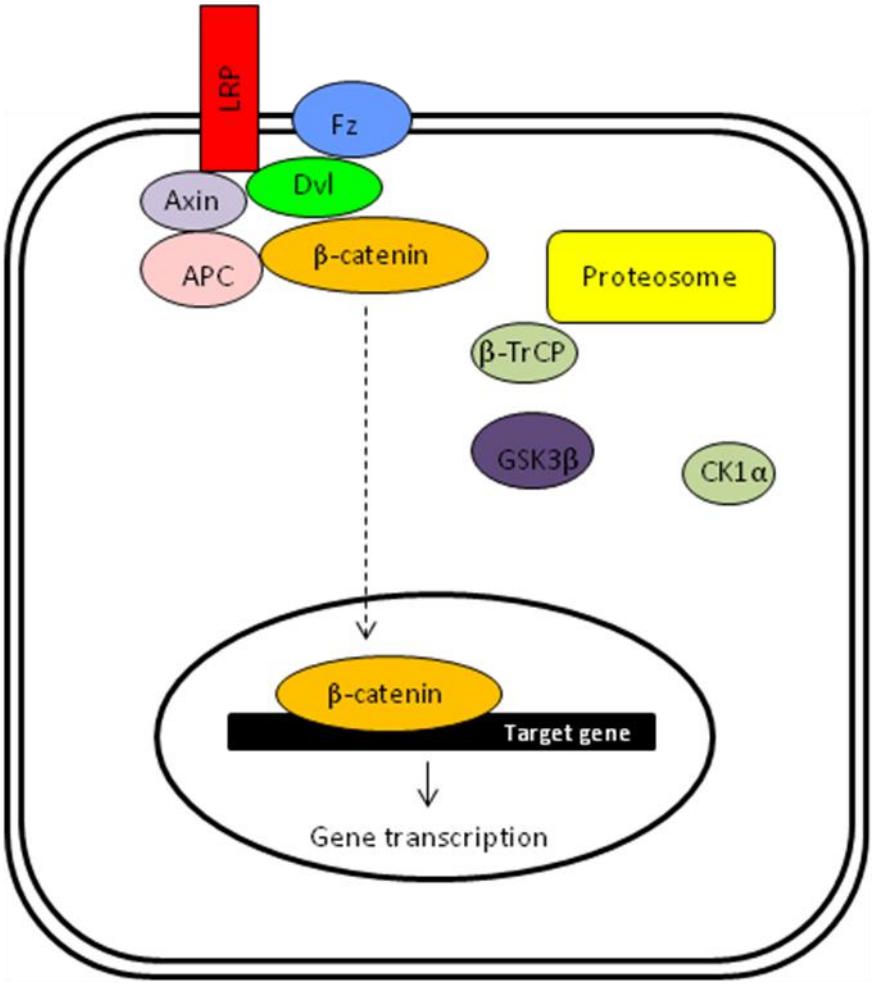

Figure 1.10: Canonical Wnt/β-catenin Pathway

β-catenin in the cytoplasm is phosphorylated by GSK-3beta, Axin, APC, PP2A, GSK2, CK1α complex (degradation complex) and undergoes polyubiquitination by β-TrCP and sent to proteosome where polu-ubiquitinated β-catenin is degraded. However, in the presence of Wnt signalling, Dvl is phosphorylated and β-catenin along with whole degradation complex (Axin, APC, etc.) binds to phosphorylated Dvl which frees β-catenin from repressive activity of GSK-3beta and β-catenin is translocated to nucleus where it binds to the DNA and assists in transcription of target genes. APC-adenomatosis polypsis coli, GSK3β-glycogen synthase kinase 3β, CK1α-casein kinase 1α.

2. Non-canonical Wnt/PCP Pathway – This pathway regulates cell differentiation during heart development and is β-catenin independent. Co-receptors involved are not clearly defined, however there are putative candidates like neurotrophin-receptor-related protein (NRH1) (Sasai *et al.*, 2004), Ryk (Lu *et al.*, 2004a; Andre *et al.*, 2012), Ror2 (Nishita *et al.*, 2006; Gao *et al.*, 2011) and PTK7 (Lu *et al.*, 2004b). The signal is transduced to Dvl which binds to Fz. Two domains of Dvl, PDZ and DEP play important role at this point they lead to two parallel pathways (Wallingford and Habas, 2005; Habas and He, 2006). Utilization of PDZ domain leads to activation of Rho pathway through Dvl-Daam1 complex. Daam1 (Dishevelled associated activator of morphogenesis 1) binds to Dvl and leads to activation of Rho GTPase. Daam1 can bind to Dvl and also to Rho GTPase, which suggests the feedback loop in the signalling pathway (Habas *et al.*, 2001). Activation of Rho GTPase leads to activation of Rho Kinase (ROCK) (Marlow *et al.*, 2002), resulting in cytoskeletal rearrangements and modifications in actin-cytoskeleton.

   When DEP domain of Dvl is utilised, it activates Rac pathway. Rac GTPase is activated, which in turn stimulates JNK (Li *et al.*, 1999; Habas *et al.*, 2003). Downstream factors of JNK are no clearly known, but have role in transcriptional regulation. Detailed explanation of non-canonical Wnt/PCP pathway will be done in section 1.6.1 keeping cardiovascular development as reference.

3. Non-canonical Wnt/Calcium Pathway – This pathway is responsible for calcium release from endoplasmic reticulum and maintaining Ca^{2+} level in the cell (figure 11). Like other 2 pathways, Wnt protein binds to Fz which activates Dvl, which upon activation binds to Fz. However, along with Dvl, trimeric G-protein is also binded to Fz and this co-stimulation activates Phospholipase C (PLC) or Phosphodiesterase (PDE), leading to 2 different pathways. If PLC is activated, it leads to activation of nuclear factor associated with T cells (NFAT) which helps in ventral patterning (Komiya

and Habas, 2008), or activation of TAK1 and NLK kinase, which inhibits canonical wnt/ β-catenin signalling (Gordon and Nusse, 2006). As this pathway controls the calcium level, it also stops the release of Ca^{2+}. If PDE is activated by co-stimulation of Dvl and G-protein, it inhibits calcium release through PKG (Komiya and Habas, 2008).

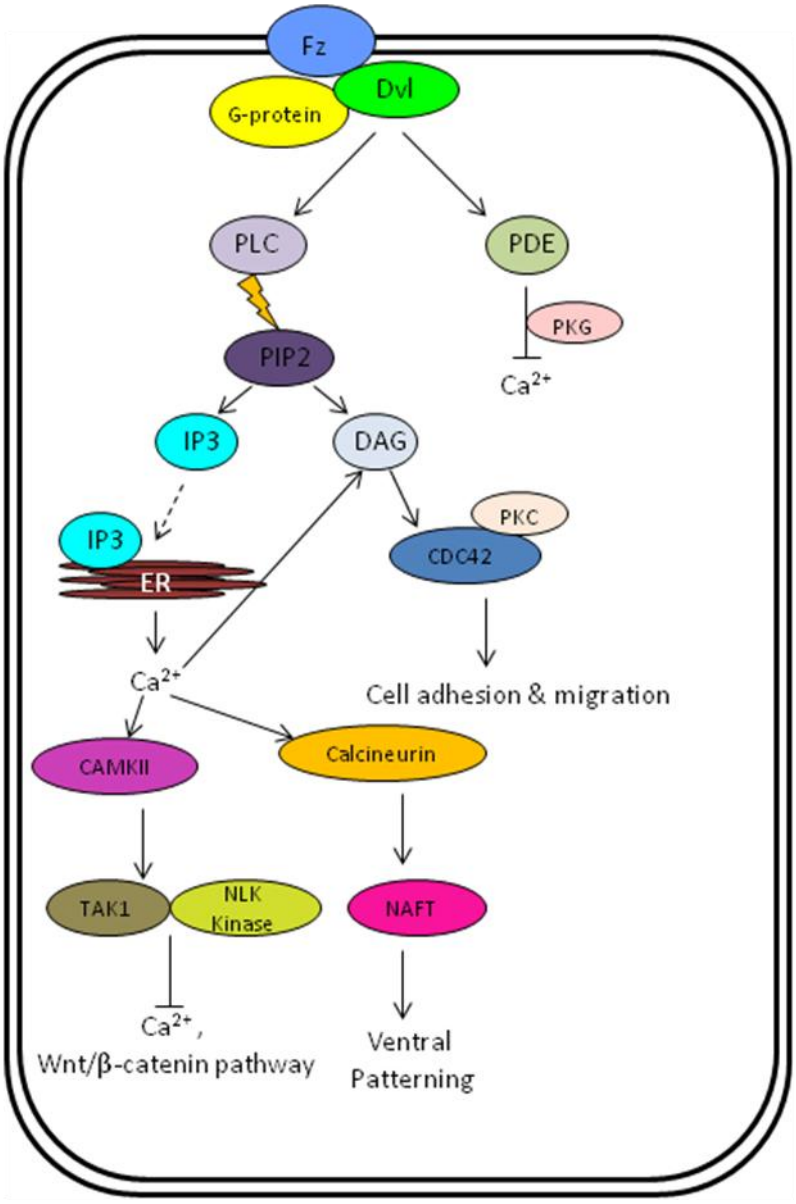

Figure 1.11: Non-canonical Wnt/Calcium Pathway

PLC-Phospholipase C, PDE-Phosphodiesterase, IP3-inositol 1,4,5-triphosphate, DAG-1,2 diacylglycerol, ER-Endoplasmic reticulum, PKC- Protein kinase C, CaMKII-calcium calmodulin-dependent protein kinase II, NAFT-nuclear factor associated with T cells.

1.5.1 Functions of Wnt signalling pathway

In both vertebrates and invertebrates, Wnt signalling plays important role in different cellular processes ranging from axis patterning to cell fate specification, proliferation and migration. In early embryonic development Wnt signalling plays an important role in establishing anteroposterior axis and dorsoventral axis in several organisms including mammals, fish and frogs. In mammals, Wnt, BMPs, Fgfs, Nodal and Retinoic acid establish axis by forming a concentration gradient, the area of their high concentration establishes the posterior and lower concentration the anterior axis. In frogs and fish, β-catenin produced by canonical wnt signalling along with BMPs elicits posterior formation. In vertebrates Wnt along with Shh establish dorsoventral axis with high Wnt signalling establishing dorsal region and high Shh signalling as ventral region (Inoki *et al.*, 2006).

Canonical Wnt signalling also mediates cell proliferation through β-catenin. Increased levels of β-catenin activate proteins like cyclin D1 and c-myc, which facilitates G1 to S phase transition during cell cycle. As there is DNA replication in S phase which leads to mitosis, the result of this rise in β-catenin is an increase cell proliferation (Nusse, 2008). For example, Wnt3a activation leads to proliferation of hematopoietic stem cells which are needed for red blood cell formation (Bakre *et al.*, 2007). Wnt signalling is also involved in cell differentiation into specific cell types such as endothelial, cardiac and smooth muscle cells (Ulloa and Martí, 2010). Wnt1 helps in self-renewal of neural stem cells and antagonizes neural differentiation. Wnt signalling is also involved in germ cell differentiation, lung tissue development, trunk neural crest cell differentiation (Van Amerongen *et al.*, 2012), and limb induction, elongation, and patterning in whichWnt5a plays the role of ligand (Gao *et al.*, 2011).

Cell migration and movement are an important aspect during embryonic development, during processes like establishment of body axis, tissue formation and limb induction. Wnt signalling facilitates this, for example during convergent extensions (CE). Both Wnt PCP and canonical signalling pathways are required for CE during gastrulation, and Wnt/Ca^{2+} signalling pathway also controls this process by inhibiting it. Migration of neuroblasts, NCC, myocytes etc are also

controlled by Wnt signalling (Woll *et al.*, 2008) which induces epithelial-mesenchymal transition (EMT) that is required for cell migration (Kaldis and Pagano, 2009). During EMT epithelial cells transform into mesenchymal cells by down regulation of cadherins which leads to cell detachment from laminin which keeps it attached to basement membrane.

1.6 Cell Polarity

Cell polarity is the difference in the spatial characteristics of the cell which leads to differences in its structure, shape and function. Polarity of a cell happens by asymmetric cell division, asymmetric localization of proteins and concentration gradients of secreted receptor proteins, and regulates both collective and individual cell movements during developmental stages. The molecules responsible for regulation of cell polarity are highly conserved between species. The polarity in epithelial cells can be divided in two distinct types; apical-basolateral polarity (ABP) and planar cell polarity (PCP) which work in coordination and are functionally linked. Polarized cells are divided into apical and basal sides and this division between the compartments is regulated by presence of adherens junctions (AJ), which are present at the border of apical and basolateral domain (Kaplan *et al.*, 2009) (basal being the cell's attachment to the basement membrane and attachment to the adjoining cells in the cell layer is the lateral) (figure 1.12). The AJ, apart from dividing the cell into two compartments, are also involved in cell-cell adhesion and migration. PCP is the polarization along the plane of the epithelial layer (perpendicular to the ABP), which divides the cell into proximal and distal sides (figure 1.12). For PCP signalling to be properly functional, the core PCP proteins are asymmetrically localized along the plane of the cell (Das *et al.*, 2004; Wu *et al.*, 2004), and ABP proteins regulate this process (Fedeles and Gallagher, 2013). Also, PCP signalling has been implicated to have a role in regulation of ABP, and directional cell migration (Tao *et al.*, 2009; Goodrich and Strutt, 2011; Tao *et al.*, 2012), for example migration of NCC has been shown to be regulated by PCP signalling in both *Xenopus* and zebrafish (De Calisto *et al.*, 2005; Matthews *et al.*, 2008), however

in mammals such a role has yet to be shown. The PCP protein Prickle1, when absent in mice, leads to death of embryos in uterus because of failure to establish ABP (Tao *et al.*, 2009). These examples show the functional link between ABP and PCP and indicate that their correct establishment and maintenance is required for normal embryonic development.

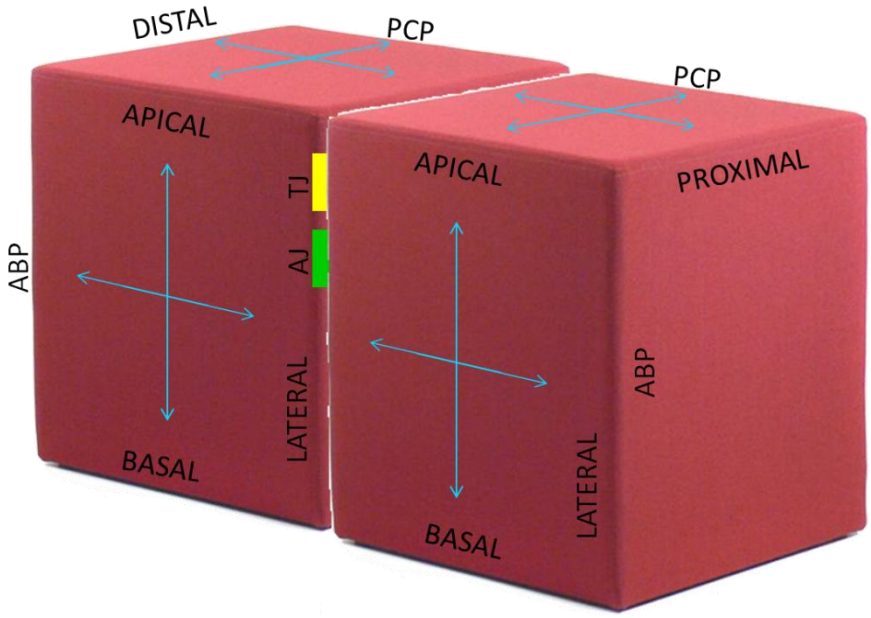

Figure 1.12: Planes of cell polarity

ABP - apical-basolateral polarity, PCP - planar cell polarity, AJ – adhesion junctions, TJ – tight junctions.

1.6.1 Planar Cell Polarity Signalling Pathway

In tissues, cells require positional information to move or orient themselves in a directed fashion and to generate polarized structures. This type of polarization of cells is known as planar cell polarity (PCP) and the pathway controlling tissue organization is the PCP pathway. The core components to PCP signalling interact to establish polarity in the field of cells. PCP helps in interpreting the anterior-posterior and left-right orientations. Disruption of PCP signalling has been shown to disrupt cell polarity and polarised cell movements in a wide range of species which results in abnormalities in morphogenesis.

PCP first came into the picture because of work on *Drosophila*, by Lawrence and Adler groups (Lawrence and Shelton, 1975; Vinson and Adler, 1987). Later genetic analysis and molecular cloning of PCP gene from *Drosophila* lead to identification of PCP factors. In *Drosophila* all adult cuticular structures show PCP features (Adler, 2002; Mlodzik, 2002; Strutt, 2003), for example hair position on thorax, compound eye organization, and patterning of wings and disruptions of PCP signalling leading to disorganization in the tissues (Wang and Nathans, 2007; Simons and Mlodzik, 2008). In wing, cells orient themselves in proximal-distal axis and have distally pointing hair, on thorax, PCP is in anterior-posterior axis and in the eye the regular arrangement of the ommatidia is because of both proximal-distal and anterior-posterior polarity (Adler, 2002; Mlodzik, 2002; Strutt, 2003).

Current evidence indicates that core PCP genes are conserved across tissues and species, instead of having different polarity regulating signalling pathways from tissue to tissue and organism to organism. In vertebrates PCP establishment and signalling pathway can be observed during CE during gastrulation (Keller, 2002; Myers *et al.*, 2002; Wallingford *et al.*, 2002). Mesodermal and ectodermal cells undergo CE, where polarised cells intercalate leading to mediolateral narrowing called convergence, and elongation along the anterior-posterior axis, which is called extension (Keller *et al.*, 2003). PCP has been shown to regulate CE movement of dorsal mesodermal cells during gastrulation and neural tube closure (Veeman *et al.*, 2003). In zebrafish and *Xenopus* as well, PCP regulates CE movements during gastrulation (Wallingford *et al.*, 2002). Other examples in

vertebrates which require PCP signalling are organisation of hair follicles, orientation of stereo-cilia in the sensory epithelium of inner ear and abnormalities in the cilia orientation in the absence of PCP signalling (Montcouquiol *et al.*, 2003; Wang and Nathans, 2007). There are many similarities between PCP in *Drosophila* and vertebrates, however there are differences too. For examples, in mouse tyrosine kinase, Ryk receptor acts as an important PCP signalling factor (Lu *et al.*, 2004b), but no similar factor has been found in *Drosophila* and none of fly Wnt genes have been implicated to have role in PCP activation, whereas in vertebrates there is evidence of involvement of Wnts in PCP signalling (Klein and Mlodzik, 2005).

PCP signalling is a multi-protein signalling pathway and in flies these components (proteins) can be divided into 2 groups, global group and core group. The global group control polarization along the tissue and body axis and include Fat (Ft), Dachsous (Ds) and Four-jointed (fj) as its components, reviewed in (Henderson and Chaudhry, 2011). The core group is mainly responsible for polarization of individual cells and members of this group are Frizzled (Fz), Dishevelled (Dvl), Vang-gogh (Vang)/Strabismus (Stbm), Prickle (Pk), Flamingo (Fmi)/starry night (stan) and Deigo (Dgo), reviewed in (Henderson and Chaudhry, 2011). Of these Fmi, Fz, Dvl and Dgo localize at distal side of the cell and Fmi, Vang and Pk localize at the proximal side resulting in an asymmetric localization of the proteins (Henderson and Chaudhry, 2011). Ft act as positive regulator of Fz and Ds as a Ft antagonist, Both Ft and Ds genetically interact with fj (Yang *et al.*, 2002; Matakatsu and Blair, 2004; Simon, 2004), which also regulates PCP as Ds and fj both act on Ft, which regulates Fz activity (Zeidler *et al.*, 1999; Zeidler *et al.*, 2000). Although PCP proteins are conserved and play similar roles in vertebrates as in fly, the mechanism of action is not shown to be conserved. As mentioned before, Wnt ligands do not activate Fz in flies, but vertebrate Wnts (Wnt4, Wnt5a and Wnt 11) are involved in PCP activation by binding to Fz. *Celsr1* and *Vangl2* are vertebrate homologues of *Fmi* and *Vang/Stbm* respectively (Formstone and Little, 2001; Montcouquiol *et al.*, 2003). Other members of this pathway are Ptk7, Scrib and Daam1. Fz after activation binds to Dvl which interacts with Daam1 and activates RhoA and in turn ROCK which controls

cytoskeleton rearrangements. Dvl can also activate Rac1 independent of Daam1 which activates JNK which impacts gene expression (figure 1.13). The downstream cascade can differ depending upon the context, for example cytoskeletal reorganisation versus transcriptional response. PCP responses can affect cytoskeletal organisation in *Drosophila* cuticular cells and mammalian inner ear epithelium (Adler, 2002; Mlodzik, 2002; Montcouquiol *et al.*, 2003; Strutt, 2003), and nuclear signalling response in Drosophila eye and mammalian hair follicle (Mlodzik, 1999; Guo *et al.*, 2004). Scrib interacts with Vangl2 and plays a role in its asymmetric localization along with Celsr1. Interaction is mediated by PDZ domain of Scrib and Vangl2 (Kallay *et al.*, 2006), and this PDZ domain is also shared with Dvl (Bastock *et al.*, 2003). Ptk7 also interacts with Vangl2, and Vangl2 recruits Pk which binds to Dvl and antagonises its binding with Fz. Fz-Dvl and Vangl2-Pk antagonise each other and are localised at opposite poles of each cell.

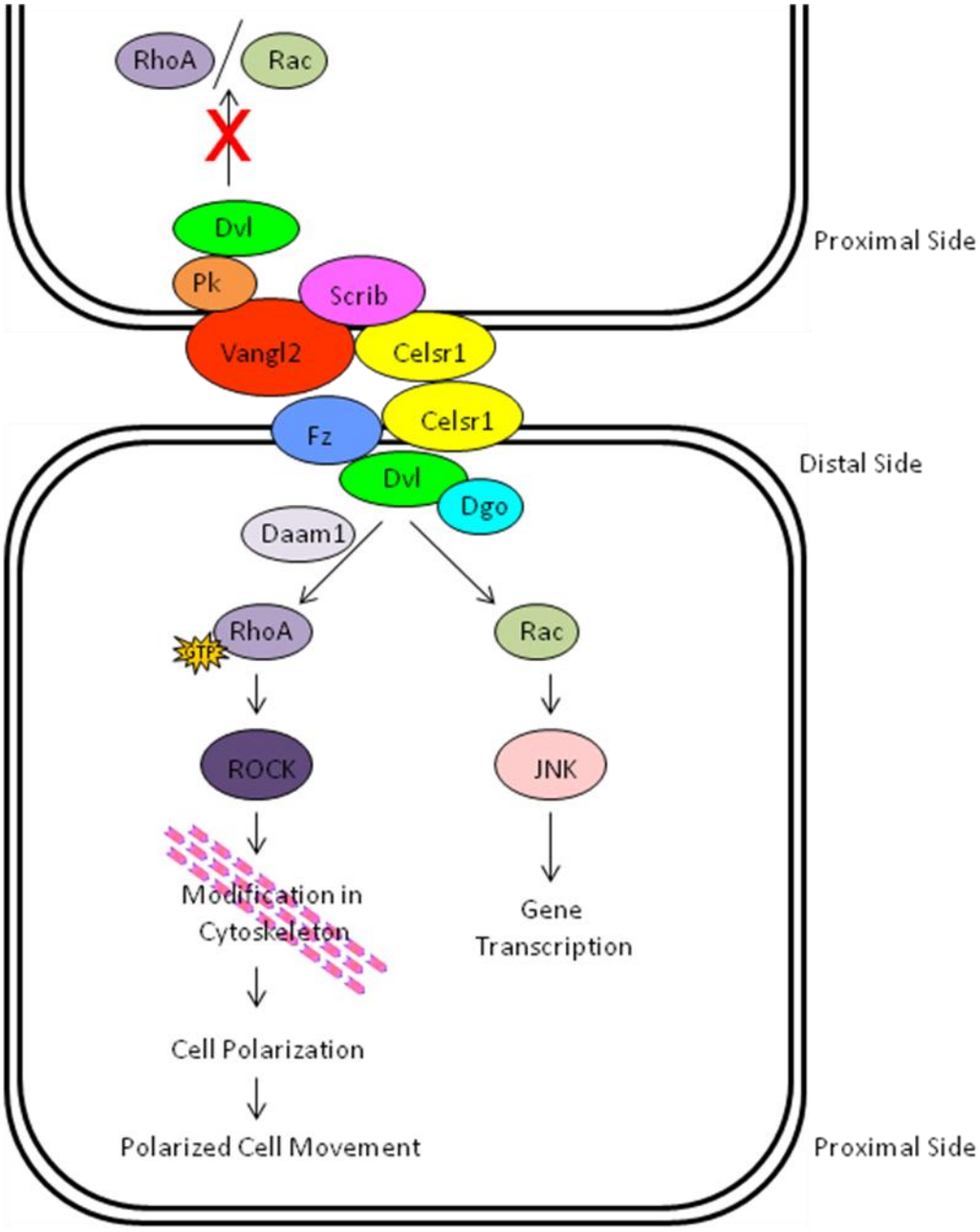

Figure 1.13: Planar Cell Polarity Signalling Pathway

Dvl-Dishevelled, Pk-Prickel Fz- Frizzled, Dgo- Deigo, Daam1- Dishevelled associated activator of morphogenesis 1, JNK- c-jun terminal kinase.

1.6.1.1 Downstream targets of PCP pathway (ROCK and Rac1)

Components of PCP pathway have been involved in cardiac outflow tract morphogenesis, with disruption of various PCP genes results in outflow tract malformations (Hamblet *et al.*, 2002; Curtin *et al.*, 2003; Phillips *et al.*, 2007; Schleiffarth *et al.*, 2007; Zhou *et al.*, 2007b; Etheridge *et al.*, 2008; Nagy *et al.*, 2010; Paudyal *et al.*, 2010; Yu *et al.*, 2010). While the mechanisms underlying these malformations are as yet unknown, there is a possibility of link between PCP signalling and the regulation of cellular migration into heart during embryogenesis. Rac1 and ROCK are both downstream targets of PCP pathway and have roles in cell adhesion, migration and polarity. Rac1 is a member of the Rho family of small guanosine triphosphatases (GTPases), which are a subgroup of Ras-superfamily of GTPases. The role of Rac1 has been investigated in cardiovascular development; in terms of cellular migration, adhesion, proliferation, transcription and apoptosis; in cardiac progenitor populations (Tan *et al.*, 2008; Bosco *et al.*, 2009; D'Amico *et al.*, 2009; Thomas *et al.*, 2010). Rho Kinase (ROCK) is a serine/threonine protein kinase downstream of the GTPase Rho A (Amano *et al.*, 2010). ROCKs phosphorylate over 20 substrate proteins primarily involved in regulating assembly of actin filaments within the cytoskeleton (Riento and Ridley, 2003). Through this mechanism it regulates a broad variety of physiological processes, including cell migration (Worthylake and Burridge, 2003), proliferation (Sahai *et al.*, 2001), transformation (EMT) (Zondag *et al.*, 2000), apoptosis (Sebbagh *et al.*, 2001), morphology (Sordella *et al.*, 2002) and establishing cell polarity (Amano *et al.*, 2010). Activation of ROCK for each function is regulated by different signalling molecule. These signalling molecules activate RhoA GTPase which in turn activates ROCK. This process of RhoA GTPase activation can be direct or indirect (Zhao and Rivkees, 2003; Loirand *et al.*, 2006).

As ROCK and Rac1 are seen to play an important role in cell migration and cell survival or cell apoptosis, their role in cardiac development is very important and raises the possibility of their involvement in congenital heart defects related to migrating cardiac progenitor populations (Bosco *et al.*, 2009; Hildreth *et al.*,

2009). Therefore, we aim to elaborate the role of PCP pathway downstream targets, Rac1 and ROCK in SHF for heart development.

1.6.1.2 PCP Signalling Pathway and Heart Development

During very early embryonic development (gastrulation), PCP signalling is involved in CE movements and abnormalities in that result in severe defects like neural tube defects (NTD), gastroschisis, axial rotation defects and cardiovascular defects (CVD) (Kibar *et al.*, 2001; Hamblet *et al.*, 2002; Curtin *et al.*, 2003; Murdoch *et al.*, 2003). Severe NTD, craniorachischisis (CRN), in which neural tube fails to close and is completely open from midbrain to tail was initially demonstrated in *Vangl2* mutant, loop-tail (*Lp*) (Strong and Hollander, 1949), and is also displayed when other PCP genes are mutated, including *Dvl1* and *Dvl2* (Hamblet *et al.*, 2002), *Celsr1* (*spin-cycle* and *crash* mutant) (Curtin *et al.*, 2003), *Scribble1* (*circle tail* mutant) (Murdoch *et al.*, 2001b; Murdoch *et al.*, 2003) and *Fz* (Wang *et al.*, 2006). However, the CVD present in these PCP mutants could be secondary defects of the primary NTD and body axis abnormalities which might lead to defective remodelling of heart during developmental stages. However, *Wnt11-/-* (Majumdar *et al.*, 2003) and *Dvl3-/-* (Etheridge *et al.*, 2008) mutants do not have NTD and have cardiac defects, which suggest that cardiac defects are not secondary to NTD in the absence of PCP signalling and disrupted polarity. However this needs to be confirmed and established.

There have been reports in zebrafish that PCP signalling might be involved in migration of cardiac precursor cells from the lateral plate mesoderm to the midline of the body where they form cardiac crescent and then the linear tube, reviewed in (Henderson and Chaudhry, 2011). *Lp* and circle-tail (*Crc*) mice with mutations in *Vangl2* and *Scribble* respectively show PCP type phenotype with abnormalities in polarization and organization of developing outflow tract and ventricular myocardium, with differences in the polarization of cardiomyocytes in the initial stages of development (Murdoch *et al.*, 2003; Phillips *et al.*, 2005; Phillips *et al.*, 2007; Phillips *et al.*, 2008). Mutation of *Wnt11*, which is a ligand for PCP pathway, in *Wnt11-/-* mice also have disorganized cardiomyocytes in the

developing ventricle along with misexpression of adhesion molecules N-cadherin and β-catenin (Nagy *et al.*, 2010). *Crc* mutant embryos also have abnormal distribution of N-cadherin and β-catenin, which are components of AJ (Phillips *et al.*, 2007). Vangl2 and Pk have also been implicated to have a role in cellular organization in the heart tube (Panáková *et al.*, 2010). PCP mutants also exhibit outflow tract defects which suggest that PCP signalling could be regulating extra-cardiac cells into the developing outflow which are responsible for the fully developed outflow tract. These cells include NCC and SHF. In frogs and zebrafish, ROCK and Rac are key effectors of the PCP pathway and are involved in NCC migration (De Calisto *et al.*, 2005; Carmona-Fontaine *et al.*, 2008b; Matthews *et al.*, 2008), but in mice PCP signalling might not be controlling long range migration of NCC, as both *Lp* and *Crc* mutant mice have normal NCC migration in the OFT (Henderson *et al.*, 2001; Phillips *et al.*, 2007). SHF cells contribute to the myocardium of the outflow tract and right ventricle and abnormalities in them while adding cells in the developing outflow could lead to improper extension and looping leading to outflow remodelling defects. There is considerable evidence the PCP signalling pathway is important in outflow tract remodelling but which cell types it majorly regulates remains unclear. I aim to increase our understanding of this regulation in this thesis. In addition PCP signalling has been shown to play a crucial role in the SHF cells, but tissue specific dissection of PCP signalling in the cell types is required to confirm this.

1.7 *Vangl2*

Vangl2 is mouse homolog of the *Drosophila* core PCP gene, *Strabismus* (*Stbm*)/*Van gogh* (*Vang*) and is a core member of the PCP pathway (Taylor *et al.*, 1998; Wolff and Rubin, 1998; Katoh, 2002). Stbm is required to establish polarity in *Drosophila* and sequence analysis of both vertebrate and invertebrate homologs show that *Stbm* is highly conserved through species (Wolff and Rubin, 1998). *Vangl2* gene encodes for a transmembrane protein with 4 transmembrane domains, a N-terminal cytoplasmic serine motif (SxxSxxSxxSxxS) and a cytoplasmic C-terminal with PDZ-binding domain (Katoh, 2002) (figure 4).

Through interactions with this PDZ domain, Vangl2 recruits various proteins, like Scrib and Magi3 (Yao *et al.*, 2004; Kallay *et al.*, 2006). The second homolog of *Stbm* in vertebrates is *Vangl1*, which encodes a protein with 73.1% total amino acid homology with Vangl2 and also has a similar overall structure (Katoh, 2002). However studies to look at tissue and cell distribution of *Vangl1* mRNA in zebrafish shows non-overlapping expression pattern with *Vangl2* (Jessen and Solnica-Krezel, 2004). In mouse there is both co-expression and important differences in the expression patterns discussed later (Jessen and Solnica-Krezel, 2004; Doudney *et al.*, 2005).

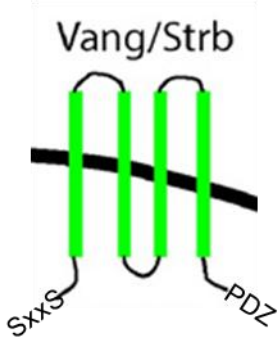

Figure 1.14: Vangl2 protein

Vangl2 along with other PCP proteins helps in regulation of coordinated polarization of the cells within the epithelial plane and is important during left-right patterning (Adler, 2002; Mlodzik, 2002; Fanto and McNeill, 2004). It co-localizes with Scrib to the basolateral plasma membrane of the polarized epithelial cells in mammals (Kallay *et al.*, 2006). It activates non-canonical Wnt/PCP signalling pathway, and activates Rac-JNK and Rho-ROCK signalling (Yao *et al.*, 2004; Ybot-Gonzalez *et al.*, 2007; Phillips *et al.*, 2008), which leads to cellular polarization and migration respectively. This cellular polarization and migration is crucial for correct patterning and morphogenesis during embryonic development e.g. during neural tube closure and organization of cardiomyocytes (Ybot-Gonzalez *et al.*, 2007; Phillips *et al.*, 2008).

Vangl2 is present on mouse 1qH3/human 1q23.2 chromosome and *Vangl1* on a duplicated block similar to the *Vangl2* locus on mouse chromosome

3qF2.2/human 1p13.1 (Doudney *et al.*, 2005). *Vangl2* is highly expressed in the brain, testis, heart, retina, lungs, neural tube, cochlea, cerebral cortex, dorsal root ganglia, tubular tissues like intestine, bronchus, and kidney during embryonic development (Kibar *et al.*, 2001; Phillips *et al.*, 2005; Tissir and Goffinet, 2006; Phillips *et al.*, 2007; Torban *et al.*, 2007). Although *Vangl2* and *Vangl1* are closely related, their expression pattern is different. *Vangl1* is expressed in neural tube like *Vangl2*; however *Vangl1* is more restricted to the floor plate region of neural tube and notochord, and *Vangl2* is expressed more broadly in the neural tube with overlapping *Vangl1* in some floor plate cells, however with no expression in notochord making it exclusively express *Vangl1* (Murdoch *et al.*, 2001a; Doudney *et al.*, 2005; Torban *et al.*, 2008). It has been suggested that *Vangl1* is not expressed in cardiac regions, whereas *Vangl2* is present in the cardiac region (Doudney *et al.*, 2005), however another study has shown *Vangl1* expression in the heart (Torban *et al.*, 2008). In *Lp* mice there was no major difference in *Vangl1* expression pattern between control and mutant mice, for example asymmetric localisation of Vangl1 in the cochlea in embryos with *Vangl2* mutation (Song *et al.*, 2010), which could be the reason for the non-redundancy between *Vangl2* and *Vangl1*, as Vangl1 does not compensate for the loss of Vangl2 in *Lp* mutants (Torban *et al.*, 2004; Doudney *et al.*, 2005). However this is not straight forward and still to be confirmed as studies show genetic interaction between *Vangl1* and *Vangl2* and have suggested redundancy between them (Torban *et al.*, 2008; Song *et al.*, 2010). Vangl1 and Vangl2 asymmetric expression is observed in hair cells of sensory epithelia of cochlea and in posterior-notochord cells (PNC) with cilia positioned randomly in their absence in PNC with turbulent nodal flow resulting in disruption of left-right asymmetry (Song *et al.*, 2010). Their localisation patterns are also consistent in regulating CE (Jessen *et al.*, 2002), indicating their genetic interaction and redundancy in PCP. A null allele of *Vangl1* (*Vangl1*^{gt}) generated using a gene-trap embryonic stem-cell line showed that *Vangl1*$^{gt/gt}$ homozygote appeared normal but had disorganisation in stereociliary bundles in cochlear hair cells (Torban *et al.*, 2008). Double heterozygous *Vangl2*$^{Lp/+}$;*Vangl1*$^{gt/+}$ also had disrupted orientation of cochlear stereociliary bundles, CRN in more than 60% cases and remaining with just looped tail and cardiac defect aberrant right

subclavian arteries (Torban *et al.*, 2008). *Vangl2*$^{Lp/+}$*;Vangl1*$^{gt/+}$ had multiple laterality defects, failed embryonic turning and heart looping (Song *et al.*, 2010).These defects have seen in *Lp/Lp*, indicating at the genetic interaction between *Vangl1* and *Vangl2*, and Vangl1's role in PCP. However there were no cardiac outflow abnormalities in *Vangl1*$^{gt/gt}$ homozygote and *Vangl2*$^{Lp/+}$*;Vangl1*$^{gt/+}$ suggesting lesser sensitivity of myocardial cells to loss of Vangl1 and confirming that Vangl2 is solely responsible for causing double outlet right ventricle in *Lp/Lp* mutants. Also NTD are also absent in *Vangl1*$^{gt/gt}$ but were present in *Vangl2*$^{Lp/+}$*;Vangl1*$^{gt/+}$, suggesting dominant role of Vangl2. Loss of *Vangl1* on its own is masked by *Vangl2* but loss of 50% or more *Vangl2* along with loss of *Vangl1* leads to developmental defects. Therefore *Vangl2* is required in dosage dependent manner. However this is only in mice, as *Vangl1* mutations have been found in human cases of NTD, even in heterozygous conditions (Torban *et al.*, 2008).

As mentioned before, Vangl2 is a core member of the PCP pathway and it has been shown that it is essential for normal neural tube closure, development of the female reproductive tract, lung and kidney branching and the organisation of sensory hair cells in the inner ear (Henderson *et al.*, 2001). Vangl2 has also been implicated to have role in AJ formation, which are essential for cell ABP (Lindqvist *et al.*, 2010). Previous studies in the Henderson laboratory suggest that Vangl2 is important for cardiac development, particularly the outflow region of the heart (Phillips *et al.*, 2005).

Preliminary data from the Henderson lab has shown that Vangl2 is expressed in the pseudo-stratified epithelium of the SHF as these cells move into the outflow region, within the myocardium of the outflow tract (which is derived from the SHF) (Phillips *et al.*, 2005). Vangl2 expression is found in pharyngeal mesoderm, but which cell type is not known. Thus, it remains possible that Vangl2 is playing crucial roles within these tissues. To determine the role of *Vangl2* a natural mutant of this gene, *Lp* mice has been looked into in great detail.

1.7.1 Natural mutant of *Vangl2*, loop-tail mice

The loop-tail (*Lp*) mouse is a naturally occurring mutant with a single nucleotide mutation in *Vangl2* (serine to asparagine substitution) producing a malfunctional protein product. In 2001 Kibar et al and Murdoch et al provided convincing evidence and identified *Ltap/Lpp1*, now called *Vangl2*, as the gene that is mutated in *Lp* mice. Mutation in *Lp* (G to A transition at position 1841) results in substitution of a highly conserved serine 464 to asparagine (S464N). The *Lp* mutations are found in the C-terminal tail of the protein, therefore it is possible that protein folding of this region in altered, leading to alteration in protein–protein interactions which are mediated by the PDZ domain at the C-terminal. Another possible explanation suggested is the serine to asparagine substitution may disrupt phosphorylation based intracellular signalling (Kapron C 2002).

Mutation in *Vangl2* leads to abnormalities in the embryo; with *Lp/+* have abnormal head movement, brain ventricle and hippocampus morphology, urogenital defects along with delayed neural tube closure giving them the characteristic 'looped' tail (Torban *et al.*, 2008). In homozygous condition, *Lp/Lp* embryos have more severe phenotype and embryos die in utero because of CRN (Strong and Hollander, 1949). *Lp/Lp* also have abnormal cochlea morphology, abnormal orientation of inner and outer hair cell stereociliary bundles, few cases of gastrochisis, and a spectrum of cardiac defects which exclusively affect the outflow region of the heart, including double outlet right ventricle, overriding aorta and ventricular septal defects (Henderson *et al.*, 2001; Montcouquiol *et al.*, 2003). Aortic arch defects are also found in most *Lp/Lp* fetuses. Non-canonical Wnt signalling is necessary for the proper development of the outflow tract and interestingly, during remodelling of the proximal outflow tract, the pattern of *Wnt-11* and *Dvl2* expression is similar to Vangl2 in the myocardium of the outflow tract and in cardiomyocytes which extend into the proximal outlet septum in the process of myocardialization (Phillips *et al.*, 2005). These migrating cardiomyocytes normally display characteristics of polarized cells, which are not seen in *Lp/Lp* mice. Therefore, it has been suggested that polarized cell movements are regulated by noncanonical Wnt signalling (Brade *et al.*, 2006).

Therefore Vangl2 is essential for normal heart development; however as the defects observed in outflow tract development in the *Lp* mouse may arise from disruptions to multiple cell types, and despite a thorough description of the cardiac defects in the *Lp/Lp* mutant it is still to be established which cell types requires Vangl2 signalling during outflow tract development and the role that Vangl2 plays in these cells. While cells from the SHF make a significant contribution to the outflow tract, including the myocardium, endocardium and smooth muscle cells (Waldo *et al.*, 2005b; Moretti *et al.*, 2006), NCC are responsible for its septation and alignment (Kirby *et al.*, 1983; Bradshaw *et al.*, 2009). Thus, the cardiac defects seen in *Lp/Lp* mice could result from disruption to either NCC or SHF cells as they are added to the heart. To unravel this, a more specific conditional knockout was required and *Vangl2flox* mice in which tissue specific deletion of the *Vangl2* gene was produced in order to dissect the tissue-specific requirement for Vangl2 signalling in the developing heart.

1.8 Aims of the project

Mutation of the *Vangl2* gene, a key component of the non-canonical Wnt/PCP signalling pathway, in the *Lp* mouse leads to a wide range of cardiac malformations. However, loss of *Vangl2* from all the cell types within the developing heart means that the *Lp* mouse cannot be used to dissect the role of *Vangl2* gene in the various cell type/s that form the heart.

It was hypothesized that *Vangl2* has a role in the establishment of PCP in the early stages of heart development and is crucial for cell organisation and movement in the developing outflow tract. Loss of *Vangl2* will result is the mislocalizaton of other proteins within the cell and a range of clinically relevant cardiac malformations.

To test these hypotheses, the main objectives of this project are:

1. To perform conditional deletions of *Vangl2* in specific tissue and cell types in an attempt to isolate the cardiac defects identified in the *Lp* mouse mutant.

- To establish whether the new *Vangl2flox* line that has been produced recapitulates the *Lp* phenotype.
- To reveal the requirement for *Vangl2* specifically in NCC and SHF, and to establish how loss of Vangl2 function in these cell types impacts on morphogenesis of the cardiac outflow tract.

2. To elucidate the normal behaviours of SHF and/or NCC as they contribute to the outflow tract, and to establish how loss of *Vangl2* affects the polarisation, directional movement and maturation of these cell types.
   - To localise Vangl2 at the sub-cellular level by attempting to co-localise it with other known proteins within the developing heart.
   - To deduce the exact role of Vangl2 in the early stages of cardiac development.
3. To determine whether PCP pathway and upstream components (Wnt5a and Ror2) and downstream targets, Rac1 and ROCK acts in the same way as Vangl2 to regulate outflow tract development (in either NCC or SHF).

Using Cre recombinase (Cre-lox) technology a floxed allele of *Vangl2* (*Vangl2flox*), *Rac1* (*Rac1flox*) and dominant negative form of *ROCK* (*ROCKDN*) have been used to dissect the tissue-specific requirement for their respective signalling in the developing heart and achieve the objectives of the project.

Chapter 2

Material and Methods

2.1 Mouse

All animals were maintained and killed according to the requirements of the Animals (Scientific Procedures) Act 1986 of the UK Government.

2.1.1 Mouse lines

Different mouse lines were used for the experiments. The *Loop-tail* mouse colony was maintained by inbreeding heterozygous males with female wild type litter-mates and mating were set up between heterozygous males and heterozygous female mice. *Vangl2*^{floxneo} mice were created in partnership with Ozgene (Australia). To generate *Vangl2*^{flox} mice, *Vangl2*^{floxneo} mice were crossed with *FlpE* (Henrich *et al.*, 2000) mice. To visualize specific cell lines and to follow their contribution to the heart development (lineage tracing), Cre recombinase technology was used with enhanced yellow fluorescent protein (eYFP) as a marker, resulting in embryos in which the *eYFP* gene was expressed in a tissue-specific manner. Hence, *Vangl2*^{flox} mice were then inter-crossed with *ROSA-Stop-eYFP* mice (Srinivas *et al.*, 2001). Table 2.1 summarises the list on mice lines used for the experiments. Cre driver lines (table 2.2) were all intercrossed with the mouse lines to for gene deletion and knockdown.

Table 2.1: Different mouse lines used in the study.

Mouse lines	
Vangl2^{floxneo}	*Neo* knockin created by Ozgene (Australia)
FlpE (Henrich et al., 2000)	*FlpE* knockin by inserting an FLPe-encoding cassette and as a deleter strain
ROSA-Stop-eYFP (Srinivas et al., 2001)	*EYFP* knockin into the *ROSA26* locus, preceded by a *loxP*-flanked stop sequence
ROCKDN (Kobayashi *et al.*, 2004)	*Cytomegalovirus (CMV)* gene promoter was fused to *chloramphenicol acetyltransferase* (CAT) gene cassette, both ends of which were flanked by *loxP* sites. A DNA fragment encoding a dominant-negative mutant for ROCK was inserted into this site.
Rac1flox (Walmsley et al., 2003)	Knockin with *loxP* site inserted between exons 3 and 4

Table 2.2: Details of *Cre* lines used in the study.

Cre-line	**Cre-containing cells**
PGK (Lallemand *et al.*, 1998), *Sox2* (Hayashi *et al.*, 2002)	*PGKcre* and *Sox2cre* transgene generated by cloning PGK-1 promoter and Sox2 promotor upstream of *cre* gene for Somatic and Germ Cells
Isl1 (Yang *et al.*, 2006)	*Cre* knockin into the endogenous *Isl1* locus, replacing the endogenous *Isl1* ATG for Second Heart Field cells
Wnt1 (Danielian *et al.*, 1998)	Cre recombinase under the control of *Wnt1* enhancer for Neural Crest Cells
Mlc2v (Chen *et al.*, 1998)	*Cre* knockin into the endogenous *Mlc2v* locus at *Xho*I site for Myocardium
Tie2 (Kisanuki *et al.*, 2001)	Cre recombinase under the control of *Tie2* enhancer for Endothelium

Mice having *eYFP* sequence have a stop codon before it, this stop codon also has *loxP* sites on its either sides. When this stop codon is present it doesn't let the fluorescent protein to express but *Cre* recognizes *loxP* sites and removes stop codon and fluorescent protein is expressed. It depends on which *Cre* is used, because on *Cre* expressing cells would have this expression. It is beneficial for lineage tracing of different cells types.

2.1.2 Timed mating

Mating were set up by putting *Vangl2*$^{flox/+}$*;Cre+* male and *Vangl2*$^{flox/flox}$*;YFP* female mice together overnight followed by separation after successful mating. Successful mating was determined by the presence of a copulation plug. Plugged females were then separated and the day was considered as embryonic day 0.5 (E0.5). This allows for timing of mating so that gestational ages can be estimated.

2.1.3 Dissection

At the desired developmental stages (E9.5-E15.5), pregnant females were sacrificed by putting them in carbon dioxide gas chamber, followed by cervical dislocation. Embryos were dissected out and placed in Dulbecco's Modified Eagle Medium (DMEM) (Gibco) or ice cold phosphate buffered saline (PBS). Embryos were washed in phosphate buffered saline (PBS) and were photographed using a stereo microscope attached to a digital camera (Leica Microscope with an attached camera). The left hind-limb of each embryo was removed for genotyping. Embryos were then fixed in 4% Paraformaldehyde (PFA) (at 4ºC) overnight, or several nights depending on age at which they were dissected (Table 4).

2.2 Genotyping

In order to identify mutant embryos, DNA from embryos of all new litters was extracted and genotyped by polymerase chain reaction (PCR) to visualise and amplify target genomic regions.

2.2.1 DNA extraction

A hind limb from each embryo and ear clip from the adult mice were taken and digested in 200µl Proteinase K Buffer (0.1M EDTA pH 8.0, 0.2M Tris-HCl pH 8.5, 1% SDS, 1mg/ml Proteinase K). The digest was incubated at 52-55°C for 3 hours – overnight, until the tissue was digested for DNA extraction. After being cooled to room temperature, 100µl of 5M potassium acetate was added to the digested samples and the tubes were vigorously shaken to mix the contents, generating a thick white protein precipitate. The tubes were left for 15 minutes on ice and then were centrifuged (13,000 rpm, 10 mins, 4°C) to pellet the protein precipitate. The resulting supernatant was transferred to a fresh tube and 1000µl of 100% ice cold ethanol was added. The contents were mixed and placed at -20°C overnight or -80°C for 20 minutes. The tubes were centrifuged (13,000 rpm, 10 mins, 4°C) to pellet the precipitated DNA and the supernatant carefully discarded as not to disturb the DNA. The DNA pellet was washed in 200µl of 70% ethanol and then centrifuged (13,000 rpm, 5mins, 4°C), the supernatant discarded and the DNA left to air-dry for 5 minutes before re-suspending the DNA in 50µl of ddH_20 and stored at -20°C until required.

2.2.2 PCR

Subsequent to genomic DNA extraction, mouse and embryo genotypes were determined by PCR using conditions optimised for each primer set specific to different genes. All amplification reactions were conducted using the PROMEGA Go-Taq polymerase kit and PTC-200 (Sensoquest labcycler). Specific primers which adhere to and amplify the particular regions of interest are described in Table 2.3.

Table 2.3: Genotyping PCR Primers

Gene	Primer Name	Primer Sequence
Vangl2 Neo	Common for	CGATCCACAGATGGGGCCAG
	Common rev	CCACTGACATCTTGCCCACG
	Neo rev	CCACTCCCACTGTCCTTTCC
Vangl2 Flox	WT_F	CCGCTGGCTTTCCTGCTGCTG
	Common Reverse	TCCTCGCCATCCCACCCTCG
	Null/Delete F	TTGACCTCAGTGCAGCGCCC
Cre	Cre/F	GCATTACCGGTCGATGCAACGAGTGATGAG
	Cre/R	GAGTGAACGAACCTGGTCGAAATCAGTGCG
Loop-tail	CrpF	AGA ATC TGA CTT ACC CAT GGT
	CrpR	GAG GGA GAA GAA TTA TGT CTG
Wnt5a	GWnt5a_wtF	GAGGAGAAGCGCAGTCAATC
	GWnt5a_mutF	GCCAGAGGCCACTTGTGTAG
	GWnt5a_com	CATCTCAACAAGGGCCTCAT
Ror2	GR0r2_ext	CTGATGTTCATCCACATACATGTGGTG
	GRor2_neo	ATCGCCTTCTATCGCCTTCTTGACGAG
	GRor2_wild	CCTACTATAGACTCTGATCCTTCTGCC
Rac1	Rac1 Primer1	ATTTTGTGCCAAGGACAGTGACAAGCT
	Rac1 Primer2	GAAGGAGAAGAAGCTGACTCCCATC
	Rac1 Primer3	CAGCCACAGGCAATGACAGATGTTC
RockDN	GRhoAF	ACTCATCTCAGAAGAGGATCTG
	GRhoKR	TTCATTCAGTTCTTTCTGATATTTG

The DNA, primers, and other reagents necessary for DNA amplification (see below), were combined to a final volume of 20µl and subjected to rounds of heating and cooling to amplify a specific region of DNA (Table 2.4).

Table 2.4: Genotyping PCR conditions

(ul)	**Vangl2 Neo**	**New Vangl2 Flox**	**Cre**	**Lp**	**Wnt5a**	**Ror2**	**Rac1**	**ROCKDN**
Genomic DNA	2	2	2	2	2	2	2	2
Primer (10uM)	1+1+1 comF+R +Neo	1+1 (WT + ComR) OR 1+1 (Null + ComR)	2 +2	2+2	1+1+1	2+2+2	1+1+1	1+1
10mM dNTP	0.4	0.2	0.2	0.2	0.2	0.3	0.2	0.2
5x Go Taq Buffer	4	-	4	-	4	4		4
5x Go Taq Flexi Buf	-	4	-	4	-	-	4	-
MgCl2 (25 mM)	-	0.8	-	3.2	-	-	2	-
Taq (Promega)	0.2	0.1	0.1	0.1	0.1	0.1	0.1	0.1
ddH_2O	10.4	10.9	9.7	6.5	10.7	7.6	8.7	11.7
Total reaction	20	20	20	20	20	20	20	20
PCR condition	95:3m 95:30s 62:30s 72:30s 72:5m 4:∞	95 C 2 min, 95 C 30 sec, 67.5 C 30 sec Decrease temperature by 0.5 C every cycle. 72 C 30 sec Goto step 2 for 15 more cycles. 95 C 30 sec, 60 C 30 sec, 72 C 30 sec Goto step 6 for 19 more cycles. 72 C 10 min, 4 C Forever.	94:2m 94:15s 58:30s 72:1m 72:5m 4: ∞	94:4m 94:1m 58:1m 72:1m 72:10m 4:∞	94:3m 94:30s 60:1m 72:1m 72:10m 4:∞	95:10m 95:1m 63:1m 73:1m 73:10m 4:∞	94:4m 94:30s 62:30s 72:30s 72:10m 4:∞	94:4m 94:1m 58:1m 72:1m 72:10m 4:∞
Cycles	33		33	30	35	30	33	35
Gel	2%	2%	2%	5%	2%	1%	2%	2%
Size	Flox420 Neo350Wt280	560bp wt 701bp Flox 203bp Delete	~400bp	140bplp/lp 150bp+/+	400bp Mutant 484bp WT	1300bp + 1000bp -	Rac1 flox 333bp Rac1+ 300bp Rac1 del 175bp	482bp Mut

2.2.3 Gel electrophoresis

The PCR products were separated by gel electrophoresis. The percentage of agarose used is specified in Table 3. The agarose gel consisted of agarose (NBS Biologicals) in 100ml 1 X TAE (40mM Tris-acetate, 1mM EDTA (pH8.3)) buffer plus one drop ethidium bromide (2.5mg/ml). A 100bp ladder (PROMEGA) (5µl DNA ladder and 1µl loading dye) was loaded to use as a size marker and 10µl of PCR product for each sample was loaded. The gel underwent electrophoresis for approximately 30 minutes at 100 volts. Visualization of the gel then took place under the UV illuminator (UVP Geldoc IT) and a photograph taken for records using UVP software.

2.3 Histology

2.3.1 Processing

After fixation, the embryos were washed in PBS to remove traces of PFA and then dehydrated by placing in 50% ethanol, on an orbital rotator, at room temperature, and then twice in 70% ethanol, on an orbital rotator, at room temperature - the length of time was dependent on developmental stage of the embryos (Table 4). After these dehydration steps the embryos could be stored at room temperature in 70% ethanol until use.

2.3.2 Embedding

2.3.2.1 Wax embedding

Before the transgenic embryos were embedded they were put through a series of dehydration steps, at room temperature, to allow full penetration of the wax. For embedding, the embryos were dehydrated in 95% ethanol, two times in 100% ethanol and two times in Histoclear (VWR). These steps were carried out by placing the embryos in glass vials on an orbital rotator. Final steps consisted of treating the embryos with 50% Histoclear-paraffin wax (VWR) and three or four times with wax alone; temperature of wax being 65ºC. The time of incubating at

each step is dependent on the age of embryo (table 2.5). Finally embryos were embedded in paraffin wax in the desired orientation.

Table 2.5: Embedding Protocol

	E9.5	**E10.5**	**E13.5**	**E14.5**	**E15.5**
4% PFA at 4ºC	1 night	1 night	2 nights	2-3 nights	2-3 nights
50% EtOH	30 mins	30 mins	2 hours	3 hours	3 hours
70% EtOH x2	30 mins 30 mins	30 mins 30 mins	2 hours 2 hours	3 hours 3 hours	3 hours 3 hours
Can store embryos in 70% EtOH at room temperature					
95% EtOH	30 mins	30 mins	2 hours	3 hours	3 hours
100% EtOH x2	30 mins 30 mins	30 mins 1 hour	2 hours O/N	3 hours O/N	3 hours O/N
Histoclear x2	10 mins 10 mins	15 mins 15 mins	20 mins 20 mins	20 mins 20 mins	30 mins 30 mins
Histoclear / Wax Heat 60-65ºC	15 mins	20 mins	30 mins	1 hour	1 hour
Wax x3 / 4 Heat 60-65ºC	20 mins 20 mins 20 mins	30 mins 30 mins 30 mins	1 hour 1 hour 1 hour	1 hour 1 hour 1 hour	1 hour 1 hour 1 hour 1 hour

(O/N = Overnight)

2.3.2.2 Cryo-embedding

Dissected embryos were washed in PBS and kept on ice. The embryos were then passed through 7.5% sucrose (in PBS), (until they sank) and then in 15% sucrose (in PBS), (until they sank), on ice. Sucrose prevents ice crystal formation in the embryo. Lastly embryos were embedded in OCT (Cell Path) in plastic moulds and frozen on dry ice. Once embedded, embryos were stored at -80^{o}C until required.

2.3.3 Sectioning

2.3.3.1 Wax sectioning

Wax embedded embryos were serially sectioned in the transverse plane at 8 micrometers using a Leica RM2235 rotary microtome. The angle of the blade was set at 5^{o}. The sections were transferred onto Histobond adhesive glass slides (Marienfield) and were allowed to dry overnight at 37ºC.

2.3.3.2 Cryo-sectioning

Cryo-embedded sections were cut on a Microm GmbH (Type HM 560MV) cryostat. The temperature of the specimen was set at -19^{o}C and the temperature of the blade was set at -21°C, the angle of the blade was 11^{o} and the sections were taken at 10µm thickness. Sections were transferred on to Histobond adhesive glass slides and air dried. Slides were stored, wrapped in foil, at -80°C.

2.3.4 Haematoxylin and Eosin staining

Wax embedded tissue sections taken from transgenic embryos were analysed using haematoxylin and eosin (H&E) staining. This type of staining results in nuclei appearing blue/black; cytoplasm, varying shades of pink; muscle fibres, pink/red; red blood cells, orange/red and fibrin, deep pink.

The dried slides were stained using Haematoxylin (which stains the nuclei) and Eosin (which stains the cytoplasm) to observe the morphology of the heart. The slides were placed in histoclear (2x 10 minutes) to remove wax from the sections

and then dehydrated through a series of ethanol steps; of 100% (x2), 90%, 70% and 50% (% ethanol in ddH_20) and ddH_20, for 2 minutes each. The slides were then placed in Harris haematoxylin solution (Raymond A. Lamb) for 10 minutes. They were then placed under running tap water until tissues turned a purple-blue colour and then dipped five times in acid alcohol (1% HCl in 70% ethanol), which removed some of the haematoxylin, until sections turned red. They were then placed under running tap water again until the sections turned back to purple-blue. After these washing steps they were placed in 1% aqueous eosin (Raymond A. Lamb) for 5 minutes, then rinsed quickly in tap water. The slides were then dehydrated through a series of ethanol steps of 50%, 70%, 90% and 100% (x2) ethanol for 2 minutes each. Lastly, slides were placed in histoclear (2x 10 minutes) before mounting them using histomount (National Diagnostics) and placing glass coverslips (VWR) on top.

2.3.5 Elastin staining

Slides were placed in histoclear (2 x 10 minutes) to remove wax from the sections and then dehydrated through a series of ethanol; of 100% (x2), 90%, 70% and 50% (% ethanol in ddH_20) and ddH_20, for 2 minutes each. After 5 minutes equilibration in PBS, slides were placed in Miller's elastin stain (Raymond A. Lamb) for 1 hour. To remove excess of stain, slides were dipped in water and then kept in 3% ferric chloride for 10 minutes to aid binding of stain to elastin fibres. Slides were counterstained with eosin for 5 minutes. After gentle rinsing under ddH_20 to remove excess eosin, slides were dehydrated in 100% ethanol and incubated in histoclear for two 10 minute cycles and mounted with histomount and dried overnight.

2.3.6 Photographs

After staining, slides were photographed using Ziess Axioplan microscope and associated software.

2.4 Slide Immunohistochemistry

2.4.1 Immunohistochemistry DAB

Slides were de-waxed with histoclear for 10 minutes (x2) and rehydrated through a series of ethanol washes (100% for 5 minutes two times, 90%, 70% and 50% ethanol for 2 minutes each) and equilibrate for 5 minutes in PBS. Antigen retrieval was done by putting the slides in citrate buffer in the microwave on high power for 10 minutes then allowed to cool at room temperature for 5 minutes, before transfer into cool ddH_20 for 10 minutes at room temperature. Slides were placed in 0.6% H_20_2 (VWR) for 5 minutes to block endogenous peroxidase activity and bleach the slide clearing the background. Following a rinse in ddH_20, the sections were washed 3 times for 5 minutes in TBS-Tx (TBS containing 0.1% Triton X-100) (Amresco), and were blocked in TBS-Tx containing 10% FCS (fetal calf serum) for 30 minutes. The slides were laid out in a humid chamber and 100µl of primary antibody added to each at the concentrations (table 2.5). Parafilm coverslips were placed over the slides to prevent evaporation and to ensure complete coverage. Slides were left overnight at 4°C. Next day the slides were washed 3 times for 5 minutes in TBS-Tx to remove any unbound antibody. They were transferred back into the humid chamber and 100 µl of the appropriate biotinylated secondary antibody (diluted in TBS-Tx containing 2% FCS) were added (Table 6). The slides, covered with parafilm coverslips, were left for 90 minutes at room temperature, and were then washed three times in TBS-Tx for 5 minutes each. Avidin-biotin complex conjugated to horseradish peroxidase (AB Complex: Vector labs) was made up according to the manufacturer's instructions and added to the slides for 30 minutes at room temperature. The slides were rinsed 3 times in TBS-Tx for 5 minutes each, and were then placed on aluminium foil. Diaminobenzidine solution (DAB: Sigma), made according to the manufacturer's instructions, was added for up to 20 minutes until brown staining was observed, then the slides were placed in PBS to stop the reaction. Slides were rinsed in ddH_2O and counterstained in 0.5 % methyl green (Sigma) for 10 minutes. Excess stain was removed in ddH_2O, and the sections were dehydrated in three 100% butanol washes. After 2 times for 10 minutes treatments in histoclear, slides were mounted with histomount and glass coverslips and left

over night for drying. After staining, slides were photographed using Ziess Axioplan microscope and associated software.

To ensure that no non-specific staining had occurred, slides as negative control were made, which were not incubated with primary antibody but secondary antibody was applied as normal and handled under the same conditions as other slides.

2.4.2 Immunofluorescence

2.4.2.1 Immunofluorescence on wax sections

Slides were de-waxed with histoclear for 10 minutes (x2) and rehydrated through a series of ethanol washes (100% for 5 minutes two times, 90%, 70% and 50% ethanol for 2 minutes each) and equilibrate for 5 minutes in PBS. Antigen retrieval was done by putting the slides in citrate buffer in the microwave on high power for 10 minutes then allowed to cool at room temperature for 5 minutes, before transfer into cool ddH_20 for 10 minutes at room temperature. Following a rinse in ddH_20, the sections were given 2 times 5 minutes washes in PBS. The sections were placed in PBS/0.5% Triton-X100 for 10 min, which make cells permeable, allowing the antibody access to the proteins within the cell. Two washes were then carried out in PBS, each for 5 minutes. Sections were then placed for 30 min in PBS/10% FCS to block any non-specific sites and then primary antibody was added. The primary antibody was diluted in PBS/2% FCS (the dilutions are antibody specific, Table 5). Of this, 100ul was pipetted on to each slide and covered with a parafilm coverslip and the slides were placed in a humidified chamber (tray with lid and wet blue roll) and incubated overnight at 4^oC. On the second day, the parafilm coverslips were carefully removed and slides were washed twice in PBS for 5 minutes each to remove the extra primary antibody and then put in PBS/10% FCS for 10 min as a second block step. The secondary antibody was diluted in PBS/2% FCS (Table 6) and pipetted onto the slides and left for 1-2 hours covered in foil to ensure complete darkness. To remove excess secondary antibody, two PBS washes were given for 5mins each and then slides were mounted in Vectashield with DAPI (Vector), which stains the nuclei, and observed under the Axio imager fluorescent microscope when the

vectashield was set. The slides were stored at 4^{o}C, in complete darkness to preserve the fluorescence.

To ensure that no non-specific staining had occurred, slides as negative control were made, which were not incubated with primary antibody but secondary antibody was applied as normal and handled under the same conditions as other slides.

2.4.2.2 Immunofluorescence on cryosections

Sections were equilibrated at room temperature, and fixed in 4% PFA (Sigma) for 10 minutes and then washed in PBS twice for 5minutes. For 10 minutes, the sections were placed in PBS/0.5% Triton-X100, which make cells permeable, allowing the antibody access to the proteins within the cell. Two washes were then carried out in PBS, each for 5 minutes. Sections were then blocked by placing in PBS/10% Fetal Calf Serum (FCS) for 30 minutes, after which the primary antibody was added. Primary antibody was diluted in PBS/2% FCS (the dilutions are antibody specific, table 2.6). Of this, 100ul was pipetted on to each slide and covered with a parafilm coverslip and the slides were placed in a humidified chamber (tray with lid and wet blue roll) and incubated overnight at 4^{o}C. On the second day, the parafilm coverslips were carefully removed and slides were washed twice in PBS for 5minutes each to remove the excess primary antibody and then put in PBS/10% FCS for 10 minutes as a second blocking step. The secondary antibody was diluted in PBS/2% FCS (Table 2.7) and pipetted onto the slides and left for 1-2 hours covered in foil to ensure complete darkness. To remove excess secondary antibody, two PBS washes were given for 5mins each and then slides were mounted in Vectashield with DAPI, which stains the nuclei and observed under the Axio imager fluorescent microscope when the vectashield was set. The slides were stored at 4^{o}C, in complete darkness to preserve the fluorescence.

To ensure that no non-specific staining had occurred, slides as negative control were made, which were not incubated with primary antibody but secondary antibody was applied as normal and handled under the same conditions as other slides.

Table 2.6: Primary Antibodies for Immunohistochemistry

Primary Antibody	Dilution
Vangl2 (in rabbit)	1/200
Chicken polyclonal anti-GFP Ab Abcam (13970)	1/100
Isl1 (in mouse) (Hybridoma Cell Bank)	1/5
Purified Mouse anti-N-Cadherin IgG1 BD Biosciences (Cat: 610920)	1/50
Purified Mouse anti-E-Cadherin IgG2a BD Biosciences (Cat: 610181)	1/50
Purified Mouse anti- β-Catenin IgG1 BD Biosciences (Cat: 610154)	1/50
Rabbit Polyclonal anti-PKCζ (C-20) Santa Cruz Biotechnology (sc-216)	1/200
Rabbit anti-Laminin Sigma-Aldrich (L9393)	1/25
Mouse monoclonal anti- Firbonectin IgG1 (EP5) Santa Cruz Biotechnology (SC 8422)	1/50
Monoclonal anti-Vinculin, produced in mouse (Clone hVIN-1, ascites fluid) Sigma (V9131)	1/100
Monoclonal anti-γ-Tubulin, produced in mouse Sigma (T6557)	1/200
Purified monoclonal Mouse anti-GM130 BD Biosciences (Cat: 610822)	1/100
Rabbit polyclonal anti-Dishevelled 2 Enzo Lifesciences (BML DA4270)	1.50
Celsr1	1/400
MF20	Undiluted (Hybridoma)

Primary Antibody	Dilution
Mouse monoclonal anti-actin, α Smooth Muscle Sigma-Aldrich (A5228)	1/300
Rat monoclonal anti-Endomucin IgG2a Santa Cruz (SC 65495)	1/50

Table 2.7: Secondary Antibodies for Immunohistochemistry

Secondary Antibody	Dilution
594 Donkey Anti-rabbit IgG (H+L) (ALEXA FLUOR)	1 in 200
488 Goat Anti-chicken IgG (H+L) (ALEXA FLUOR)	1 in 200
488 Donkey Anti-mouse IgG (H+L) (ALEXA FLUOR)	1 in 200
488 Goat Anti-mouse IgG_1 (γ_1) (ALEXA FLUOR)	1 in 200
488 Donkey Anti-rabbit IgG (H+L) (ALEXA FLUOR)	1 in 200
594 Donkey Anti-mouse IgG (H+L) (ALEXA FLUOR)	1 in 200
568 Goat Anti-rat IgG (H+L) (ALEXA FLUOR)	1 in 200

2.5 Recombination efficiency of *Cre* line

2.5.1 RNA extraction

Frozen tissue samples (not fixed) from embryos were homogenized by passing through fine needles in 1ml TRIzol reagent (Life Tecnologies), which is used to break the cells. Homogenized sample was incubated at room temperature for 5 minutes and then mixed with 200µl chloroform (Sigma), which dissolves the fat and layers out everything. Tube was vigorously shaken for 15 seconds and then incubated at room temperature for 2-3 minutes. Samples were then centrifuged at 12,000rpm at 4°C for 15 minutes; separating the solution into lower red phenol-chloroform organic phase, an interphase with white precipitated DNA, and a colourless upper aqueous phase. The aqueous phase was transferred to a new tube and precipitated with 500µl isopropanol (for cleaning and removing trizol and chloroform) and incubated for 10minutes at room temperature before centrifuging at 12000 rpm for 10 minutes at 4°C. The supernatant was discarded after centrifugation and the RNA pellet was washed with 75% DEPC-ethanol at 7500 rpm for 5 minutes at 4°C. After brief air drying, the RNA pellet was dissolved in RNase-free DEPC-H_2O and stored -80°C until use. Concentration of RNA was check using Nanodrop (ND 800 Labtech International).

2.5.2 cDNA synthesis

RNA synthesised was treated with DNAase before using it to make cDNA, to remove all traces of DNA. For 1µg RNA, 2µl buffer and 2µl DNAase buffer (Ambion) was used with ddH20 to make a solution mix of total 20µl. This mix was incubated at 37°C for 10 minutes. Then 2µl EDTA was added to the mix to remove Ca^{2+} ions which stops DNAase from working. The mix was incubated at 65°C for 5 minutes. EDTA deactivates DNAase and 65°C denatures whatever traces of DNAase are left. RNA procured after this was DNA free and was used to synthesise cDNA.

Applied Bioscience High Capacity cDNA Kit was used for cDNA synthesis. The RNA (DNAase treated), random primers, and other reagents necessary for cDNA

synthesis (see below), were combined to a final volume of 40µl and subjected to rounds of heating and cooling (table 2.8)

Table 2.8: cDNA synthesis conditions

Amount in (ul)	
RNA	20
Random Primer (10uM)	4
10mM dNTP	1.6
Buffer	4
Reverse Transcriptase	2
RNAase Inhibitor	2
DEPC H_2O	6.4
Total reaction	40
Condition	25:10m 37:120 m 85:5m 4:∞

2.5.3 RT-PCR

The generated cDNA from 1µg of total RNA was used for RT-PCR (Reverse transcriptase PCR) for gene amplification. All amplification reactions were conducted using the PROMEGA Go-Taq polymerase kit and PTC-200 (Sensoquest labcycler). Specific primers which adhere to and amplify the particular regions of interest are described in table 2.9.

Table 2.9: RT-PCR primers

Gene	Primer Name	Primer Sequence
Vangl2	Forward primer	TGAGGGCCTCTTCATCTCC
	Reverse primer	ACCAATAACTCCACGGG
Beta Actin	Actb-fw	CCCGCGAGCACAGCTTCTTTG
	Actb-rev	CGACCAGCGCAGCGATATCGT

The cDNA, primers, and other reagents necessary for cDNA amplification (table 2.9), were combined to a final volume of 20µl and subjected to rounds of heating and cooling to amplify a specific region of cDNA (Table 2.10).

Table 2.10: RT-PCR conditions

(ul)	**Vangl2**	**β-Actin**
cDNA	5	2
Primer(10uM)	0.1 + 0.1	0.5 + 0.5
10mM dNTP	0.2	0.5
5x Go Taq Buffer	4	4
Taq (Promega)	0.1	0.2
ddH_2O	10.5	12.3
Total reaction	20	20
PCR condition	94:2m 94:1m 58:1m 72:1m 72:10m 4: ∞	94:2m 94:30s 58:40s 72:40s 72:10m 4: ∞
Cycles	33	35
Gel	2%	2%
Size	535bp	90bp

2.6 Protein analysis

2.6.1 Western blotting

Frozen tissue samples (not fixed) from embryos were lysed with 500µl 1X laemmli buffer (2% SDS, 5% BME (Betamercaptoethanol), 10% Glycerol, 0.05%w/v Bromophenol blue, 0.0625M Tris HCL pH 6.8; made solution without BME and added BME just before use), by homogenizing passing through fine needles. Samples were heated at 95°C for 5 minutes to break open the protein tertiary structure and then centrifuged at full speed for 5 minutes. Finally samples were cooled at room temperature for 5 minutes and were ready to use. At this point samples can be stored at -20°C.

Once the samples were ready, they were run on premade gel (Bio-Rad) at 90V for initial few minutes till the samples cross the stacking gel passing into resolving gel. Then the gel was run at 180V for 30-35 minutes in the running buffer (2.5mM Tris pH 8, 19mM Glycine, 0.01% SDS). While the samples are running on the gel, membrane preparation was done by treating membrane and four blotting papers with methanol for 30 seconds and then in distilled water for 5 minutes. After that the membrane and four blotting papers along with 2 sponges were transferred to ice cold transfer buffer (48Mm Tris pH 8, 39mM Glycine, 0.04% SDS, 20% Methanol) for 20 minutes. Once the gel was fully run and the dye front of the samples reached the bottom of the gel, the gel was taken out and it was sandwiched with the membrane (sponge/2 blotting paper/gel/membrane/2 blotting paper/sponge) and run at 100V for 1 hour at 4°C with transfer buffer. The gel was positioned towards the negative side and membrane towards positive. After the bands (of protein ladder) have completely transferred on the membrane, the membrane was stained with Ponceau stain to check for presence of protein bands in the samples. The membrane was put in methanol for 30 seconds, then in Ponceau stain for 5 minutes and then in 5% Acetic acid (x2) to remove the background staining so that band become visible. Then the membrane was rinsed in TBST (TBS, 0.1% Tween 20; TBS – 2.423%w/v Trizma Hydrochloride, 8.006%w/v Sodium Chloride at pH 7.6) a few times to remove Ponceau. The membrane was then blocked in 5%milk/TBST at room temperature for 1 hour on a shaker, after which primary antibody (Vangl2; table 2.10) was added and

incubated overnight on a roller at 4°C. The next day, membrane was washed in 5%milk/TBST for 10 minutes (x4) to remove excess primary antibody and then incubated with secondary antibody (table 2.10) for 1 hour at room temperature. Membrane was then washed in 5%milk-TBST for 10 minutes (x4) and then in TBST for 10 minutes (x4) to remove excess antibody. During the washes, the developer was turned on 30 minutes before use and chemilluminescence substrate was prepared (1 ml A + 1 ml B). Membrane was then incubated with the substrate in the dark room for 5 minutes and developed using developing films.

The same membrane was stripped and then reprobed to check if equal amount of protein was loaded for control and mutant. Membrane was washed in stripping buffer (1.5%w/v Glycine, 0.1%w/v SDS, 1% Tween 20, with pH set at 2.2) two times for 10 minutes each. Then two times in PBS for 10 minutes each and finally in TBST for 2 x 5 minutes washes. After these washes membrane was again blocked in 5%milk/TBST at room temperature for 1 hour on a shaker, and then primary antibody (alpha-actin, GAPDH; table 2.10) was added and incubated overnight on a roller at 4°C. The next day, membrane was washed in 5%milk/TBST for 10 minutes (x4) to remove excess primary antibody and then incubated with secondary antibody (table 2.10) for 1 hour at room temperature. Membrane was then washed again in 5%milk-TBST for 10 minutes (x4) and then in TBST for 10 minutes (x4) to remove excess antibody. During the washes, the developer was turned on 30 minutes before use and chemilluminescence substrate was prepared (1 ml A + 1 ml B). Membrane was then incubated with the substrate in the dark room for 5 minutes and developed using developing films.

Table 2.10: Antibodies for western blotting

Primary Antibodies (in 5%milk/TBST)		**Secondary Antibodies (in 5%milk/TBST)**	
Antibody	**Dilution**	**Antibody**	**Dilution**
Vangl2	1/2500	Polyclonal swine anti-rabbit immunoglobulins/HRP	1/2500
GAPDH	1/25000	Polyclonal swine anti-rabbit immunoglobulins/HRP	1/10000
Alpha-Actin	1/1000	Polyclonal goat anti-mouse immunoglobulins/HRP	1/3000

Chapter 3

Characterization of *Vangl2*^{flox} mouse and establishing the tissue that requires *Vangl2* for normal heart development

3.1 Introduction

To understand the role *Vangl2* plays in embryonic development a lot of work has been done on loop-tail mice (*Lp*), which is a naturally occurring mutant and has *Vangl2* mutated in all body cells (Strong and Hollander, 1949). *Lp/Lp* mice suffer from neural tube defects, along with cardiac defects (Henderson *et al.,* 2001). However, because Vangl2 expression is disrupted in all body cells of *Lp* mice, it is not possible to tell unequivocally which cell types require Vangl2 and are crucial during heart development. Looking at the cardiac defects present in *Lp* mice, primarily the outflow tract is affected. The main cell types involved in development of the outflow tract are NCC (Hutson and Kirby, 2007) and cells derived from the SHF (Buckingham *et al.,* 2005). Therefore, my main focus was to genetically dissect the role of Vangl2 specifically in NCC and SHF cells, for which a new *Vangl2*^{flox} line was used.

The classical approach to study the function of a gene using mouse models is to analyse the effect of loss of function by deleting the expression of the gene in every cell or a particular cell type. This approach was applied to look at the role the PCP gene *Vangl2* is playing during heart development. A gene can be targeted specifically using gene targeting technology in embryonic stem (ES) cells (Müller, 1999; Prosser and Rastan, 2003). Using this approach, a DNA construct containing the gene of interest (or a portion of the gene) and a marker, such as a *neomycin (neoR)* cassette, is transfected into ES cells (Prosser and Rastan, 2003). The latter allows selection of cells successfully transfected with the targeted construct. However, the presence of the *neoR* resistance expression cassette can actually affect the level of expression and hence the function of the gene of interest and create a hypomorph (Meyers *et al.*, 1998; Kist *et al.*, 2007). Any mutation or change in the genetic makeup can lead to a change in gene expression.

Hermann J. Muller classified such mutations as amorph and hypomorph. He termed hypomorphic mutants as 'lesser-normal'; therefore when gene function is reduced but not absent compared with the normal wild type level. In contrast, amorph is when the mutation results in complete loss of functional expression of the gene (Muller, 1932). For example, *Fgf8neo* and *Pax9neo* homozygotes have defects because of reduction in functional gene expression due to presence of the neo cassette (Meyers *et al.*, 1998; Kist *et al.*, 2007). It has also been reported that the neo cassette has cryptic splice sites which can be responsible for interfering with the gene expression (Jacks *et al.*, 1994; Carmeliet *et al.*, 1996). During normal gene expression, the mRNA is transcribed from the endogenous DNA sequence, and subsequently the functional protein is translated. Introns are removed through a process of splicing, allowing the correct exon to be joined together. However, the presence of cryptic splice sites within the *neoR* cassette can interfere with this process as it can cause aberrant splicing, hence altering the gene sequence and hence gene expression.

To decipher the role of Vangl2 in specific cell types, a floxed line was produced which would remove exon 4 from the sequence of *Vangl2* gene. Exon 4 encodes the trans-membrane domains of Vangl2 and removing this exon results in a frame shift and stop codon which result in the formation of a non-functional and truncated protein. The gene sequence was altered by a process of recombination, mediated by the site-specific DNA recombinase sequences, *Cre* and *FLP*. The targeted region of the gene was engineered to be flanked by *loxP* and *FRT* sites, and these sequences are identified by *Cre* or *FLP*, respectively (Meyers *et al.*, 1998). *LoxP* sites are inserted on either side of the gene of interest (or exons within a gene). The *Cre* enzyme recognizes these sequences and recombines the DNA between those two points, leaving one *loxP* site. Similarly, the *neoR* cassette can be removed by inserting *FRT* sites on either side and using *FLP* to identify those sites and allowing recombination between the two *FRT* sites, hence removing the *neoR* cassette.

The first aim of this chapter was to establish whether the new $Vangl2^{flox}$ line that had been produced recapitulated the *Lp* phenotype, which is a functional null mutant of Vangl2. Having established that the $Vangl2^{flox}$ line behaved as expected,

we wanted to reveal the requirement for the Vangl2 specifically in SHF and NCC, and to establish how loss of Vangl2 function in these cell types impacts on morphogenesis of the cardiac outflow tract.

3.2 Results

3.2.1 Construction of *Vangl2*^{floxneo} mice

Vangl2^{floxneo} mice were created by Ozgene (Australia) for the Henderson lab by inserting *loxP* sites on either side of exon 4 of the *Vangl2* gene (containing the transmembrane domains, required for Vangl2 activity) and *neoR* cassette, by homologous recombination in ES cells (figure 3.1). *NeoR* cassette allows selection of cells successfully transfected with the targeted construct, and was flanked by *FRT* sites so it could be deleted.

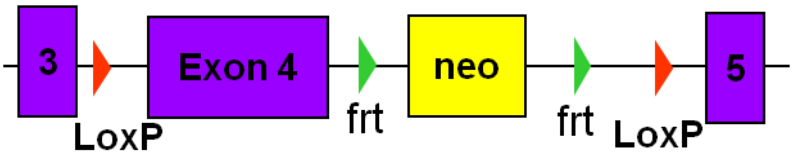

Figure 3.1: *Vangl2*^{floxneo} construct

Exon 4 of *Vangl2* gene (containing the transmembrane domains, required for Vangl2 activity) flanked by l*oxP* sites on both side and *neoR* cassette downstream to it with *FRT* sites on either sites for recombination.

3.2.1.1 Vangl2^{floxneo} *is hypomorphic allele of Vangl2*

Previous studies have shown that the *neoR* cassette can be responsible for creating a hypomorph (Meyers *et al.*, 1998; Kist *et al.*, 2007), so it was checked if the presence of neo cassette in our construct was also giving a similar result, creating a hypomorph with reduced level of functional expression of Vangl2.

To confirm this, crosses were set up between *Vangl2*$^{floxneo/+}$ parents (figure 3.2b) and 2 litters were collected at embryonic day (E) 14.5. Mendelian ratios of

expected genotypes were obtained from total 12 embryos (25% *Vangl2*$^{+/+}$, 50% *Vangl2*$^{floxneo/+}$, 25% *Vangl2*$^{floxneo/floxneo}$) (figure 3.2c). To compare the *Vangl2*^{floxneo} phenotype with *Lp* phenotype, crosses were also set up between *Lp*/+ parents and 2 litters were dissected out at E14.5, which also showed Mendelian percentage of embryo genotypes from total 16 embryos (25% *Lp*+/+, 50% *Lp*/+, 25% *Lp/Lp*). Phenotypic analysis showed open neural tube, suggesting mutation and loss of Vangl2 function, however genotypes were confirmed using specific primers for both crosses.

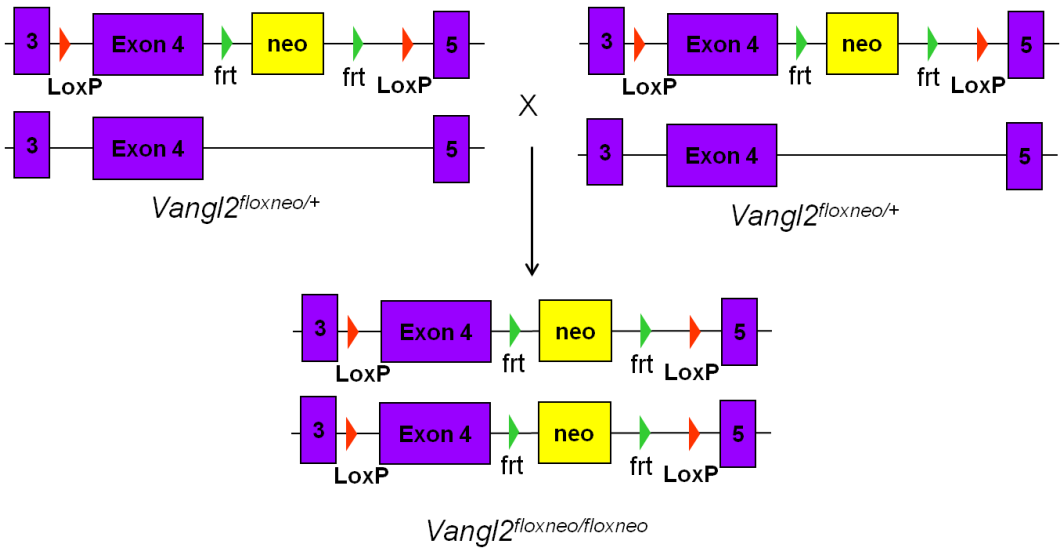

Figure 3.2: *Vangl2*^{floxneo} cross

Cross between *Vangl2*$^{floxneo/+}$ parents with *neoR* present on one allele and other allele being wild type, giving *Vangl2*$^{floxneo/floxneo}$.

The presence of the *neoR* cassette on both of the alleles; *Vangl2*$^{floxneo/floxneo}$; homozygous embryos, resulted in the neural tube defect (NTD) craniorachischisis (figure 3.3f arrows showing open brain and spinal cord, and arrowhead showing looped tail because of delay in closure of posterior neuropore (Copp *et al.*, 1994)) (2/12 embryos; table 3.1). This is identical to the NTD defects seen in *Lp/Lp* embryos (figure 3.3e, g) (4/16 embryos; table 3.1). One *Lp/Lp* embryo also showed gastroschisis, which is very unusual (figure 3.3g with arrow pointing at open body line resulting in protrusion of abdominal contents). Gastrochisis was not seen in *Vangl2*$^{floxneo/floxneo}$ embryos. But presence of *neoR* cassette on both alleles not only gives craniorachischisis but a variable external phenotype was also observed; where in 1 embryo the neural tube was open only at the posterior trunk, known as spina bifida (figure 3.3h arrows showing closed brain and spinal cord, and arrowhead showing failure in closure of posterior trunk region). In heterozygous embryos, the presence of *neoR* cassette on one allele (*Vangl2*$^{floxneo/+}$), had no effect as these embryos were phenotypically normal (figure 3.3d) (6/12 embryos; table 3.1). In *Lp* mice the heterozygous embryos and adult mice (*Lp/+*) had a looped tail (figure 3.3c) (8/16 embryos; table 3.1), however this phenotype was not seen in our *Vangl2*$^{floxneo/+}$embryos (figure 3.3d arrowhead showing normal tail) or adult mice. As delayed closure of posterior neuropore in Lp/+ leads to looped tail (Copp *et al.*, 1994), the results suggest that there is no delay in neural tube closure when *neoR* cassette is present on only one allele in *Vangl2*$^{floxneo/+}$. Table 3.1 summarizes the external phenotypic defects observed in *Lp/Lp* and *Vangl2*$^{floxneo/floxneo}$ embryos.

Table 3.1: External phenotypic defects seen in *Lp/Lp* and *Vangl2*$^{floxneo/floxneo}$ mutants at E14.5

Genotype	Number of embryos	Looped tail	Craniorachischisis	Spina bifida	Gastroschisis
Lp/+	8/16	8	0	0	0
Lp/Lp	4/16	4	4	0	1
Vangl2$^{floxneo/+}$	6/12	0	0	0	0
Vangl2$^{floxneo/floxneo}$	3/12	3	2	1	0

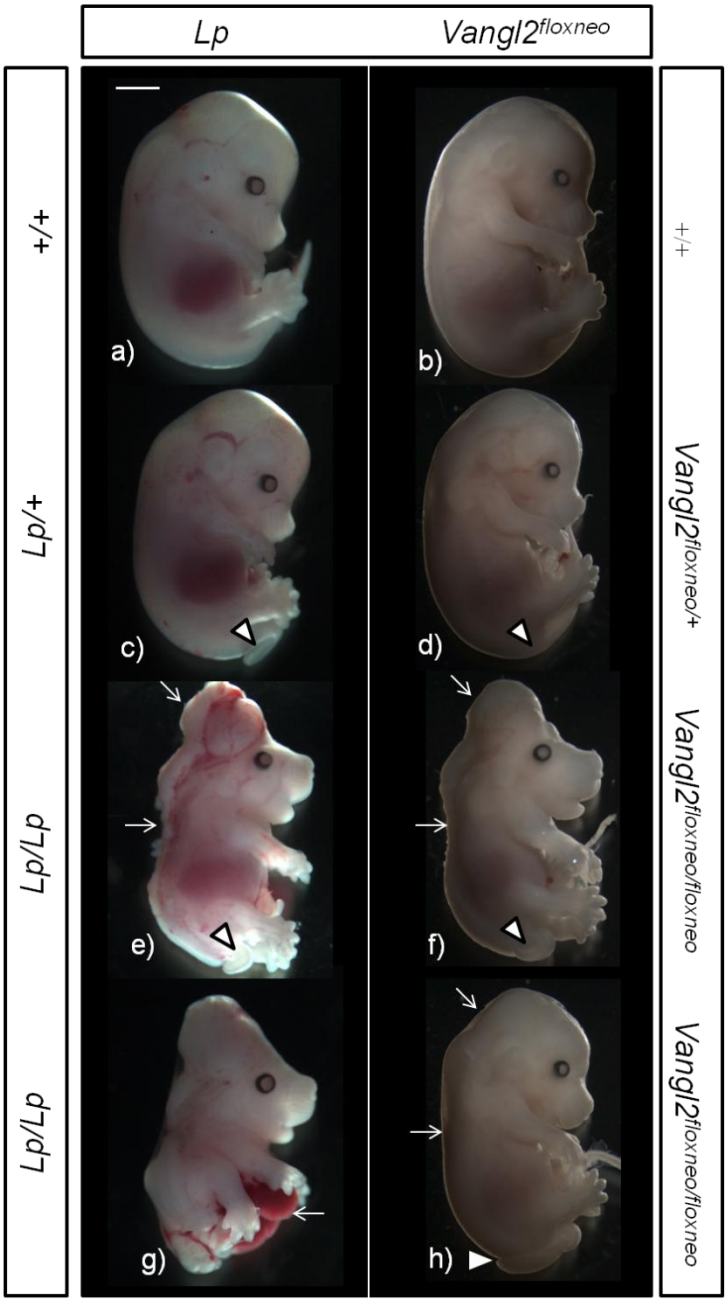

Figure 3.3: External phenotypic defects in *Lp* and *Vangl2*^{floxneo} hypomorphic embryos at E14.5

Whole mount embryos from *Lp*/+ x *Lp*/+ cross and *Vangl2*$^{floxneo/+}$x *Vangl2*$^{floxneo/+}$ litter. **a, b)** +/+ embryos for both the crosses with normal external phenotype. **c, d)** *Lp*/+ embryo showing a looped tail (arrowhead) and *Vangl2*$^{floxneo/+}$embryo with normal external phenotype (c; arrowhead showing no loop in tail). **e, f)** *Lp/Lp* (e) and *Vangl2*$^{floxeo/floxneo}$ (f) phenotype with craniorachischisis (arrows pointing at open neural tube and arrowhead showing looped tail). **g, h)** *Lp/Lp* embryo with gastrochisis (g; arrow pointing at protruding liver) and *Vangl2*$^{floxneo/floxneo}$ embryo showing external phenotypic defect, spina bifida (h; arrows showing closed neural tube and arrowhead showing at opening at the posterior region). Scale – 2000µm.

3.2.1.2 Cardiac defects in Lp and Vangl2^{floxneo} embryos

Lp and *Vangl2*^{floxneo} embryos were embedded in wax and transverse sections were taken (figure 4i shows the plane of section through the embryo) and hematoxylin and eosin (H&E) staining was carried out to look at the morphology of the heart. Heart sections of *Lp/Lp* embryos showed spectrum of cardiac defects (table in figure 3.4) which has been previously reported (Henderson *et al.*, 2001). *Lp/Lp* embryos had double outlet right ventricle (figure 3.4c), aortic arch defect retroesophageal subclavian artery (figure 3.4e) and ventricular septal defect (figure 3.4g). *Vangl2*$^{floxneo/floxneo}$ homozygote embryos after analysis of the heart sections also showed the same cardiac defect as *Lp/Lp* (table in figure 3.4). They had double outlet right ventricle (figure 3.4d) with the aorta incorrectly connected to the right ventricle instead of left ventricle; retroesophageal subclavian artery (figure 3.4e), with subclavian artery forms a ring around the oesophagus which would result in its constriction; and ventricular septal defect (figure 3.4h), which would result in mixing of oxygenated and deoxygenated blood. The *Vangl2*$^{floxneo/floxneo}$ embryo which did not show craniorachischisis and had only spina bifida present also had double outlet right ventricle (figure 3.4h), which suggests that cardiac defects are not secondary to craniorachischisis. Presence of a *neoR* cassette on only one allele (*Vangl2*$^{floxneo/+}$) resulted in normal external phenotype and a normal heart (figure 3.4b) meaning that the *Vangl2* gene is not haploinsufficient.

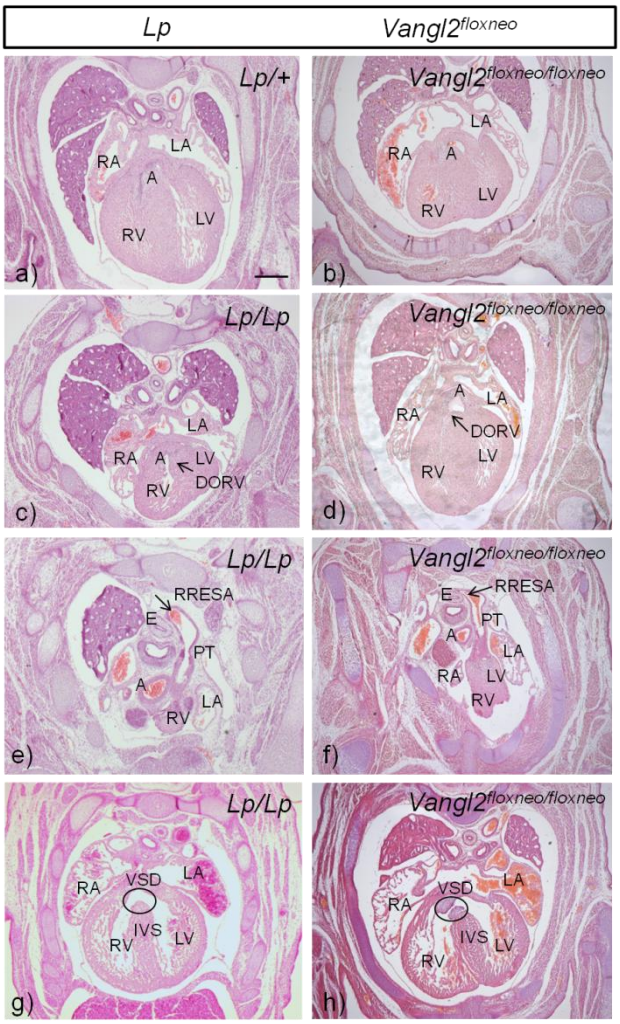

Cardiac defects	Lp/Lp (n=4)	*Vangl2*$^{floxneo/floxneo}$ (n=3)
DORV	4 (100%)	3 (100%)
VSD	4 (100%)	3 (100%)
RRESA	2 (50%)	1 (33.3%)

Figure 3.4: Cardiovascular defects in *Lp* and *Vangl2*^{floxneo} hypomorphic embryos at E14.5

Transverse sections of heart from *Lp/+* x *Lp/+* and *Vangl2*$^{floxneo/+}$ x *Vangl2*$^{floxneo/+}$ litter. **a,b)** Transverse section through heart of *Lp/+* (a) and *Vangl2*$^{floxneo/+}$ (b) embryo showing normal heart development. **c-h)** *Lp/Lp* and *Vangl2*$^{floxneo/floxneo}$ embryo with double outlet right ventricle (c,d; arrow pointing at aorta coming from right ventricle instead of left ventricle as seen in *Lp/+* and *Vangl2*$^{floxneo/+}$embryo), retroesophageal subclavian artery (e,f; arrow), and ventricular septal defect (g,h; circle). **i)** Plane of the section. Table shows different defects seen in *Lp/Lp* and *Vangl2*$^{floxneo/floxneo}$ embryos. RA-right atria, LA-left atria, RV-right ventricle, LV-left ventricle, A-aorta, PT-pulmonary trunk, RRESA-retroesophageal subclavian artery, DORV-double outlet right ventricle, VSD-ventricular septal defect, E-esophagus, IVS-interventricular septum. Scale - 20µm.

The similarities and differences between *Lp* and *Vangl2*^{floxneo} embryos are summarized in table 3.2, which is suggestive that *Vangl2*^{floxneo} is a hypomorph.

Table 3.2: Comparison between *Lp* and *Vangl2*^{floxneo} phenotype.

Similarities/Differences		***Lp***	***Vangl2*^{floxneo}**
External Phenotype	Tail	*Lp/+* have a looped/kinked tail	*Vangl2*$^{floxneo/+}$ have a normal tail
	Neural Tube	*Lp/Lp* have neural tube completely open (CRN)	*Vangl2*$^{floxneo/floxneo}$ have neural tube open but in variation, from completely open (CRN) to just in the posterior region (Spina bifida)
Cardiac Defects		*Lp/Lp* have cardiovascular defects (double outlet right ventricle, ventricular septal defect, aortic arch defects)	*Vangl2*$^{floxneo/floxneo}$ have cardiovascular defects (double outlet right ventricle, ventricular septal defect, aortic arch defects)

3.2.2 Construction of *Vangl2*^{flox} line (removal of *neoR* cassette)

After establishing that *Vangl2*^{floxneo} is likely to be a hypomorphic allele of *Vangl2*, it was essential to remove *neoR* cassette from the construct and generate *Vangl2*^{flox} line for further experiments to eliminate any effect presence of *neoR* could cause. *NeoR* construct was flanked by *FRT* sites and was removed by causing recombination at the *FRT* sites by crossing *Vangl2*^{floxneo} mice with *FLPe* mice (Henrich *et al.*, 2000) to give rise to *Vangl2*^{flox} mice (figure 3.5).

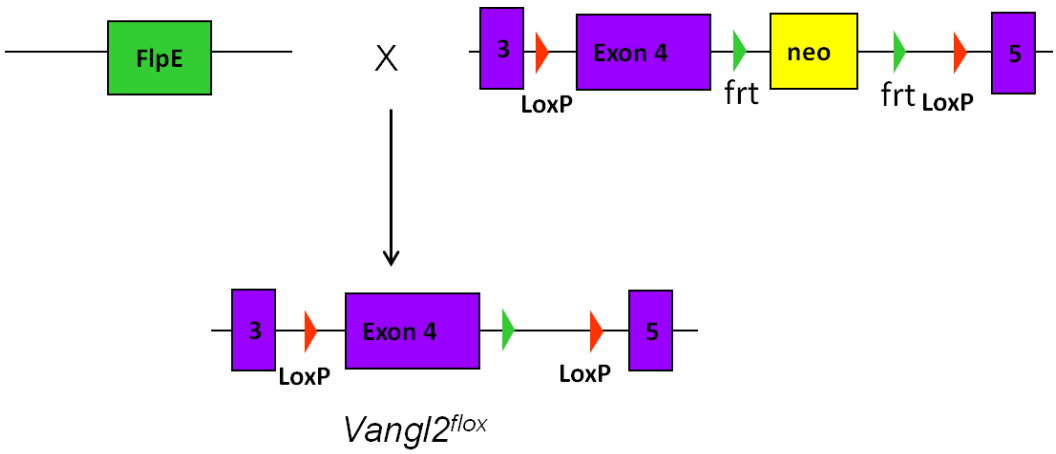

Figure 3.5: *Vangl2*^{flox} line

Cross between *FLPe* mice and *Vangl2*^{floxneo} to remove *neoR* cassette from the construct by recombination at *FRT* sites, giving the new *Vangl2*^{flox} line.

The *Vangl2*^{flox} mice produced were then inter-crossed with mice carrying a floxed enhanced yellow fluorescent protein sequence (*ROSA-Stop-eYFP*) (Srinivas *et al.*, 2001) so that when different *Cre* lines are crossed with the *Vangl2*^{flox} line, the *Cre*, as well as removing exon 4 of *Vangl2* would also result in the expression of this enhanced yellow fluorescent protein (eYFP). Once *Vangl2*^{flox} line had *eYFP* sequence in it, it was crossed with different *Cre* lines to drive *Cre* expression in different cell types to produce a *Vangl2*$^{flox/+}$*;Cre* males, which would have Vangl2 expression on one allele. These *Vangl2*$^{flox/+}$*;Cre* males were crossed with *Vangl2*$^{flox/flox}$ females for the further experiments (Figure 3.6). Recombination due to the activity of the enzyme *Cre* deletes exon 4, creates a frame shift and a stop codon that truncates the protein at amino acid 78.

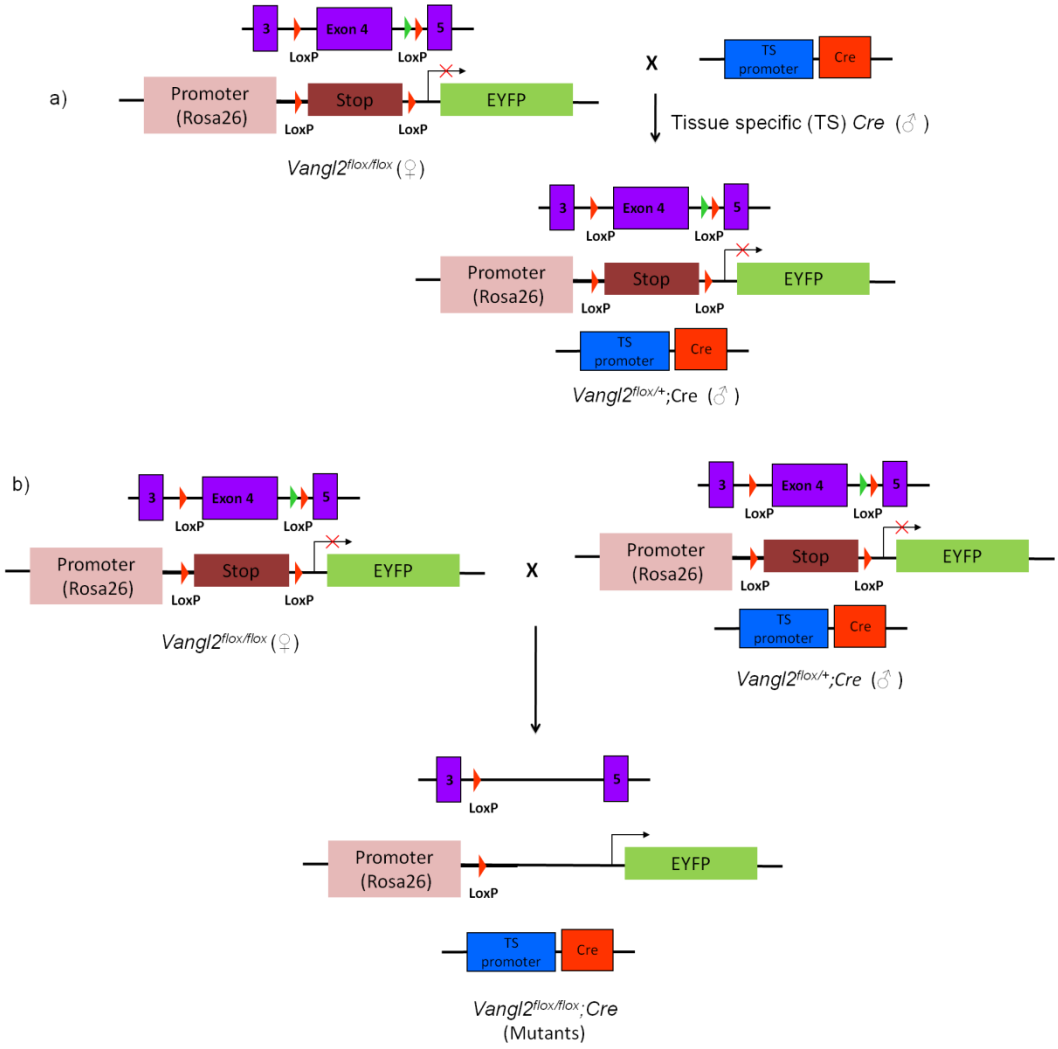

Figure 3.6: Crosses to delete *Vangl2* from different tissues

All *Vangl2*^{flox} mice used for the study were incorporated with *eYFP* sequence, by inter-crossing with mice carrying a floxed enhanced yellow fluorescent protein sequence (*ROSA-Stop-eYFP*) **a)** Cross between *Vangl2*$^{flox/flox}$ and a *Cre* line (which can be any tissue specific Cre or universally expressing *Cre*) to get *Vangl2*$^{flox/+}$*;Cre* mice. **b)** Cross between *Vangl2*$^{flox/flox}$ and *Vangl2*$^{flox/+}$*;Cre* mice to produce mice which had *Vangl2* deletion on both alleles and eYFP protein expression by *Cre* drived recombination.

3.2.3 *Vangl2*^{flox} line recapitulates Lp phenotype (using *PGK-Cre* and *Sox2-Cre*)

The next question was whether a global knockout of *Vangl2* using the *Vangl2*^{flox} allele recapitulated the *Lp/Lp* phenotype. To test this a globally expressing *Cre*, *PGK-Cre* was used (Lallemand *et al.*, 1998). *PGK-Cre* was crossed into our *Vangl2*^{flox} line, which would remove *Vangl2* in all cells that are expressing *Cre*, that is all cells in this case.

Vangl2$^{flox/+}$*;PGK-Cre* mice were crossed with *Vangl2*$^{flox/flox}$ mice (shown in figure 3.7) and embryos were collected at E14.5. These embryos were then compared with *Lp* embryos for their external as well as internal phenotype. Embryos were genotyped using *Vangl2*^{flox} primers and *Cre* primers. Of these embryos, *Vangl2*$^{flox/flox}$*;PGK-Cre* were expected to recapitulate *Lp/Lp* phenotype.

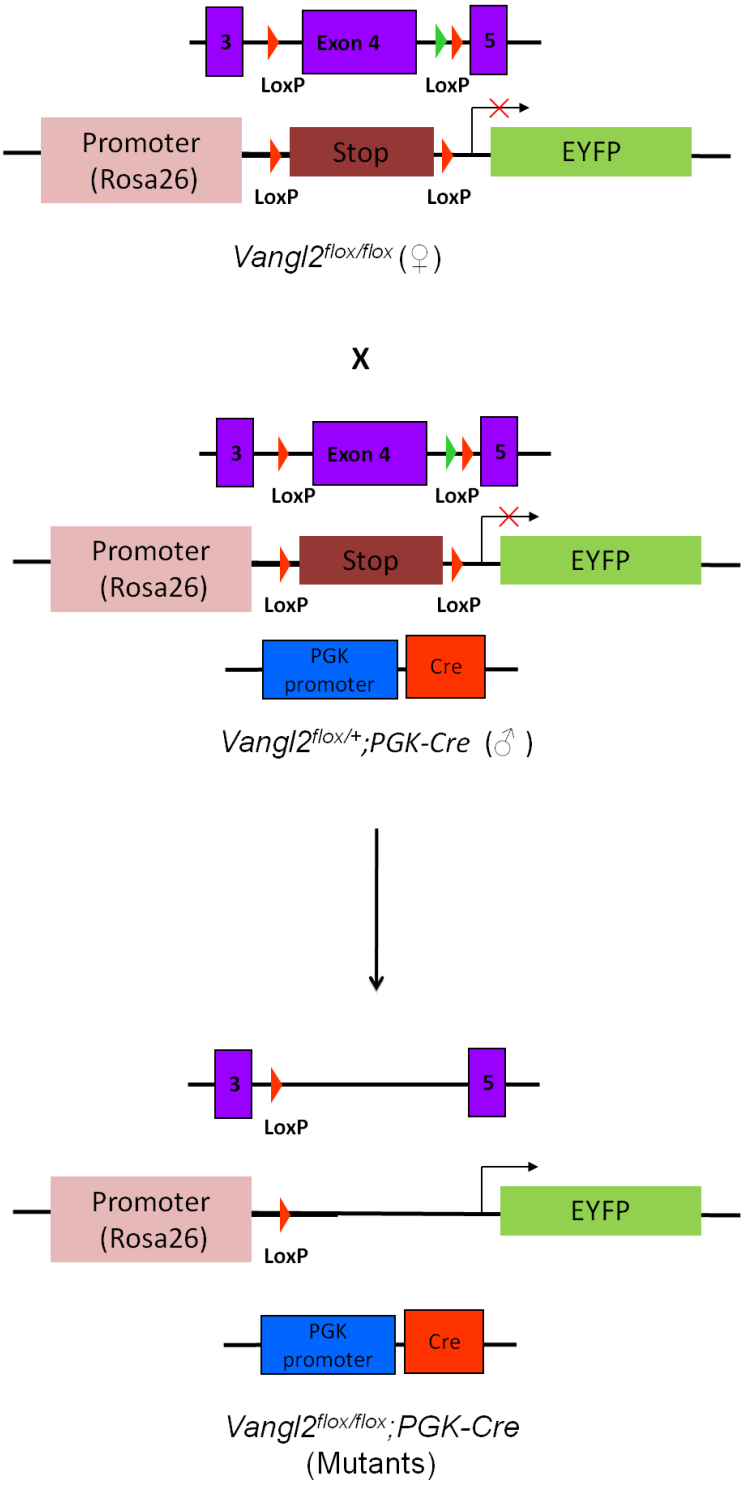

Figure 3.7: *Vangl2*^{flox} cross with *PGK-Cre*

Vangl2$^{flox/+}$*;PGK-Cre* x *Vangl2*$^{flox/flox}$ cross to have full deletion of exon 4 of *Vangl2* gene. Exon 4 has *loxP* sites on either sides (shown in red), which gets removed with the expression of *Cre*. Resulting genotype would be devoid of exon 4 and have *eYFP* expression in all the cells which express *Cre* (in this case all body cells, as *PGK-Cre* is a universally expressing *Cre*).

A total of 6 mutants (*Vangl2*$^{flox/flox}$*;PGK-Cre*) from 3 litters (total 24 embryos) were used for the phenotype analysis. These 6 mutant embryos had the same neural tube defect as *Lp/Lp* mice; where the complete neural tube was open (craniorachischisis), although the neural tube was closed rostral to the mid-brain:hindbrain boundary, just like in *Lp* (Copp *et al.*, 1994). *Vangl2*$^{flox/flox}$*;PGK-Cre* also had looped tail as seen in *Lp/Lp* embryos, although *Vangl2*$^{flox/+}$*;PGK-Cre* embryos didn't have looped tail. Figure 3.8 shows a control embryo with a normal phenotype, with closed neural tube (figure 3.8a) compared to *Vangl2*$^{flox/flox}$*;PGK-Cre* embryos with craniorachischisis (arrows in figure 3.8b,c,d) and looped tail (arrow head in figure 3.8b,c,d), as seen in *Lp/Lp* (figure 3.3e). This phenotype had 100% penetrance and was observed in all mutant embryos with equal amount of severity. Table 3.3 summarizes the external phenotypic defects observed in *Lp/Lp* and *Vangl2*$^{flox/flox}$*;PGK-Cre* embryos.

Table 3.3: External phenotypic defects seen in *Lp/Lp* and *Vangl2*$^{flox/flox}$*;PGK-Cre* mutants at E14.5

Genotype	Number of embryos	Looped tail	Craniorachischisis	Spina bifida	Gastroschisis
Lp/+	8/16	8	0	0	0
Lp/Lp	4/16	4	4	0	1
Vangl2$^{flox/+}$*; PGK-Cre*	6/24	0	0	0	0
Vangl2$^{flox/flox}$*; PGK-Cre*	6/24	6	6	0	0

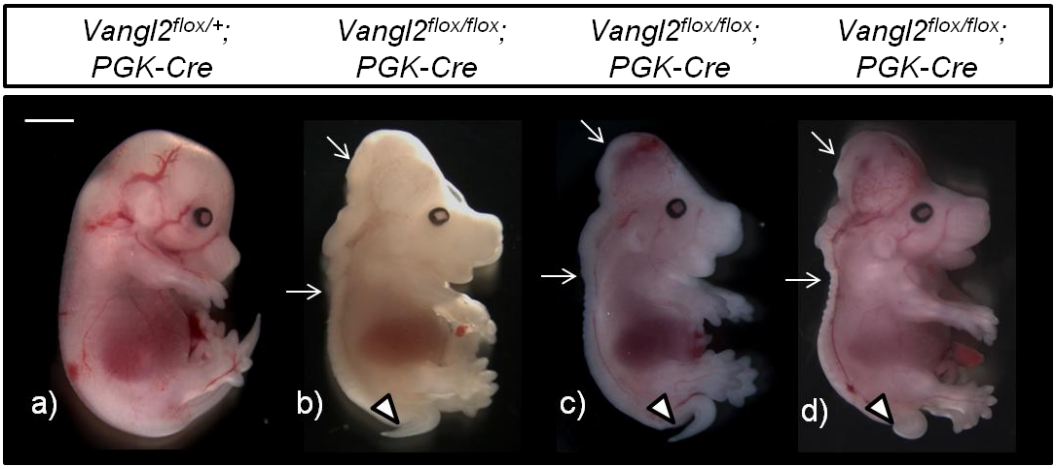

Figure 3.8: Neural Tube defects in *Vangl2$^{flox/flox}$;PGK-Cre* embryos at E14.5

Whole embryos from *Vangl2$^{flox/+}$;PGK-Cre* x *Vangl2$^{flox/flox}$* litter. **a)** *Vangl2$^{flox/+}$;PGK-Cre* embryo with normal external phenotype. **b, c, d)** *Vangl2$^{flox/flox}$;PGK-Cre* embryo showing external phenotypic defect, craniorachischisis (arrows showing open neural tube and arrowhead pointing at looped tail). Scale - 2000µm.

Once the external phenotype was established, the *Vangl2$^{flox/+}$;PGK-Cre* and *Vangl2$^{flox/flox}$;PGK-Cre* embryos were fixed and wax embedded. Transverse sections were taken (figure 10a showing the plane of section) and H&E stained to look at heart morphology. When only one allele was floxed (*Vangl2$^{flox/+}$;PGK-Cre*) there was normal heart development (Figure 10b), as in *Lp/+* embryos. On the other hand, when both alleles were floxed (*Vangl2$^{flox/flox}$;PGK-Cre*) and had Vangl2 truncated in all body cells, heart defects were observed. These included double outlet right ventricle (figure 3.9c arrow), ventricular septal defect (figure 3.9e circle) and aortic arch defect retroesophageal subclavian artery (figure 3.9g arrow).

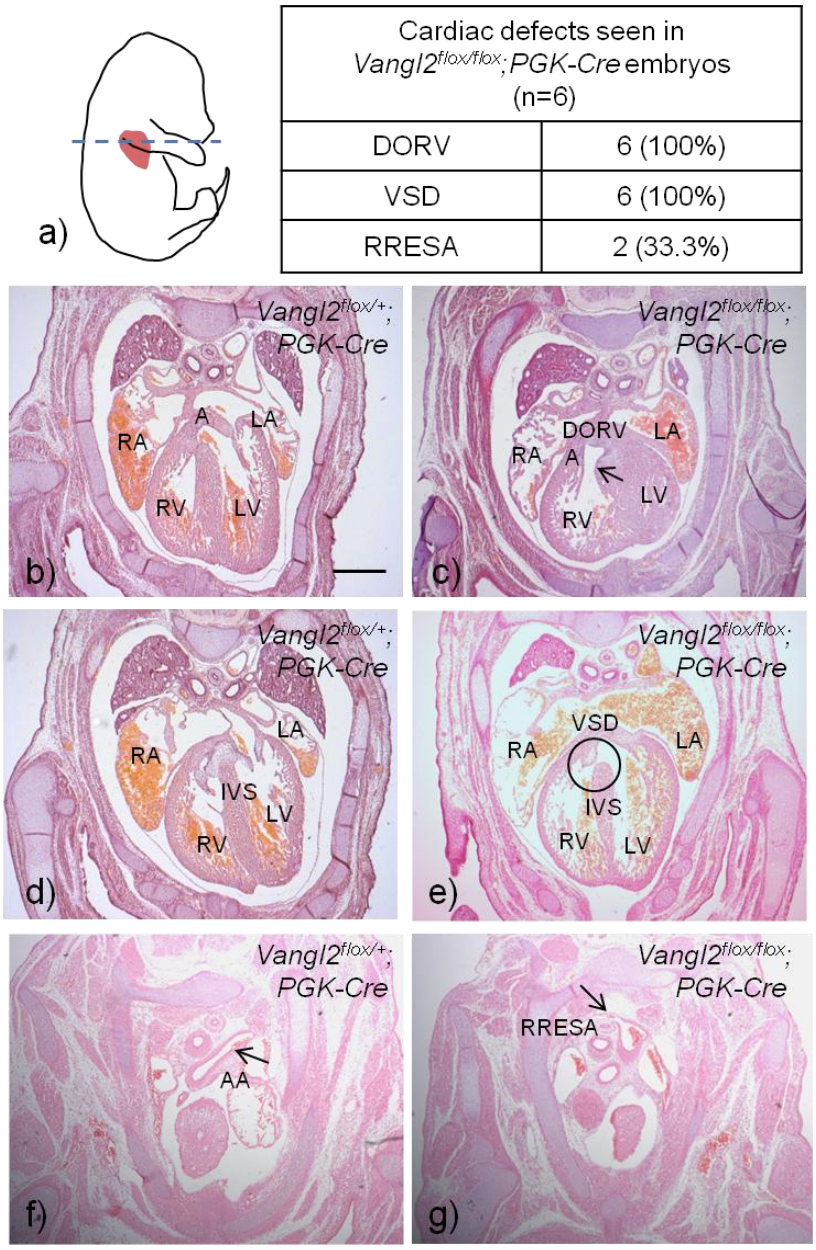

Figure 3.9: Cardiovascular defects in *Vangl2$^{flox/flox}$;PGK-Cre* embryos at E14.5

Transverse sections of heart from *Vangl2$^{flox/+}$;PGK-Cre* x *Vangl2$^{flox/flox}$* litter. The table shows different defects seen in *Vangl2$^{flox/flox}$;PGK-Cre* embryos. **a)** Plane of the section. **b)** Transverse section through heart of *Vangl2$^{flox/+}$;PGK-Cre* embryo showing normal heart development. **c)** Heart section from *Vangl2$^{flox/flox}$;PGK-Cre* embryos showing double outlet right ventricle. **d)** Section of *Vangl2$^{flox/+}$;PGK-Cre* embryo showing interventricular septum. **e)** Section of *Vangl2$^{flox/flox}$;PGK-Cre* embryo showing ventricular septal defect. **f,g)** Normal left sided aortic arch in *Vangl2$^{flox/+}$;PGK-Cre* embryo and retroesophageal subclavian artery in *Vangl2$^{flox/flox}$;PGK-Cre* (g). RA-right atria, LA-left atria, RV-right ventricle, LV-left ventricle, A-aorta, PT-pulmonary trunk, DORV-double outlet right ventricle, VSD-ventricular septal defect, IVS-interventricular septum, RRESA-retroesophageal subclavian artery. Scale - 20µm.

Table 3.4 is used as a summary to look at the phenotype of *Vangl2*$^{flox/flox}$*;PGK-Cre* and compare it with *Lp/Lp* and *Vangl2*$^{floxneo/floxneo}$ phenotype. The table shows that there was 100% penetrance of heart defects along with external phenotypic defect suggesting that *PGK-Cre* gives a complete knockout of *Vangl2* and resembles the defective phenotype seen in *Lp* mice (Henderson *et al.*, 2001).

Table 3.4: Comparison between *Lp*, *Vangl2*^{floxneo} and *Vangl2*^{flox}*;PGK-Cre* phenotype.

Phenotypes		***Lp/Lp***	***Vangl2*$^{neo/neo}$**	***Vangl2*$^{flox/flox}$*;PGK-Cre***
External Phenotype	**Tail**	*Lp/+* - looped/ kinked tail *Lp/Lp* - looped/ kinked tail	*Vangl2*$^{floxneo/+}$ - normal tail *Vangl2*$^{floxneo/floxneo}$ - looped/ kinked tail	*Vangl2*$^{flox/+}$*;PGK-Cre* - normal tail *Vangl2*$^{flox/flox}$*;PGK-Cre* - looped/ kinked tail
	Neural Tube	*Lp/Lp* - open neural tube (CRN)	*Vangl2*$^{floxneo/floxneo}$ - open neural tube, but in variation(CRN to Spina bifida)	*Vangl2*$^{flox/flox}$*;PGK-Cre* - open neural tube (CRN)
Cardiac Defects		*Lp/Lp* - cardiovascular defects (double outlet right ventricle, ventricular septal defect, aortic arch defects)	*Vangl2*$^{floxneo/floxneo}$ - cardiovascular defects (double outlet right ventricle, ventricular septal defect, aortic arch defects)	*Vangl2*$^{flox/flox}$*;PGK-Cre* - cardiovascular defects (double outlet right ventricle, ventricular septal defect, aortic arch defects)

3.2.3.1 PGK-Cre is not expressed in all body cells

Looking at the phenotype, we got full recapitulation of *Lp* phenotype in our *Vangl2*^{flox} line using *PGK-Cre*. To confirm that there was full loss of Vangl2 in our *Vangl2*$^{flox/flox}$*;PGK-Cre* mutant embryos, western blotting was carried out using protein samples from whole embryos at E14.5. *PGK-Cre* is a globally expressing *Cre* and is used to produce global knockouts (ref), which would be expected to delete Vangl2 from all cells. However there was a Vangl2 band in the *Vangl2*$^{flox/flox}$*;PGK-Cre* sample, as in *Vangl2*$^{flox/+}$*;PGK-Cre* control (figure 3.10a). This was checked with 3 different control and mutant samples. To confirm that equivalent levels of proteins were loaded, the same membrane was reprobed for β-actin and similar levels of protein was observed in control and mutant (figure 3.10a). Thus, although the levels of Vangl2 appeared slightly reduced, it was still present. To understand and explain this, the expression of *PGK-Cre* in sections was looked at using anti-GFP antibody. Heart sections from 3 controls and 3 mutants were taken at E9.5 and using immunohistochemistry techniques, were immunostained for anti-GFP antibody, which recognizes the eYFP protein in the sections. Ideally a universally expressing *Cre* like *PGK-Cre* should have eYFP labelled on all cells, but there were regions where staining wasn't present in both *Vangl2*$^{flox/+}$*;PGK-Cre* control and *Vangl2*$^{flox/flox}$*;PGK-Cre* mutant embryo sections (figure 3.10b,c asterisk), suggesting that eYFP isn't expressed in these cells. These results suggest that *PGK-Cre* isn't driving expression in all body cells.

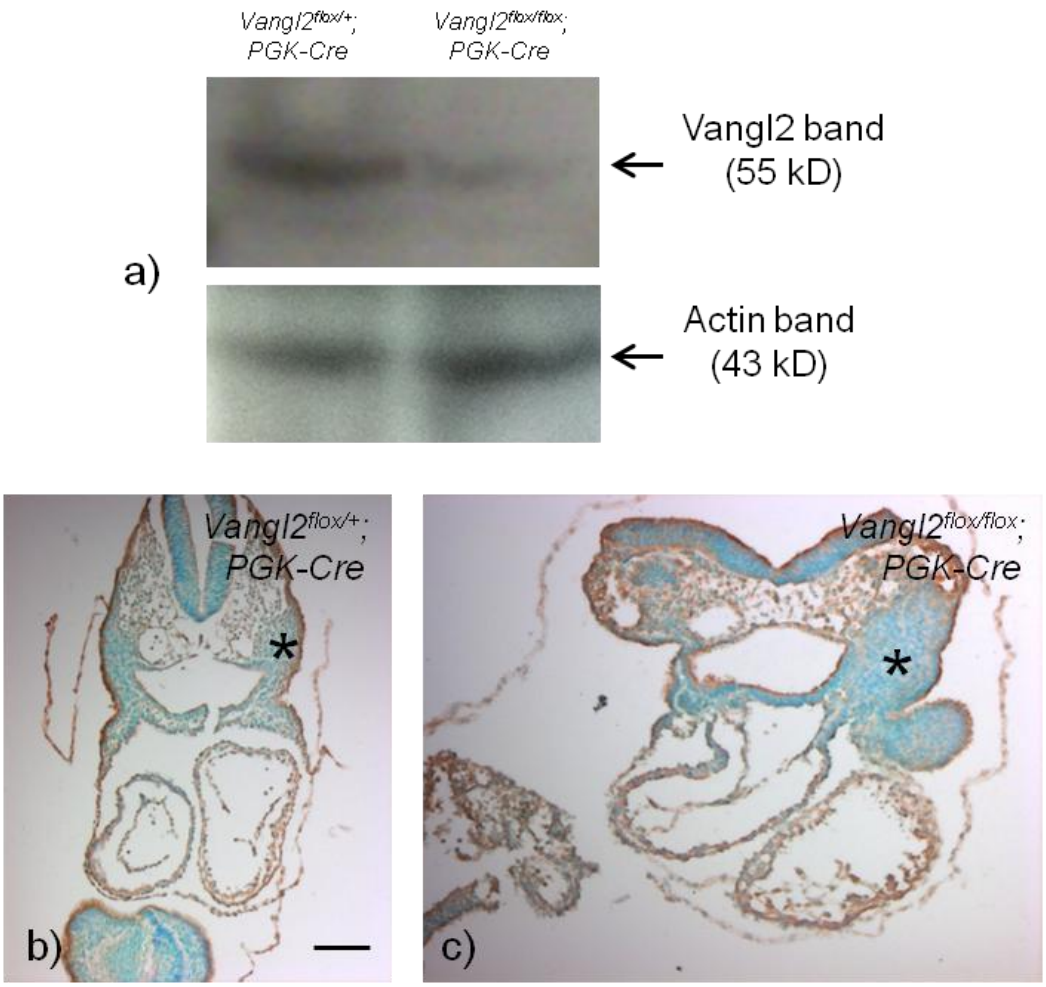

Figure 3.10: Vangl2 expression not completely lost in the presence of *PGK-Cre*

a) Western blot showing a faint Vangl2 band in *Vangl2$^{flox/flox}$;PGK-Cre* mutant embryo at E14.5, with similar levels of β-actin protein. **b,c)** Immunostaining using GFP-DAB on E9.5 embryos, brown cells showing cells expressing eYFP. *Vangl2$^{flox/+}$;PGK-Cre* embryo (b) showing regions which are not expressing eYFP (blue, asterisk), similar expression in *Vangl2$^{flox/flox}$;PGK-Cre* embryo (c) with blue region (asterisk). Scale - 100µm.

3.2.3.2 Sox2-Cre as the new universal Cre line

Sox2-Cre is another universally expressing Cre with efficient recombination and effective removing of a gene (Hayashi *et al.*, 2002). Therefore *Sox2-Cre* mice were intercrossed with *Vangl2*^{flox} line (cross shown in figure 3.11). Embryos were collected at E15.5 for western blotting and at E9.5 for immunohistochemistry. *Vangl2*$^{flox/flox}$*;Sox2-Cre* were taken as mutants and *Vangl2*$^{flox/+}$*;Sox2-Cre* as controls and were detected by PCR.

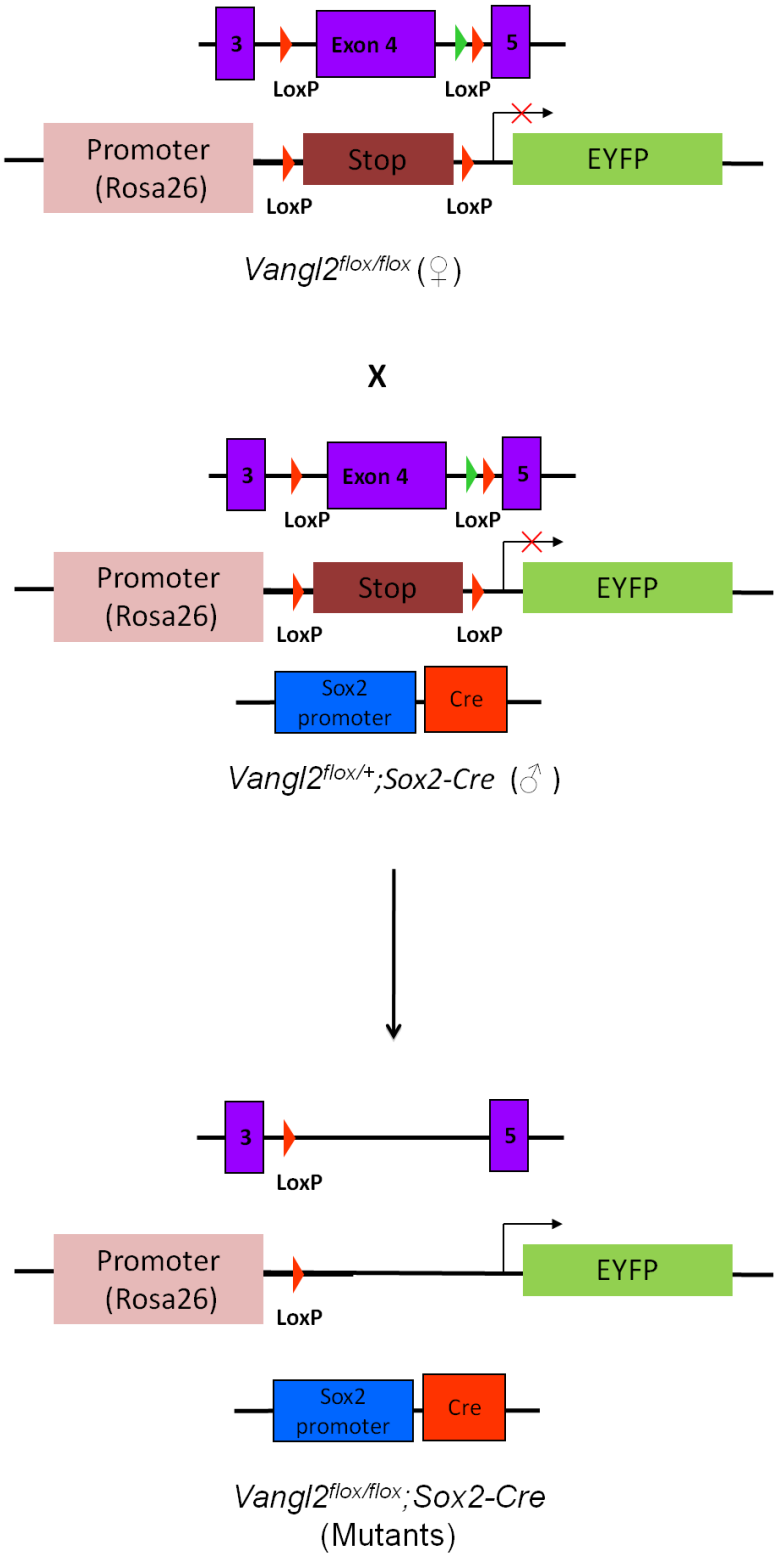

Figure 3.11: *Vangl2*^{flox} cross with *Sox2-Cre*

Vangl2$^{flox/+}$*;Sox2-Cre* x *Vangl2*$^{flox/flox}$ cross to have full deletion of exon 4 of *Vangl2* gene. Resulting genotype would be devoid of exon 4 and have eYFP expression in all the cells which express *Cre* (in this case all body cells, as *Sox2-Cre* is a universally expressing *Cre*).

Similar experiment using anti-GFP antibody was done on 3 *Vangl2*$^{flox/+}$*;Sox2-Cre* and 3 *Vangl2*$^{flox/flox}$*;Sox2-Cre* embryos as was done on embryos with *PGK-Cre* present. More widespread expression of eYFP was observed, with labelling detected the brown colour of DAB (figure 3.12a). It should be noted that in the regions where eYFP expression was not observed with in *Vangl2*$^{flo+}$*;PGK-Cre* embryos (figure 3.10b,c) also had uniform staining (shown with arrows in figure 3.12a). RT PCR of cDNA and western blot of the protein sample from 3 different control and mutant embryos were done to check for presence of Vangl2 transcript and protein respectively. RT-PCR showed complete loss of Vangl2 at the RNA level, as no Vangl2 band was observed in *Vangl2*$^{flox/flox}$*;Sox2-Cre* as compared to a clear band in *Vangl2*$^{flox/+}$*;Sox2-Cre* lane (figure 3.12b). β-actin was used to check the levels of cDNA for RT PCR, which showed same levels in both control and mutant. There was significant loss of Vangl2 at the protein level as well detected by western blot (figure 3.12c). Membrane was reprobed to check the levels of protein added, by checking GAPDH protein, which did not show equivalent level of protein in control and mutant (figure 3.12c), however using densitometry analysis the levels were equalised and still showed significant reduction of Vangl2 in *Vangl2*$^{flox/flox}$*;Sox2-Cre.* This confirms that expression of Vangl2 was reduced and recombination directed by *Sox2-Cre* was more efficient as compared to *PGK-Cre*.

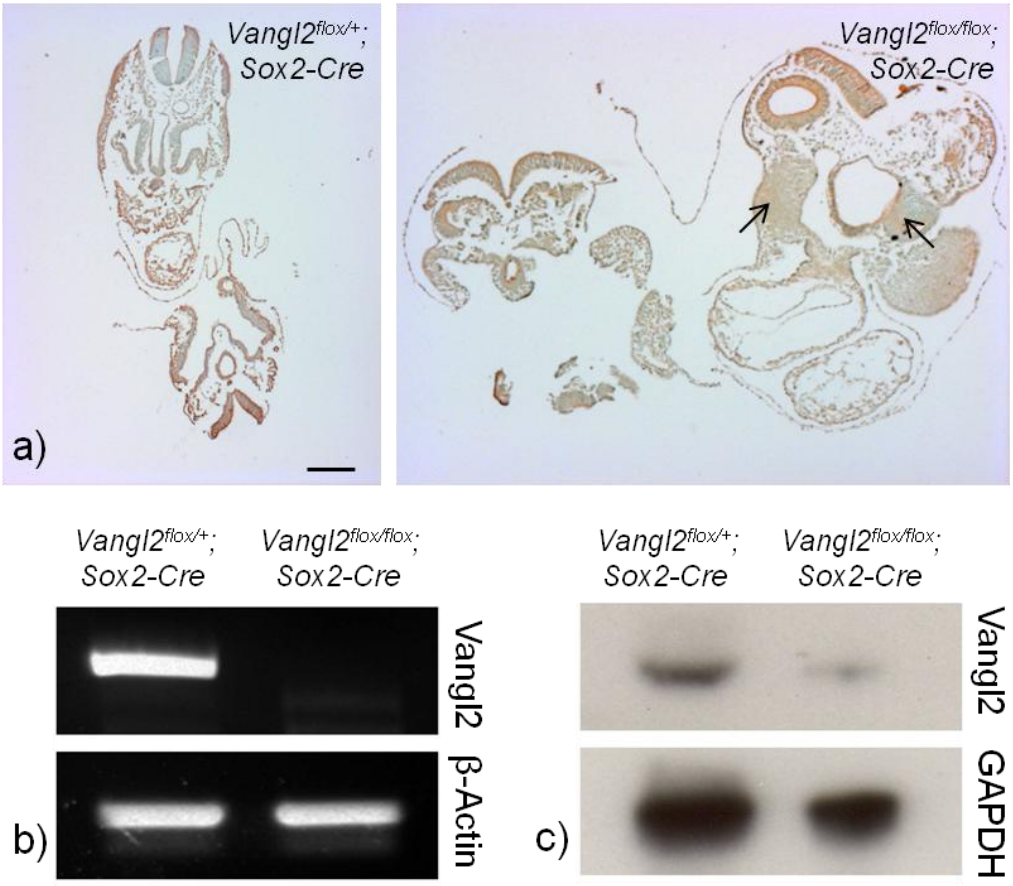

Figure 3.12: Vangl2 expression lost in the presence of *Sox2-Cre*

a) Immunostaining using GFP-DAB, brown cells showing cells expressing *Cre*. *Vangl2$^{flox/+}$;Sox2-Cre* embryo and in *Vangl2$^{flox/flox}$;Sox2-Cre* embryo (arrows pointing at region where *Cre* expression was not observed in *Vangl2^{flox};PGK-Cre* embryos) at E9.5. **b)** RT PCR showing complete loss of Vangl2 band in *Vangl2$^{flox/flox}$;Sox2-Cre* embryo at RNA level at E15.5. **c)** Western blot showing significant reduction in Vangl2 protein level in *Vangl2$^{flox/flox}$;Sox2-Cre* embryo at E15.5. Scale - 100µm.

To check the loss of Vangl2 from the embryo co-expression of Vangl2 with anti-GFP antibody was checked using immunofluorescence. Anti-GFP antibody which detects eYFP protein in *Cre* expressing cells was used along with Vangl2 antibody. Secondary antibodies having fluorescence probes were used. Figure 3.13a,b shows the position of outflow tract in *Vangl2*$^{flox/+}$*;Sox2-Cre* and *Vangl2*$^{flox/flox}$*;Sox2-Cre* sections. *Vangl2*$^{flox/+}$*;Sox2-Cre* embryos showed eYFP expression (in green, figure 3.13c) throughout the embryo in uniform manner along with Vangl2 expression (in red, figure 3.13e). This was in contrast with *Vangl2*$^{flox/flox}$*;Sox2-Cre* section, where eYFP expression (in green, figure 3.13d) was similar to controls, but no staining was observed for Vangl2 (figure 3.13f) at the same exposure as for the control section. This was repeated on 3 different controls and mutants with similar expression pattern and therefore adds on to our confirmation that Vangl2 was deleted by *Sox2-Cre* mediated recombination.

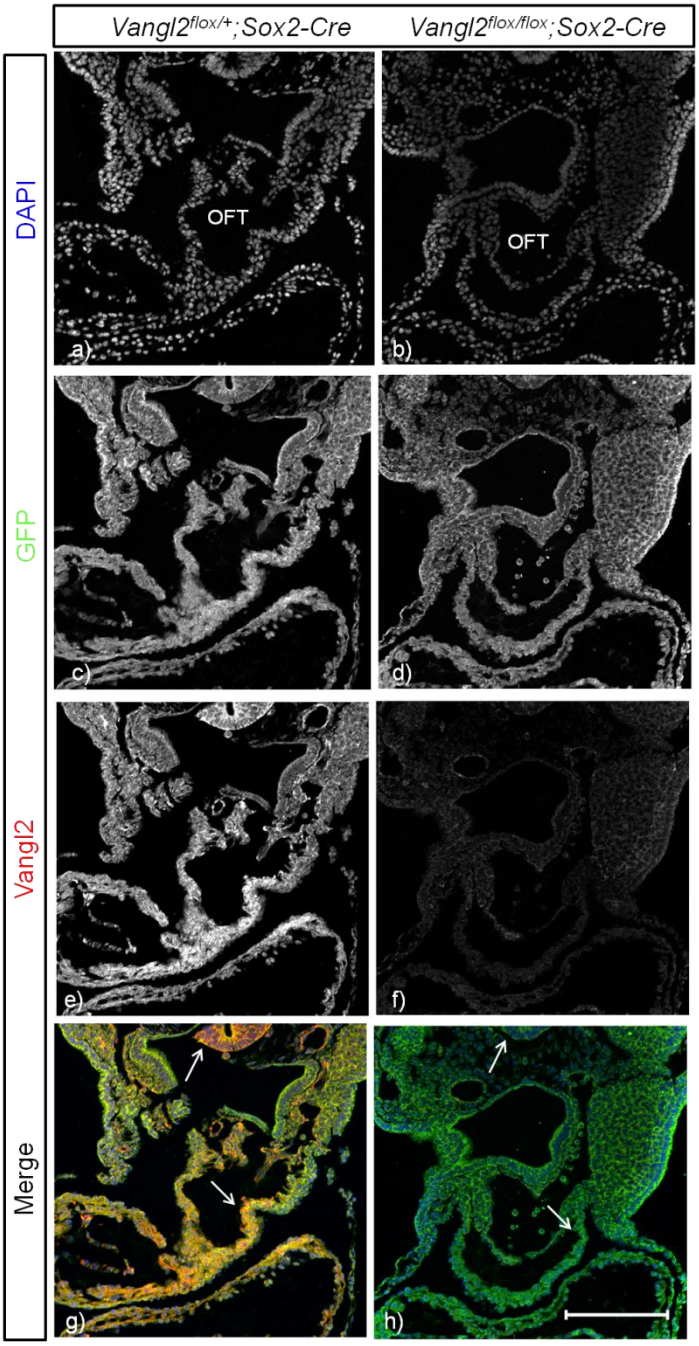

Figure 3.13: Vangl2 expression completely lost in the presence of *Sox2-Cre*

Different panels for Immunofluorescence for co-expression of Cre (GFP antibody) and Vangl2 in *Vangl2$^{flox/+}$;Sox2-Cre* and *Vangl2$^{flox/flox}$;Sox2-Cre* embryo. **a,b)** DAPI marking nucleus of cells showing outflow tract in *Vangl2$^{flox/+}$;Sox2-Cre* (a) and *Vangl2$^{flox/flox}$;Sox2-Cre* (b) section. **c,d)** Anti-GFP antibody labeling eYFP in *Vangl2$^{flox/+}$;Sox2-Cre* (c) and *Vangl2$^{flox/flox}$;Sox2-Cre* (d) showing similar expression throughout the section. **e,f)** Vangl2 expression in *Vangl2$^{flox/+}$;Sox2-Cre* (e) and *Vangl2$^{flox/flox}$;Sox2-Cre* (f) where no Vangl2 expression is seen. **g,h)** Coexpression of eYFP and Vangl2 in *Vangl2$^{flox/+}$;Sox2-Cre* (g) with yellow regions (arrows, neural tube and outflow tract) where both are expressed and *Vangl2$^{flox/flox}$;Sox2-Cre*(h) where no coexpression is seen (arrows). Scale - 200µm.

3.2.3.3 Vangl2^{flox};Sox2-Cre recapitulates Lp and Vangl2^{flox};PGK-Cre phenotype

After establishing that recombination using *Sox2-Cre* is more efficient and effective, the embryonic phenotype of *Vangl2$^{flox/flox}$;Sox2-Cre* embryos was analysed at E15.5 and compared with phenotype of *Vangl2$^{flox/flox}$;PGK-Cre* mutants to check if it was same or more severe phenotype. Also recapitulation of *Lp* phenotype was checked.

Embryos were dissected at E15.5 and were genotyped. Six mutant embryos (*Vangl2$^{flox/flox}$;Sox2-Cre*) were obtained and showed open neural tube (craniorachischisis) as seen in *Vangl2$^{flox/flox}$;PGK-Cre* and *Lp/Lp* embryos, while *Vangl2$^{flox/+}$;Sox2-Cre* had a normal external phenotype. Figure 3.14 shows *Vangl2$^{flox/+}$;Sox2-Cre* embryo with closed neural tube and no looped-tail and *Vangl2$^{flox/flox}$;Sox2-Cre* embryos with craniorachischisis (arrows) and looped-tail (arrowhead). Table 3.5 summarizes the external phenotypic defects observed in *Lp/Lp* and *Vangl2$^{flox/flox}$;Sox2-Cre* embryos.

Table 3.5: External phenotypic defects seen in *Lp/Lp* and *Vangl2$^{flox/flox}$;Sox2-Cre* mutants at E15.5

Genotype	Number of embryos	Looped tail	Craniorachischisis	Spina bifida	Gastroschisis
Lp/+	8/16	8	0	0	0
Lp/Lp	4/16	4	4	0	1
Vangl2$^{flox/+}$; Sox2-Cre	6/24	0	0	0	0
Vangl2$^{flox/flox}$; Sox2-Cre	6/24	6	6	0	0

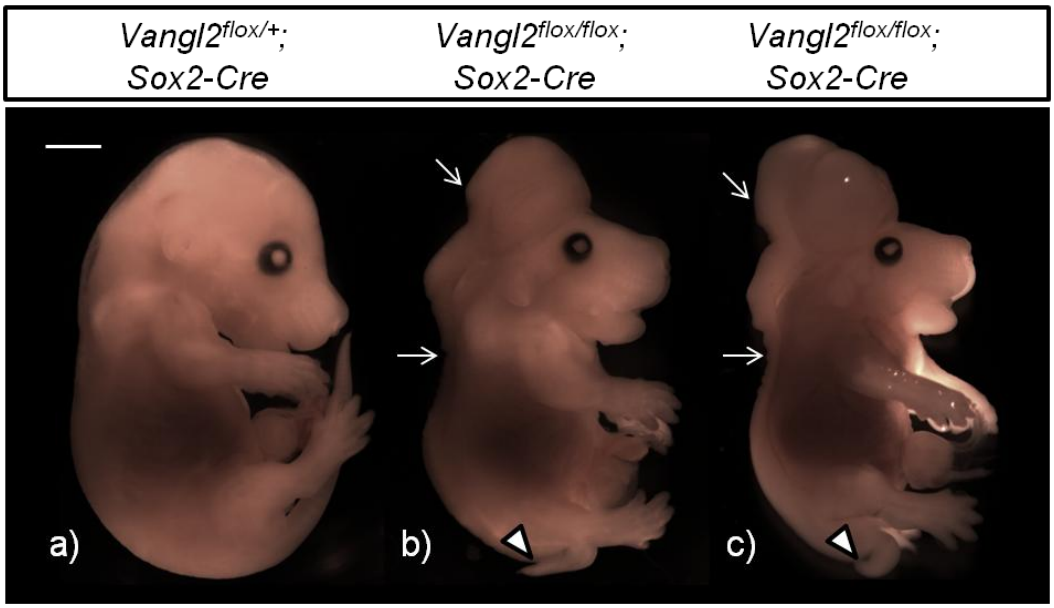

Figure 3.14: Neural Tube defects in *Vangl2$^{flox/flox}$;Sox2-Cre* embryos at E15.5

Whole embryos from *Vangl2$^{flox/+}$;Sox2-Cre* x *Vangl2$^{flox/flox}$* litter. **a)** *Vangl2$^{flox/+}$;Sox2-Cre* embryo with normal external phenotype. **b, c)** *Vangl2$^{flox/flox}$;Sox2-Cre* embryo showing external phenotypic defect, craniorachischisis (arrows showing open neural tube and arrowhead pointing at looped tail). Scale - 2000µm.

Transverse heart sections of wax embedded embryos were taken (figure 3.15a, f) and stained with H&E to analyse the heart morphology. *Vangl2$^{flox/+}$;Sox2-Cre* had a normal heart phenotype (figure 3.15b), whereas all 6 *Vangl2$^{flox/flox}$;Sox2-Cre* mutant embryos showed double outlet right ventricle (figure3.15c, d) and ventricular septal defect (figure3.15e). Of these 2 mutants also had retroesophageal subclavian artery (figure 3.15g) which are the same defects as seen in *Vangl2$^{flox/flox}$;PGK-Cre* and *Lp/Lp* embryos.

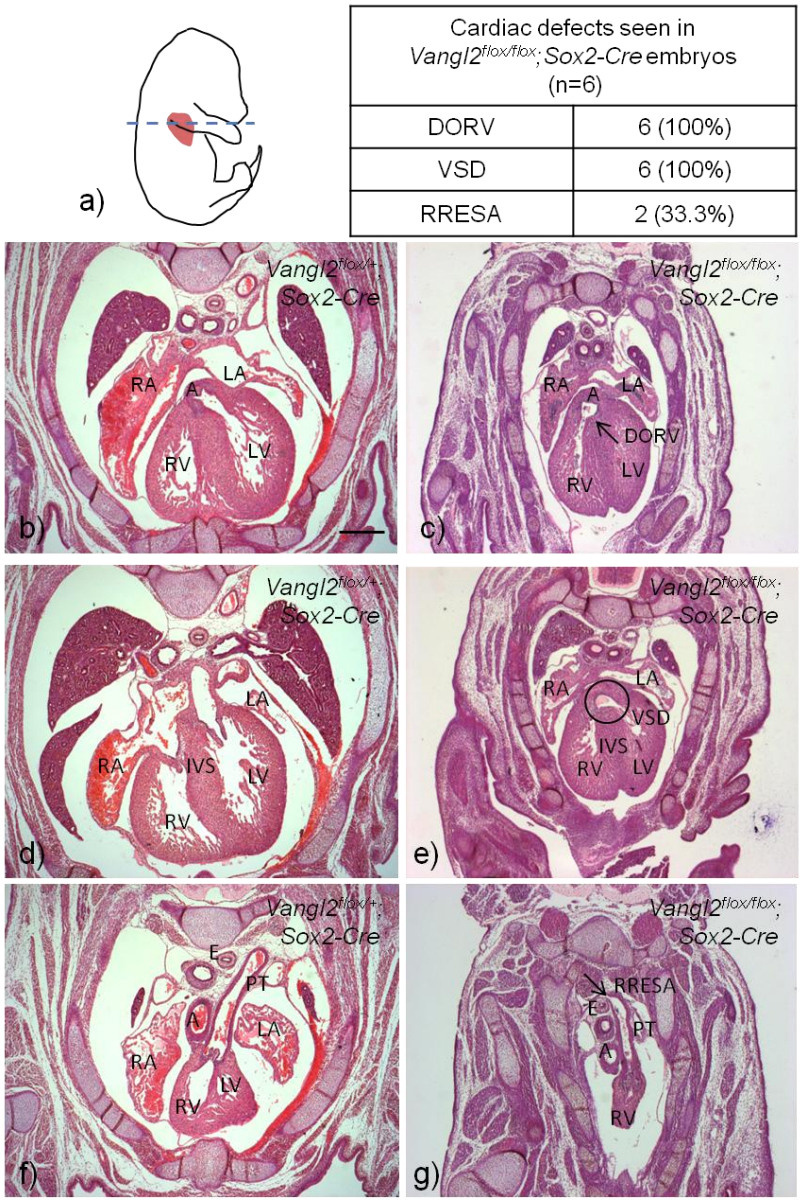

Figure 3.15: Cardiovascular defects in *Vangl2$^{flox/flox}$;Sox2-Cre* embryos at E15.5

Transverse sections of heart from *Vangl2$^{flox/+}$;Sox2-Cre* x *Vangl2$^{flox/flox}$* litter. Table shows different defects seen in *Vangl2$^{flox/flox}$;Sox2-Cre* embryos. **a)** Plane of the section. **b)** Transverse section through heart of *Vangl2$^{flox/+}$;Sox2-Cre* embryo showing normal heart development. **c)** Heart section from *Vangl2$^{flox/flox}$;Sox2-Cre* embryos showing double outlet right ventricle. **d)** Heart section of *Vangl2$^{flox/+}$;Sox2-Cre* embryo showing interventricular septum. **e)** Heart section from *Vangl2$^{flox/flox}$;Sox2-Cre* embryos showing ventricular septal defect. **f)** Heart section of *Vangl2$^{flox/+}$;Sox2-Cre* embryo showing normal left sided aortic arch. **g)** Heart section from *Vangl2$^{flox/flox}$;Sox2-Cre* embryos showing retroesophageal subclavian artery. RA-right atria, LA-left atria, RV-right ventricle, LV-left ventricle, A-aorta, PT-pulmonary trunk, DORV-double outlet right ventricle, VSD-ventricular septal defect, IVS-interventricular septum, RRESA-retroesophageal subclavian artery. Scale - 20µm.

3.2.4 *Vangl2*^{flox} allele fails to complement *Lp* allele

When two different genes in their recessive form give the same phenotype, but when crossed together to be present in the same genome give a wild-type phenotype, the effect is called 'complementation'. For complementation to occur, the mutations have to be in different genes. The wild type allele of each gene will compensate for the loss of the other gene and resulting in the wild-type phenotype. If the mutation is in same gene, complementation will not occur; therefore if mutant phenotype is observed in the crossed strains it means that they are allelic in nature. Reduced protein stability and expression in *Lp/Lp* has been reported suggesting *Lp* as a null allele (Montcouquiol *et al.*, 2006; Torban *et al.*, 2007). However, another study showed dominant negative effect of *Lp* mutation by comparing severity of *Vangl2* knockouts with *Vangl2* knockout mouse intercrossed with *Lp* mutants (Yin *et al.*, 2012).

To establish if *Lp* is a null allele and *Vangl2*^{flox} and *Lp* are allelic in nature, crosses were set up between *Lp/+* and *Vangl2*$^{flox/+}$*;PGK-Cre* (and *Vangl2*$^{flox/+}$*;Sox2-Cre*)(cross shown in figure 19). Possible genotypes of the offsprings are shown in the figure, and if presence of *Lp* and *Vangl2*^{flox}*;Cre* (*PGK-Cre/Sox2-Cre*) in one embryo produces a wild-type phenotype it would mean that these two complement each other and are not allelic but give the same phenotype in recessive condition. However, if presence of *Lp* and *Vangl2*^{flox}*;Cre* produces a mutant phenotype which is same as phenotype they produce in the individual recessive forms it would mean that these two fail to complement and are allelic in nature. Therefore, *Vangl2* deletion from one allele by *Cre* recombination producing *Lp* phenotype would mean that *Lp* is a null/loss of function mutation.

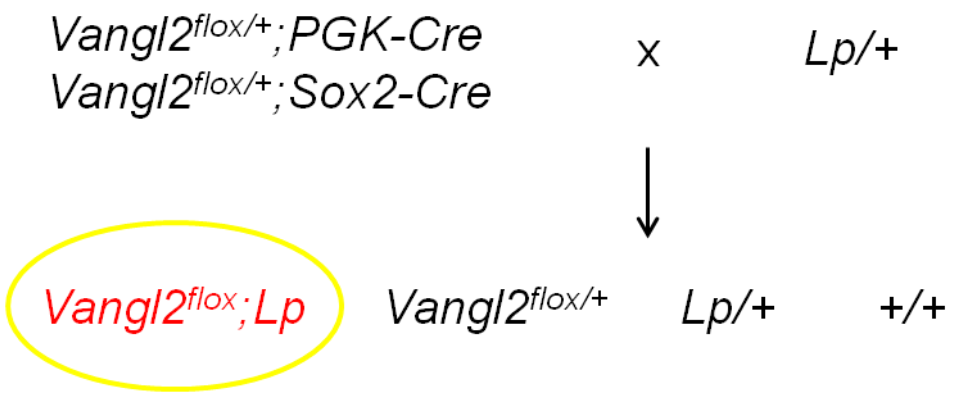

Figure 3.16: *Lp* cross with *Vangl2*$^{flox/+}$;Cre (PGK-Cre/Sox2-Cre)

Vangl2$^{flox/+}$;Cre (PGK-Cre/Sox2-Cre) x *Lp/+* cross to check complementation between these two alleles. Different possible genotypes from the cross are also shown.

Embryos were collected at E14.5 and genotyped using *Lp* primers and *Vangl2*^{flox} primers. *Vangl2*^{flox}*;Lp;PGK-Cre* and *Vangl2*^{flox}*;Lp;Sox2-Cre* embryos had craniorachischisis (figure 3.18a,b) (n=4), as observed in *Lp/Lp* (figure 3.3e) and *Vangl2* knockouts (figure 3.8b, 3.14b). To look at the heart morphology, embryos were embedded in wax and transerve sections through heart were taken. Heart sections after H&E staining revealed outflow tract defect and aortic arch defects. *Vangl2*^{flox}*;Lp;PGK-Cre* and *Vangl2*^{flox}*;Lp;Sox2-Cre* embryo had double outlet right ventricle (figure 3.18c,e) and retroesophageal subclavian artery (figure 3.18d,f), which are seen in *Lp/Lp* embryos (figure 3.4c,e) as well as knockout embryos of *Vangl2* using *PGK-Cre* (figure 3.9c,g) and *Sox2-Cre* (figure 3.15c,g). Table 3.6 summarizes the external phenotypic defects and cardiac defects observed *Vangl2*^{flox}*;Lp;PGK-Cre* and *Vangl2*^{flox}*;Lp;Sox2-Cre* embryos, along with different genotype combinations from *Lp* and *Vangl2*^{flox} allele and their external phenotype shown in figure 3.17.

Table 3.6: External phenotypic defects and cardiac defects seen in *Vangl2^{flox};Lp;PGK-Cre* and *Vangl2^{flox};Lp;Sox2-Cre* embryos at E14.5

Genotype	Number of embryos	Looped tail	Craniorachischisis	DORV	VSD	RRESA
+/+	4/13	0	0	0	0	0
Lp/+	3/13	3	0	0	0	0
Vangl2$^{flox/+}$	3/13	0	0	0	0	0
Vangl2^{flox}; Lp	4/13	4	4	4	4	4

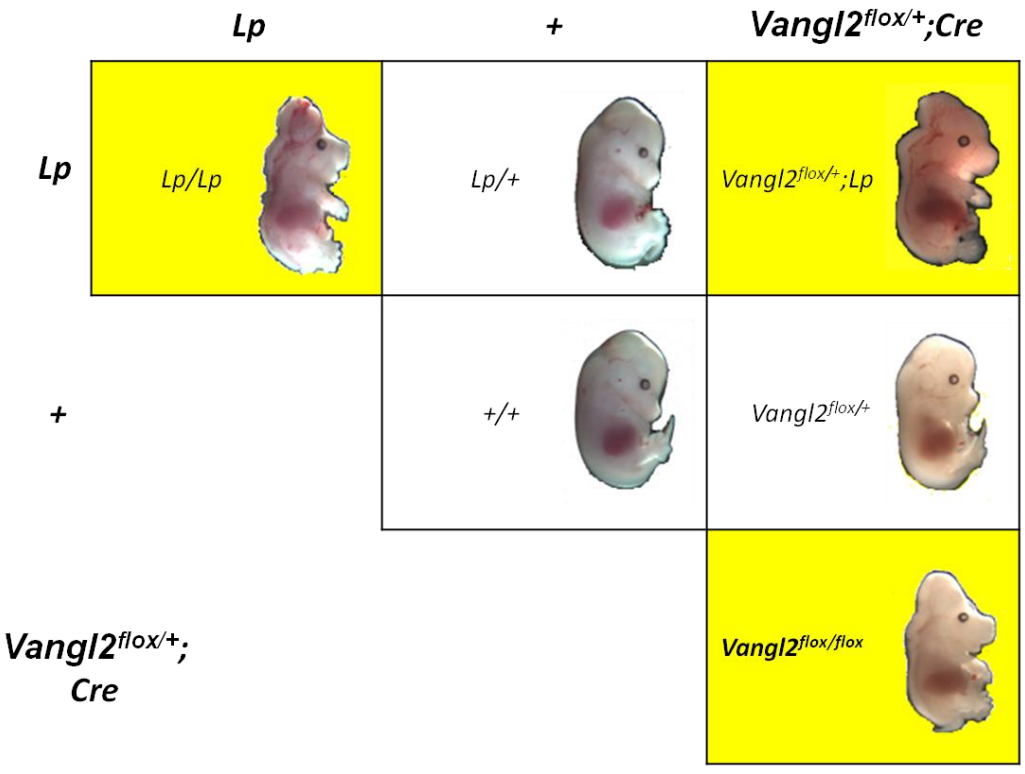

Figure 3.17: Different genotype combinations from *Lp* and *Vangl2^{flox}* allele

Different genotype combinations from *Lp* and *Vangl2^{flox}* allele and external phenotype obtained with those allele combinations.

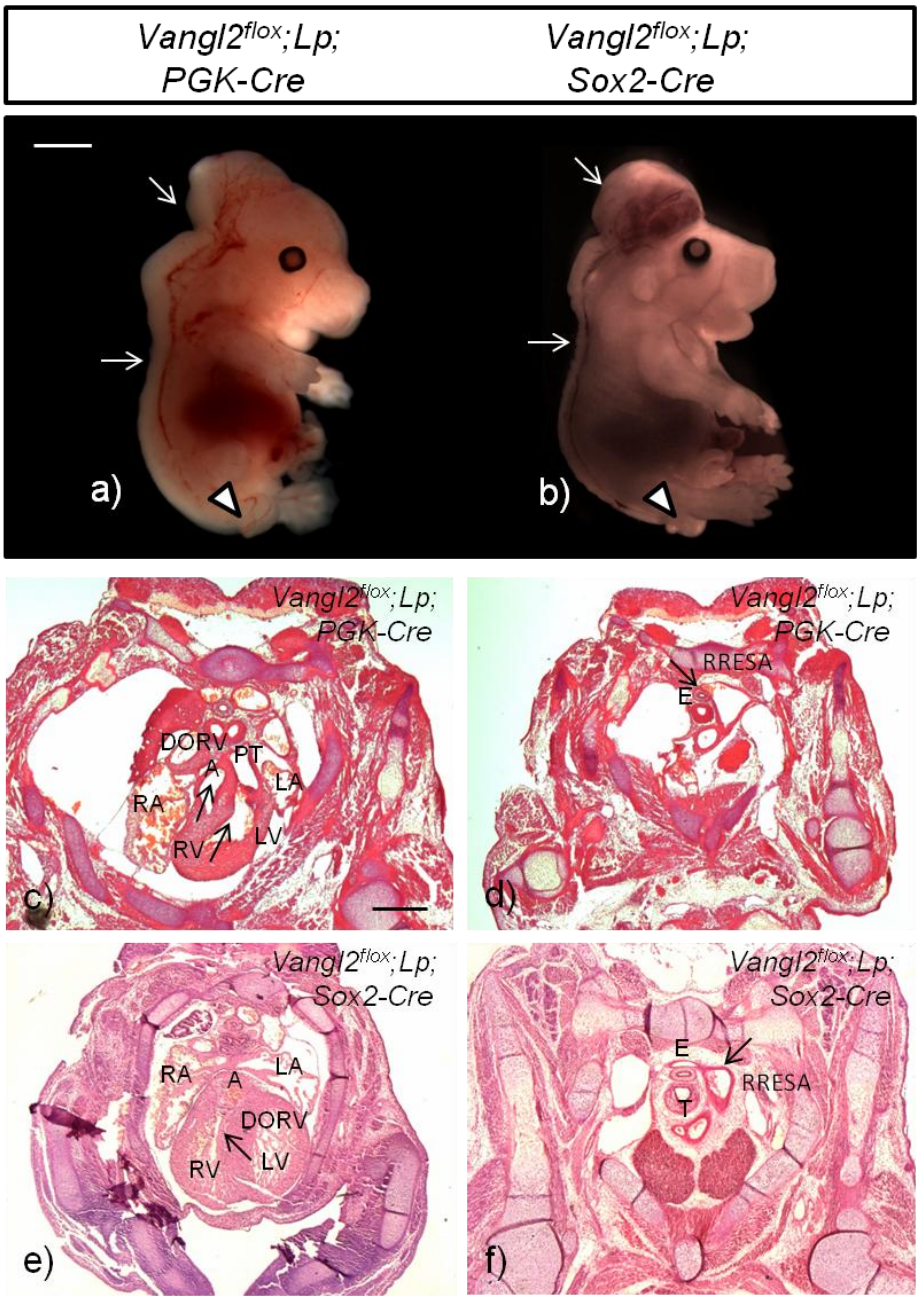

Figure 3.18: Neural Tube and Cardiovascular defects in *Vangl2^{flox};Lp;Cre* embryos at E14.5

a,b) Whole mount embryos from *Vangl2$^{flox/+}$;Cre* x *Lp/+* litter. *Vangl2^{flox};Lp;PGK-Cre* embryo (a) and *Vangl2^{flox};Lp;Sox2-Cre* embryo (b) showing external phenotypic defect, craniorachischisis (arrows showing open neural tube and arrowhead pointing at looped tail). Scale - 2000µm. **c-f)** Transverse sections of heart from *Vangl2^{flox};Lp;PGK-Cre* embryo showing double outlet right ventricle (c) and retroesophageal subclavian artery (d), and *Vangl2^{flox};Lp;Sox2-Cre* embryo showing double outlet right ventricle (e) and retroesophageal subclavian artery (f). Scale - 20µm. RA-right atria, LA-left atria, RV-right ventricle, LV-left ventricle, A-aorta, DORV-double outlet right ventricle, E-esophagus, RRESA- retroesophageal subclavian artery.

Thus, *Lp* and *Vangl2*^{flox} are allelic and both appear to act as loss of function/null mutations**.** Our results confirm that the *Vangl2*^{flox} allele, when knocked out globally, recapitulated *Lp* phenotype and subsequently was a useful tool for genetically dissecting the role of *Vangl2* in specific cell types.

3.2.5 *Vangl2* is not required in NCC for heart development

Studies have suggested that several extra-cardiac cell populations contribute in the development of heart and its remodelling. Neural crest cells (NCC) are essential for outflow tract development and are required for its septation and alignment (Anderson et al., 2012; Kirby et al., 1983; Phillips et al., 2013). Their ablation and functional disruption leads to a number of cardiovascular defects reflecting the various functions NCC perform during the process of cardiac development (Creazzo *et al.,* 1998).

The heart defects seen in *Lp* mice, like outflow defect and arch artery defects, are an indication that possibly NCC are also regulated by Vangl2 and loss of Vangl2 may cause abnormal behaviour of NCC leading to these defects. Although migration of NCC in *Lp/Lp* embryos is shown to be normal (Henderson *et al.*, 2001), it is essential to look at the role of *Vangl2* in NCC because the latter are playing a key role in outflow tract development.

To delete *Vangl2* specifically in NCC, *Wnt1-Cre* was used (Danielian *et al.*, 1998). As *Wnt1* is expressed in NCC very early and is turned off as the cells migrate away from the neural tube, *Wnt1-Cre* is frequently used for lineage tracing of NCC (Danielian *et al.*, 1998; Hutson and Kirby, 2007). Our aim was to determine if Vangl2 is required in NCC, and if any heart defects are observed in its absence from this cell type.

Crosses were set up between *Vangl2*$^{flox/+}$*;Wnt1-Cre* and *Vangl2*$^{flox/flox}$ mice (figure 3.19a) and embryos were collected at E14.5. Embryos were obtained with genotypes in accordance with expected Mendelian ratios. *Vangl2*$^{flox/flox}$*;Wnt1-Cre* were considered the mutants (n=8). Externally, these embryos were indistinguishable from the control littermates. Figure 3.19b shows

Vangl2$^{flox/+}$*;Wnt1-Cre* embryo (control) along with *Vangl2*$^{flox/flox}$*;Wnt1-Cre* embryos (mutant) (figure 3.19c). Table 3.7 summarizes the external phenotypic defects observed in *Vangl2*$^{flox/flox}$*;Wnt1-Cre* embryos.

Table 3.7: External phenotypic defects seen in *Vangl2*$^{flox/flox}$*;Wnt1-Cre* mutants at E14.5

Genotype	Number of embryos	Looped tail	Craniorachischisis	Spina bifida	Gastroschisis
Vangl2$^{flox/+}$*; Wnt1-Cre*	8/30	0	0	0	0
Vangl2$^{flox/flox}$*; Wnt1-Cre*	8/30	0	0	0	0

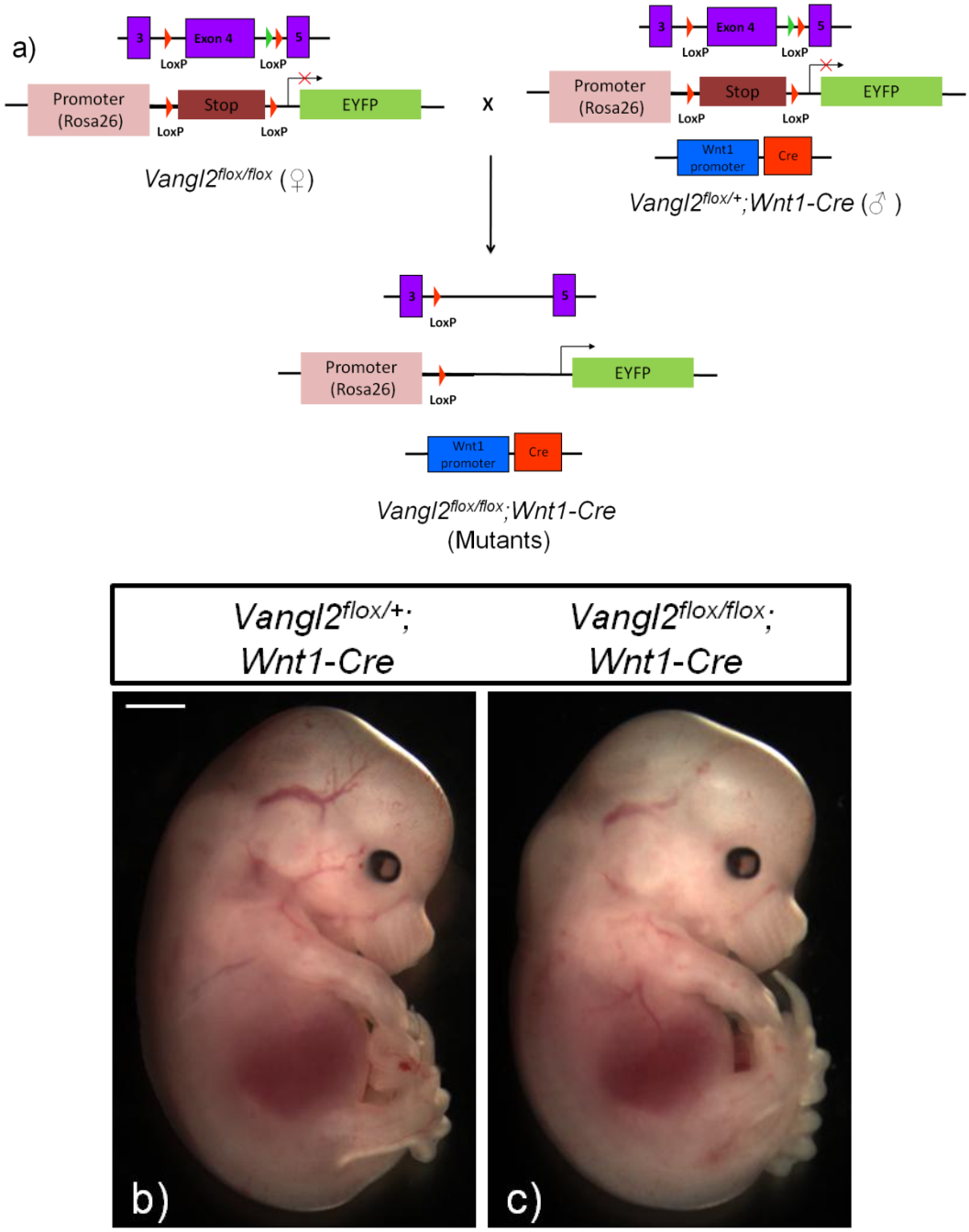

Figure 3.19: *Vangl2*^{flox} cross specifically within NCC, using *Wnt1-Cre*

a) *Vangl2*$^{flox/+}$*;Wnt1-Cre* x *Vangl2*$^{flox/flox}$ cross to have deletion of *Vangl2* gene specifically in NCC. **b)** Whole mount *Vangl2*$^{flox/+}$*;Wnt1-Cre* embryo with normal external phenotype. **c)** *Vangl2*$^{flox/flox}$*;Wnt1-Cre* embryo also showing normal external phenotypic. Scale - 2000µm.

After establishing that loss of *Vangl2* in NCC does not cause any external phenotypic defect, it was checked if any cardiac defects were present in the mutants. To look at the heart phenotype, embryos were embedded in wax and transverse sections through heart were taken (figure 3.20a), which were stained with H&E. The heart phenotype of controls as well as mutant embryos was normal with no outflow tract defect. Figure 3.20 shows heart section of *Vangl2*$^{flox/+}$*;Wnt1-Cre* (figure 3.20b) embryo with normal heart development with aorta coming out from left ventricle and complete interventricular septum fused with the outflow tract and atrio-ventricular cushions. Similarly, heart section of *Vangl2*$^{flox/flox}$*;Wnt1-Cre* emrbyo also showed normal heart development (figure 3.20c) with no double outlet right ventricle, ventricular septal defect or aortic arch defect as seen in *Lp/Lp* and global knock out of *Vangl2*. Ablation of NCC not only results in cardiovascular phenotype but non-cardiovascular phenotype is also reported, including hypoplasia or aplasia of the thymus (Bockman and Kirby, 1984), and formation of dorsal root ganglia (Epstein *et al.,* 2000). Results show that there is no hypoplasia or aplasia of thymus or abnormality in formation of dorsal root ganglia in *Vangl2*$^{flox/flox}$*;Wnt1-Cre* mutant embryos (figure 3.20f) when compared to *Vangl2*$^{flox/+}$*;Wnt1-Cre* control embryos (figure 3.20e).

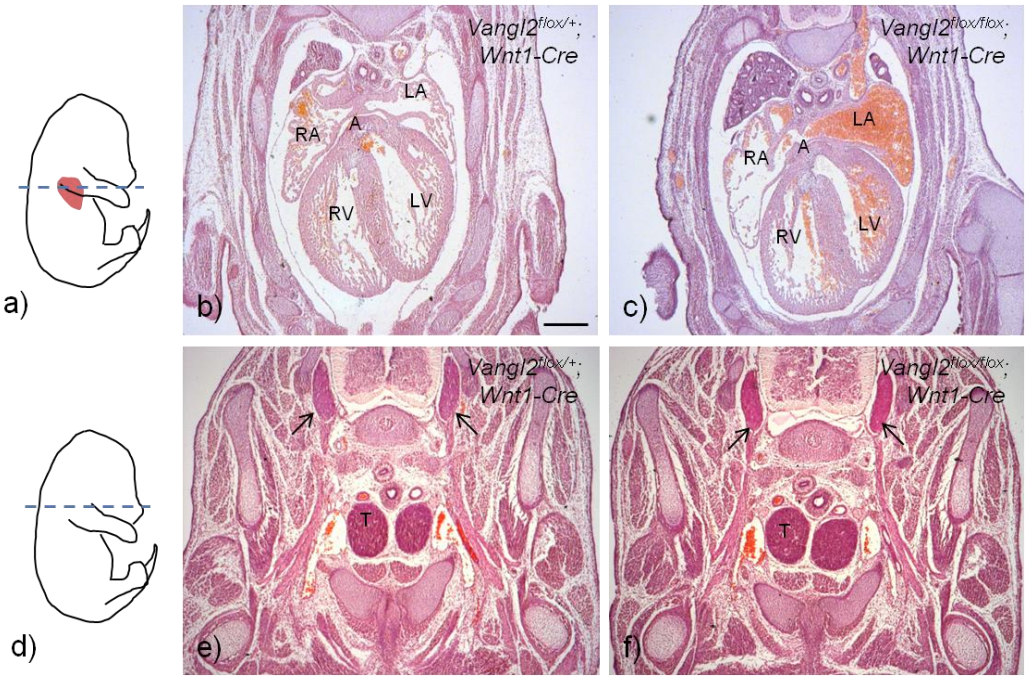

Figure 3.20: Cardiac phenotype and non-cardiac structures in *Vangl2^{flox};Wnt1-Cre* embryos at E14.5

Transverse sections of embryos from *Vangl2$^{flox/+}$;Wnt1-Cre* x *Vangl2$^{flox/flox}$* litter. **a)** Plane of the section. **b)** Transverse section through heart of *Vangl2$^{flox/+}$;Wnt1-Cre* embryo showing normal heart development. **c)** Heart section from *Vangl2$^{flox/flox}$;Wnt1-Cre* embryo also showing normal heart. **d)** Plane of the section. **e,f)** Transverse section shows normal thymus and dorsal root ganglia formation (arrow) in *Vangl2$^{flox/+}$;Wnt1-Cre* control embryos (e) as well as in *Vangl2$^{flox/flox}$;Wnt1-Cre* mutant embryo (f). RA-right atria, LA-left atria, RV-right ventricle, LV-left ventricle, A-aorta, PT-pulmonary trunk, T-Thymus. Scale - 20µm.

To confirm whether there was deletion of *Vangl2* in NCC by *Wnt1-Cre* recombination and to confirm whether Vangl2 is expressed in NCC, immunofluorescence was carried out to check for loss of Vangl2 expression in mutants and colocalization of NCC and Vangl2 in controls. Anti-GFP antibody was used to label cells expressing eYFP protein in the presence of *Cre*, *Wnt1-Cre* in this case, therefore labelling all NCC. Vangl2 antibody was used along with anti-GFP antibody to look at the expression of Vangl2 protein in NCC in 3 controls and 3 mutants. Embryos were collected at E9.5 while the heart is developing and cells are migrating into the outflow tract. Figure 3.21 shows *Vangl2*$^{flox/+}$*;Wnt1-Cre* heart section (figrue 3.21a) with eYFP expression (shown in green) and Vangl2 expression (shown in red). It appeared that NCC are not expression Vangl2 and co-expression cannot be seen (figure 3.21a). Heart sections of *Vangl2*$^{flox/flox}$*;Wnt1-Cre* (figure 3.21b) had eYFP and Vangl2 expression as observed in the control. This shows that Vangl2 is not expressed in NCC, which justifies the lack of outflow tract defect in *Vangl2*$^{flox/flox}$*;Wnt1-Cre* mutants.

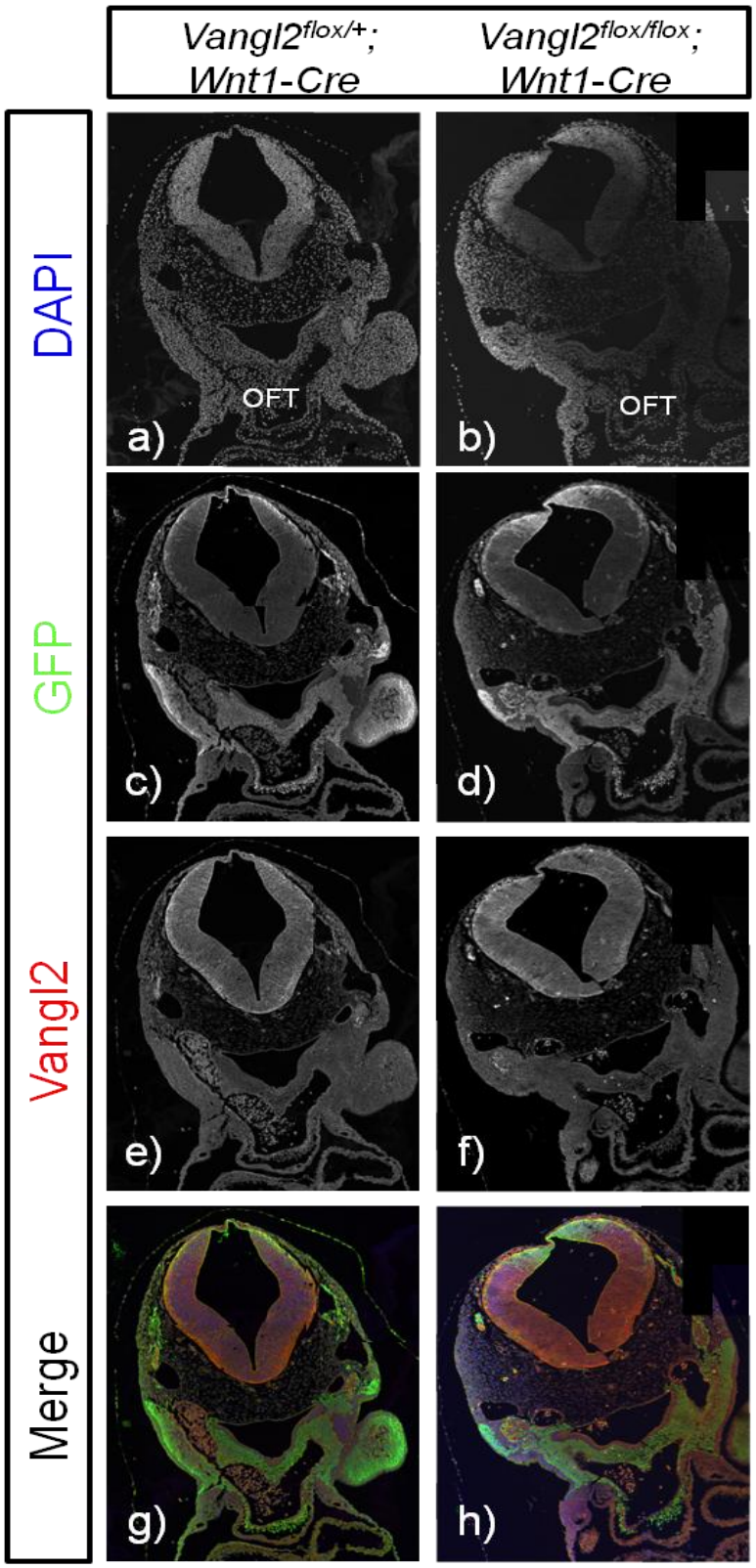

Figure 3.21: Vangl2 expression in NCC

a,b) Immunofluorescence for co-expression of *Wnt1-Cre* (GFP antibody) and Vangl2 in *Vangl2$^{flox/+}$;Wnt1-Cre* E9.5 embryo (a) and *Vangl2$^{flox/flox}$;Wnt1-Cre* embryo(b) where no co-expression is seen. OFT-outflow tract. Scale - 100µm.

To rule out any subtle defects because of loss of *Vangl2* from NCC and confirm that mutants were healthy and didn't have any heart defects or late onset defects, two litters were taken at post natal day (P) 28. These 4 weeks old mice were genotyped and mutants (n=4) were viable, healthy and indistinguishable from their control littermates. Their hearts were dissected out to compare the heart morphology of controls and mutants, which showed normal looking heart (figure 3.22a,b). Hearts were embedding in wax and sectioned transversally, then stained with H&E. Both the control (figure 3.22c) and mutant (figure 3.22d) showed normal outlets of aorta and pulmonary trunk from left ventricle and right ventricle respectively.

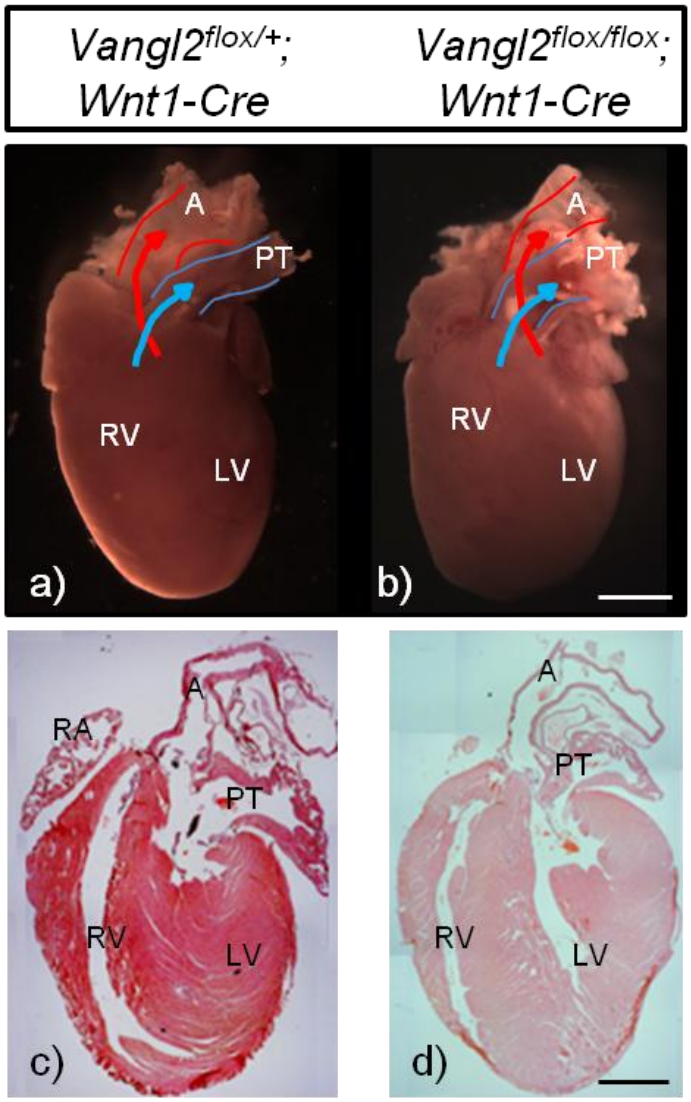

Figure 3.22: Adult heart of *Vangl2^{flox};Wnt1-Cre* mice at P28

a) Whole heart of *Vangl2$^{flox/+}$;Wnt1-Cre* adult mice (P28). **b)** Whole heart of *Vangl2$^{flox/flox}$;Wnt1-Cre* mutant adult mice (P28). Scale - 2000µm. **c,d)** Section of *Vangl2$^{flox/+}$;Wnt1-Cre* heart (c) and *Vangl2$^{flox/flox}$;Wnt1-Cre* heart (d). RA-right atria, RV-right ventricle, LV-left ventricle, A-aorta, PT-pulmonary trunk. Scale - 20µm.

Thus, the reason for no cardiac outflow tract or extra-cardiac abnormalities in *Vangl2$^{flox/flox}$;Wnt1-Cre* mutants that Vangl2 is not expressed in NCC. Hence, *Vangl2* is not required in NCC for normal cardiac outflow tract development.

3.2.6 *Vangl2* is indispensable in SHF cells for heart development

The cardiac defects seen in *Lp* embryos and our *Vangl2*^{flox} global knock out embryos (using *PGK-Cre* and *Sox2-Cre*) are double outlet right ventricle, ventricular septal defect and aortic arch defects and of these double outlet right ventricle in particular would require disturbance in alignment of aorta and pulmonary trunk to left and right ventricle respectively. In this particular region SHF cells are playing a key role in extension and alignment. These observations led us to think that *Vangl2* may be playing a key role in SHF cells and disruption in its expression is resulting in the defects.

To delete *Vangl2* specifically in SHF cells, *Isl1-Cre* was used (Yang *et al.*, 2006) which is a tissue specific *Cre* line targeting SHF cells. Crosses were set up between *Vangl2*$^{flox/+}$*;Isl1-Cre* and *Vangl2*$^{flox/flox}$ mice (figure 3.23a) and embryos were collected at E14.5. Embryos were genotyped to identify mutants and controls, as none of the embryos showed any external phenotypic defect. Of these *Vangl2*$^{flox/flox}$*;Isl1-Cre* were considered as mutants embryos. Figure 3.23 shows *Vangl2*$^{flox/+}$*;Isl1-Cre* control embryo (figure 3.23b) along with *Vangl2*$^{flox/flox}$*;Isl1-Cre* mutant embryo (figure 3.23c) (n=11) showing normal external phenotype of all embryos. Table 3.8 summarizes the external phenotypic defects observed in *Vangl2*$^{flox/flox}$*;Isl1-Cre* embryos.

Table 3.8: External phenotypic defects seen in *Vangl2*$^{flox/flox}$*;Isl1-Cre* mutants at E14.5

Genotype	Number of embryos	Looped tail	Craniorachischisis	Spina bifida	Gastroschisis
Vangl2$^{flox/+}$*; Isl1-Cre*	8/30	0	0	0	0
Vangl2$^{flox/flox}$*; Isl1-Cre*	8/30	0	0	0	0

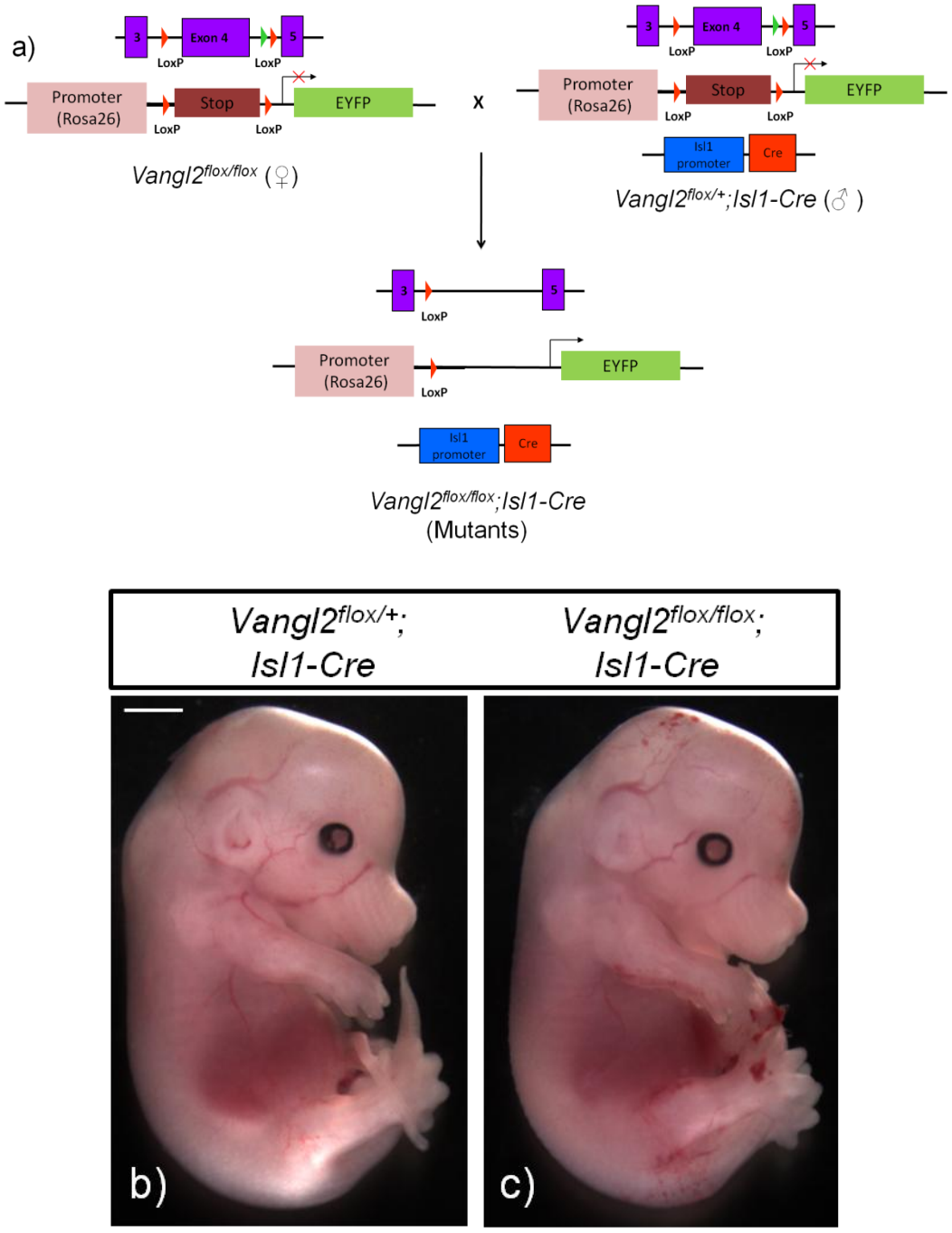

Figure 3.23: *Vangl2*^{flox} cross specifically within SHF cells, using *Isl1-Cre*

a) *Vangl2*$^{flox/+}$*;Isl1-Cre* x *Vangl2*$^{flox/flox}$ cross to have deletion of Vangl2 gene specifically in SHF cells. **b)** Whole embryo *Vangl2*$^{flox/+}$*;Isl1-Cre* at E14.5 with normal external phenotype. **c)** *Vangl2*$^{flox/flox}$*;Isl1-Cre* embryo at E14.5 also showing normal external phenotypic. Scale - 2000µm.

To look at the heart morphology of the embryos, they were embedded in wax and then sectioned transversally (figure 3.24a) and stained with H&E. *Vangl2*$^{flox/+}$*;Isl1-Cre* showed a normal heart phenotype (figure 3.24b), however heart sections of *Vangl2*$^{flox/flox}$*;Isl1-Cre* mutant embryos revealed they had double outlet right ventricle (figure 3.24c) and ventricular septal defect (figure 3.24d). These defects are same as seen in *Lp* mice and there was 100% penetrance of this phenotype in the mutants (table in figure 3.24). Although SHF cells enter the inflow tract as well as are responsible for formation of parts of atria, inflow defects like atrial septal defects were not observed in the mutants, along with no aortic arch defect, retroesophageal subclavian artery as seen in *Lp/Lp* (figure 3.4e).

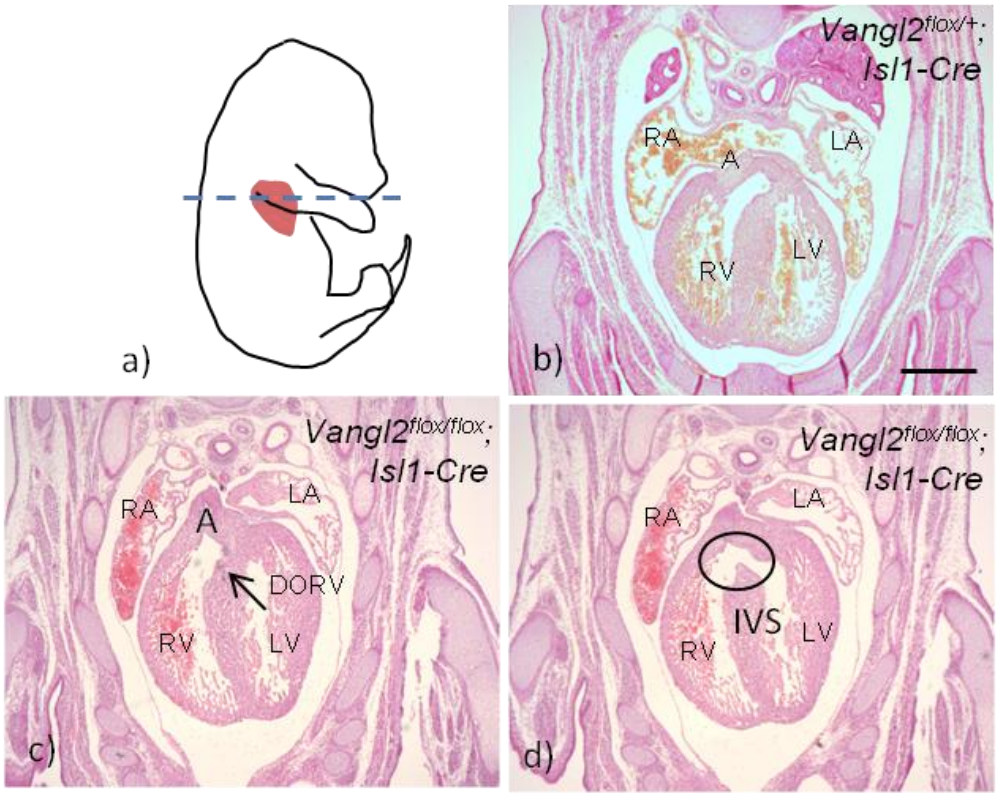

Cardiac defects seen in *Vangl2*$^{flox/flox}$;*Isl-Cre* embryos (n=11)	
DORV	11 (100%)
VSD	11 (100%)
RRESA	0 (0%)

Figure 3.24: Cardiovascular defects in *Vangl2*$^{flox/flox}$;*Isl1-Cre* embryos at E14.5

Transverse sections through heart of embryos from *Vangl2*$^{flox/+}$;*Isl1-Cre* x *Vangl2*$^{flox/flox}$ litter. **a)** Plane of the section. **b)** Transverse section through heart of *Vangl2*$^{flox/+}$;*Isl1-Cre* embryo showing normal heart development. **c,d)** Heart section from *Vangl2*$^{flox/flox}$;*Isl1-Cre* embryo showing double outlet right ventricle (c) and ventricular septal defect (d). Table shows different defects seen in *Vangl2*$^{flox/flox}$;*Isl1-Cre* embryos. Table RA-right atria, LA-left atria, RV-right ventricle, LV-left ventricle, A-aorta, DORV-double outlet right ventricle, VSD-ventricular septal defect, IVS-interventricular septum, RRESA- retroesophageal subclavian artery. Scale - 20µm.

Looking at our results it can be said that *Vangl2* is playing a key role in regulating SHF and its disruption specifically in SHF is leading to cardiac defects. However, to confirm that *Vangl2* was actually knocked out in these cells and had no Vangl2 expression, immunofluorescence labelling was done. Three controls and 3 mutant embryos were collected at a younger development stage, E9.5, when SHF cells are moving into the outflow tract. Embryos were embedding in wax and transverse sections were taken, which were immunofluorescently labelled using anti-GFP antibody to label eYFP protein in cells expressing *Cre*, along with Vangl2 antibody. Figure 3.25 shows *Vangl2*$^{flox/+}$*;Isl1-Cre* control embryo (figure 3.25a) with eYFP positive cells (SHF cells) in green while Vangl2 expression is seen in red. Regions which are yellow show the co-localization of SHF cells and Vangl2 (figure 3.25a arrows). It can be seen that in the outflow tract there is clear co-localization between SHF cells and Vangl2, showing that Vangl2 is expressed in these cells. When similar staining was done on *Vangl2*$^{flox/flox}$*;Isl1-Cre* mutant embryos (figure 3.25b) it was seen that there was no co-localization between *Cre* positive cells (SHF) and Vangl2, that is Vangl2 is not being expressed in SHF cells. Figure 3.25b shows that in the outflow tract there is green staining showing the presence of SHF, but there isn't any Vangl2 staining (shown in red, arrows). However in the same section Vangl2 staining can be seen in the neural tube and left ventricle where SHF cells are not present (figure 3.25c, arrows), confirming conditional knock out of *Vangl2*.

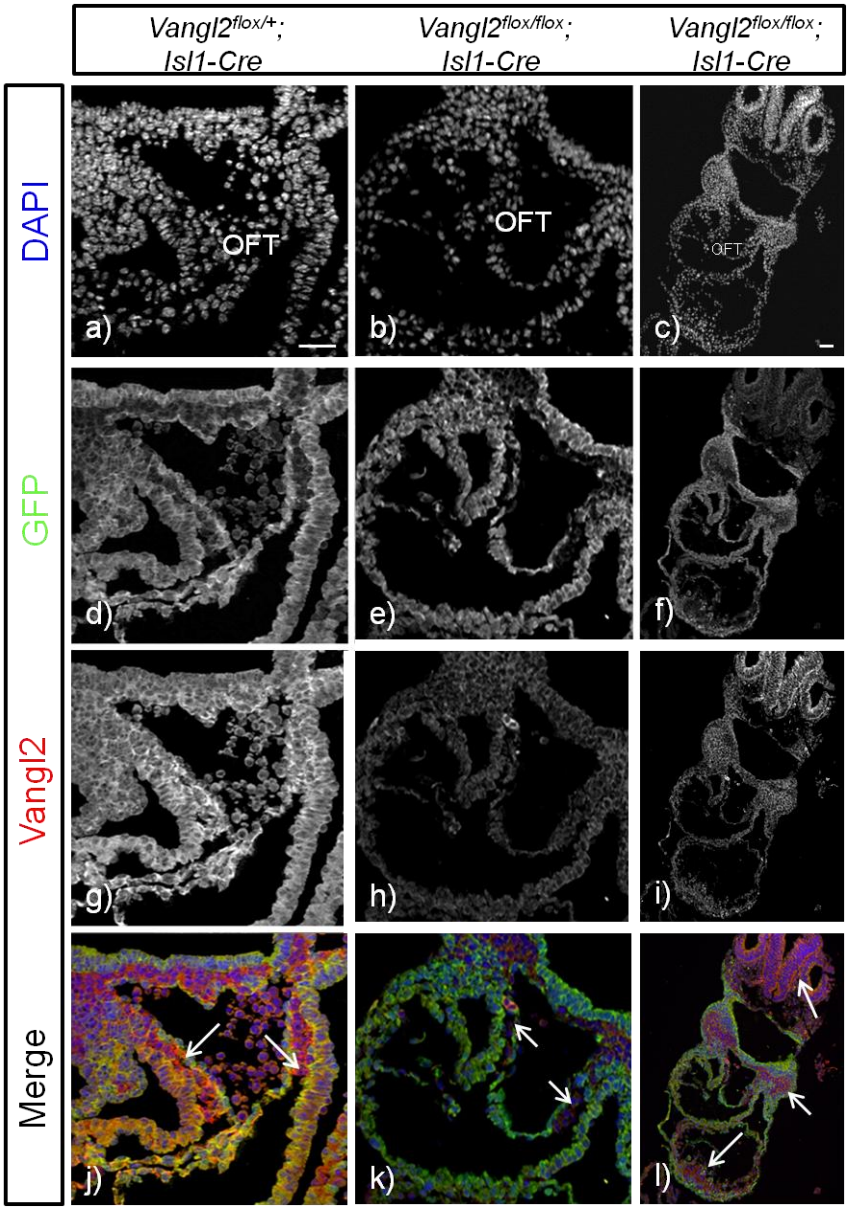

Figure 3.25: Vangl2 expression lost in SHF cells in the presence of *Isl1-Cre*

Different panels for Immunofluorescence for co-expression of *Isl1-Cre* (GFP antibody) and Vangl2 in *Vangl2$^{flox/+}$;Isl1-Cre* and *Vangl2$^{flox/flox}$;Isl1-Cre* embryo. **a,b,c)** DAPI marking nucleus of cells, showing outflow tract in *Vangl2$^{flox/+}$;Isl1-Cre* (a) and *Vangl2$^{flox/flox}$;Isl1-Cre* (b,c) section. **d,e,f)** GFP staining in *Vangl2$^{flox/+}$;Isl1-Cre* (d) and *Vangl2$^{flox/flox}$;Isl1-Cre* (e,f) showing similar expression of cells derived from SHF magnified in outflow tract (e) and whole section (f). **g,h,i)** Vangl2 staining in *Vangl2$^{flox/+}$;Isl1-Cre* (g) and *Vangl2$^{flox/flox}$;Isl1-Cre* (h,i) where no Vangl2 expression is seen in SHF cells magnified in outflow tract (h) and whole section (i). **j,k,l)** Coexpression of GFP and Vangl2 in *Vangl2$^{flox/+}$;Isl1-Cre* (j) with yellow regions (arrows) where both are expressed and *Vangl2$^{flox/flox}$;Isl1-Cre* (k,l) where no coexpression is seen (arrows in k showing outflow tract) and Vangl2 expression is seen in areas where SHF cells are not present (arrows in l showing neural tube, pharyngeal region and left ventricle).OFT-outflow tract. Scale - 100µm.

Thus, it is evident that deletion of *Vangl2* in SHF cells leads to double outlet right ventricle and ventricular septal defect as seen in *Lp* mice, but not retroesophageal subclavian artery, which confirms that *Vangl2* is regulating SHF cells in the outflow region of the heart and its absence leads to the defects observed.

3.2.6.1 Vangl2$^{flox/flox}$;Isl1-Cre mutants are able to survive

We were also interested in looking if these mutants would survive with these heart defects. Litters were taken and culled at P28 (4 weeks old mice). Interestingly the litter size was normal, but had a few mice which were quite small in size. The mice were ear clipped and genotyped and it was confirmed that the mice which were smaller in size were *Vangl2$^{flox/flox}$;Isl1-Cre*. Figure 3.26 shows the comparison of a *Vangl2$^{flox/+}$;Isl1-Cre* control mice and *Vangl2$^{flox/flox}$;Isl1-Cre* mutant mice in size and weight.

Cardiac defects seen in *Vangl2*$^{flox/flox}$;*Isl1-Cre* embryos (n=3)	
DORV	3 (100%)
VSD	3 (100%)
RRESA	0 (%)

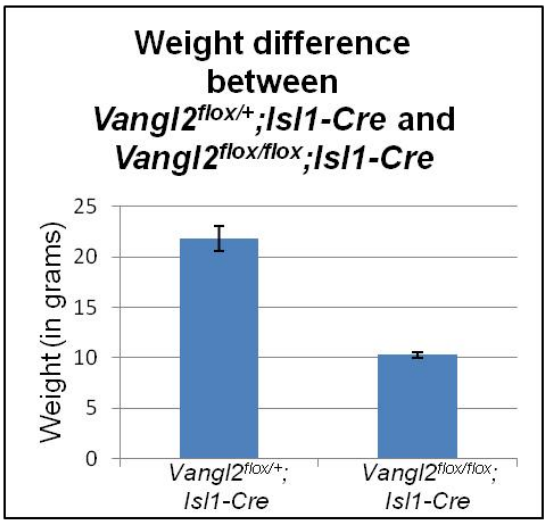

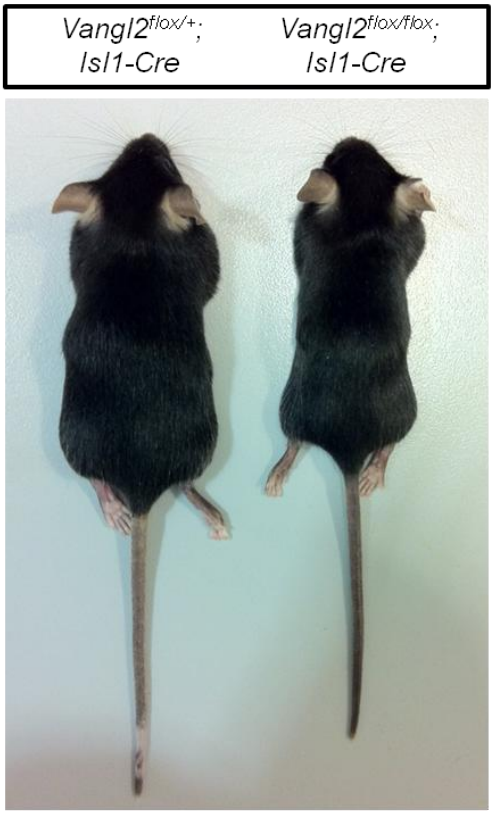

Figure 3.26: Adult mice from *Vangl2*^{flox}*;Isl1-Cre* litter at P28

Table shows the number of mutants got from 3 litters, 5/25 pups were *Vangl2*$^{flox/flox}$*;Isl1-Cre*, however 2 pups were dead at birth so couldn't be analysed. Adult mice shown with *Vangl2*$^{flox/+}$*;Isl1-Cre* as normal size and *Vangl2*$^{flox/flox}$*;Isl1-Cre* smaller in size and graph shows the difference in the weight of controls and mutants, with controls with normal weight and mutants lighter in weight.

To look if these mice had heart defects, the heart was dissected out. Figure 3.27 shows that in *Vangl2*$^{flox/+}$*;Isl1-Cre* mice the heart phenotype was normal and in figure 3.27a we can see that aorta and pulmonary trunk are coming out of left and right ventricles respectively. Whereas in *Vangl2*$^{flox/flox}$*;Isl1-Cre* it looked like both aorta and pulmonary trunk are coming out from the right ventricle (figure 3.27c). To confirm this, these adult hearts were embedded in wax, sectioned and stained with H&E. Sections confirmed that *Vangl2*$^{flox/+}$*;Isl1-Cre* heart section had aorta and pulmonary trunk coming out from left and right ventricle respective (figure 3.27b), and *Vangl2*$^{flox/flox}$*;Isl1-Cre* adult mice had double outlet right ventricle with both aorta and pulmonary trunk coming out from the right ventricle (figure 3.27d).

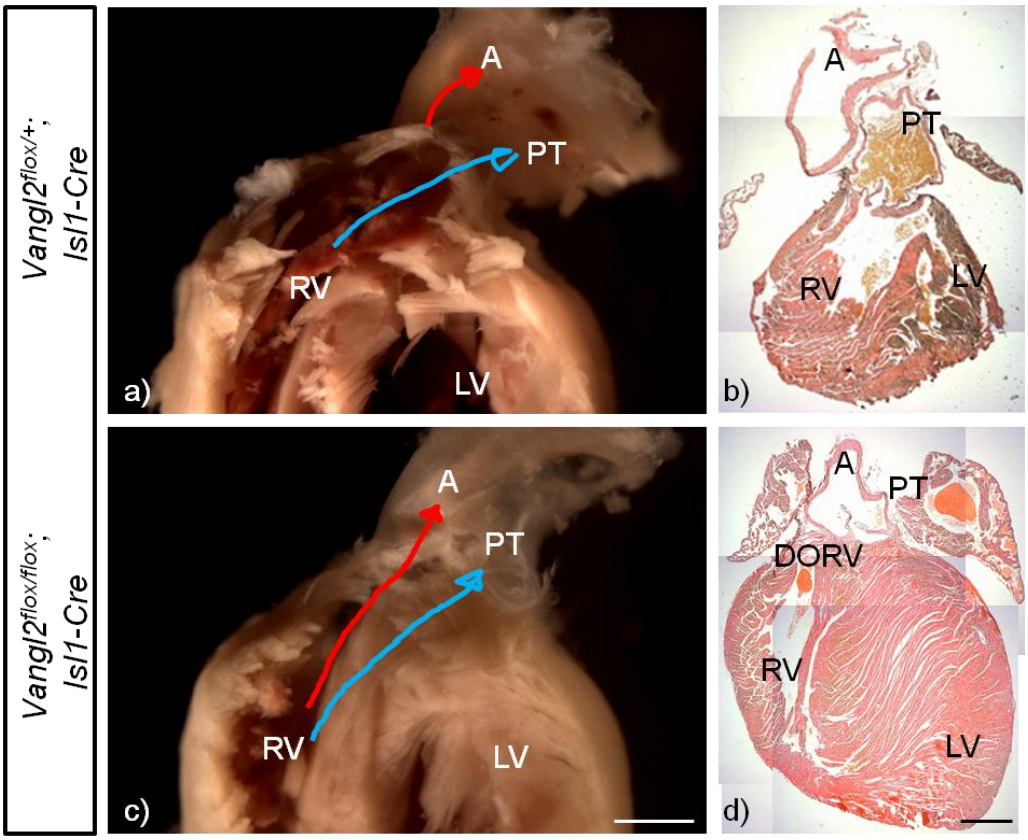

Figure 3.27: Heart phenotype of *Vangl2*^{flox}*;Isl1-Cre* adult mice

a) Whole heart of *Vangl2*$^{flox/+}$*;Isl1-Cre* control adult mice (P28). **c)** Whole heart of *Vangl2*$^{flox/flox}$*;Isl1-Cre* mutant adult mice (P28). Scale - 1000µm. **c,d)** Section of *Vangl2*$^{flox/+}$*;Isl1-Cre* heart (c) and *Vangl2*$^{flox/flox}$*;Isl11-Cre* heart (d) showing double outlet right ventricle. RA-right atria, LA-left atria, RV-right ventricle, LV-left ventricle, A-aorta, PT-pulmonary trunk, DORV-double outlet right ventricle. Scale - 20µm.

Thus, Vangl2 is expressed in SHF cells and is playing an essential role as its deletion in SHF cells (*Vangl2$^{flox/flox}$;Isl1-Cre*) leads to double outlet right ventricle and ventricular septal defect. Hence, *Vangl2* is required in SHF cells for normal cardiac outflow tract development.

3.2.7 *Vangl2* is required in undifferentiated precursor SHF cells

Undifferentiated SHF cells differentiate into myocardium and endothelial cells in the heart. Isl1-Cre labels all SHF cells; therefore, *Vangl2* was deleted specifically in ventricular myocardium by using *Mlc2v-Cre (Chen et al., 1998). Vangl2$^{flox/flox}$* mice were crossed with *Vangl2$^{flox/+}$;Mlc2v-Cre* mice and embryos were collected at E14.5. *Vangl2$^{flox/flox}$;Mlc2v-Cre* (n=7) were used as mutants after genotyping. They showed no external defects and were indistinguishable from their control littermates (figure 3.28a,b). Embryos were embedded in wax, sectioned transversally and H&E stained. Heart sections showed that there was no outflow defects in the mutants (figure 3.28c,d), indicating Vangl2 is not regulating differentiated SHF cells. Table 3.9 summarizes that there were no incidences of external or cardiac outflow tract defects when Vangl2 was deleted from ventricular myocardium.

Table 3.9: External phenotypic and cardiac defects in *Vangl2$^{flox/flox}$;Mlc2v-Cre* mutants at E14.5

Genotype	Number of embryos	External defects	Outflow defects
Vangl2$^{flox/+}$;Mlc2v-Cre	9/35	0	0
Vangl2$^{flox/flox}$;Mlc2v-Cre	7/35	0	0

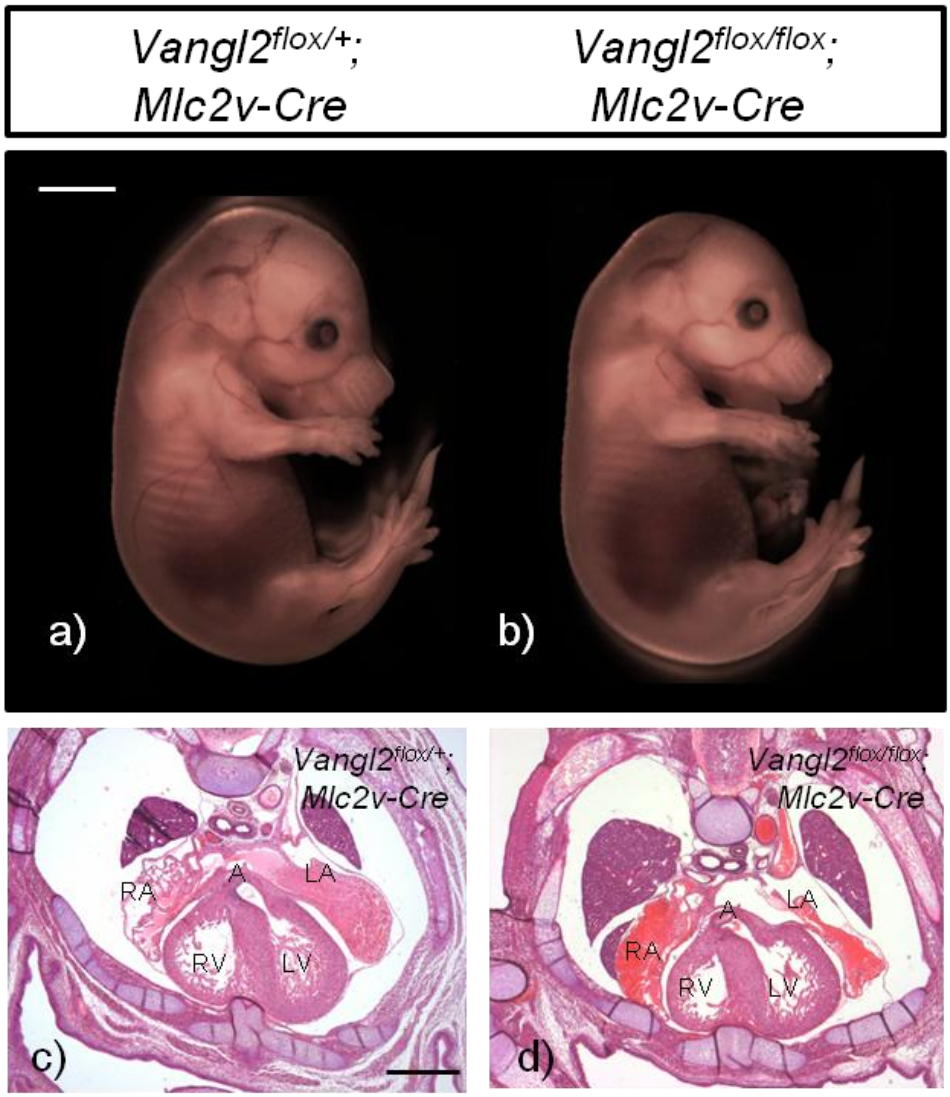

Figure 3.28: External and heart phenotype of *Vangl2^{flox};Mlc2v-Cre* embryos at E14.5

a,b) Whole embryo at E14.5 with normal external phenotype of *Vangl2$^{flox/+}$;Mlc2v-Cre* control embryo (**a**) and *Vangl2$^{flox/flox}$;Mlc2v-Cre* mutant embryo (**c**). Scale - 2000µm. **c**) Transverse section through heart of *Vangl2$^{flox/+}$;Mlc2v-Cre* control embryo showing normal heart development with aorta exiting left ventricle. **d**) Transverse section through heart of *Vangl2$^{flox/flox}$;Mlc2v-Cre* mutant embryo also showing no outflow tract defect. RA-right atria, LA-left atria, RV-right ventricle, LV-left ventricle, A-aorta. Scale - 20µm.

To check the importance of Vangl2 in endothelial cells, Tie2-Cre was used (Kisanuki *et al.*, 2001). *Vangl2*$^{flox/flox}$ mice were crossed with *Vangl2*$^{flox/+}$*;Tie-Cre* mice. Embryos were collected at E14.5 and genotyped. *Vangl2*$^{flox/flox}$*;Tie2-Cre* (n=4) mutant embryos had no external defects (figure 3.29b). However, 2 *Vangl2*$^{flox/flox}$*;Tie2-Cre* had craniorachischisis exhibiting full recombination, were excluded from the analysis. The 4 *Vangl2*$^{flox/flox}$*;Tie2-Cre* mutants(with no external defects) were further used to look at the heart morphology. Embryos were embedded in wax, sectioned transversally and H&E stained. Heart sections of both control and mutants showed normal outflow tract with aorta exiting left ventricle (figure 3.29c,d). Table 3.10 summarizes that there were no incidences of external or cardiac outflow tract defects when Vangl2 was deleted from endothelial cells.

Table 3.10: External phenotypic and cardiac defects in *Vangl2*$^{flox/flox}$*;Tie2-Cre* mutants at E14.5

Genotype	Number of embryos	External defects	Outflow defects
Vangl2$^{flox/+}$*;Tie2-Cre*	6/25	0	0
Vangl2$^{flox/flox}$*;Tie2-Cre*	4/25	0	0

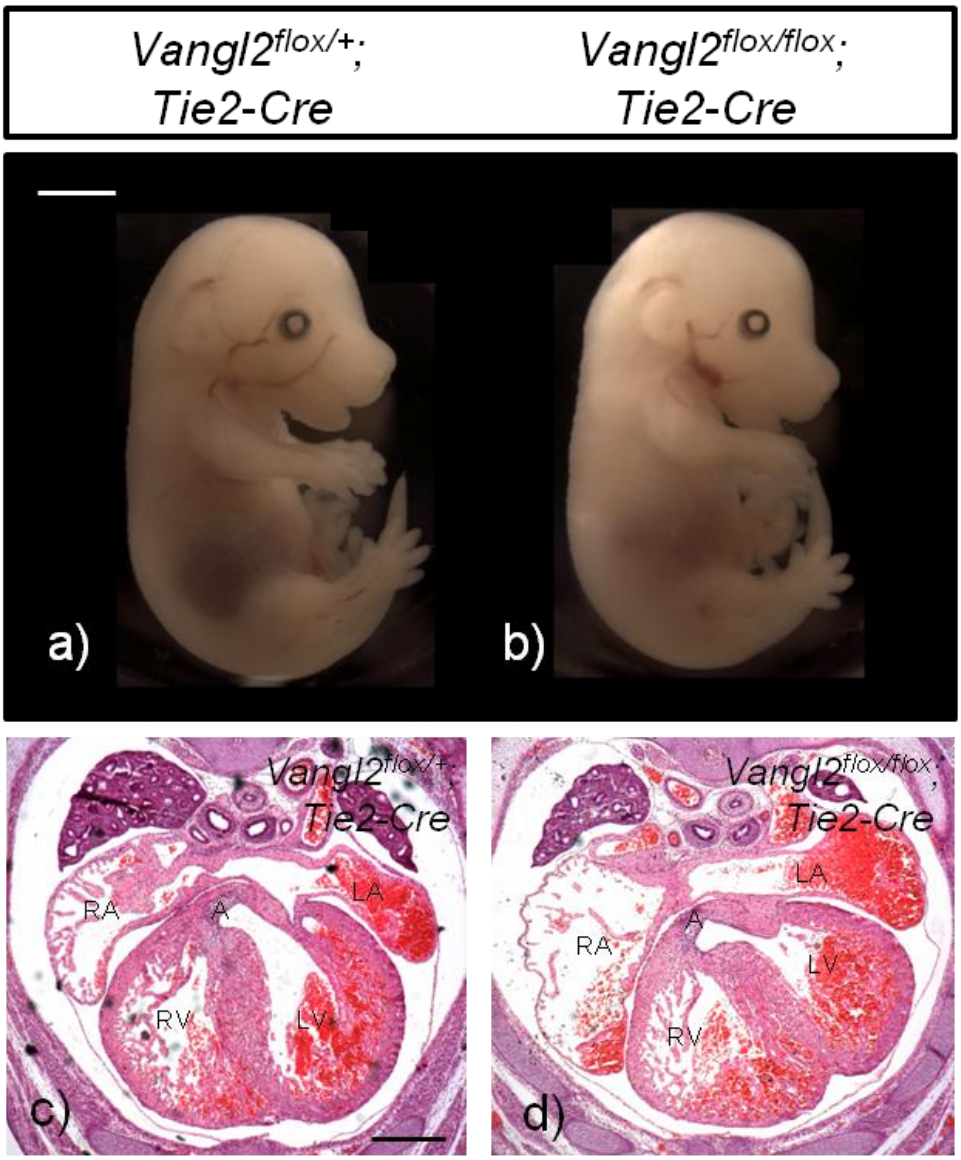

Figure 3.29: External and heart phenotype of *Vangl2^{flox};Tie2-Cre* embryos at E14.5

a,b) Whole embryo at E14.5 with normal external phenotype of *Vangl2$^{flox/+}$;Tie2-Cre* control embryo (**a**) and *Vangl2$^{flox/flox}$;Tie2-Cre* mutant embryo (**c**). Scale - 2000µm. **c**) Transverse section through heart of *Vangl2$^{flox/+}$;Tie2-Cre* control embryo showing normal heart development with aorta exiting left ventricle. **d**) Transverse section through heart of *Vangl2$^{flox/flox}$;Tie2-Cre* mutant embryo also showing no outflow tract defect. RA-right atria, LA-left atria, RV-right ventricle, LV-left ventricle, A-aorta. Scale - 20µm.

Deletion of *Vangl2* from myocardium derived from SHF cells and endothelial cells showed normal outflow tract development. Thus, defects like double outlet right ventricle and ventricular septal defect in *Vangl2*$^{flox/flox}$*;Isl1-Cre* suggests the importance of *Vangl2* in undifferentiated precursor SHF cells. Hence, *Vangl2* is required only in undifferentiated precursor SHF cells for normal cardiac outflow tract development.

3.3 Discussion

Lp mice are a naturally occurring *Vangl2* mutant and have been characterized with numerous developmental defects (Strong and Hollander, 1949; Henderson *et al.*, 2001; Montcouquiol *et al.*, 2003; Torban *et al.*, 2008). *Vangl2* is essential for normal heart development; however despite a thorough description of the cardiac defects in the *Lp/Lp* mutant (Henderson *et al.*, 2001), it is still to be established which cell type requires *Vangl2* signalling during outflow tract development and the role that *Vangl2* plays in these cells. The cardiac defects, double outlet right ventricle and ventricular septal defect, which are seen in *Lp/Lp* mutants, can be associated with CNCC or SHF abnormalities, given their role during outflow tract morphogenesis (Buckingham *et al.*, 2005; Hutson and Kirby, 2007). However it has been suggested previously that migration and differentiation of CNCC is normal in *Lp/Lp* and there is normal development of neural crest derived structures including cranial ganglia, dorsal root ganglia and thymus (Henderson *et al.*, 2001). SHF cells ablation also results in alignment defects of the outflow tract (Buckingham *et al.*, 2005), therefore it is possible that Vangl2 might also act in this cell type. An abnormality in heart looping during developmental stages can compromise remodelling and positioning of great vessels (aorta and pulmonary trunk) and ventricles leading to outflow tract defects like double outlet right ventricle and ventricular septal defect in *Lp/Lp* embryos (Henderson *et al.*, 2001). Therefore *Lp* mutants have a range of defects that overlap with those seen when either the contribution of neural crest cells, or the addition of second heart field cells to the heart being disrupted. To unravel which cell type out of NCC and SHF is responsible for this phenotype, *Vangl2*^{flox} mice were produced to delete *Vangl2* gene in particular cell types to dissect the tissue-specific requirement for *Vangl2* signalling in the developing heart.

The two aims of the chapter were to establish whether the *Vangl2*^{flox} line recapitulates the *Lp* phenotype and to reveal the requirement for the *Vangl2* gene specifically in NCC and cells derived from SHF. Initially, *Vangl2*^{flox} line had *neoR* cassette present in the construct, but as it was established that *Vangl2*^{neo} is a hypomorphic allele of *Vangl2* and that *neoR* disrupts the function of *Vangl2* gene.

The results show that in the presence of *neoR*, the external phenotype produced and the heart defects were similar to those seen in the *Lp/Lp* mutant. However, there were some variations with respect to external phenotype and lung morphology. Presence of *neoR* cassette on both alleles not only gives craniorachischisis but a variable external phenotype was also observed; where neural tube was open only at the tail region (known as spina bifida). This observation shows that *Vangl2* function is only reduced to certain extent giving a variable phenotype. Even in the absence of craniorachischisis, double outlet right ventricle was present in *Vangl2*$^{floxneo/floxneo}$ embryo, which shows that heart defects produced are not secondary to craniorachischisis. Therefore, it can be stated that in the *Vangl2*^{neo} mice produced, *neoR* disrupts the function of *Vangl2* and that *Vangl2*^{neo} is a hypomorphic allele of *Vangl2*, although it is yet to be studied to what extent the function is disrupted. Recently another hypomorph, *Vangl2R259L* has been reported to have a mild NTD phenotype (no craniorachischisis, just a looped or kinky tail in 47% and spina bifida in 12% homozygous mutant embryos (Guyot *et al.*, 2011)). This mutant also lacked other PCP phenotypes including outflow tract defects in the heart, failure of eyelid closure, severe ear polarity defects, and imperforate vagina in affected females as seen in homozygous *Lp* mutants (Henderson *et al.*, 2001). This milder functional defect suggests that dosage is an important modulator of the severity of the PCP defective phenotypes (Guyot *et al.*, 2011). Therefore, because of the different natures of different hypomorphs, the extent of gene level of expression should be established.

These results add further evidence to the current literature that the presence of a *neoR* cassette can disrupt the gene function resulting in a hypomorphic mutation. Although it is not certain if the *Vangl2* function is disrupted because of the *neoR* cassette causing abnormal and divergent splicing or affecting through some other mechanism. Looking together at the genetic and molecular results, it is confirmed

that the external phenotype and heart phenotype of embryos with *neoR* cassette are similar to *Lp* but not as severe. Hence, *neoR* was removed for further experiments so that a universal or tissue specific *Cre* could be used to completely knockout *Vangl2* in all body cells or specific tissues respectively.

To establish the efficiency of our *Vangl2*^{flox} line, *PGK-Cre* was used to delete *Vangl2* from all body cells to establish whether it recapitulates the *Lp* phenotype. *Vangl2* deletion with *PGK-Cre* resulted in embryos with neural tube defects same as in *Lp/Lp* mutants, and also heart defects including double outlet right ventricle, retroesophageal subclavian artery and ventricular septal defect were observed. However, our results from western blotting showed a Vangl2 band in the *Vangl2*$^{flox/flox}$*;PGK-Cre* mutant, suggesting that *PGK-Cre* may not be expressed in all body cells. However, it must be quite widely expressed as its recombination gives the full *Lp/Lp* phenotype. It has been reported that *PGK-Cre* expression is not uniform (McBurney *et al.*, 1994). A study used X-gal staining to recognize *PGK-LacZ* transgene observed that at different embryonic developmental stages the intensity of staining varied and expression was widespread but was not uniform (McBurney *et al.*, 1994). Therefore it seems that it is the *PGK-Cre* which isn't expressed 'universally' and not that our *Vangl2*^{flox} line isn't suitable for our purpose.

Therefore, another universally expressing *Cre*, *Sox2-Cre* was used. Looking at the RNA expression level, protein level and embryo phenotype it is established that *Vangl2*$^{flox/flox}$*;Sox2-Cre* results in successful recombination and marked deletion of *Vangl2*. We saw the same external phenotypic and cardiac abnormalities in *Vangl2*$^{flox/flox}$*;Sox2-Cre* mutants as in *Vangl2*$^{flox/flox}$*;PGK-Cre* and *Lp/Lp* mutants. This suggests that for our purpose *PGK-Cre* is acceptable to use as it clearly deleted expression in the relevant heart forming regions, however on the basis of the results, it is clear that *Sox2-Cre* mediated recombination is more effective compared to *PGK-Cre* recombination.

The nature of the *Lp* mutation is not clear, if it is null mutation or dominant negative. Loss of Vangl2 protein from samples isolated from *Lp/Lp* brain indicate *Lp* is a null mutation (Montcouquiol *et al.*, 2006), however another study has

shown *Lp* intercrossed with *Vangl2* knockout mice line had severe defects in the inner ear than *Vangl2* knockout homozygotes and the mutant protein produced altered the distribution of Vangl1 and Pk2 along with Vangl2, suggestive dominant negative nature of *Lp* mutation during inner ear development (Yin *et al.*, 2012). A similar analysis is done keeping heart development as reference and *Lp* were intercrossed with *Vangl2* knockouts (with *PGK-Cre* and *Sox-Cre*) and results show that external and heart phenotype was same in *Lp/Lp, Vangl2$^{flox/flox}$;PGK-Cre, Vangl2$^{flox/flox}$;Sox2-Cre, Vangl2^{flox};Lp;PGK-Cre* and *Vangl2^{flox};Lp;Sox2-Cre* embryos. Thus, *Lp* and *Vangl2^{flox}* are allelic and both appear to act as loss of function/null mutations during heart development.

To check which cell type requires Vangl2, tissue specific *Cre* lines were used and as SHF and NCC are important for normal heart development and we hypothesis that *Vangl2* plays a key role in their movement and polarization through non-canonical Wnt PCP pathway. When *Vangl2* was deleted only in NCC, no external or heart defects were observed, confirming that *Vangl2* is not required in NCC, which are contributing to the development of the heart. Although there is evidence that planar cell polarity is required for NCC migration and function in *Xenopus*, zebrafish and chick (De Calisto *et al.*, 2005; Carmona-Fontaine *et al.*, 2008a; Matthews *et al.*, 2008; Shnitsar and Borchers, 2008; Sisson and Topczewski, 2009; Banerjee *et al.*, 2011; Topczewski *et al.*, 2011; Theveneau *et al.*, 2013; Ulmer *et al.*, 2013; Mayor and Theveneau, 2014), a similar role in mammals is still to be established. However there are reports of loss of PCP components in NCC leading to cardiac defects in mice (Thomas *et al.*, 2010; Phillips *et al.*, 2013), the results here show that *Vangl2* is not regulating NCC. Defects in NCC can lead to a range of outflow tract anomalies like common arterial trunk and double outlet right ventricle, of which double outlet right ventricle is a characteristic feature of *Lp* cardiac phenotype, but they also exhibit common arterial trunk (Henderson *et al.*, 2001; Anderson *et al.*, 2012).

When *Vangl2* was specifically deleted only in SHF cells, embryos showed heart defects but the external phenotype was normal. Similar heart defects were observed as seen in *Lp/Lp* mutants but with normal external phenotype, which adds to the conclusion that heart defects are primary and not secondary to the

neural tube defects. Because the heart defects seen in *Lp* mice were recapitulated when *Vangl2* was specifically deleted in SHF, it can be said that *Lp* mice is a SHF mutant with respect to heart development. Although, the aortic arch abnormality, retroesophageal subclavian artery seen in *Lp, Vangl2*$^{flox/flox}$*;PGK-Cre* and *Vangl2*$^{flox/flox}$*;Sox2-Cre* mutants, may be secondary to the neural tube defects or abnormalities in body form, as they are only observed in the presence of craniorachischisis. SHF cells can be present in undifferentiated precursor state or in differentiated state. Deletion of *Vangl2* in differentiated myocardium and endothelial cells showed that Vangl2 is not required in differentiated SHF cells, but only regulates and plays an important role in proginetor SHF cells.

SHF cells play a role in outflow tract alignment with the ventricles, and if these cells behave abnormally, their function is hampered which might lead to alignment of outflow tract being disturbed leading to double outlet right ventricle. No inflow defects were seen in *Vangl2*$^{flox/flox}$*;Isl1-Cre* mutants, therefore from the results, it can be concluded that *Vangl2* is indispensable in SHF for outflow tract development and is acting as a key regulator of SHF cells. Another PCP protein, Dvl2 has also been shown to regulate SHF cells for outflow tract development (Sinha *et al.*, 2012), indicating importance of PCP in SHF. It can also be stated that SHF do not contribute to the neural tube defects but are responsible for heart morphogenesis. Co-localization of Vangl2 with SHF cells was done. It was observed that there is co-localization between Vangl2 and SHF in the cells of the dorsal pericardial wall, distal outflow tract, and the differentiated myocardium of the right ventricle of the heart concluding that these cells express Vangl2 in respective regions of heart and validates the histological results observed showing heart defects in *Vangl2* SHF mutants. This set of results established the key role *Vangl2* plays in SHF which led us to characterize these cells and their behaviour in presence as well as absence of *Vangl2*. The mechanism and the reason behind these changes in cellular behaviour need to be established, which will form the basis of next chapter.

Chapter 4

Characterization of SHF phenotype – Loss of *Vangl2* disrupts polarity in SHF cells

4.1 Introduction

The requirement for the PCP gene *Vangl2* specifically in SHF and how the loss of Vangl2 function in these cells impacts on the morphogenesis of the cardiac outflow tract was established in the previous chapter. This chapter seeks to establish how loss of *Vangl2* affects the polarisation, organisation, and maturation of SHF derived cells.

During heart development, SHF reside in the anterior pharynx and move together into the poles (both venous/inflow and arterial/outflow) of the heart after formation of the linear heart tube (Kelly *et al.*, 2001; Snarr *et al.*, 2007) (figure 4.1a). These cells do not migrate individually but as a sheet of cells moving together (Van Den Berg *et al.*, 2009), which is similar to the movement of epithelial cells in other organs (Guillot and Lecuit, 2013). Figure 4.1c (red arrows) illustrates SHF cells in the heart at both outflow and inflow tracts on a sagittal section through an embryo at E9.5 (figure 4.1b), while figure 4.1e (red arrows) shows SHF cells only in the outflow tract on a transverse section (figure 4.1d) at E9.5. Similarly to *Lp/Lp* mutants, *Vangl2*$^{flox/flox}$*;Isl1-Cre* mutants had the alignment defect, double outlet right ventricle, therefore the outflow region was focussed upon to study the pattern and behaviour of SHF in this region. Hence figure 4.1e was taken as reference section for all the analysis and experiments to understand cellular behaviour in the outflow tract.

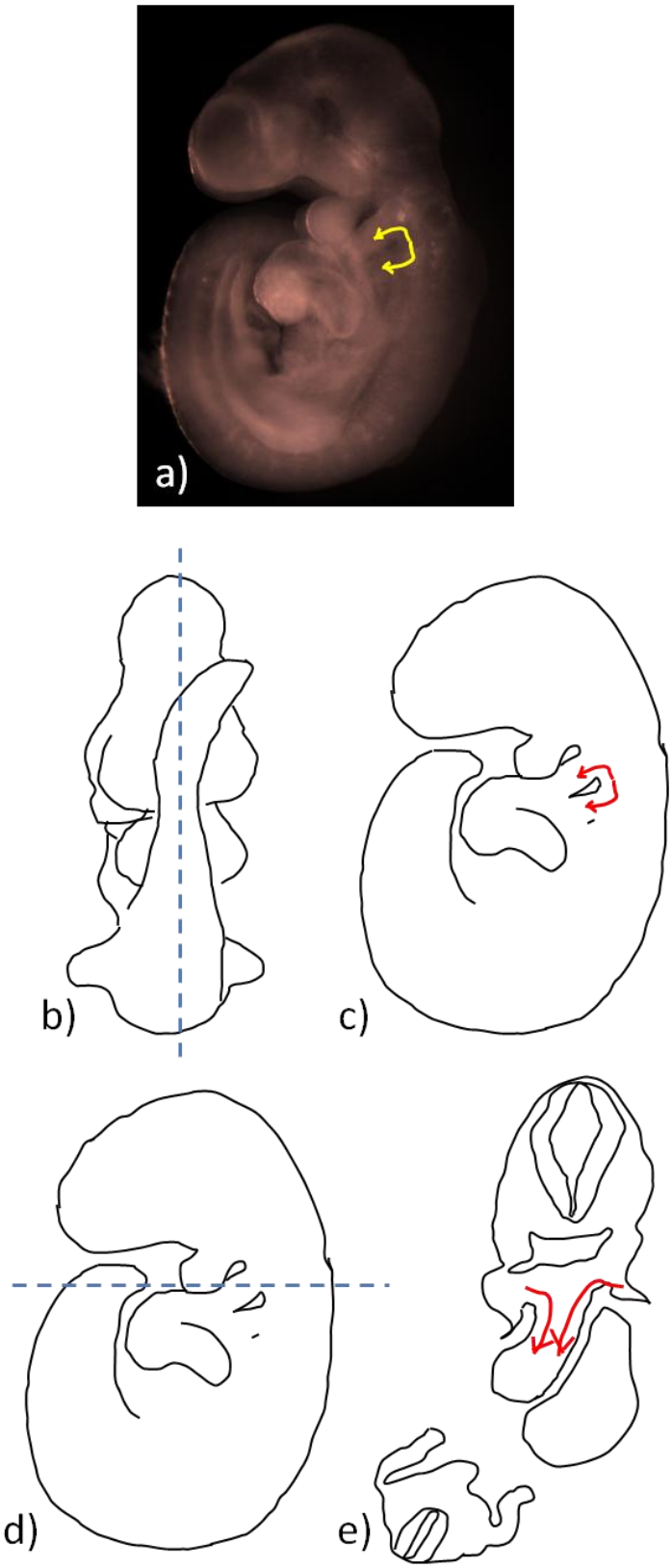

Figure 4.1: Movement of SHF into the developing heart at E9.5

a) E9.5 embyro with arrows showing the direction in which SHF cells move into the developing heart through the outflow and inflow. **b)** Plane of sagittal section shown in **(c)**. **d)** Plane of transverse section shown in **(e)**.

SHF remain in their precursor state for a longer duration as compared to FHF, with prolonged expression of Isl1, whereas in the FHF Isl1 is expressed only transiently (Cai *et al.*, 2003). Previous work in *Lp/Lp* mutants in the Henderson lab by Dr Jun Hong Rhee, showed that there is disorganisation of *Isl1* positive cells in the distal outflow tract instead of normal uniform distribution in the outflow tract wall. The expression of Isl1 at E9.5 in SHF indicates they are still in precursor state in the distal outflow tract and work on *Lp/Lp* suggests that there could be a movement defect/delay. Therefore, it was important to understand the movement of SHF cells in control embryos and see if it changes in mutants. As Vangl2 is a polarity protein and cell polarity plays an important role in directional movement of the cells and their organization, it was considered relevant to look at the polarity of SHF derived cells while they are entering the outflow tract. The possible reason for the disorganisation of SHF derived cells in the distal outflow tract in *Lp/Lp* mice could be the disruption in polarity of cells.

Epithelial cells are compartmentalised into apical and basal sides, also known as apical-basolateral polarity (ABP). This division between the compartments is regulated by presence of adherens junctions (AJ) and tight junctions (TJ), which are present at the border of apical and basolateral domain (Kaplan *et al.*, 2009). The basal side of a cell is where it is attached to the basement membrane and its attachment to the adjoining cells is at the lateral side (Figue 4.2). The AJ, apart from dividing the cell into two compartments, are also responsible for cell-cell adhesion and migration by improving cell coordination during collective migration and promote cell motility by transducing signals that actively participate in controlling directed cell migration and providing polarity cues (Etienne-Manneville, 2012). SHF cells instead of migrating as an individual cells, move as a sheet of cells exhibiting epithelial nature (Van Den Berg *et al.*, 2009) and cell polarity regulates both collective and individual cell movements during developmental stages (Muñoz-Soriano *et al.*, 2012). Apart from ABP, epithelial cells also exhibit planar cell polarity (PCP), which involves asymmetric localization of core PCP components like Vangl2. The functional link between ABP and PCP, and their requirement for normal embryonic development is well established (Djiane *et al.*, 2005).

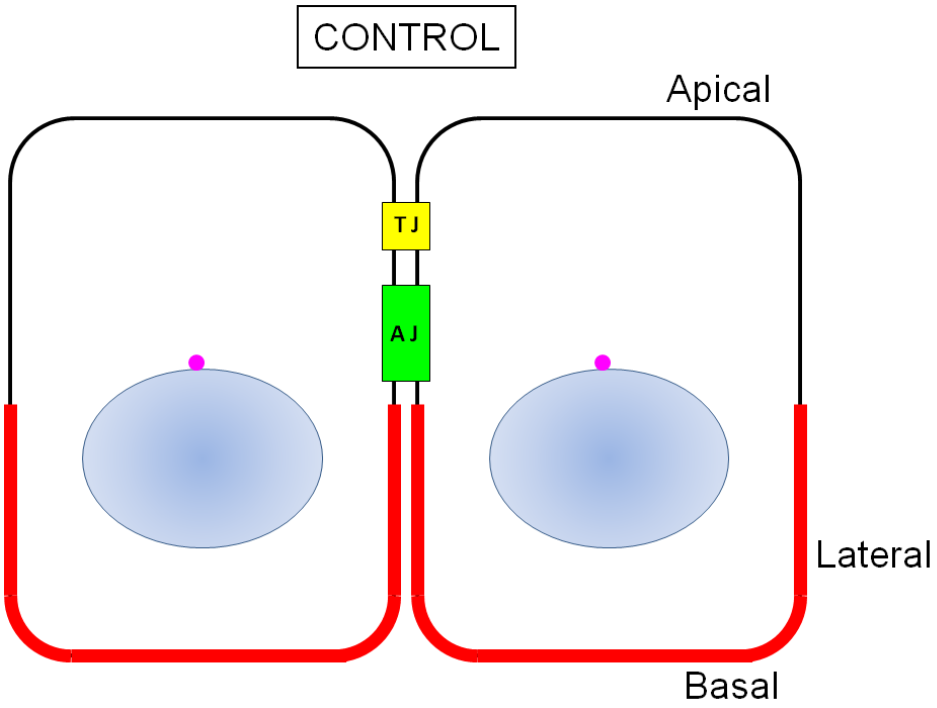

Figure 4.2: Apical-Basolateral Polarity in epithelial cells

Cells exhibiting apical-basolateral polarity with adherens junctions and tight junctions dividing the cell into apical and basal compartments. TJ-tight junction, AJ- adherens junction.

E-cadherin, N-cadherin and β-catenin are components of AJ (Tepass, 2002; Hartsock and Nelson, 2008). Cadherins are the heart of these junctions; they are present on membrane and recruit β-catenin onto their intracellular regions. β-catenin forms an association with α-catenin that binds to actin filaments (James Nelson, 2008). This complex organises and regulates actin cytoskeleton and plays important role in cell-cell adhesion and movement (James Nelson, 2008). Another protein, vinculin, is also associated with AJ along with establishment of focal adhesion and its loss prevents cell adhesion by formation of fewer focal adhesions and a decrease in spreading of cells (Goldmann and Ingber, 2002).

Apart from AJ, there are TJ present just above the AJ (figure 4.2). Recent studies have revealed the importance of the PAR-PKCζ complex in cell polarity (Joberty *et al.*, 2000; Lin *et al.*, 2000; Ohno, 2001). In mammalian epithelial cells PAR-3, PAR-6, and PKCζ colocalize and form a complex in the apical most part of the

cell where TJ are formed. This ternary complex co-localizes with TJ protein ZO-1 (Suzuki *et al.*, 2001). Point mutation in PKCζ (PKCζ-kn, dominant negative form of PKCζ which lacks kinase activity) leads to mislocalization of PAR3 and PAR6 along with TJ proteins Z0-1, occludin and claudin-1 (Ohno, 2001). Also there is mislocalization of apical and basolateral membrane proteins because of loss of PCKζ activity. These studies confirm that PCKζ is required for the establishment of epithelial cell polarity.

To look at the ABP of SHF, AJ and TJ markers were examined and also markers which were specific to each compartment. This was done by looking at components of AJ (E-cadherin, N-cadherin and β-catenin), different polarised cell organelles like microtubule organising centre (MTOC) (Magdalena *et al.*, 2003) which is specific to the apical domain (MTOCs shown as pink dots in figure 4.2), laminin and fibronectin which are extracellular markers present at the basal side of the cell, and polarity marker PKCζ which is present in TJ and is also responsible for the formation of AJ (Colosimo *et al.*, 2010). Fibronectin is an extracellular matrix molecule that is involved in cell-matrix adhesion and migration and has been implicated to play a role in the localization, composition and functioning of AJ (Lefort *et al.*, 2011). Laminin is also involved in adhesion and cell migration and is present in basal lamina, which is one of the layers of basement membrane (Timpl *et al.*, 1979).

Apart from ABP, cells also exhibit PCP. Vangl2 is a part of PCP complex, along with other polarity proteins, like Dvl2 and Celsr1, which work in coordination with Vangl2. Therefore all these markers were shortlisted to look at the polarity of SHF.

Finally, this chapter focuses on the SHF derivatives. SHF can give rise to three major cell lineages of the heart: cardiomyocytes, smooth muscle cells and also endothelial cells (Moretti *et al.*, 2006). Different markers, specific for each derivative, were used to analyse if there is any difference in their expression in control and mutant embryos.

As SHF are important for normal heart development and deletion of *Vangl2* specifically in these cells leads to the outflow tract defect, double outlet right

ventricle, it was hypothesised that Vangl2 plays a key role in their organization, movement and polarization through non-canonical Wnt/PCP pathway.

4.2 Results

4.2.1 Transition of SHF from precursor state to differentiated cells in distal outflow tract

Previous work on *Lp* mice suggested that there might be a defect in organisation of SHF as they enter the distal outflow tract from the dorsal pericardial wall, as there was disorganisation of *Isl1* positive cells in the distal region in *Lp/Lp* mutants as compared to controls, along with a shortened outflow tract at E10.5 (figure 4.3a-d red arrows) (Ramsbottom et al, 2014). Isl1 antibody labels all cells which are actively expressing Isl1. In SHF there is persistent expression of Isl1, which is subsequently down regulated as cells differentiate (Cai *et al.*, 2003), meaning that Isl1 marks SHF in their precursor state. It was expected that similar phenotype would be seen in *Vangl2*$^{flox/flox}$*;Isl1-Cre* mutants as in *Lp/Lp*, and to confirm this, a similar experiment was performed on *Vangl2*$^{flox/flox}$*;Isl1-Cre* mutants at E10.5 similarly to *Lp* embryos, using an Isl1 antibody.

Embryos were collected at E10.5 and were embedding in wax. Sections were taken in traverse orientation as shown in figure 4.1e. Isl1 antibody expression in *Vangl2*$^{flox/flox}$*;Isl1-Cre* mutant embryos was similar to *Lp/Lp* mutant embryos, appearing disorganised in the distal outflow tract (figure 4.3g,h red arrows) as compared to control (figure 4.3e,f red arrows). Isl1 antibody expression was analysed on 3 control and 3 mutant embryos and similar results were seen. This supported the probable abnormality in SHF in the absence of Vangl2. It was also observed that the mutants had shortened outflow tract (figure 4.3g black double sided arrow) and the outflow tract wall was thicker (figure 4.3h black double sided arrow), as compared to controls (figure 4.3e,f black double sided arrow).

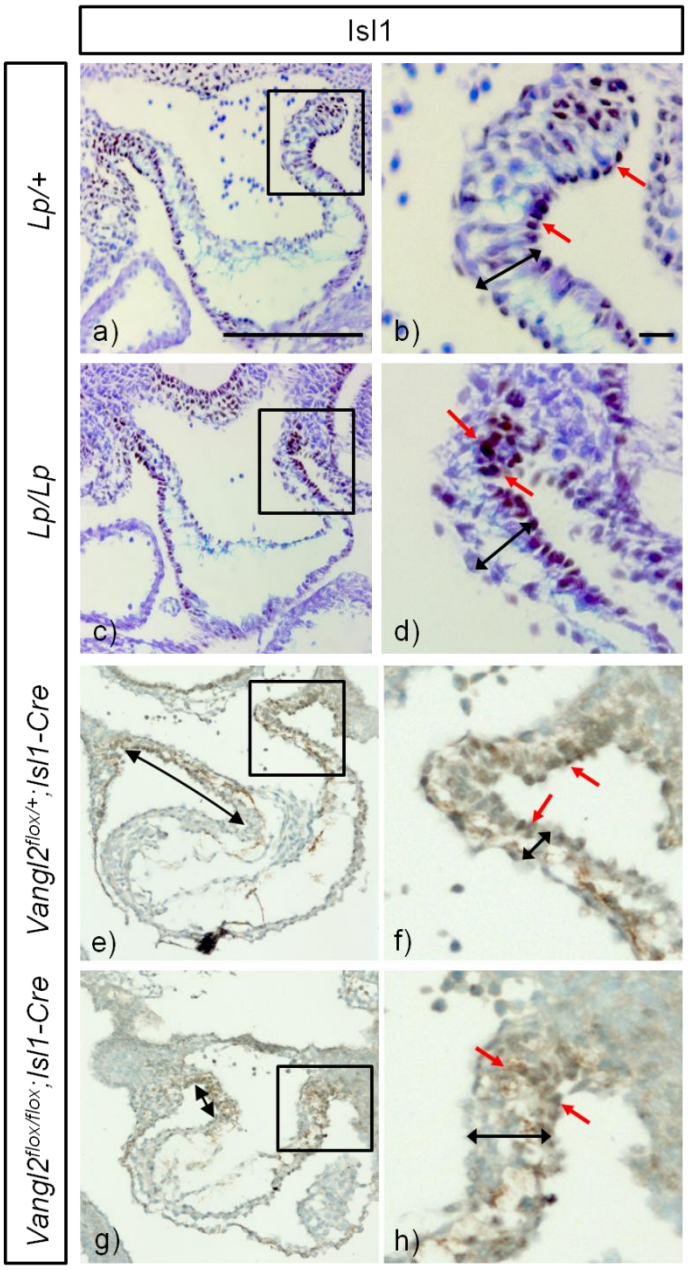

Figure 4.3: Disorganisation of Isl1 positive SHF cells in distal outflow tract at E10.5

Isl1 antibody staining to mark SHF actively expressing Isl1. The box represents the magnified region. **a,b)** SHF expressing Isl1 (brown cells) in an organised manner in the distal outflow tract in *Lp/+* embryo and higher magnification in b (red arrows). **c,d)** Disorganisation of Isl1 positive cells in distal outflow tract of *Lp/Lp* embryo with cells arranged is a disorganised manner in d (red arrows) (Images taken by Dr Hong Jun Rhee). **e-h)** Similar expression was seen in *Vangl2^{flox};Isl1-Cre* control and mutant embryos, with SHF cells expressing Isl1 in the distal outflow tract in *Vangl2$^{flox/+}$;Isl1-Cre* embryo (e, f red arrows) and disorganised Isl1 positive cells in distal outflow tract of *Vangl2$^{flox/flox}$;Isl1-Cre* embryo (g, h red arrows) with a shorter and thicker outflow tract as compared to control (black double sided arrows in e-h). Scale - 100µm.

SHF cells enter the outflow tract in the precursor state, but differentiate as they move proximally to form the outflow tract myocardium and ventricular myocardium. While Isl1 marks the SHF in precursor state, expression of myosin heavy chain (marked by MF20) marks the differentiated myocardium derived from SHF cells. Therefore, MF20 was used to mark differentiated SHF. Transverse sections of wax embedded E9.5 embryos when stained with MF20 showed no expression in dorsal pericardial wall, and started with low expression in the distal outflow tract and became stronger towards the proximal outflow tract when all of the cells were fully differentiated in *Vangl2*$^{flox/+}$*;Isl1-Cre* control embryo (figure 4.4e,f arrowheads) (n=3). MF20 expression overlapped with Isl1 expression in the distal outflow tract, and this overlapping region was termed as Transition Zone, which marked the transition of undifferentiated SHF cells into differentiated cardiomyocytes (figure 4.5). In *Vangl2*$^{flox/flox}$*;Isl1-Cre* mutant embryo there was no gradual increase in MF20 expression, but an abrupt appearance was observed (figure 4.4g,h arrowhead) (n=3). Hence, transition zone appeared to be shifted distally in *Vangl2*$^{flox/flox}$*;Isl1-Cre* mutants.

Dr Simon Ramsbottom looked at Isl1 expression in *Vangl2*$^{flox/flox}$*;Isl1-Cre* mutant embryo and compared it with *Vangl2*$^{flox/+}$*;Isl1-Cre* control embryo (n=3). It was observed that nuclear expression of Isl1 was lost more distally in the mutants as compared to controls (figure 4.4c,d arrows), indicating loss of precursor phenotype earlier in mutants as compared to controls (figure 4.4a,b arrows).

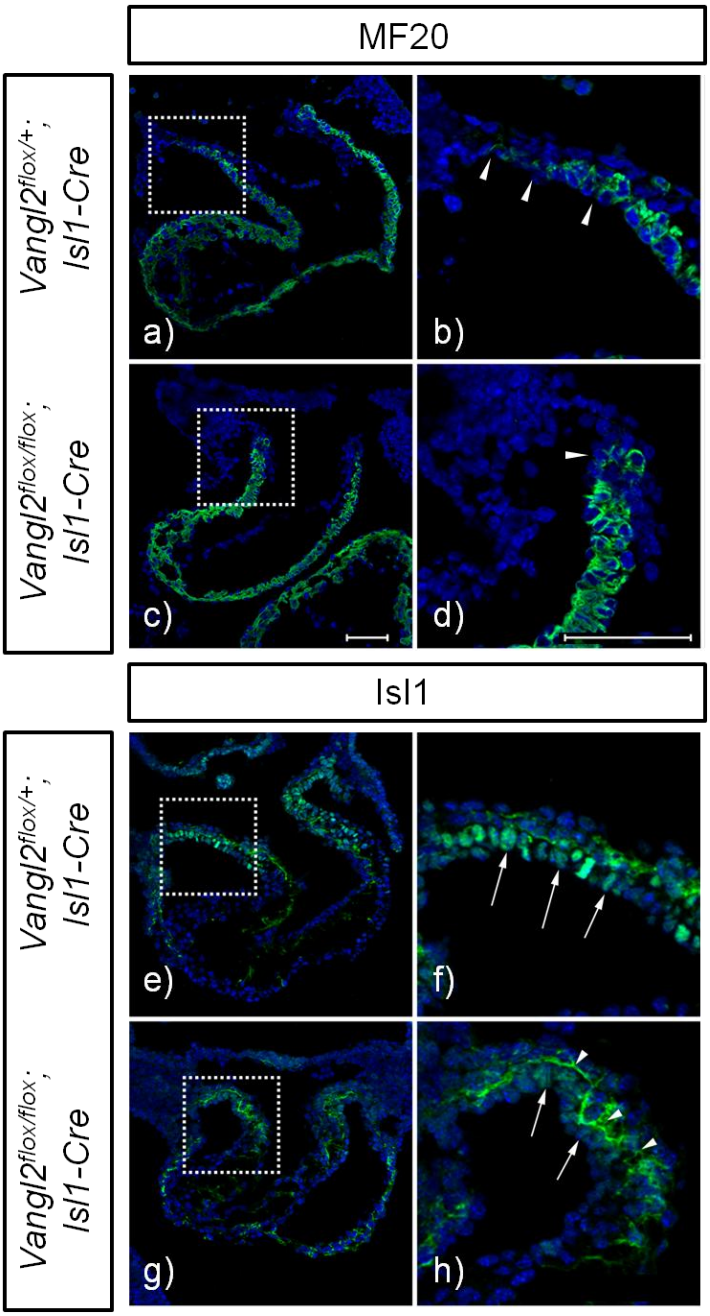

Figure 4.4: Loss of SHF precursor phenotype in distal outflow tract at E9.5

Isl1 and MF20 labeling precursor and differentiated SHF respectively. The box represents the magnified region. **a,b)** MF20 expression marking cardiomyocytes in *Vangl2*$^{flox/+}$*;Isl1-Cre* control embryo with gradual increase in expression to a more stronger expression from distal to proximal outflow tract (arrowheads in b). **c,d)** Abrupt appearance of strong MF20 expression in *Vangl2*$^{flox/flox}$*;Isl1-Cre* mutant embryo more distally (arrowheads in d). **e,f)** Isl1 expression in *Vangl2*$^{flox/+}$*;Isl1-Cre* control embryo showing nuclear expression of Isl1 in the distal outflow tract and expression going off as cells move proximally (arrows in f). **g,h)** Loss of nuclear expression of Isl1 in the distal outflow tract of *Vangl2*$^{flox/flox}$*;Isl1-Cre* mutant embryo (arrows in h). Images were taken by Dr Simon Ramsbottom. Scale - 100µm.

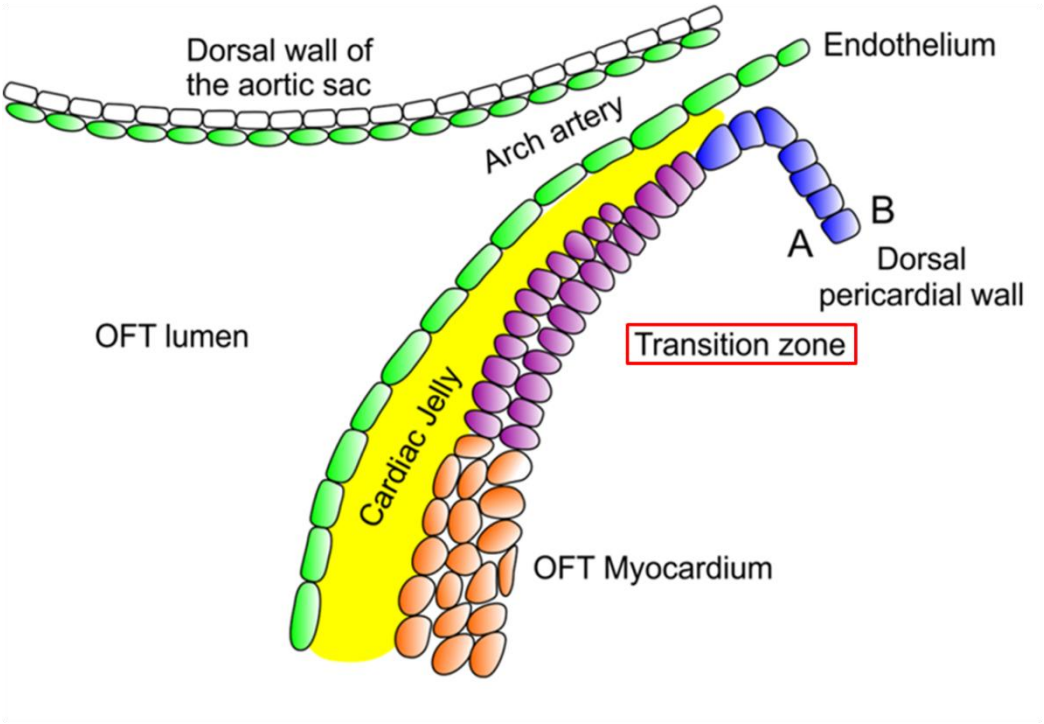

Figure 4.5: Transition Zone (undifferentiated SHF cells into differentiated cardiomyocytes)

Representation of Transition zone with SHF in progenitor state entering from dorsal pericardial wall into the distal outflow tract and differentiates into myocardium while moving proximally. OFT-outflow tract.

4.2.2 Expression of Vangl2 in the transition zone

In the previous chapter it was established that there was co-localization between Vangl2 and *Isl1-Cre* expressing SHF using Vangl2 and GFP antibody (figure 3.24). Vangl2 expression was seen in the undifferentiated precursor SHF in the distal outflow tract and in the differentiated myocardium of the proximal outflow tract and ventricles. To address the abnormality seen in SHF derived cells in the distal outflow tract, Vangl2 expression was examined in that region. Interestingly, Vangl2 expression in *Vangl2*$^{flox/+}$*;Isl1-Cre* controls was not uniform in all the cells analysed in sections from 3 embryos at E9.5. Figure 4.6b-d shows that the expression of Vangl2 changes in SHF at different positions in the outflow tract. Vangl2 expression localized to cell membrane in the distal outflow tract as these precursor cells enter the outflow tract (figure 4.6b,c1-3 arrowheads) and changes to cytoplasmic as the cells move to the proximal outflow tract and reach the right ventricle and differentiate into myocardium (figure 4.5b,d1-3). SHF changes from epithelium while entering into heart, into myocardium as they reach right ventricle. Change in Vangl2 expression in the transition zone can be seen as representation in figure 4.5a. Localisation of Vangl2 at the cell membrane supports the idea that cells are polarised in the distal outflow tract.

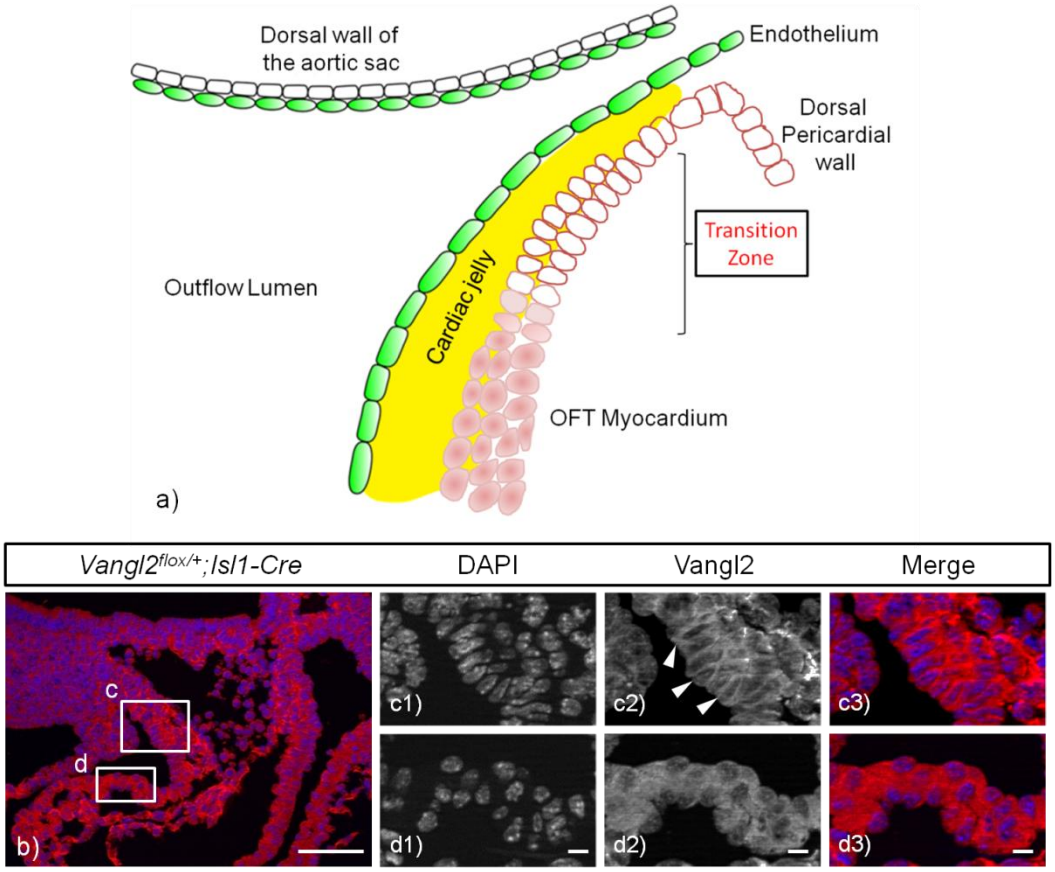

Figure 4.6: Vangl2 expression in transition zone at E9.5
a) Representation of Transition zone with SHF cells in progenitor state entering from dorsal pericardial wall into the distal outflow tract and differentiates into myocardium while moving proximally. **b)** Representation of Vangl2 expression in the transition zone with being localised to cell membrane in the zone but becoming cytoplasmic in the differentiated SHF cells. **c)** Vangl2 antibody staining (in red) showing change in expression as SHF cells moves towards proximal outflow tract and right ventricle with membrane localized expression in the transition zone (d arrowheads, box in c representing the magnified region) and cytoplasmic expression after that (e, box in c representing the magnified region). OFT-outflow tract. Scale - 100µm.

4.2.3 SHF cell behavior in absence of *Vangl2*

It was shown that during outflow tract development, SHF derived cells appear disorganised in the distal outflow tract in *Vangl2$^{flox/flox}$;Isl1-Cre* mutants. To understand the reason behind this, it was important to look at cellular behaviour in this region. SHF cells move from the mesothelial dorsal pericardial wall into the distal outflow tract as a sheet of epithelial cells. Vangl2 expression during this is membrane localised (figure 4.6), indicating PCP might be acting at this point as in other epithelial structures. It is important for the cells to possess polarity which helps them in their adhesion and movement. As Vangl2 is a polarity protein, its loss could possibly affect cell polarity. Therefore, we hypothesised that loss of *Vangl2* in SHF leads to disruption in cellular polarity. To confirm this, markers which are responsible for cell polarity along with indicators of polarity were looked at.

4.2.3.1 Adherens Junctions disrupted in absence of Vangl2

AJ help in cell-cell adhesion and also in giving apical-basal polarity to cells. AJ consist of the cadherin–catenin complex (Niessen, 2007). Therefore, expression of E-cadherin, N-cadherin and β-catenin was checked at to look at the position of AJ in the transition zone in distal outflow tract. E-cadherin is a classical epithelial markers and its presence in the outflow tract confirmed that tissue is the distal outflow tract is epithelium. Previous work has shown that mutation in PCP components, *Scribble* and *Wnt11* causes mis-expression of N-cadherin and β-catenin (Phillips *et al.*, 2007; Nagy *et al.*, 2010), which makes it more likely that AJ might be affected by the loss of *Vangl2*.

E-cadherin, N-cadherin and β-catenin expression was investigated on *Vangl2$^{flox/+}$;Isl1-Cre* controls and *Vangl2$^{flox/flox}$;Isl1-Cre* mutants at E9.5 (n=3), while the SHF derived cells enter into the outflow tract. Embryos were wax embedded, sectioned transversally and labeled individually with N-cadherin, E-cadherin and β-catenin antibodies. In the distal outflow tract, N-cadherin expression was seen in the cell membrane with strong apical staining in controls (figure 4.7a-h arrowheads). However in the mutants, this localization was lost and

uniform expression and distribution at the cell membrane was seen (figure 4.7i-p arrowheads).

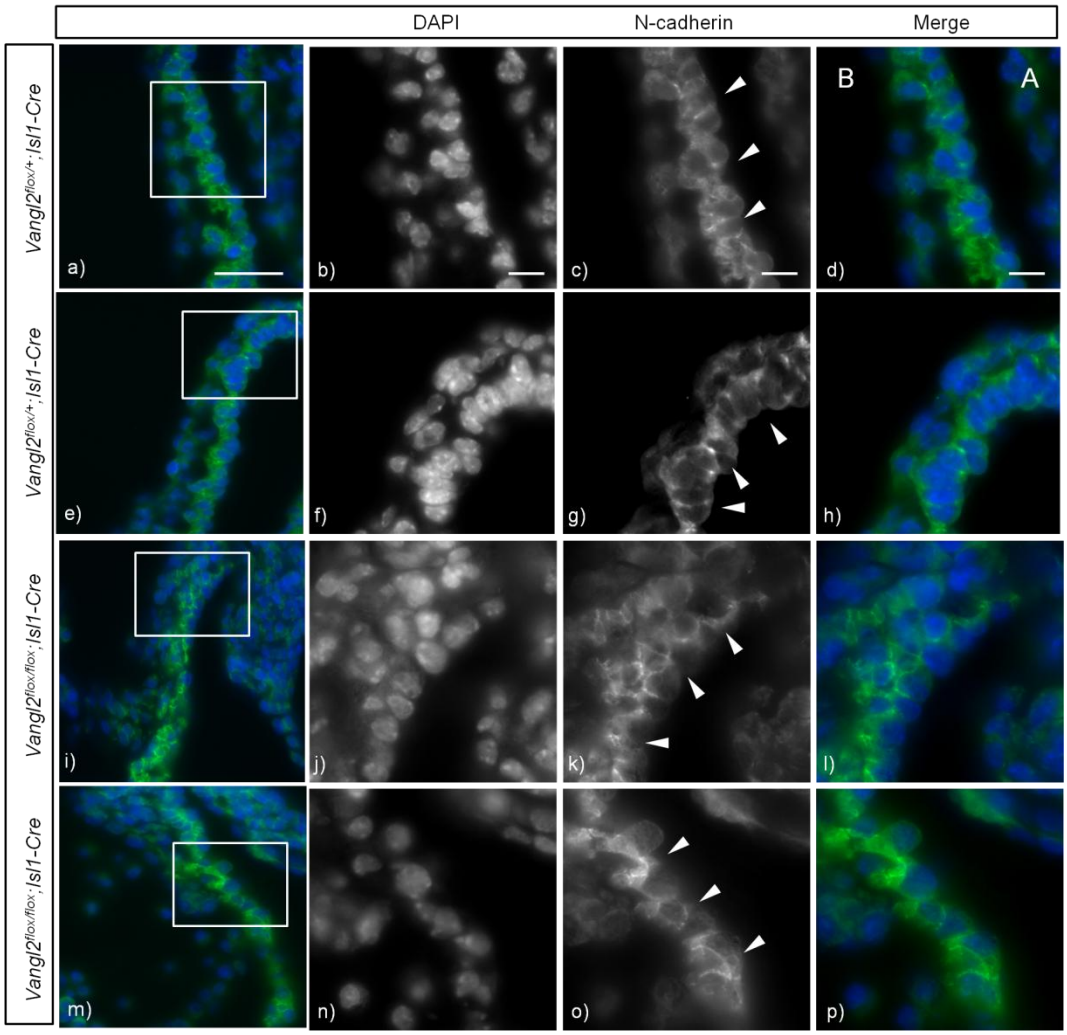

Figure 4.7: Loss of apical localization of N-cadherin expression in the transition zone at E9.5

N-cadherin antibody staining on *Vangl2;Isl1-Cre* control and mutant sections. The boxed region marks the transition zone and is magnified. **a-h)** N-cadherin expression (in green) in *Vangl2$^{flox/+}$;Isl1-Cre* controls (a,e) showing apical expression (arrowheads in c,g). i-p) N-cadherin expression in *Vangl2$^{flox/flox}$;Isl1-Cre* mutants (l,m) with loss of apical expression but uniform expression around cells in the transition zone (arrowheads in k,o). A-apical, B-basal. Scale - 100µm.

Another cadherin, E-cadherin (epithelial cadherin), also showed abnormal expression in mutants in the distal outflow tract. It was observed that the expression of E-cadherin was localized at cell membrane in controls at the apical-basal boundary of cells in the distal outflow tract (figure 4.8a-h arrowheads); however in mutants this expression was altered with some cells showing expression at the basolateral compartment (figure 4.8i-p arrowheads).

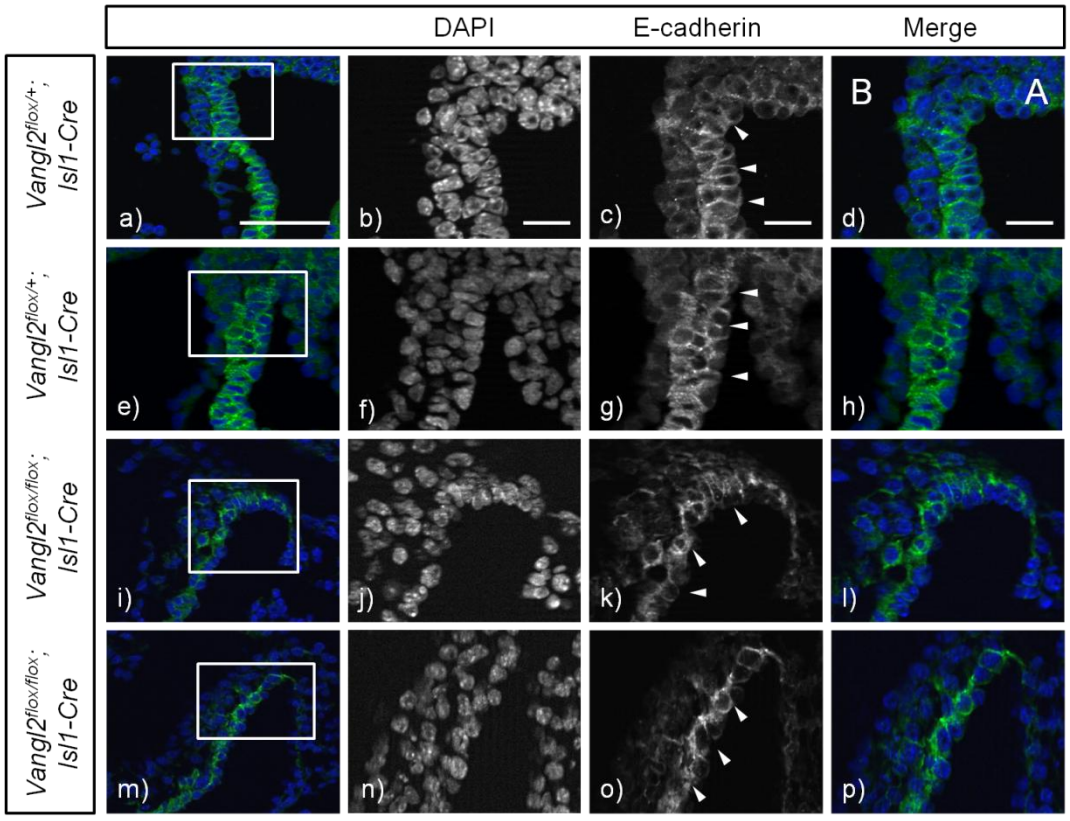

Figure 4.8: Loss of apical-basal localization of E-Cadherin expression in the transition zone at E9.5
E-cadherin antibody staining on *Vangl2;Isl1-Cre* control and mutant sections. The boxed region marks the transition zone and is magnified. **a-h)** E-cadherin expression (in green) in *Vangl2*$^{flox/+}$*;Isl1-Cre* controls (a,e) showing apical –basal expression (arrowheads in c,g). i-p) E-cadherin expression in *Vangl2*$^{flox/flox}$*;Isl1-Cre* mutants (l,m) with expression at basolateral compartment of some cells in the transition zone (arrowheads in k,o). A-apical, B-basal. Scale - 100µm.

Distribution of β-catenin also looked abnormal and not uniform in the *Vangl2*$^{flox/flox}$*;Isl1-Cre* mutants when compared to stage-matched controls. β-catenin expression was seen on cell membranes in the distal outflow tract cells, marking the basolateral compartment in control embryos (figure 4.9a-h arrowheads), whereas in mutants although the expression was present at the cell membrane, there was disorganisation of cellular architecture in the distal outflow tract (figure 4.9i-p arrowheads).

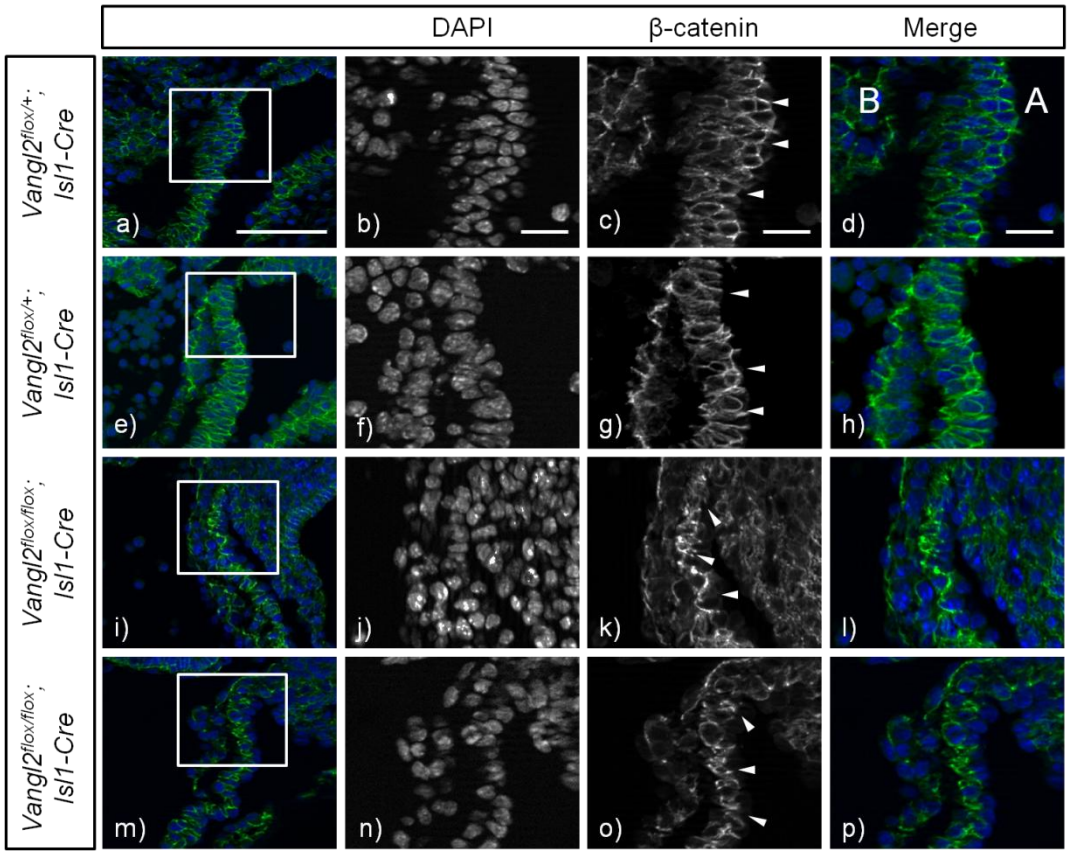

Figure 4.9: Disorganised expression of β-catenin in the transition zone at E9.5

β-catenin antibody staining on Vangl2 SHF controls and mutants sections. The boxed region marks the transition zone and is magnified. **a-h)** β-catenin expression (in green) in *Vangl2*$^{flox/+}$*;Isl1-Cre* controls (a,e) showing membrane bound expression (arrowheads in c,g). i-p) β-catenin expression in *Vangl2*$^{flox/flox}$*;Isl1-Cre* mutants (l,m) disorganized expression in some cells in the transition zone (arrowheads in k,o). A-apical, B-basal. Scale - 100μm.

Expression of these markers was looked at another region than transition zone to check if the effect was isolated to the transition zone or not. Isl1 positive cells are present in the lateral and ventral regions of the pharynx, the dorsal wall of aortic sac and in distal outflow tract. As N-cadherin is not expressed in dorsal wall of aortic sac (figure 4.10a,e arrowhead), its expression in the proximal outflow tract was analysed. For E-cadherin and β-catenin dorsal wall of aortic sac was examined. It was observed that all these adhesion proteins are expressed in a comparable manner in controls and mutants in regions other than transition zone (figure 4.10). These regions have Vangl2 expression as well, therefore in *Vangl2*$^{flox/flox}$*;Isl1-Cre* mutants Isl1 positive cells in these regions would have Vangl2 knocked down and comparable expression in controls and mutants shows specificity of defect to the transition zone only. This solidifies the argument of Vangl2 regulating SHF in the transition zone.

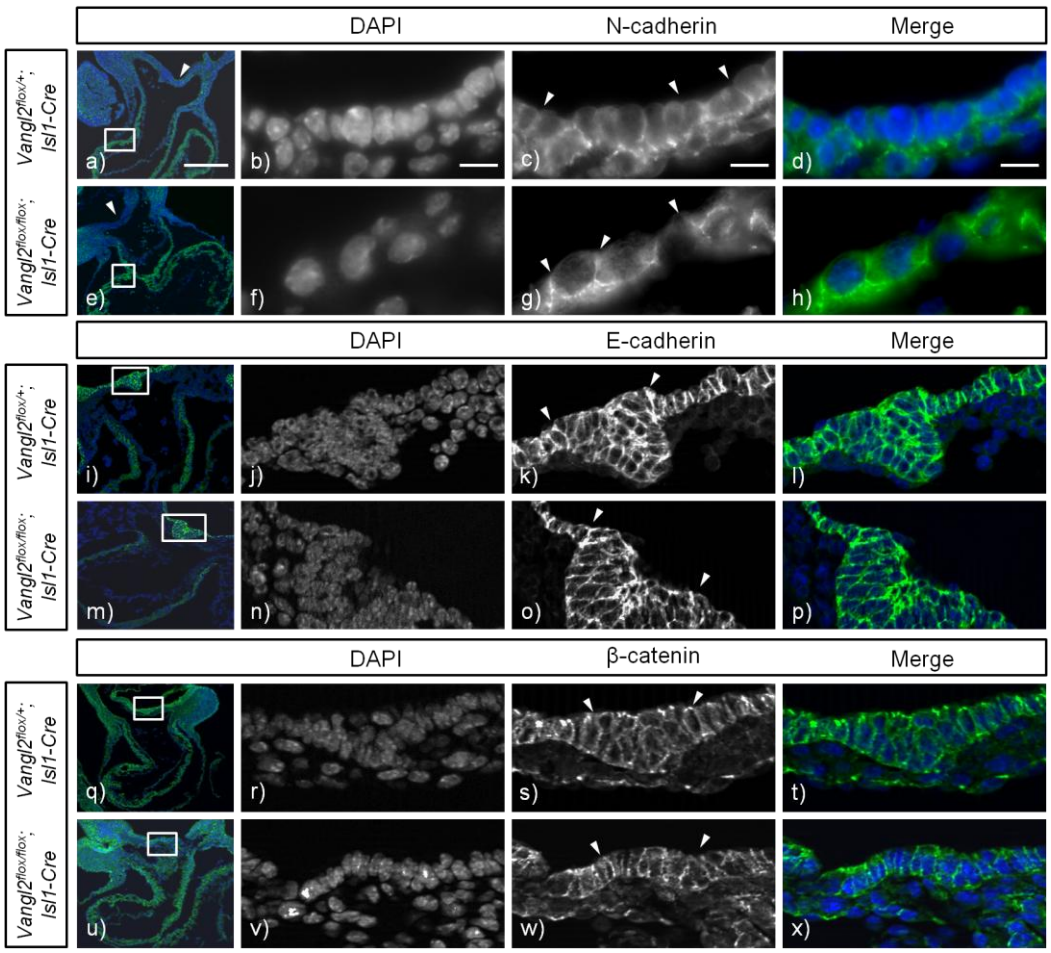

Figure 4.10: Comparable expression of N-cadherin, E-cadherin and β-catenin in controls and mutants outside transition zone

N-cadherin, E-cadherin and β-catenin antibody staining on *Vangl2;Isl1-Cre* control and mutant sections in other regions than transition zone. The box represents the magnified area. **a-h)** N-cadherin expression (in green) in *Vangl2*$^{flox/+}$*;Isl1-Cre* control (a-d) showing apical expression (arrowheads in c) and in *Vangl2*$^{flox/flox}$*;Isl1-Cre* mutant (e-h) also with apical expression between cells in the proximal outflow tract (arrowheads in g). **i-p)** E-cadherin expression (in green) in *Vangl2*$^{flox/+}$*;Isl1-Cre* control (i-l) showing apical–basal expression (arrowheads in k) and in *Vangl2*$^{flox/flox}$*;Isl1-Cre* mutant (m-p) also with apical-basal expression in cells in the dorsal wall of aortic sac (arrowheads in o). **q-x)** β-catenin expression (in green) in *Vangl2*$^{flox/+}$*;Isl1-Cre* control (q-t) showing membrane bound expression (arrowheads in s) and in *Vangl2*$^{flox/flox}$*;Isl1-Cre* mutant (u-x) also showing membrane bound expression in cells in the dorsal wall of aortic sac (arrowheads in w). Scale - 100µm.

Disrupted expression of N-cadherin and E-cadherin along with disorganization of β-catenin suggests disruption of AJ in the cells in distal outflow tract at E9.5. As AJ are present at the border of apical and basal compartments, this is suggestive of the imbalance between the apical and basal compartments of the cell, indication disruption in ABP.

4.2.3.2 Tight Junctions disrupted in absence of Vangl2

TJ are a characteristic feature of epithelial cells, and are present just above the AJ. They help in acting as a barrier for material transport and maintain the osmotic balance of cells, apart from dividing the apical and basal domains of the cell along with AJ. PKCζ is known to be compartmentally localized in epithelial cells, was chosen as the marker because of its dual function that it is present in TJ and is also responsible for the formation of AJ (Colosimo *et al.*, 2010).

Transverse sections of wax embedded embryos at E9.5 were taken and were examined for PKCζ expression. Figure 4.11a-h (arrowheads) shows *Vangl2*$^{flox/+}$*;Isl1-Cre* control embryo showing PCKζ staining in the apical region of the cells in distal outflow tract wall, at the point of TJ, however this apical expression was lost when cells enter the outflow tract in *Vangl2*$^{flox/flox}$*;Isl1-Cre* mutants (figure 4.11i-p arrowheads). It was observed that PCKζ was mislocalized only in transition zone, as there was apical localization of PCKζ expression at TJ of cells before entering the outflow tract in controls (figure 4.11c arrowhead) and in mutants (figure 4.11k,o arrowhead). This result indicates that absence of Vangl2 results in mislocalization of PCKζ expression, suggesting disruption of epithelial ABP and altered expression on these epithelial markers in *Vangl2*$^{flox/flox}$*;Isl1-Cre* mutants also indicate at loss of epithelial nature of SHF cells in the absence of Vangl2.

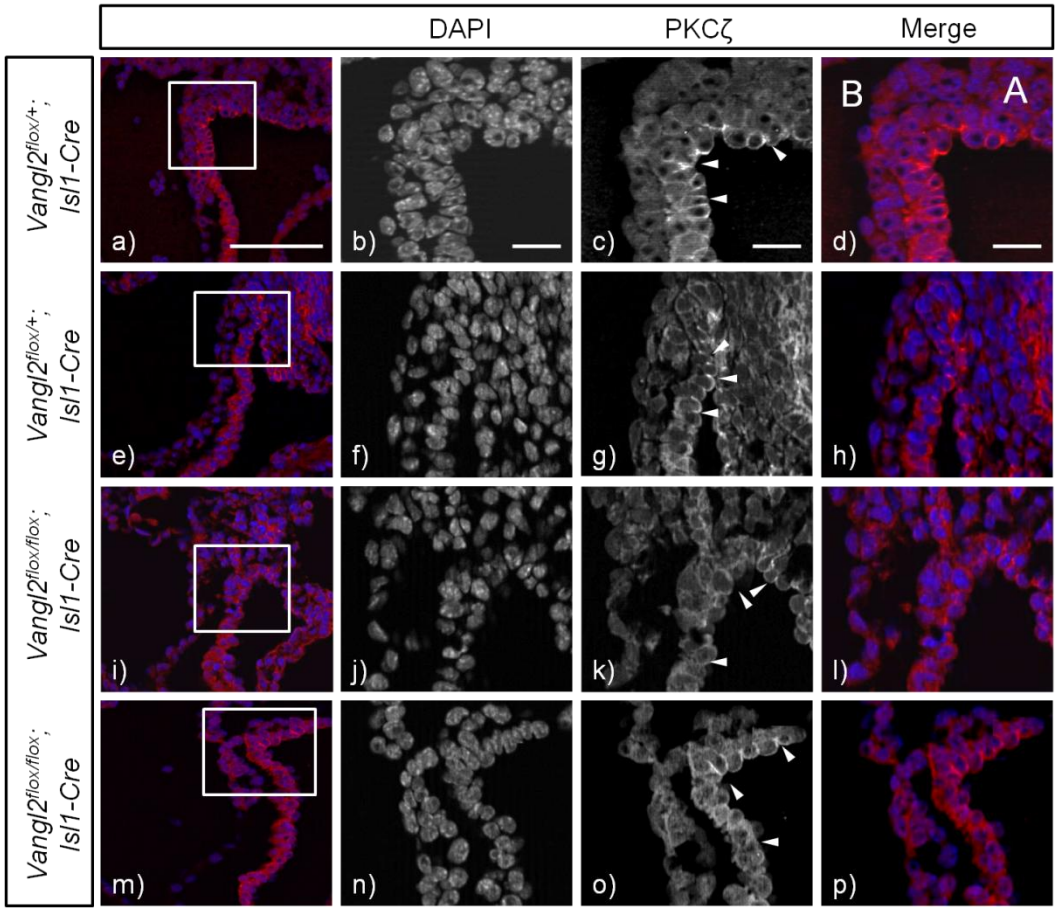

Figure 4.11: Mislocalization of PKCζ expression in transition zone at E9.5

PKCζ antibody staining on *Vangl2;Isl1-Cre* control and mutant sections. The boxed region marks the transition zone and is magnified. **a-h)** PKCζ expression (in red) in *Vangl2$^{flox/+}$;Isl1-Cre* controls (a,e) showing apical localization at tight junctions (arrowheads in c,g). i-p) PKCζ expression in *Vangl2$^{flox/flox}$;Isl1-Cre* mutants (l,m) with mislocalized expression in cells in the transition zone (arrowheads in k,o). A-apical, B-basal. Scale - 100µm.

4.2.3.3 Mislocalisation of basal markers in Vangl2$^{flox/flox}$;Isl1-Cre mutants

Apical-basolateral polarity means that cell is divided into apical and basal zones which are different from each other with respect to the different proteins and determinants specific to each zone. Fibronectin and laminin are extra-cellular markers and were used as they both have roles in adhesion and cell movement and mark the basal side of the side. To check interaction of cells with extra-cellular matrix, vinculin was used which assists in the focal adhesions of the cells. Polarised organelle like MTOC is specific to the apical side of the epithelial cells and was used as apical marker. All these markers were checked in transition zone to test if basal and apical determinants are restricted to their respective compartments.

Three *Vangl2$^{flox/+}$;Isl1-Cre* control and 3 *Vangl2$^{flox/flox}$;Isl1-Cre* mutant embryos were collected at E9.5 and wax embedded. Transverse sections were taken and immunostained with marker specific antibodies. Laminin had basal expression in the control embryos associated with the basal compartment of the distal outflow tract wall cells in the transition zone (figure 4.12a-h arrowheads). However, in *Vangl2$^{flox/flox}$;Isl1-Cre* mutants expression was irregular and not limited to basal side of the cells and completely surrounded some on the cells in the transition zone (figure 4.12i-o arrowheads).

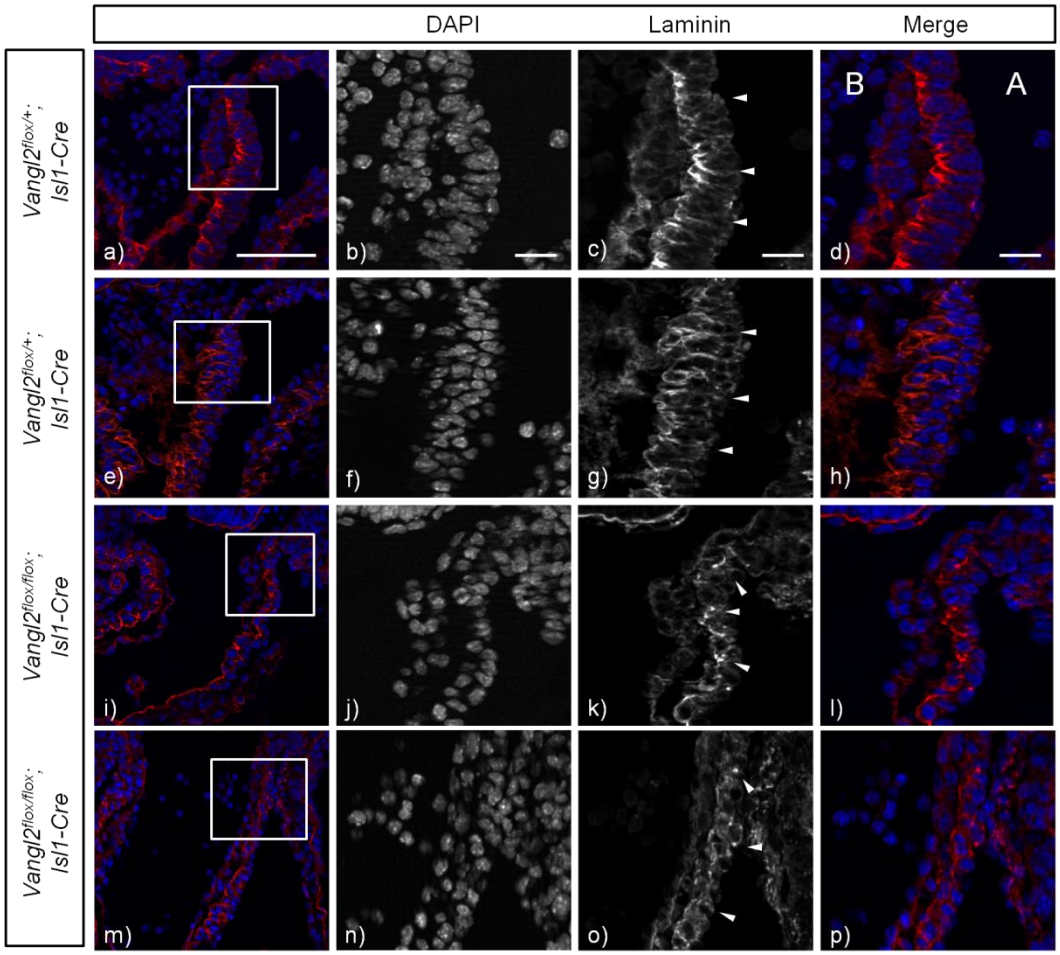

Figure 4.12: Disruption of laminin basal expression in transition zone at E9.5

Laminin antibody staining on *Vangl2;Isl1-Cre* control and mutant sections. The boxed region marks the transition zone and is magnified. **a-h)** Laminin expression (in red) in *Vangl2*$^{flox/+}$*;Isl1-Cre* controls (a,e) showing uniform basal expression (arrowheads in c,g). i-p) Laminin expression in *Vangl2*$^{flox/flox}$*;Isl1-Cre* mutants (l,m) with disrupted expression with not being limited to basal side of the cells in the transition zone (arrowheads in k,o). A-apical, B-basal. Scale - 100µm.

In contrast, laminin was comparable between *Vangl2*$^{flox/flox}$*;Isl1-Cre* mutants and stage matched controls in the proximal outflow tract, where the cells had differentiated to cardiomyocytes (figure 4.13). This again indicates that the abnormalities were restricted to the distal outflow region.

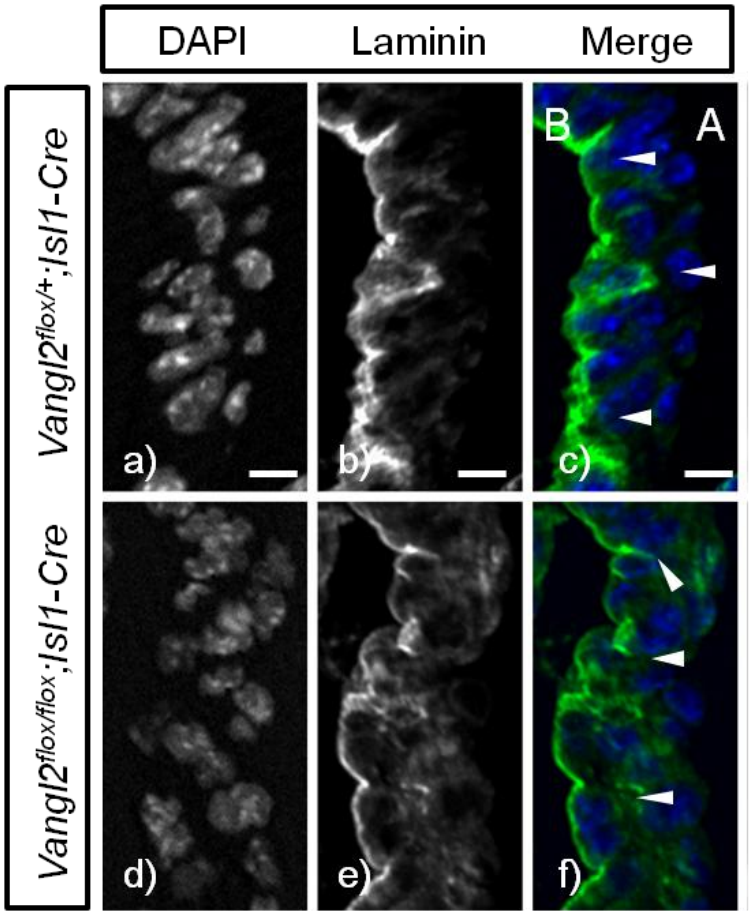

Figure 4.13: Basal expression of laminin in proximal outflow tract at E9.5
a-c) Laminin expression (in green) in *Vangl2*$^{flox/+}$*;Isl1-Cre* control showing basal expression between the basement membrane and the cells (arrowheads in c). **d-f)** Laminin expression in *Vangl2*$^{flox/flox}$*;Isl1-Cre* mutants showing basal expression similar to control (f arrowheads). A-apical, B-basal. Scale - 100µm.

Similarly to laminin, fibronectin also has a basal expression between the basement membrane and the cells, which can be seen in controls (figure 4.14a-h arrowheads). However, in all the 3 *Vangl2*$^{flox/flox}$*;Isl1-Cre* mutants, basal expression of fibronectin was disrupted in cells in the transition zone (figure 4.14i-p arrowheads) and a more non-uniform and dispersed expression was seen.

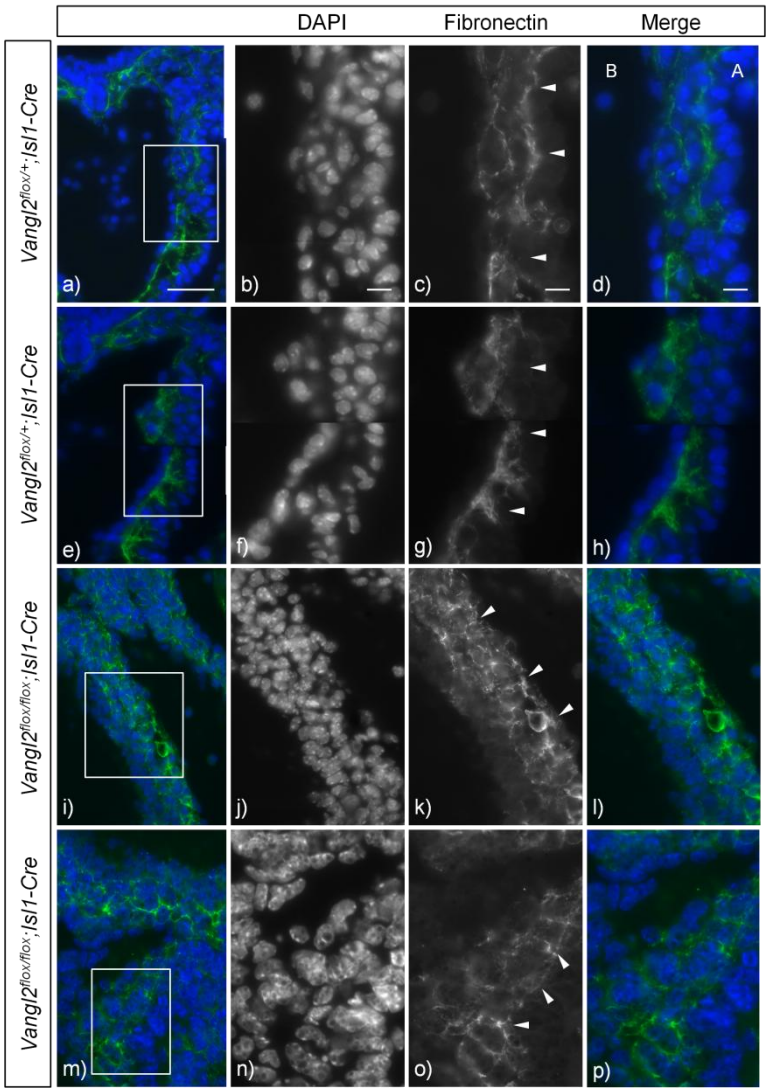

Figure 4.14: Disruption of fibronectin basal expression in transition zone at E9.5

Fibronectin antibody staining on *Vangl2;Isl1-Cre* control and mutant sections. The boxed region marks the transition zone and is magnified. **a-h)** Fibronectin expression (in green) in *Vangl2*$^{flox/+}$*;Isl1-Cre* controls (a,e) showing basal expression between the basement membrane and the cells (arrowheads in c,g). i-p) Fibronectin expression in *Vangl2*$^{flox/flox}$*;Isl1-Cre* mutants (l,m) with disrupted, non-uniform and dispersed expression in cells in the transition zone (arrowheads in k,o). A-apical, B-basal. Scale - 100µm.

Vinculin, which marks the focal adhesions, was not affected in mutants (figure 4.15i-p arrowheads) and was similar to the expression seen in controls (figure 4.15a-h arrowheads). However, cells in the region looked disorganised, although cell-matrix adhesion appears to be normal in the absence of Vangl2 in SHF cells in the outflow tract.

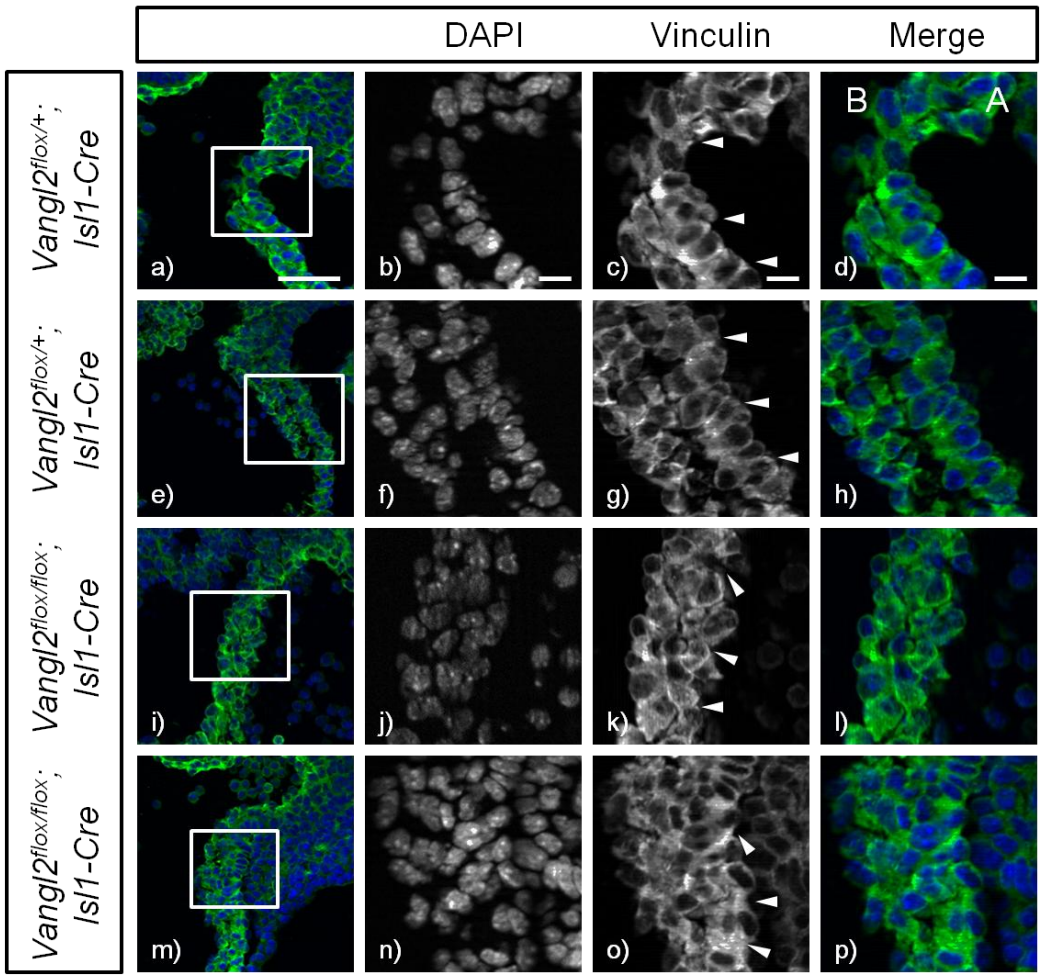

Figure 4.15: Disorganized expression of vinculin in transition zone at E9.5

Vinculin antibody staining on *Vangl2;Isl1-Cre* control and mutant sections. The boxed region marks the transition zone and is magnified. **a-h)** Vinculin expression (in green) in *Vangl2*$^{flox/+}$*;Isl1-Cre* controls (a,e) showing uniform membranous expression (arrowheads in c,g). i-p) Vinculin expression in *Vangl2*$^{flox/flox}$*;Isl1-Cre* mutants (l,m) showing disorganized cells in the transition zone (arrowheads in k,o). A-apical, B-basal. Scale - 100µm.

4.2.3.4 Mislocalisation of apical marker in Vangl2$^{flox/flox}$;Isl1-Cre mutants

To investigate whether there was any abnormality in apical determinants; the position of MTOCs was examined, which are present towards the apical side of epithelial cells. To establish loss of polarity as a result of *Vangl2* mutation in SHF cells, two possibilities were proposed, one that either the cells will lose MTOCs as loss of AJ leads to loss of apical determinants of the cell (Kaplan *et al.*, 2009) or MTOCs will not be restricted to apical compartment of the cell (figure 4.15a, black dots being MTOCs), both causing disturbance in polarity in SHF. In our experiments, γ-tubulin was used to label the MTOCs on 3 *Vangl2$^{flox/+}$;Isl1-Cre* controls and 3 *Vangl2$^{flox/flox}$;Isl1-Cre* mutant embryo sections at E9.5. Transition zone was analysed and γ-tubulin staining showed that in controls MTOCs were restricted to the apical compartment of the cells, while in mutants they were not restricted to the apical side of the cell. Figure 4.16 shows transverse sections of outflow tract as results showed that position of MTOCs was more apical in controls (figure 4.16b-i arrowheads) as compared to mutants (figure 4.16j-q arrowheads).

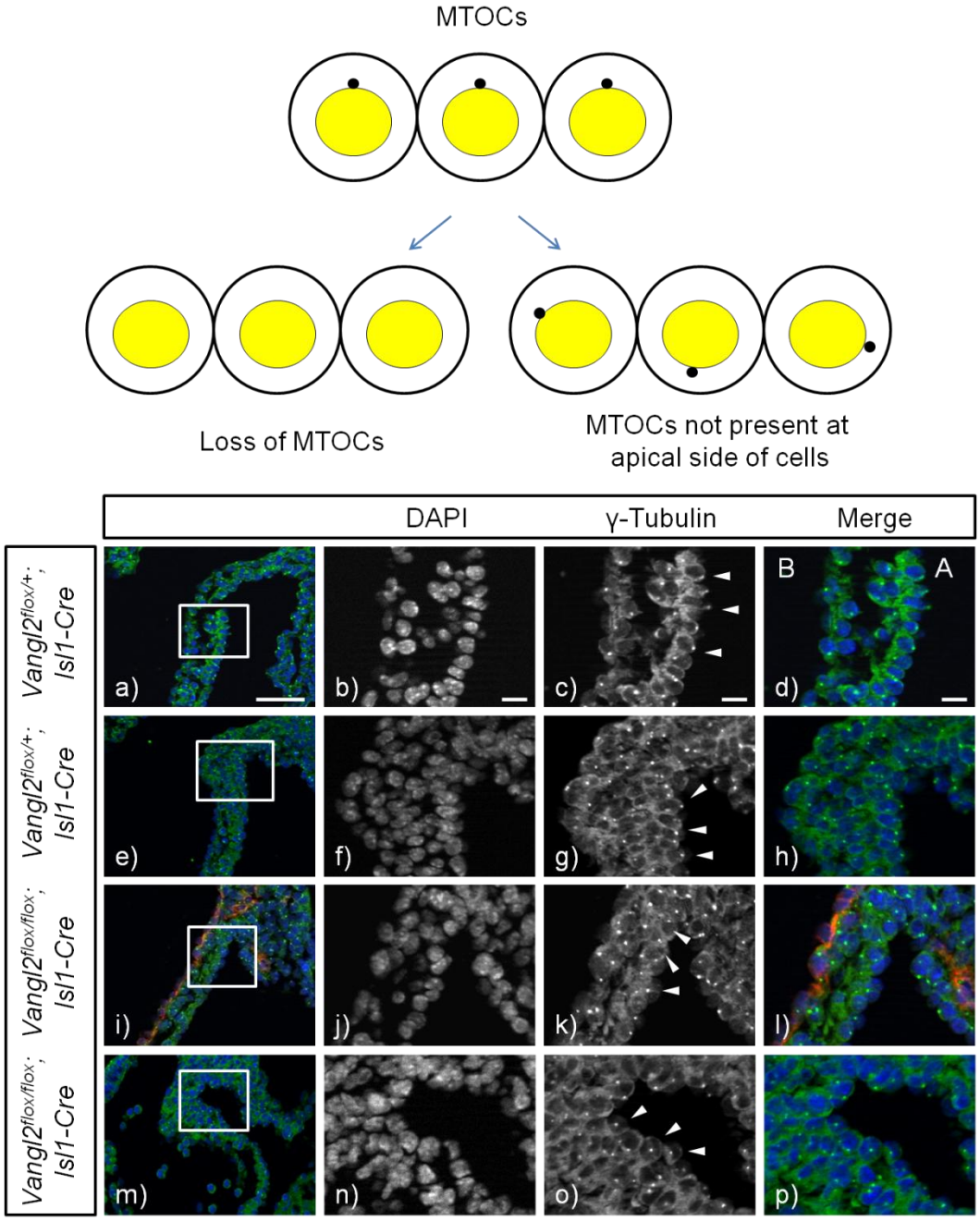

Figure 4.16: Loss of apical localization of MTOCs in transition zone at E9.5

Black dots showing MTOC pointing in apical direction in polarized cells and loss of polarity could lead to either loss of MTOCs or MTOCs being pointing at different direction. γ-tubulin antibody staining on *Vangl2;Isl1-Cre* control and mutant sections. The boxed region marks the transition zone and is magnified. **a-h)** γ-tubulin (marking MTOCs) expression (in green) in *Vangl2*$^{flox/+}$*;Isl1-Cre* controls (a,e) showing apical localization of MTOCs (arrowheads in c,g). i-p) γ-tubulin expression in *Vangl2*$^{flox/flox}$*;Isl1-Cre* mutants (l,m) showing MTOCs being present at basal side of some cells in the transition zone (arrowheads in k,o). A-apical, B-basal. Scale - 100µm.

To establish whether there was decrease in MTOC numbers, cell counting was done using Fiji software with total number of cells and total MTOCs. There was no evident decrease in number of MTOCs in the mutants as compared to controls when this quantitative analysis by cell counting was done (table and graph in figure 4.17). To solidify our finding about the loss of apical positioning of MTOC in *Vangl2*$^{flox/flox}$*;Isl1-Cre* mutants, higher magnification images were taken to look at the position of MTOCs. To check the position of MTOC, 100 cells were labelled in controls and mutants. These cells were divided into apical and basal compartments and then position of MTOC was observed by measuring the angle from the centre of the cell using Fiji software. These sections showed evident difference in position of MTOCs (average angles of controls and mutants are mentioned in the table in figure 4.17). In controls they are present on apical side of the cells (figure 4.16c) and in mutants they were present all around the cells (figure 4.17f). These results of MTOC position in cells gives a strong evidence for the possible disruption is ABP in the absence of Vangl2 in SHF cells with MTOC being an apical determinant isn't restricted to the apical compartment of the cells.

	Control	Mutant
Total cells (DAPI)	417	413
MTOCs	308	301
Average Percentage of MTOCs	73.86	72.88
Average angle (°) of MTOCs (n=100) Apical <90° Basal >90°	13.64°	117.84°

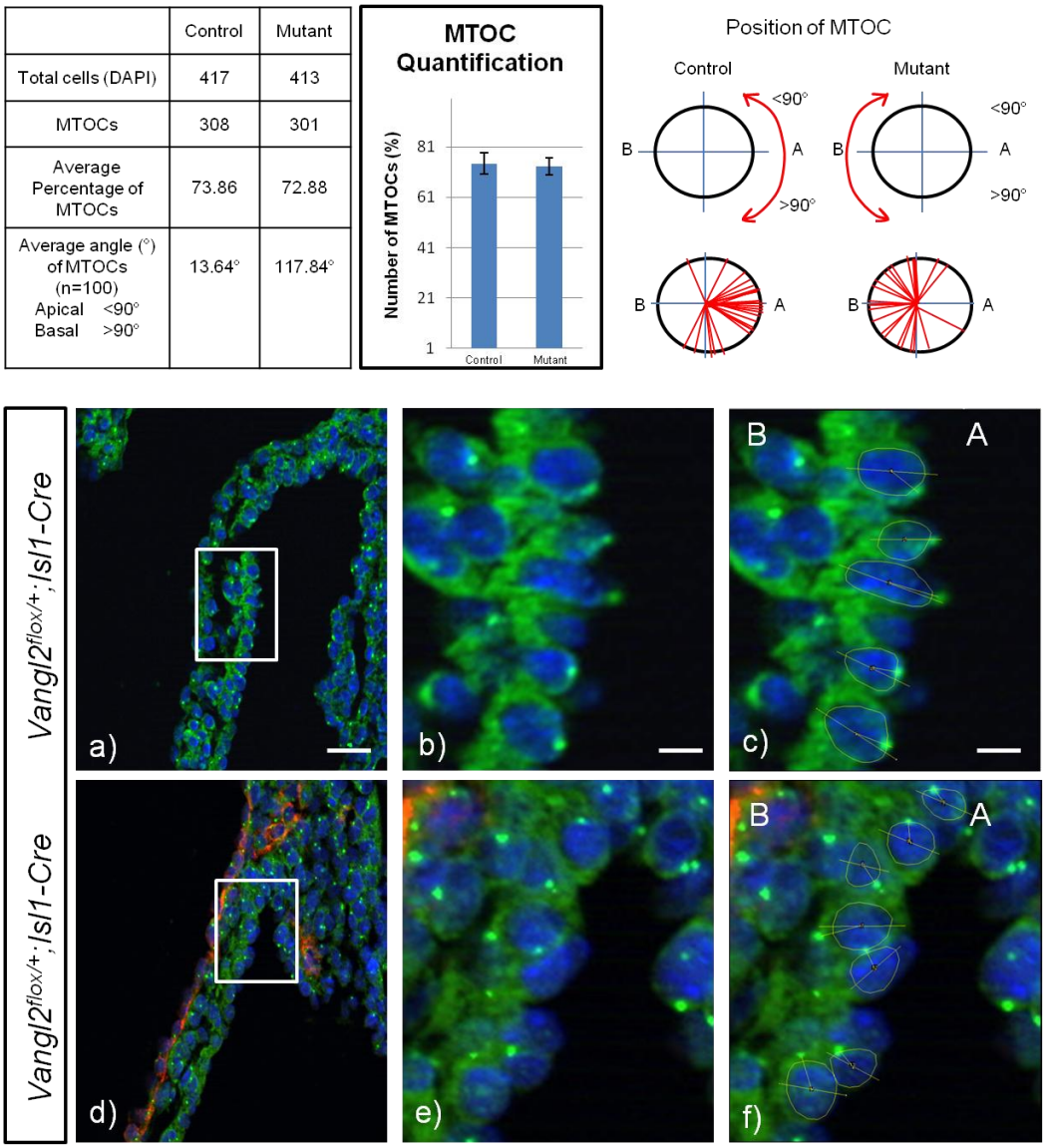

Figure 4.17: Quantification and position analysis of MTOCs

Table showing quantification of MTOCs in *Vangl2*$^{flox/+}$*;Isl1-Cre* controls (n=3) and *Vangl2*$^{flox/flox}$*;Isl1-Cre* mutants (n=3) and average angle of of MTOC from the centre of the cell. Graph showing no signification difference in their numbers and representation of position of MTOC around the cell at apical/basal side. **a-c)** MTOCs (green dots) in *Vangl2*$^{flox/+}$*;Isl1Cre* control (a) with magnified region showing MTOCs pointing towards the apical side of the cells (c). **d-f)** MTOCs (green dots) in *Vangl2*$^{flox/flox}$*;Isl1-Cre* mutant embryo section (d) with magnified region showing MTOCs pointing towards the basal side of the cells (f). MTOC-microtubule organising centre, A-apical, B-basal. Scale - 100µm.

4.2.3.5 Loss of planar cell polarity in absence of Vangl2

Our results confirm the loss of ABP in SHF derived cells in the distal outflow tract in the absence of Vangl2; however, epithelial cells apart from exhibiting ABP also exhibit PCP along the plane of epithelium and because Vangl2 is a core PCP protein it was hypothesised that its absence along with loss of ABP leads to loss of planar polarity as well.

PCP signaling pathway is a multi-protein pathway and requires all the proteins involved to work in coordination (Henderson and Chaudhry, 2011). We checked if in absence of Vangl2 in SHF cells two other members of the PCP signaling pathway, Dvl2 and Celsr1, are recruited to the membrane. Our previous result about Vangl2 expression during heart development in SHF cells showed that Vangl2 expression is membrane bound in the dorsal pericardial wall and in the distal outflow tract in transition zone, but becomes cytoplasmic towards proximal outflow tract and after reaching the right ventricle of heart where SHF are differentiated into myocardium (section 4.2.2). Dvl2 and Celsr1 when observed in *Vangl2*^{flox} embryos had similar expression like Vangl2, with membrane localisation in the distal outflow tract and cytoplasmic expression in proximal outflow tract. Embryos were collected at E9.5 and sectioned transversally after wax embedding to analyze the transition zone (n=3).

Figure 4.18 compares Dvl2 and Celsr1 expression in *Vangl2*$^{flox/+}$*;Isl1-Cre* control embryo (figure 4.18a-e and 4.18i-l respectively) and *Vangl2*$^{flox/flox}$*;Isl1-Cre* mutant embryo (figure 4.18e-h and 4.18m-p respectively). In control embryos both Dvl2 and Celsr1 expression was membrane localized in cells in the transition zone in distal outflow tract (figure 4.18c1 and k1 respectively; arrowheads), while this is not seen in the mutant embryos for both the proteins (figure 4.18g1 and o1 respectively; arrowheads). However when looked in the differentiated myocardium in the proximal outflow tract, expression of both Dvl2 and Celsr1 remained cytoplasmic in both controls and mutant embryo sections (figure 4.18c2,g2 and k2,o2 respectively; arrowheads), which was comparable to Vangl2 expression in the same region (figure 4.6).

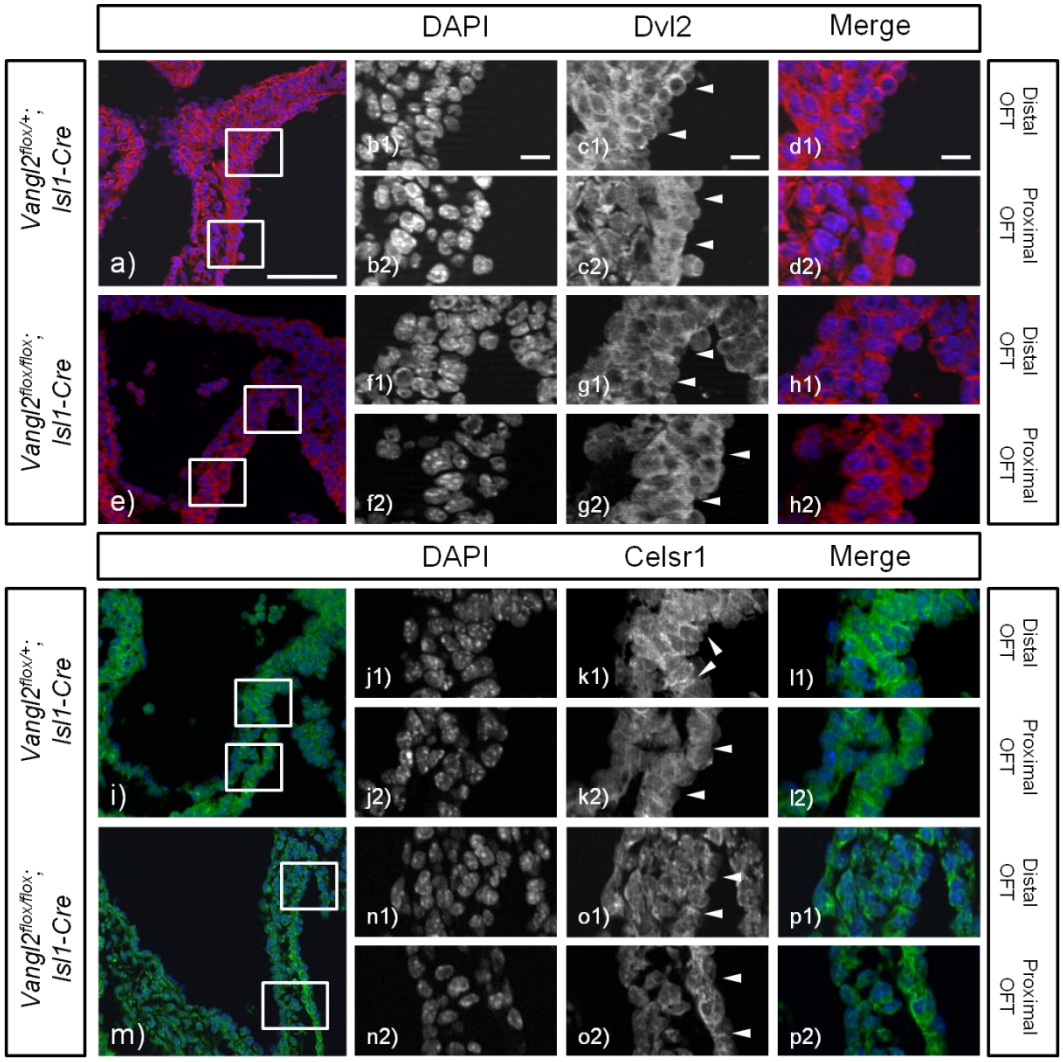

Figure 4.18: Loss of polarity proteins, Dvl2 and Celsr1 in the absence of Vangl2 in transition zone at E9.5

Dvl2 and Celsr1 antibody staining on *Vangl2;Isl1-Cre* control and mutant sections. The boxed region marks the transition zone and proximal outflow tract. **a-d)** Dvl2 expression (in red) in *Vangl2$^{flox/+}$;Isl1-Cre* control embryo showing change in expression as SHF cells moves towards proximal outflow tract with membrane localized expression in the transition zone (c1 arrowheads) and cytoplasmic expression after that (c2 arrowheads). **e-h)** Loss of Dvl2 membrane localized expression in *Vangl2$^{flox/flox}$;Isl1-Cre* mutant embryo in transition zone (g1 arrowheads) and cytoplasmic expression after that (g2 arrowheads). **i-l)** Celsr1 expression (in green) in *Vangl2$^{flox/+}$;Isl1-Cre* control embryo showing change in expression as cells moves towards proximal outflow tract with membrane localized expression in the transition zone (k1 arrowheads) and cytoplasmic expression after that (k2 arrowheads). **m-p)** Loss of Celsr1 membrane localized expression in *Vangl2$^{flox/flox}$;Isl1-Cre* mutant embryo in transition zone (o1 arrowheads) and cytoplasmic expression after that (o2 arrowheads). A-apical, B-basal, OFT-outflow tract. Scale - 100µm.

Results show that loss of Vangl2 leads to non-recruitment of Dvl2 and Celsr1 at the cell membrane in the transition zone, possibly leading to the PCP complex to be not formed and resulting in disruption of the whole signaling pathway.

4.2.4 Abnormal differentiation of SHF in absence of *Vangl2*

After looking at the polarity of SHF cells during heart morphogenesis, it is also essential to check if the derivatives of these cells are formed and functioning in the usual manner or have some abnormal behaviour in the absence of Vangl2. SHF cells can give rise to three major cell lineages of the heart: cardiomyocytes, smooth muscle cells and endothelial cells (Moretti *et al.*, 2006). Transverse sections of 3 control and 3 mutant wax embedded embryos were taken and labelled with specific antibodies for these derivatives.

Cardiomyocytes constitute the cardiac muscle cells (myocardium) and are labelled by MF20 antibody. At E10.5 our mutants showed that although formation of cardiomyocytes was normal as compared to controls, there was a difference in cell shape. Cells in the distal outflow tract marked by MF20 show extended membrane protrusions in *Vangl2*$^{flox/+}$*;Isl1-Cre* controls (figure 4.19a-d arrowheads) but no protrusions are seen in the cells in *Vangl2*$^{flox/flox}$*;Isl1-Cre* mutant embryos and had a rounded appearance (figure 4.19e-h arrowheads). Similar expression of MF20 has been reported *Lp* controls and mutants (Phillips *et al.*, 2005), however in this case the analysis was done at E13.5 and termed as myocardialization defect leading to failure in movement of myocardial cells.

Smooth muscle cell are the major component of the great arteries and blood vessels. Their expression was also looked at, at E10.5 and at later stages of development, E14.5 when the heart is fully developed, using αSMA antibody. At E10.5 there was αSMA expression in both controls and mutants (figure 4.19i-p) suggesting formation of smooth muscle cells at early developmental stages is normal, however it was observed in all 3 mutant embryos that the expression comes on more distally (figure 4.19o arrowheads) as compared to controls (figure 4.19k arrowheads). In controls the expression starts in the transition zone, however in the mutants expression came on at the beginning of the distal outflow tract, suggestion early differentiation in the absence of Vangl2.

The other cell type which is derivative of SHF cells is endothelial cells, which form the interior surface of blood vessels in outflow tract. Endothelial cells were marked using endomucin antibody and its expression was unchanged in mutants with respect to controls (figure 4.19q-x) when checked at E9.5 in the transition zone, indicating that the overall organization of the endothelial tissue as cells move into the developing outflow tract is maintained.

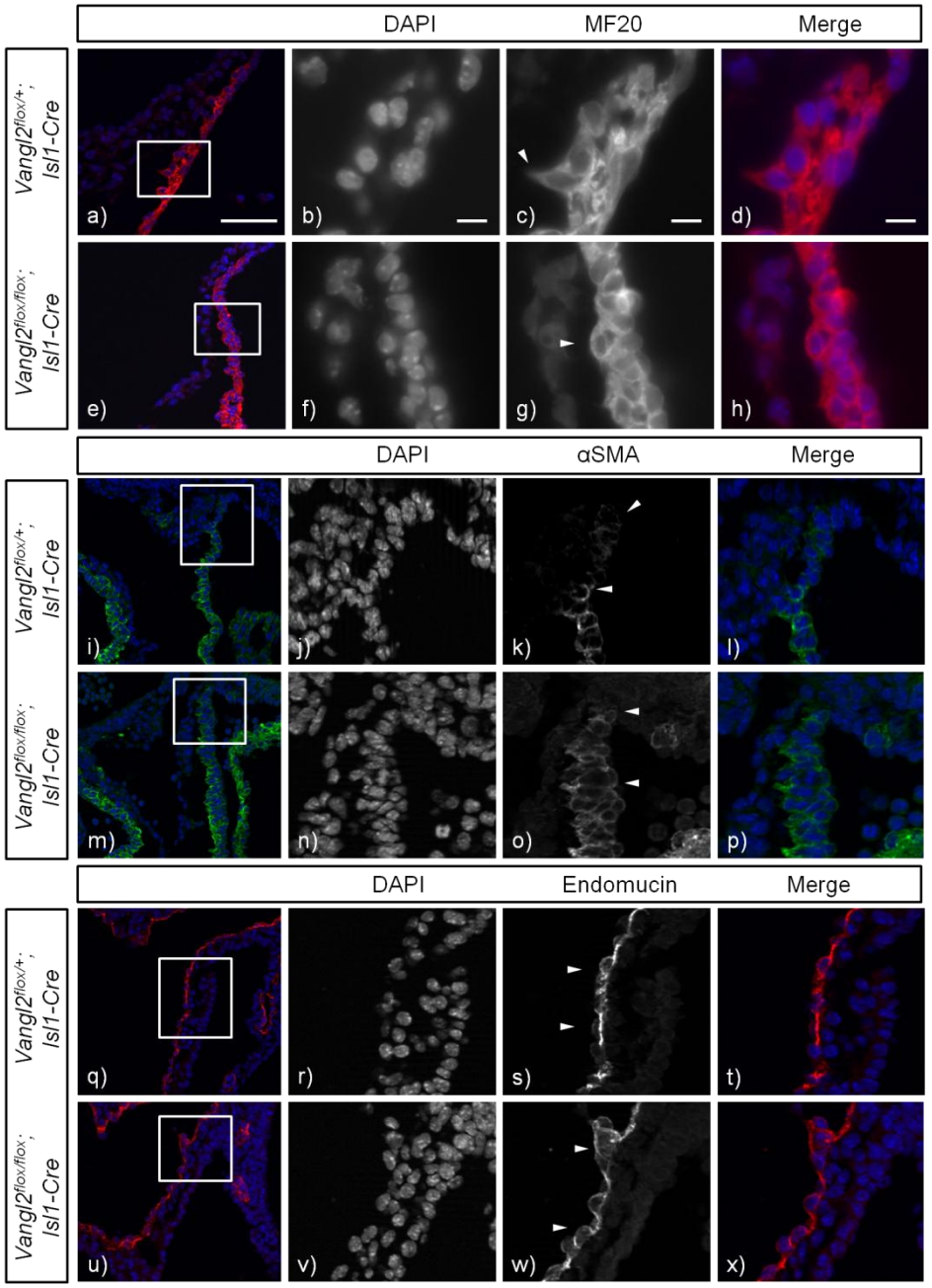

Figure 4.19: Derivatives of SHF cells

MF20, α-sma and endomucin antibody staining on *Vangl2;Isl1-Cre* control and mutant sections. The boxed region marks the transition zone and is magnified. **a-h)** MF20 labelling the cardiomyocytes in the transition zone with extended protusions in *Vangl2*$^{flox/+}$*;Isl1-Cre* control embryo section (c arrowhead) and rounded appearance with no protusions in *Vangl2*$^{flox/flox}$*;Isl1-Cre* mutant embryo section (g arrowhead)**. i-p)** αSMA labelling smooth muscle cells showing early expression in *Vangl2*$^{flox/flox}$*;Isl1-Cre* mutant embryo section (o arrowheads) as compared to *Vangl2*$^{flox/+}$*;Isl1-Cre* control embryo section (k arrowheads). **q-x)** Endomucin expression labelling the endothelial cells with no difference in *Vangl2*$^{flox/+}$*;Isl1-Cre* control (s arrowheads) and *Vangl2*$^{flox/flox}$*;Isl1-Cre* mutant (w arrowheads). Scale - 100µm

When αSMA expression was looked at later stage of development, E14.5 when the heart is fully septated, there was lack of expression at the aortic root in all 3 mutants (figure 4.20). Figure 4.20a,b show *Vangl2*$^{flox/+}$*;Isl1-Cre* control embryo showing aortic root, at the level of the aortic valves with αSMA labelling smooth muscle cells in brown colour (using DAB), and in *Vangl2*$^{flox/flox}$*;Isl1-Cre* mutants the expression is similar, however there is lack of staining in the outer region of the aortic arterial wall (figure 4.20c,d arrows). Smooth muscle cells were normal in aortic arch region in mutants (figure 4.20f) and were comparable to controls (figure 4.20e).

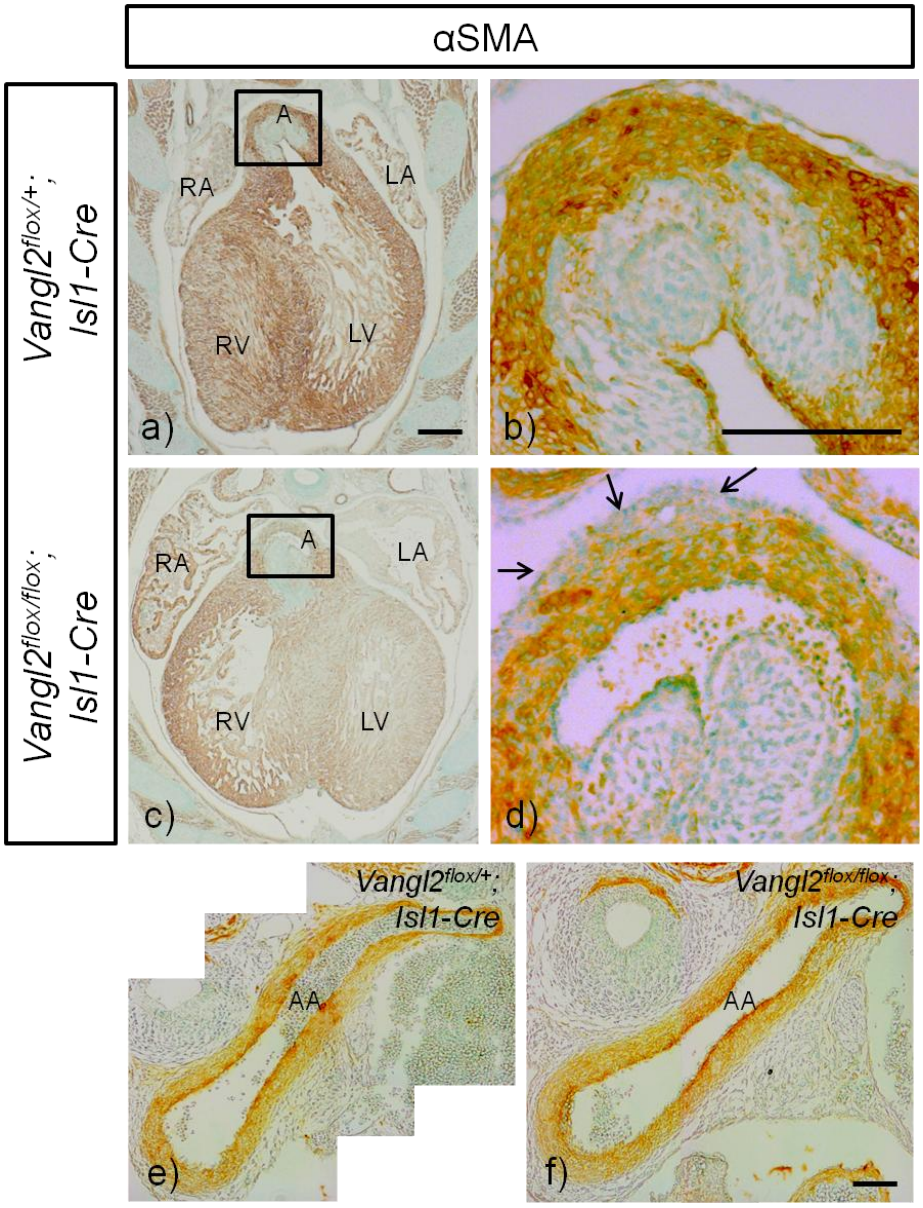

Figure 4.20: Smooth muscle cells expression at E14.5

α-sma staining on *Vangl2;Isl1-Cre* control and mutant sections. The boxed region represents the magnified area. **a,b)** Smooth Muscle Cells staining using DAB (marked in brown) at aortic root level in *Vangl2*$^{flox/+}$*;Isl1-Cre* control. **c,d)** Smooth Muscle Cells expression at aortic root level in *Vangl2*$^{flox/flox}$*;Isl1-Cre* mutant with lack of staining in the outer region of the aortic arterial wall (d arrows). **e,f)** Smooth muscle expression at aortic arch level with similar expression in control (e) and mutant (f).). RA-right atria, LA-left atria, RV-right ventricle, LV-left ventricle, A-aorta, AA-aortic arch. Scale - 20µm.

Smooth muscle cells give rise to elastin fibres in the arteries. These elastin fibres are present in extra-cellular matrix (Liu *et al.*, 2004) and are produced from fibroblasts and smooth muscle cells (Kagan and Trackman, 1991; Bökenkamp *et al.*, 2006), and is involved in smooth muscle cell proliferation (Karnik *et al.*, 2003). When observed in *Vangl2;Isl1-Cre* embryos at E14.5, there was a drastic decrease in elastin fibres, when layers of elastin fibres were counted (figure 4.21f graph) in the aortic root in mutants (figure 4.21c,d arrows) as compared to controls (figure 4.21a,b arrows) (n=3), suggesting the role of abnormal SHF in either origin of these elastin fibres.

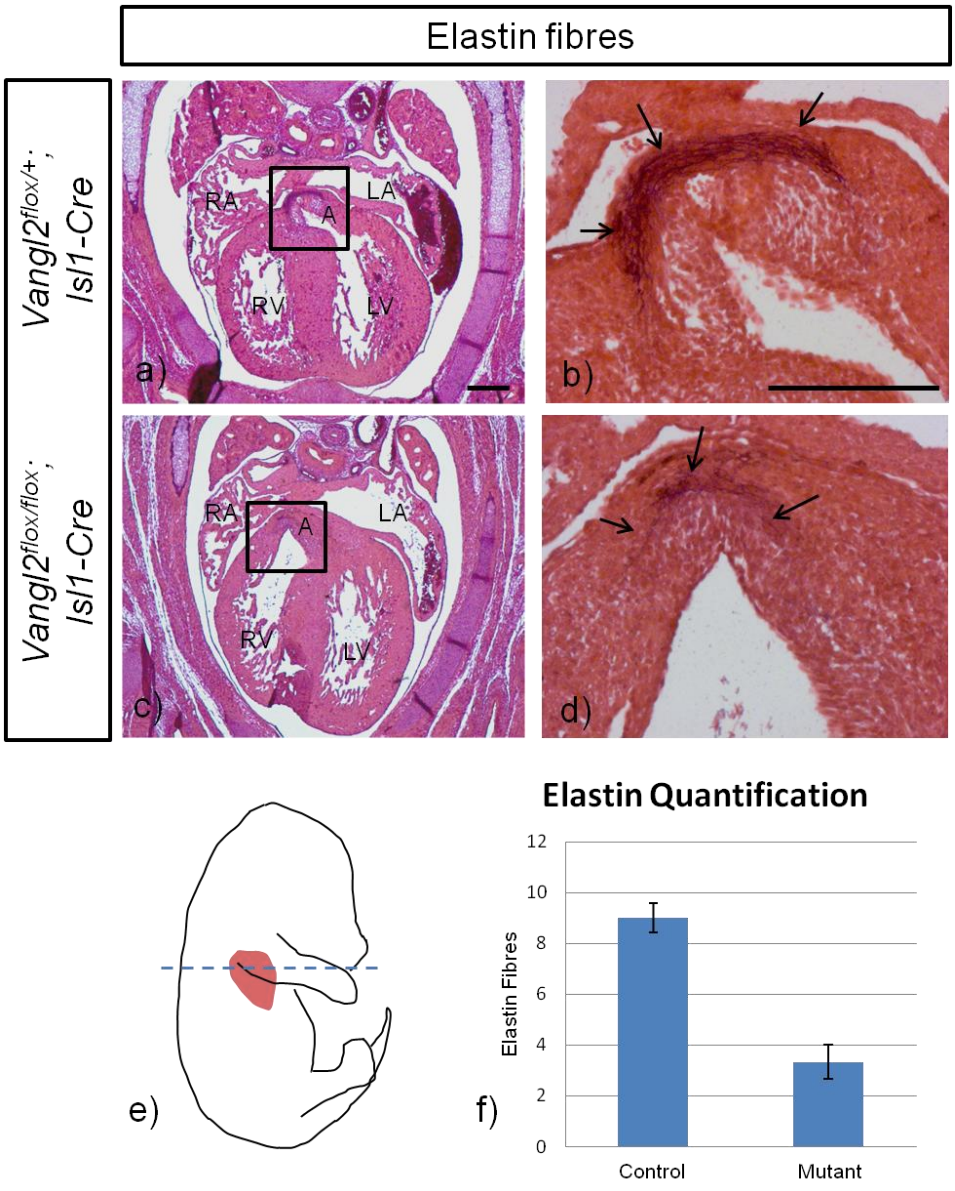

Figure 4.21: Reduction of elastin fibres in absence of Vangl2 at E14.5

Elastin staining on *Vangl2;Isl1-Cre* control and mutant sections. The boxed region represents the magnified area. **a,b)** Elastin fibres at aortic root level in *Vangl2$^{flox/+}$;Isl1-Cre* control. **c,d)** Elastin fibres at aortic root level in *Vangl2$^{flox/flox}$;Isl1-Cre* mutant showing decrease in fibres (d arrows). **e)** Plane of transverse section of embryo at E14.5. **f)** Graph showing quantification of elastin fibres with decrease in mutants as compared to controls. RA-right atria, LA-left atria, RV-right ventricle, LV-left ventricle, A-aorta. Scale - 20µm.

4.3 Discussion

The project seeks to establish the role of the *Vangl2* gene, a key component of the non-canonical Wnt/PCP signalling pathway, in regulating polarisation of SHF in the outflow tract of the developing heart. After establishing that our new *Vangl2*^{flox} line recapitulates *Lp/Lp* phenotype, we proved that *Lp* is a SHF mutant with respect to heart development. *Lp/Lp* mutants have outflow tract defect that was recapitulated in our *Vangl2*$^{flox/flox}$*;Isl1-Cre* mutants, confirming that SHF cells require Vangl2 in their undifferentiated precursor form and absence of Vangl2 leads to double outlet right ventricle. Our next aim was to elucidate the characteristic behaviour of SHF cells as they contribute to the outflow tract, and to establish how loss of Vangl2 changes their behaviour and affects polarisation and maturation of these cells.

We showed that Vangl2 co-localises with Isl1 expressing cells while they contribute to the developing heart, and its sub-cellular localisation changes while SHF derived cells enter the distal outflow tract and move towards proximal outflow tract. At E9.5 these cells enter the outflow tract through dorsal pericardial wall and are in multipotent progenitor state, but after entering outflow tract there is a transition from their undifferentiated precursor state to differentiated state as they move more proximally. This zone where both undifferentiated and differentiated SHF cells are present and transition from one form to another occurs in the distal outflow tract was termed as ‘transition zone’. Interestingly, Vangl2 expression in this transition zone was localized to cell membrane whereas it becomes cytoplasmic as cells move more proximally and differentiate into myocardium. Mutation in *Vangl2*, which results in *Lp* phenotype leads to loss of membrane bound expression of Vangl2 (Torban *et al.*, 2007), indicating membrane association of Vangl2 is important for its function. Hence Vangl2 localisation to cell membrane in transition zone suggests it is functional in this region. This shows the polarized nature of the undifferentiated SHF in the transition zone, therefore transition zone became the key zone for the analysis. In the absence of Vangl2 (seen in *Lp/Lp* and *Vangl2*$^{flox/flox}$*;Isl1-Cre* mutants) the SHF derived cells appear disorganised in the distal outflow tract instead of moving in uniformly, suggesting that the alignment defects in the outflow tract

seen later in gestation could be because the SHF are unable to successfully add on to the distal end of the outflow tract.

Vangl2 is a key component of multi-protein complex in PCP pathway and plays a role in cell polarity (Henderson *et al.*, 2006). Loss of *Vangl2* leads to disrupted polarity in tissues. In fly *Vang/Stbm* mutation leads to loss of polarity in ommatidia of the compound eye and hair of the wing and thorax making them point in various directions (Klein and Mlodzik, 2005). In mice as well there is loss in cell polarity when *Vangl2* is mutated. Mutation in *Vangl2* results in abnormal orientation of stereociliary bundles in cochleae in *Lp/Lp* embryos (Montcouquiol *et al.*, 2003). There have been suggestions about there being a polarity defect in *Lp/Lp* mutants (Phillips *et al.*, 2005), leading to the cardiac defects observed in *Lp/Lp* mutants. However, polarity of SHF hasn't been reported before in the absence of Vangl2. As the cardiac outflow tract defect observed in *Lp/Lp* was recapitulated in *Vangl2$^{flox/flox}$;Isl1-Cre* mutants, it was hypothesised that it was a polarity defect and that loss of Vangl2 leads to loss of polarity in SHF resulting in their abnormal behaviour.

To look at polarity of cell it is essential to look at its complete behaviour, how it interacts with neighbouring cells, their adhesion and directional movement. Epithelial nature of SHF cells while they move in the outflow tract was established, and loss of polarity in the cells was confirmed by checking the polarized organelles in cell and the complexes which play a role in polarity. Epithelial cells have AJ and TJ which divide the cell in apical and basal compartment, imparting ABP. Our results show that both these junctions are impaired in *Vangl2$^{flox/flox}$;Isl1-Cre* mutants. There have been reports on β-catenin localization assists in establishing cell polarity in some tissues and its loss leading to a disruption of AJ (Wu *et al.*, 2010). Change in cadherins expression and evident disorganisation of cells in the transition zone indicated loss of epithelial nature of the SHF. To look at TJ, expression of PKCζ was seen. The PAR-PKCζ complex has an important role in cell polarity (Joberty *et al.*, 2000; Lin *et al.*, 2000; Ohno, 2001). In mammals, epithelial cells have colozalization of PAR-3, PAR-6, and PKCζ, which forms a complex in the apical most part of the cell

where TJ are formed. Mutation of PKCζ results in the complex being not formed and hence loss of polarity (Ohno, 2001). *Vangl2*$^{flox/flox}$*;Isl1-Cre* mutant also had the same fate as PKCζ expression was mislocalised in the transition zone, however it was localised apically in the cells before they enter the transition zone. Laminin and fibronectin expression which are normally localised basally to the cells was spread to the apical side and MTOCs which are present on the apical side of cells were present even at the basal side of some cells in the mutants. Reports suggest that polarized alignment of MTOC along with cytoskeleton is required for directional cell movement (Kupfer *et al.*, 1982; Kupfer *et al.*, 1983; Magdalena *et al.*, 2003). *Vangl2*$^{flox/+}$*;Isl1-Cre* controls showed MTOC mostly towards the apical side of cells as compared to mutants which had MTOCs not limited to apical side but had them towards the basal side of some cells. Therefore cell's apical and basal domains were not separate and markers specific to each domain were no longer exclusive. This indicates that loss of Vangl2 from SHF cells leads them to behave abnormally owing to disrupted apical-basolateral domain mixing and loss of ABP (figure 4.22b). However, apart from disruption of ABP, another possibility is abnormal orientation of cells which makes these apical and basal determinants look misoriented (figure 4.22c). Mislocalisation of MTOCs could be because of the abnormal orientation of cells, but as laminin is an extra cellular marker, disruption in its basal expression is indicative of loss of ABP. Hence, it could be a combination of both the factors.

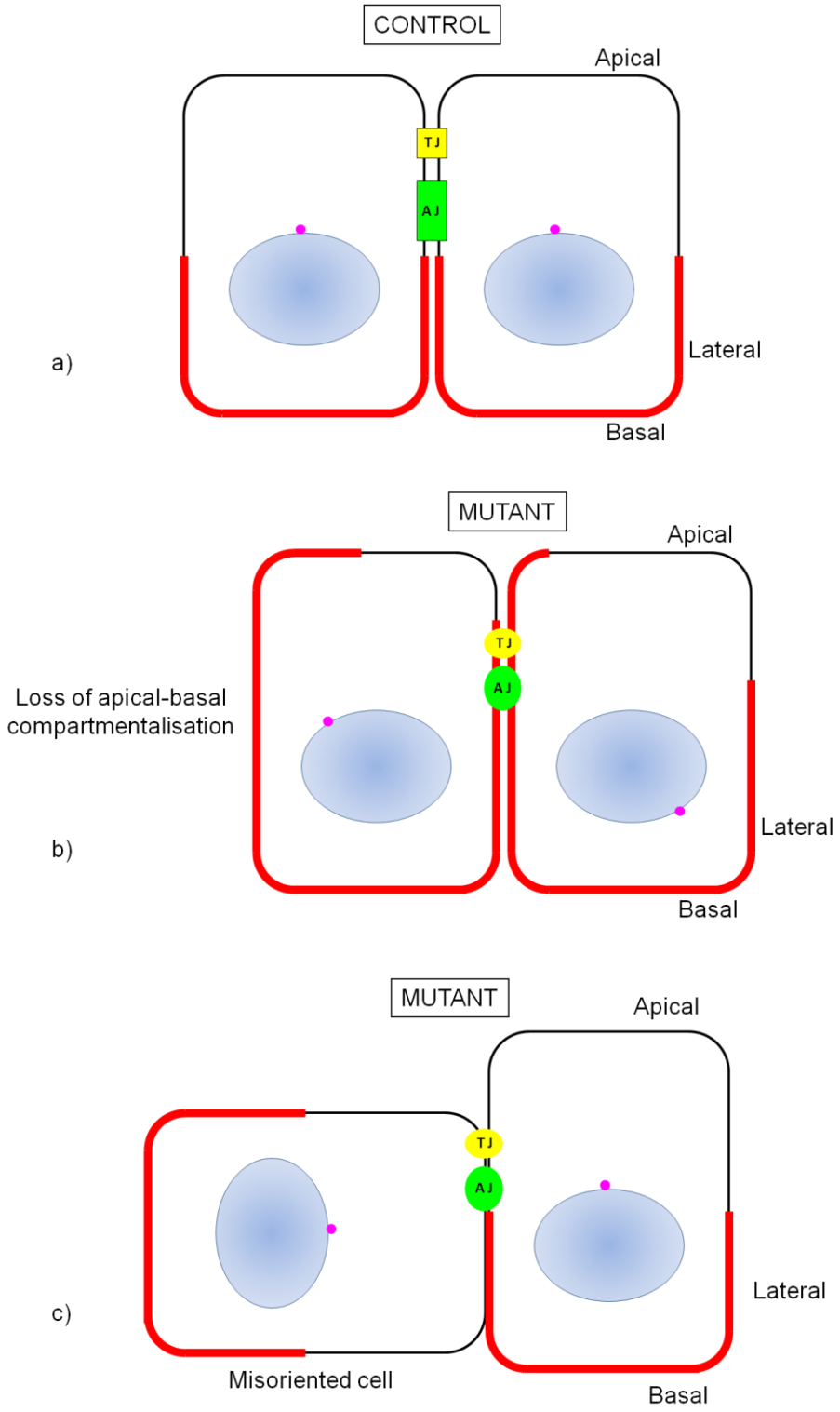

Figure 4.22: Comparison of ABP in control and mutants.

Control shows proper demarcation between apical and basolateral domains (a), divided by adhesion junctions (AJ) and tight junctions (TJ). However, in mutants, when AJ and TJ are disrupted, the apical and basolateral domains lose their boundaries and don't stick to it (b), and there is misorientation of cells leading to abnormal positioning of apical and basal determinants (c).

To look at PCP, two other members of PCP pathway, Dvl2 and Celsr1 were checked in the transition zone. In controls their expression in the transition zone was comparable to Vangl2 expression, with expression localized at cell membrane; however in the absence of Vangl2, their expression was also lost from the membrane, suggesting PCP complex is not formed in the absence of one of the core member. All this evidence is supporting our hypothesis that loss of Vangl2 in SHF leads to loss of their polarity. Together all the results suggests that in the absence of Vangl2, SHF lose their polarity and epithelial nature in the transition zone in distal outflow tract leading to disorganisation of cells, which in turn results in minimal extension of outflow tract (figure 4.23). During outflow tract formation, maximal extension is required for the proper alignment of the base of the aorta with the left ventricle during aorto-pulmonary septation (Sugishita *et al.*, 2004). Therefore, disturbances in the SHF because of loss of Vangl2 leads to reduced extension of the outflow tract resulting in alignment abnormalities.

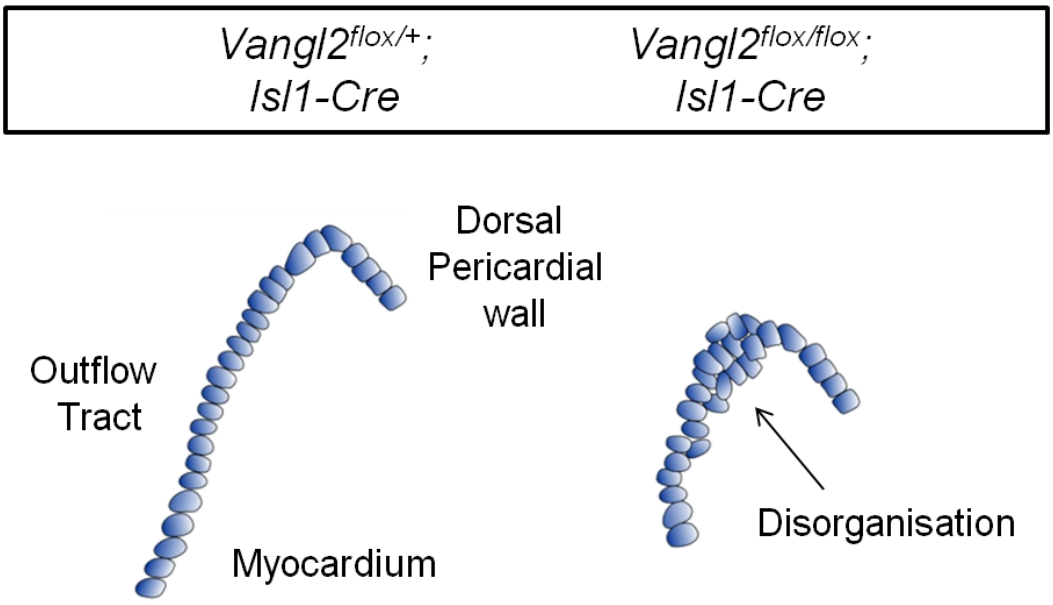

Figure 4.23: Disorganisation of SHF cells

In control SHF cells enter in an organised manner facilitating maximal extention and lengthening of the outflow tract, however in mutants there is disorganisation of cells, which leads to reduced extension of the outflow tract and ultimately resulting in alignment abnormalities.

SHF give rise to cardiomyocytes, smooth muscle cells and to endothelial cells (Moretti *et al.*, 2006). The cardiomyocytes have myocardialization defect in *Lp/Lp* mutants where *Lp/+* controls have extended protusions as lamellipodia and filopodia into the flanking cushion tissue showing the characteristics of motile polarized cells and *Lp/Lp* mutants has rounded cells and no extensions in E13.5 embryos (Phillips *et al.*, 2005). Similar behaviour was seen in *Vangl2$^{flox/flox}$;Isl1-Cre* mutants although at a younger stage as compared to *Lp/Lp*. At E10.5 *Vangl2$^{flox/+}$;Isl1-Cre* embryos showed extensions in the cells, however *Vangl2$^{flox/flox}$;Isl1-Cre* had rounded cells with no protrusions or extensions indicating unpolarized nature of cells in the mutants. At E9.5 as well there was different in expression pattern as in controls there was a gradual increase of MF20 expression in the distal outflow tract and become strong as cells move more proximally showing gradual transition of precursor SHF into differentiated myocardium. However, high level expression was seen abruptly in *Vangl2$^{flox/flox}$;Isl1-Cre* mutants. Smooth muscle cells also showed expression more distally in the *Vangl2$^{flox/flox}$;Isl1-Cre* mutants as compared to controls. Isl1 expression at E9.5 showed loss of nuclear expression more distally in the mutants. Hence, loss of Isl1 expression more distally, abrupt appearance of strong MF20 expression and early expression of smooth muscle cells indicates loss of precursor phenotype of SHF and early differentiation (figure 4.24).

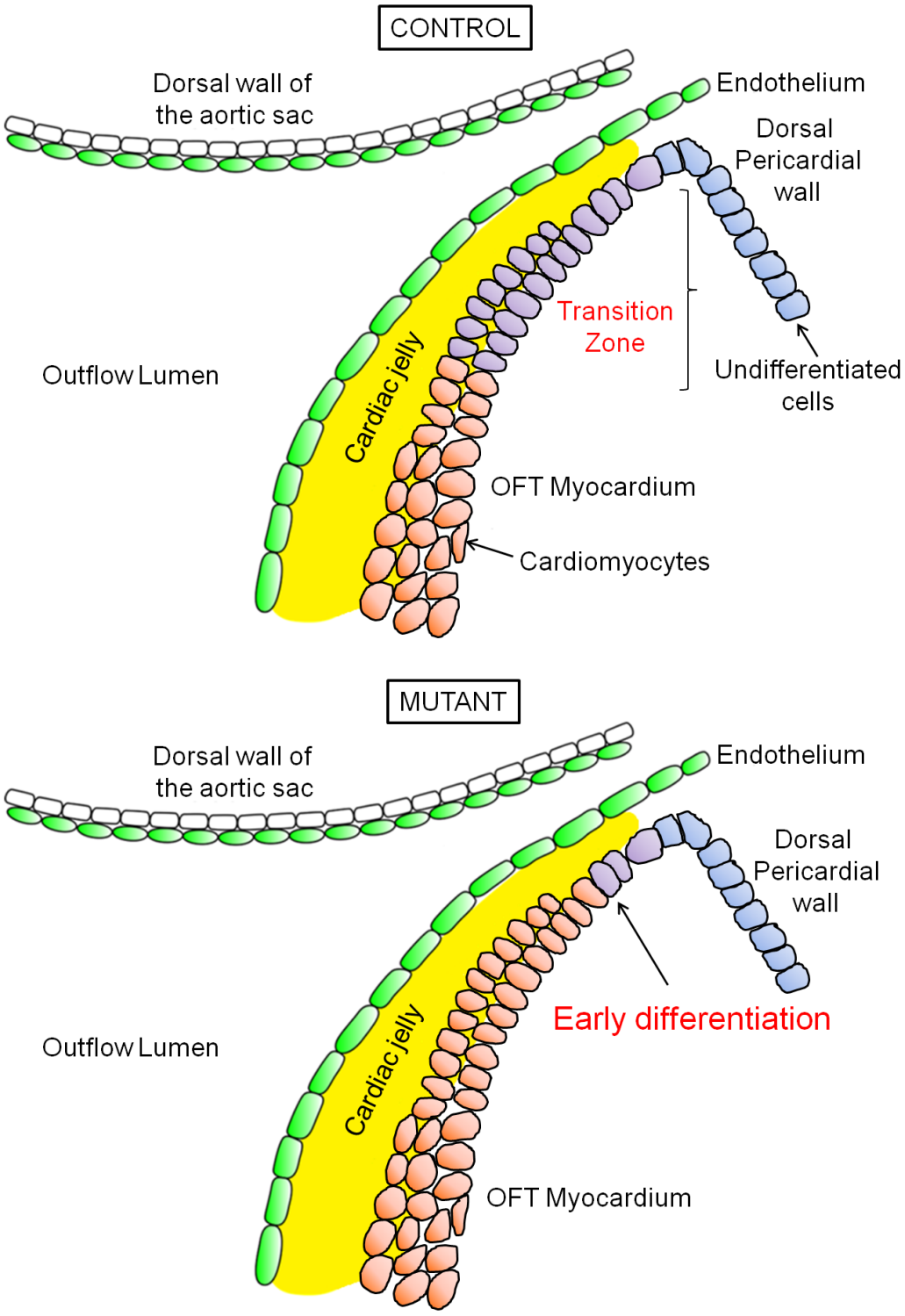

Figure 4.24: Early differentiation of precursor SHF cells in mutants

SHF cells enter the outflow tract in the precursor state and differentiate as they move proximally to form the outflow tract myocardium with a transition zone which there is transition from precursor to differentiated cells in control condition. In contrast, mutants show premature differentiation of SHF cells.

When looked at later stage, E14.5, smooth muscle cells expression appeared to be absent at the outer region of the aortic arterial wall at the aortic root along with loss of elastin fibres in mutants, which are derived from smooth muscle cells. Smooth muscle cells at the base of aorta and pulmonary trunk are derived from SHF cells while at the arch level are derived from NCC (Waldo *et al.*, 2005b). Our results were in consistency with the Waldo model of different origins of smooth muscle cells as SHF specific *Vangl2*$^{flox/flox}$*;Isl1-Cre* mutant showed normal expression of smooth muscle cells at the aortic arch, where the smooth muscle cells are derived from NCC. These results suggest that loss of Vangl2 specifically from the SHF cells affects the maturation of these cells owing to the difference in smooth muscle cells expression and elastin levels in controls and mutants, confirming Vangl2 plays a key role in SHF cells. Together the results suggest that loss of Vangl2 leads to disruption of epithelialisation and polarisation of SHF cells and their premature differentiation in the distal outflow tract. This results in disorganisation of SHF cells while they entering the outflow tract leading to impairment in outflow tract lengthening process, which ultimately results in double outlet right ventricle in *Vangl2*$^{flox/flox}$*;Isl1-Cre* mutants.

Outflow tract defects are common in mice with mutations in PCP genes (Henderson *et al.*, 2001; Hamblet *et al.*, 2002; Curtin *et al.*, 2003; Paudyal *et al.*, 2010), indicating their importance in SHF. I therefore decided to look at upstream and downstream targets of Vangl2 in the PCP pathway and establish whether they also play an important role in SHF for normal heart development. This forms the basis of the next chapter.

Chapter 5

Upstream and Downstream of Vangl2

5.1 Introduction

The requirement of the PCP gene, *Vangl2* specifically in SHF cells is established in the previous chapters. Loss of Vangl2 function in these cells impacts on morphogenesis of the cardiac outflow tract by failing to regulate polarisation and organisation of SHF cells into and within the developing outflow tract in the transition zone. However, as other components of PCP pathway have been involved in cardiac outflow tract morphogenesis (Hamblet *et al.*, 2002; Curtin *et al.*, 2003; Phillips *et al.*, 2007; Schleiffarth *et al.*, 2007; Zhou *et al.*, 2007b; Etheridge *et al.*, 2008; Nagy *et al.*, 2010; Paudyal *et al.*, 2010; Yu *et al.*, 2010), it was considered relevant to look at the signalling and transcription factors working upstream and downstream of Vangl2.

5.1.1 Upstream of PCP signalling

The Wnt family plays a role in different cell processes, and can be divided into two classes. The first Wnt class, which includes Wnt1, Wnt3a, Wnt8, activates the canonical β-catenin pathway and regulates cell proliferation and cell fate (Cadigan and Nusse, 1997; Sokol, 1999). The second class is the Wnt5a class, which includes Wnt5a and Wnt11, and activates non-canonical Wnt pathway and have been reported to regulate planar cell polarity and convergent extension movements in *zebrafish* and *Xenopus* (Moon *et al.*, 1993; Heisenberg *et al.*, 2000; Sokol, 2000; Tada and Smith, 2000; Wallingford *et al.*, 2000). In mouse, Wnt5a interacts with Vangl2 during cochlear extension, neural tube closure, cilia orientation (Qian *et al.*, 2007) and during limb elongation (Gao *et al.*, 2011). This interaction of Wnt5a with Vangl2 is through Ror2 as it induces Ror2-Vangl2 complex and regulates cell polarity (Gao *et al.*, 2011). Ror2 is a receptor belonging to Ror family of receptor tyrosine kinases (RTKs) and has cysteine rich domains (CRD). Wnt5a binds extracellularly to the cysteine rich domain of Ror2 (Oishi *et al.*, 2003) and induces a complex formation between Ror2 and Vangl2. This complex between Ror2 and Vangl2 is formed through phosphorylation of

Vangl2 via tyrosine kinase (TK) domain present on Ror2 intracellularly and CKIδ (Casein Kinase 1) (Gao *et al.*, 2011), which is shown to be a mandatory factor in PCP signalling in Drosophila (Klein *et al.*, 2006; Strutt *et al.*, 2006) (Figure 5.1). This complex is known to regulate cell polarity.

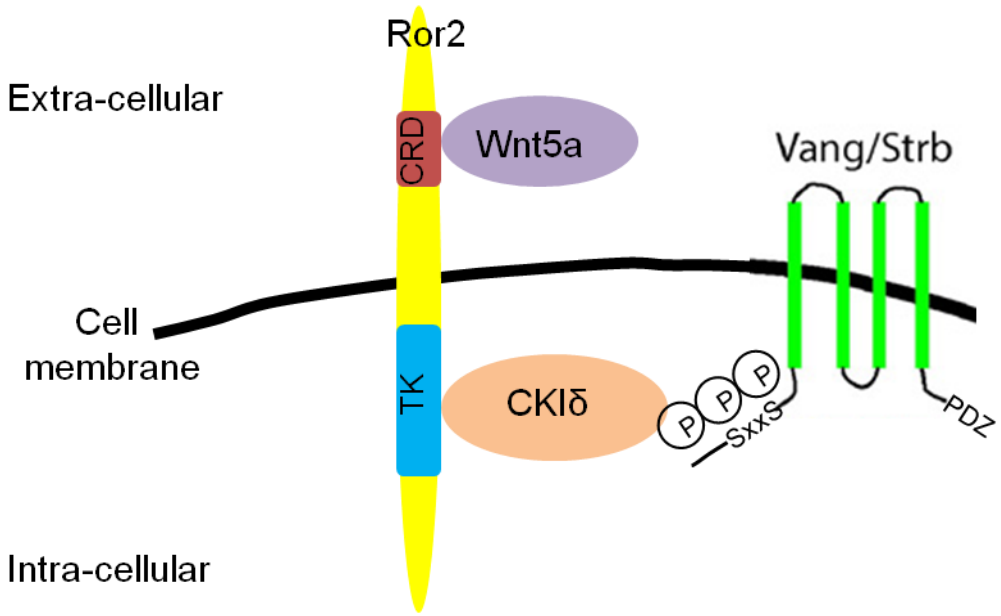

Figure 5.1: Vangl2 phosphorylation by Ror2 and Wnt5a
Wnt5a interacts with Ror2 through its cysteine rich domains (CRD) present extra-cellularly and the tyrosine kinase (TK) domain present intra-cellularly interacts with Vangl2 and phophorylates it via casein kinase 1 (CKIδ).

Wnt5a and *Ror2* have a similar expression pattern and are expressed in the developing face, limbs, heart and lungs (Yamaguchi *et al.*, 1999; DeChiara *et al.*, 2000; Takeuchi *et al.*, 2000; Li *et al.*, 2002). Mutations in both genes individually lead to respiratory dysfunction, cardiac defects and shortened-limb dwarfism known as Robinow Syndrome in humans (Van Bokhoven *et al.*, 2000; Gao *et al.*, 2011). A similar phenotype is seen in *Wnt5a* and *Ror2* mouse mutants (Yamaguchi *et al.*, 1999; DeChiara *et al.*, 2000; Takeuchi *et al.*, 2000; Oishi *et al.*, 2003), and similar expression pattern indicate a physical and functional interaction between Wnt5a and Ror2, which has been demonstrated before (Oishi

et al., 2003). Mutation in both *Ror2* and *Wnt5a* also leads to cardiac defects (Oishi *et al.*, 2003). Wnt5a null mice show 100% penetrance for outflow tract defects like common arterial trunk and also exhibit aortic arch defects in some nulls, while Ror2 null mice exhibit ventricular septal defects (Oishi *et al.*, 2003; Schleiffarth *et al.*, 2007). Similar external phenotype of *Wnt5a* null, *Ror2* null and *Lp/Lp* mutants having shortened anterior-posterior body axis and shortened limbs suggests *Vangl2*, *Ror2* and *Wnt5a* have similar roles and are present in the same signalling pathway. Their interaction with *Vangl2* hasn't been studied before in heart but because of their interaction with *Vangl2* in other developmental processes (Gao *et al.*, 2011), it may be that they play important roles in heart as well.

5.1.2 Downstream of PCP signalling

Vangl2 interact with PCP signalling molecules and activates Rac-JNK and Rho-ROCK signalling cascades (Katoh, 2002; Torban *et al.*, 2004; Katoh, 2005). ROCK and Rac1 are both downstream effectors of the PCP pathway, and have roles in cell adhesion, migration and polarity (Bosco *et al.*, 2009; Amano *et al.*, 2010). PCP proteins present at the cell membrane activate downstream signalling via the small GTPases RhoA and Rac. This activation leads to activation of Rho kinases (ROCK) and c-jun terminal kinase (JNK) respectively, which helps in reorganization of the cell cytoskeleton and effects cell movements (figure 5.2).

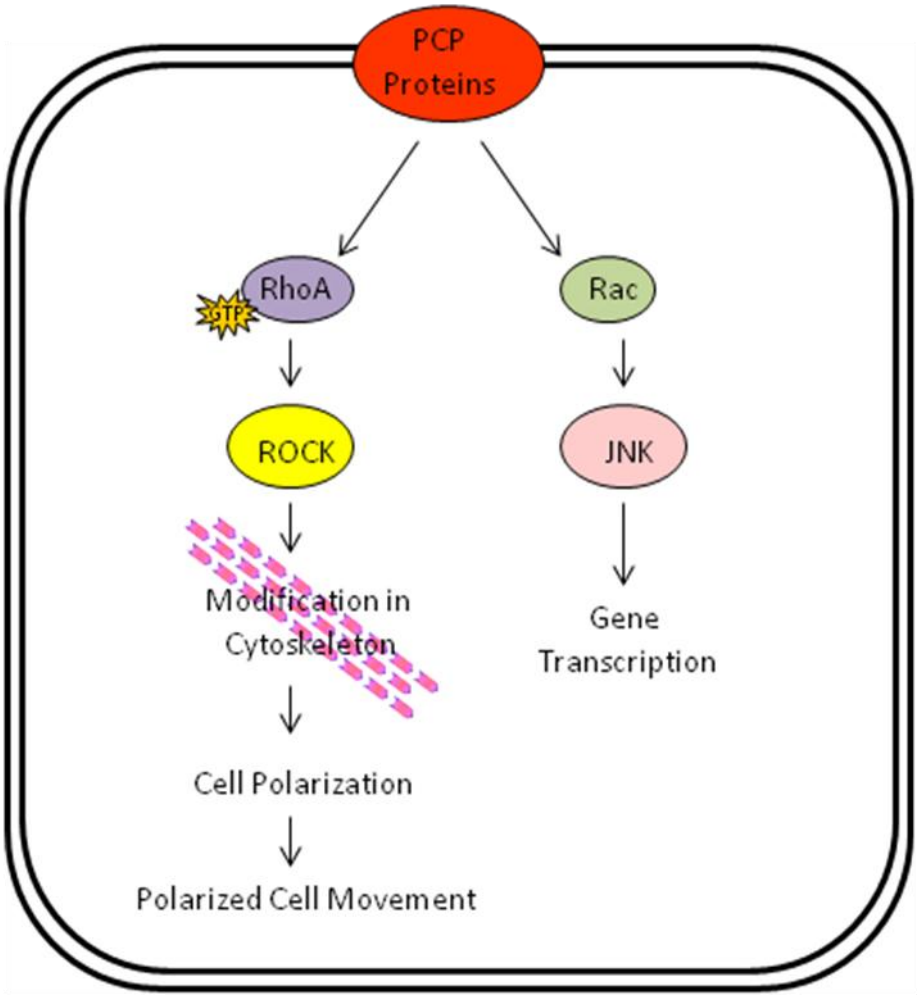

Figure 5.2: ROCK and Rac1 as downstream targets of PCP signalling.

PCP proteins activate RhoA and Rac, which leads to activation of ROCK leading to reorganization in cell cytoskeleton and polarized cell movement, and JNK which helps in transcription process.

ROCK is a serine/threonine protein kinase downstream of the GTPase Rho A (Amano *et al.*, 2010). ROCKs phosphorylate over 20 substrate proteins primarily involved in regulating assembly of actin filaments within the cytoskeleton (Riento and Ridley, 2003). Through this mechanism it regulates a broad variety of physiological processes, including cell migration (Worthylake and Burridge, 2003), proliferation (Sahai *et al.*, 2001), transformation (EMT) (Zondag *et al.*, 2000), apoptosis (Sebbagh *et al.*, 2001), morphology (Sordella *et al.*, 2002) and establishing cell polarity (Amano *et al.*, 2010). ROCK is present in the form of 2 isoforms (Rock 1 and 2), which are highly conserved serine/threonine kinases (Satoh *et al.*, 2011) and have similar expression patterns and roles during embryonic development (Thumkeo *et al.*, 2005). ROCK is key effector of RhoA signalling and ROCK1 is co-expressed with RhoA in the myocardial cushion interface and this co-expression is disrupted by the mutation of the *Vangl2* gene (Brade *et al.*, 2006). Knockout of ROCK1 and ROCK2 independently does not result in cardiac defects (Thumkeo *et al.*, 2003; Thumkeo *et al.*, 2005), however, disruption of ROCK signalling using the specific chemical inhibitor Y27632 in chick embryos results in a range of cardiac anomalies (Wei *et al.*, 2001). It has been known that ROCK plays an important role in cell movement and development of their polarity (Raftopoulou and Hall, 2004) and loss of its function in Isl1 expressing cells prevents normal movement of SHF cells within the developing heart in mouse (Hildreth *et al.*, 2009). This leads to defects like atrioventricular septal defects and hypoplastic venous valves in the inflow region of the heart (Hildreth *et al.*, 2009). As SHF cells contribute to the outflow region as well in addition to inflow region of heart, ROCK activity was looked in the outflow tract.

Rac1 is a member of the Rho family of small guanosine triphosphatases (GTPases), which are a subgroup of Ras-superfamily of GTPases. It regulates focal adhesion and reorganization of actin-cytoskeleton in cellular protrusions (Ridley, 2001) and plays a fundamental role in cellular processes like cytoskeleton organization, gene transcription, DNA synthesis, superoxide production, cell migration, cell proliferation and apoptosis (Bosco *et al.*, 2009). All these roles of Rac1 has been investigated in cardiovascular development in

terms of cardiac progenitor populations (Tan *et al.*, 2008; Bosco *et al.*, 2009; D'Amico *et al.*, 2009; Thomas *et al.*, 2010). It regulates proliferation of vascular smooth muscle cell and their migration, cardiomyocyte hypertrophy, and realignment of endothelial cells (Sawada *et al.*, 2010). Deletion of Rac1 specifically in endothelial cells leads to embryonic lethality (Fiedler, 2009), and in neural crest cells mutant embryos have craniofacial abnormalities with cardiac defects like common arterial trunk and aberrant remodelling of pharyngeal arch arteries (Thomas *et al.*, 2010).

As ROCK and Rac1 are seen to play an important role in cell migration and cell survival or cell apoptosis, their role in cardiac development is very important and raises the possibility of their involvement in congenital heart defects related to migrating cardiac progenitor populations. Therefore, we aim to investigate the role of PCP pathway downstream targets, Rac1 and ROCK in SHF for heart development and relate them to the defects in the *Vangl2;Isl1-Cre* mutants.

To genetically dissect the role of *Rac1* and *ROCK* in SHF cells, expression of Rac1 and ROCK was specifically deleted/knocked down in cells derived from SHF. For tissue specific removal of *Rac1*, *Rac1flox* mice (Walmsley *et al.*, 2003) were used, and for *ROCK*, a dominant negative form of *ROCK* was used, called *ROCKDN* (Kobayashi *et al.*, 2004). ROCKDN protein has a point mutation in the RhoA binding site, therefore cannot bind to RhoA. It instead binds to endogenous ROCK1 and ROCK2 and inhibits the function of the kinase domain preventing functional activity of both ROCK isoforms (Kobayashi *et al.*, 2004). There is a *CAT* gene cassette ahead of *ROCKDN* in the sequence which does not let it express, however this *CAT* cassette has *lox P* sites on its either sides and can be removed using *Cre* resulting in expression of ROCKDN. The SHF specific promoter, *Isl1-Cre* (Yang *et al.*, 2006) was used to drive SHF specific deletion/knockdown (deletion in case of *Rac1* and knockdown in case of *ROCKDN*).

5.2 Results

5.2.1 Wnt5a and Ror2 regulating Vangl2 expression

To look at cardiac defects in the absence of Wnt5a and Ror2, null mutants of each ($Wnt5a^{-/-}$ and $Ror2^{-/-}$) were analysed. Genetic interaction between Vangl2, Wnt5a and Ror2 was looked at using Lp mice, without using Cre lines. Finally, cellular behaviour was analysed in transition zone of the outflow tract of Wnt5a and Ror2 null embryos for cell adhesion and polarity using specific markers.

5.2.1.1 Wnt5a and Ror2 mutation leads to external and cardiac defects

$Wnt5a^{+/-}$ heterozygous mice, and separately *$Ror2^{+/-}$* heterozygous mice were crossed together to generate *$Wnt5a^{-/-}$* and *$Ror2^{-/-}$* embryos, which were collected at E14.5 to look at external and cardiac phenotype. *$Wnt5a^{-/-}$* and *$Ror2^{-/-}$* embryos (n=4) showed external abnormalities and this phenotype was similar to the external phenotype seen in *Lp/Lp* mutant embryos (table), exhibiting shortened frontonasal processes (figure 5.3b,c,e,f,h,i bold white arrow), shortened body along P-D axis and shortened limbs (figure 5.3j red lines and graph). These range of external defects are summarized in table 5.1.

Table 5.1: External defects in *Lp/Lp*, *$Wnt5a^{-/-}$* and *$Ror2^{-/-}$* at E14.5

External defects	*Lp/Lp* (n=4)	*$Wnt5a^{-/-}$* (n=4)	*$Ror2^{-/-}$* (n=4)
CRN	4 (100%)	2 (50%)	2 (50%)
Oedema	0 (0%)	2 (50%)	0 (0%)
Shortened limbs	4 (100%)	4 (100%)	4 (100%)

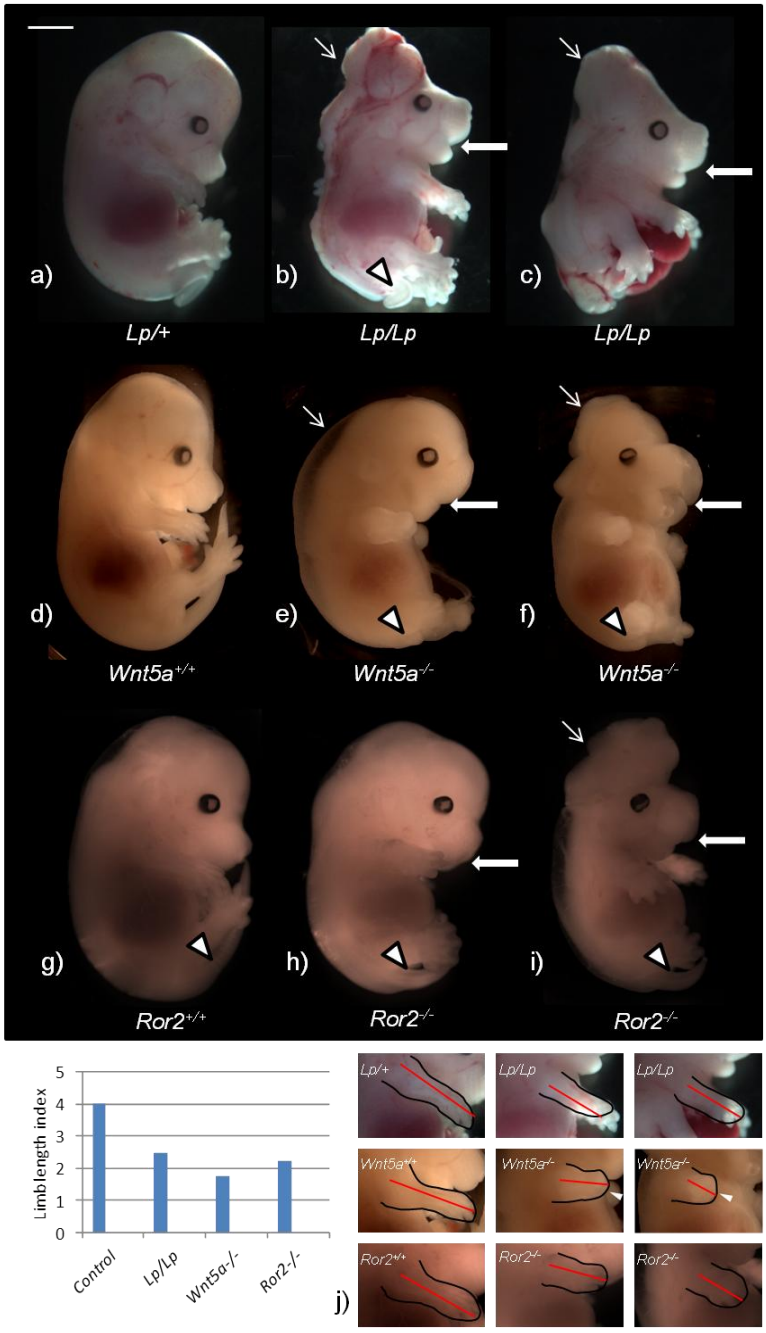

Figure 5.3: External defects in *Lp/Lp, Wnt5a*$^{-/-}$ and *Ror2*$^{-/-}$embryos at E14.5

Whole embryos at E14.5 with external defects. **a-c**) *Lp* embryos with normal external phenotype of *Lp/+* embryo (**a**), *Lp/Lp* embryos showing open neural tube (CRN) (b) and another *Lp/Lp* embryo showing open neural tube along with gastrochitisis (c), with shortened frotonasal processes (**b,c** bold white arrow). **d-f)** *Wnt5a*$^{+/+}$ embryo with normal external phenotype (d) and *Wnt5a*$^{-/-}$ embryo with oedema (**e**, arrow), open neural tube (**f,** arrow) with shortened frotonasal processes (e,f bold white arrow). **g-i)** *Ror2*$^{+/+}$ embryo with normal external phenotype (g) and *Ror2*$^{-/-}$ embryo open neural tube (**i,** arrow) with shortened frotonasal processes (h,i bold white arrow). **j)** Short limbs in *Lp/Lp*, *Wnt5a*$^{-/-}$ and *Ror2*$^{-/-}$ embryos as compared to *Lp/+*, *Wnt5a*$^{+/-}$ and *Ror2*$^{+/-}$ embryos (red lines) and graph showing limb length index of the embryos. Scale - 2000µm.

To check the presence of cardiac defects, embryos were embedded in wax and then transverse sections through heart (figure 5.4a) were stained with H&E. Both *Wnt5a*$^{-/-}$ and *Ror2*$^{-/-}$ embryos showed cardiac defects, which were also present in the outflow region as seen in *Lp/Lp* mutants. Table in figure 4 shows cardiac defects and their occurrence in *Lp/Lp*, *Wnt5a*$^{-/-}$ and *Ror2*$^{-/-}$ embryos. *Lp/Lp* mutants exhibit double outlet right ventricle, ventricular septal defect (figure 5.4b,c) and aortic arch defect. Outflow defects were seen in *Wnt5a*$^{-/-}$ embryos (n=4), having common arterial trunk (figure 4d) and ventricular septal defect (figure 5.4e) in all null embryos. However, 25% (1/4) *Ror2*$^{-/-}$ embryos had double outlet right ventricle (figure 5.4f) and 50% (2/4) penetrance of ventricular septal defects (figure 5.4g).

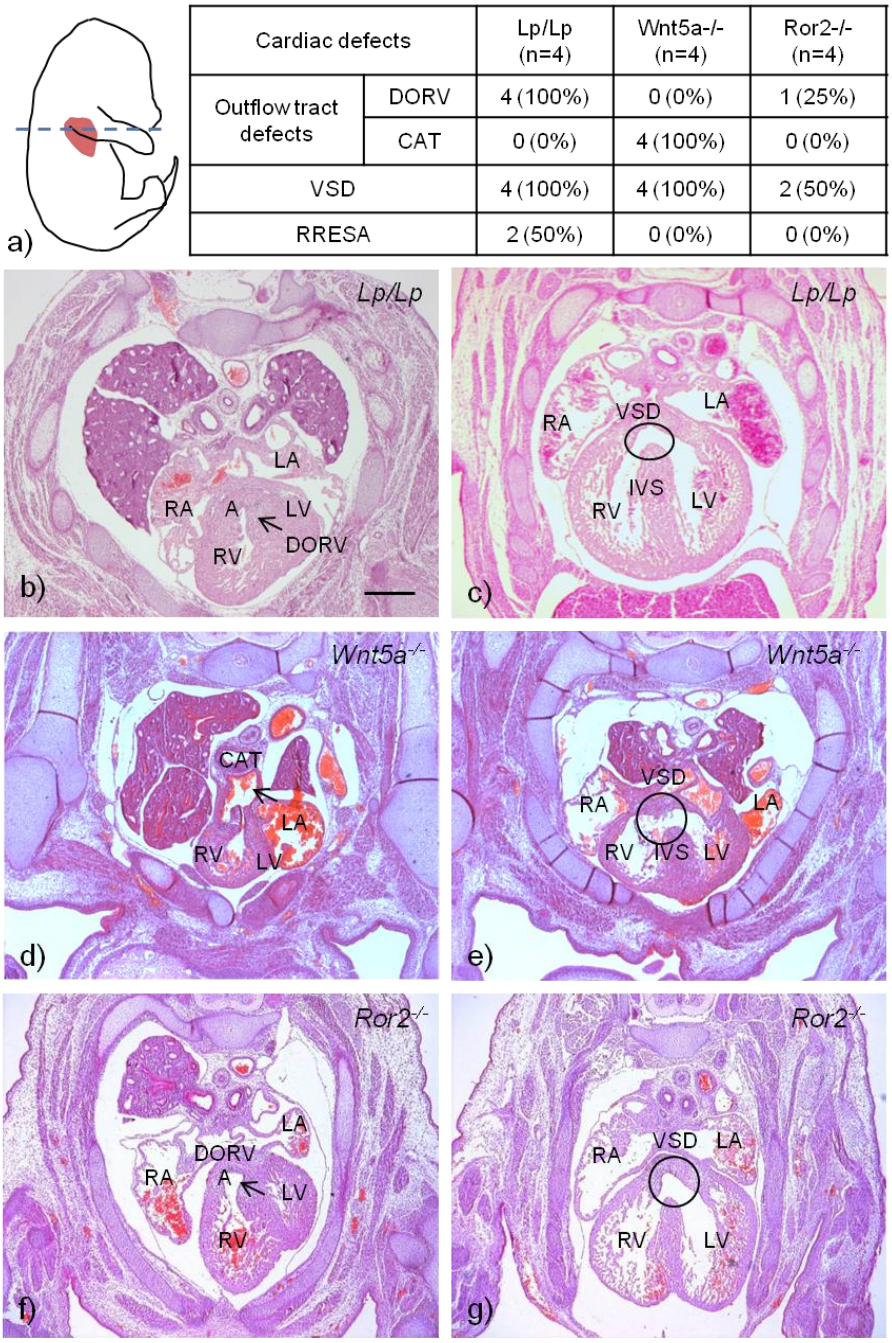

Cardiac defects		Lp/Lp (n=4)	Wnt5a-/- (n=4)	Ror2-/- (n=4)
Outflow tract defects	DORV	4 (100%)	0 (0%)	1 (25%)
	CAT	0 (0%)	4 (100%)	0 (0%)
VSD		4 (100%)	4 (100%)	2 (50%)
RRESA		2 (50%)	0 (0%)	0 (0%)

Figure 5.4: Cardiac defects in *Lp/Lp*, *Wnt5a*$^{-/-}$ and *Ror2*$^{-/-}$embryos at E14.5

a) Plane of the section with table showing different cardiac defects observed in *Lp/Lp*, *Wnt5a*$^{-/-}$ and *Ror2*$^{-/-}$ embryos. b,c) Transverse sections through heart of *Lp/Lp* mutant embryos showing double outlet right ventricle (b) and ventricular septal defect (c). **d,e**) Transverse sections through heart of *Wnt5a*$^{-/-}$ embryos showing common arterial trunk (d) and ventricular septal defect (e). **f,g)** Transverse sections through heart of *Ror*$^{2-/-}$ embryo showing double outlet right ventricle (f) and ventricular septal defect (**g**). RA-right atria, LA-left atria, RV-right ventricle, LV-left ventricle, A-aorta, PT-pulmonary trunk, CAT-common arterial trunk, VSD-ventricular septal defect, DORV-double outlet right ventricle. Scale - 20µm.

5.2.1.2 Disruption of adherens junction in Wnt5a-/- and Ror2-/- embryos

Wnt5a$^{-/-}$ and *Ror2*$^{-/-}$ embryos were collected at E9.5 stage to match the analysis of *Vangl2*$^{flox/flox}$*;Isl1-Cre* mutants described in the previous chapter. At this point SHF cells are entering into the outflow tract and disruption in their organization and polarity at this stage leads to defects in the fully formed heart. *Lp* mice was established as SHF mutant with respect to heart development by genetically dissecting the role of *Vangl2* in SHF cells using our *Vangl2*$^{flox/flox}$*;Isl1-Cre* mice. Given the interaction of *Wnt5a* and *Ror2* with *Vangl2*, it was hypothesised that their deletion would also lead to abnormalities in SHF cells within the outflow tract as seen in our *Vangl2*$^{flox/flox}$*;Isl1-Cre* mutants. Therefore cellular organization was looked at using β-catenin, presence of epithelial nature and adherens junction was analysed by looking at apical localization of E-cadherin, presence of tight junctions through PKCζ and apical-basal polarity (ABP) in the cells by basolateral localization of laminin in *Wnt5a*$^{-/-}$ and *Ror2*$^{-/-}$ embryos (n=3).

Adherens junctions (AJ) have a role in establishing cell polarity (Wu *et al.*, 2010) and cadherin-catenin complex is an important component of AJ. In E9.5 *Vangl2*$^{flox/flox}$*;Isl1-Cre* mutant embryos, there was mislocalisation of E-cadherin apical expression in the distal outflow tract (figure 5.5 c,g arrow heads). Similar expression pattern was seen in *Wnt5a*$^{-/-}$ and *Ror2*$^{-/-}$ embryos. Figure 5.5 shows the expression of E-cadherin in the distal outflow tract in *Wnt5a* and *Ror2* control and null embryos. The expression in the *Wnt5a*$^{+/+}$ and *Ror2*$^{+/+}$ embryos in the distal outflow tract (figure 5.5 k,s arrow heads) was seen at the apico-basal boundary, however there was mislocalisation of E-cadherin expression in *Wnt5a*$^{-/-}$ (figure 5.5 o arrow heads) and *Ror2*$^{-/-}$ (figure 5.5 w arrow heads) embryos as it was seen more towards basolateral compartment with no expression on apical side.

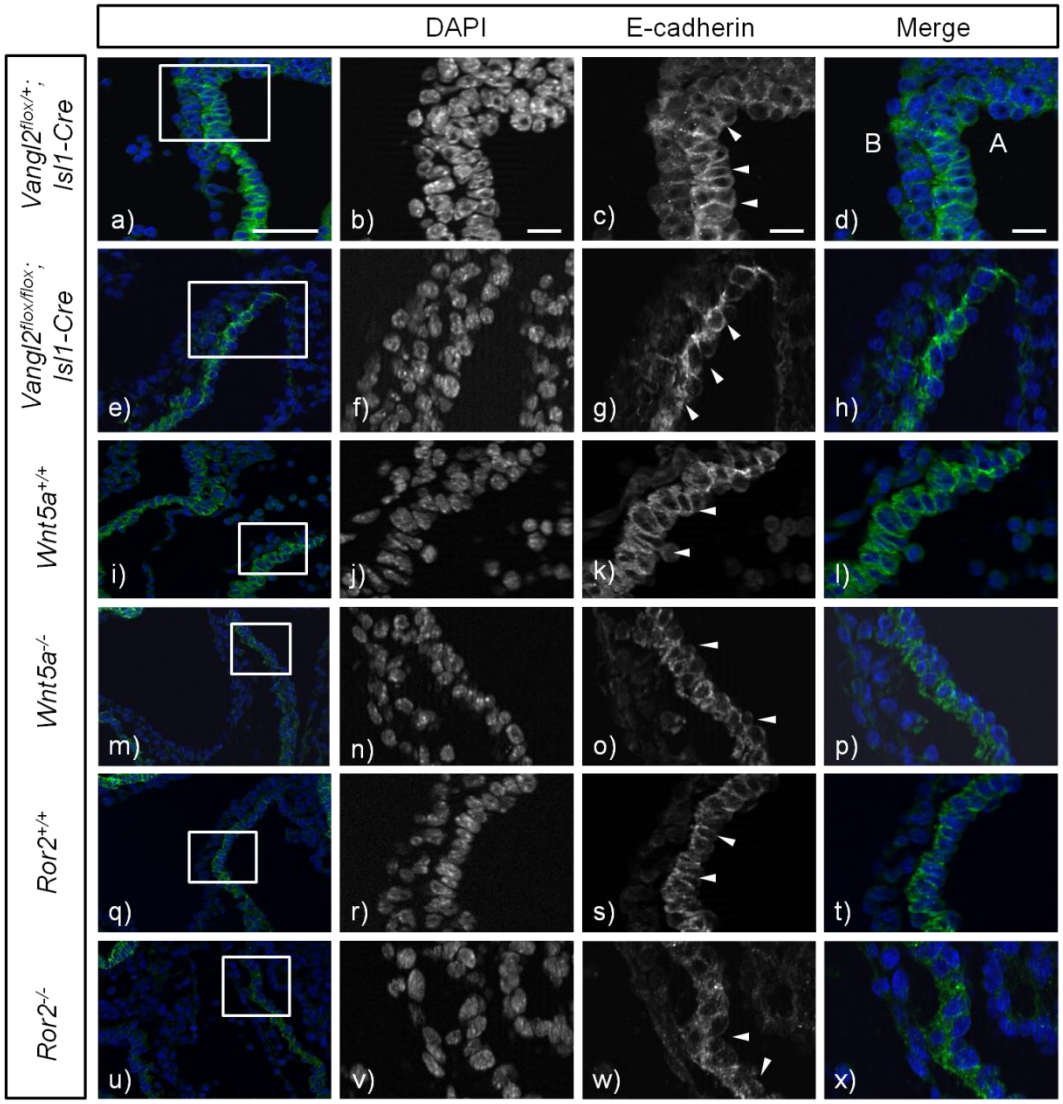

Figure 5.5: Loss of apical-basal localization of E-Cadherins expression in transition zone of *Vangl2*$^{flox/flox}$*;Isl1-Cre*, *Wnt5a*$^{-/-}$ and *Ror2*$^{-/-}$ mutants at E9.5

a-d) E-cadherin expression (in green) in *Vangl2*$^{flox/+}$*;Isl1-Cre* control (a) showing apical –basal expression (arrow heads in c). **e-h)** E-cadherin expression in *Vangl2*$^{flox/flox}$*;Isl1-Cre* mutant (e) with expression at basolateral compartment of some cells in the transition zone (arrow heads in g). **i-l)** E-cadherin expression in *Wnt5a*$^{+/-}$ control (i) showing apical –basal expression (arrow heads in k). **m-p)** E-cadherin expression in *Wnt5a*$^{-/-}$ mutant (m) with disruption of expression in some cells in the transition zone (arrow heads in o). **q-t)** E-cadherin expression in *Ror2*$^{+/-}$ control (q) showing apical –basal expression (arrow heads in s). **u-x)** E-cadherin expression in *Ror2*$^{-/-}$ mutant (u) with disrupted expression at cell boundary and expression at basolateral compartment of some cells in the transition zone (arrow heads in w). A-apical, B-basal. Scale - 100µm.

In *Vangl2*$^{flox/flox}$*;Isl1-Cre* mutant embryos, expression of β-catenin showed disrupted cellular organization (figure 5.6 c,g arrow heads). β-catenin expression in *Wnt5a* and *Ror2* embryos showed it was present localised at the membrane of distal outflow tract wall cells marking their basolateral compartment in *Wnt5a*$^{+/+}$ and *Ror2*$^{+/+}$ embryos (figure 5.6 k,s arrow heads). The expression was present in the cells in the distal outflow tract in both *Wnt5a*$^{-/-}$ (figure 5.6 o arrow heads) and *Ror2*$^{-/-}$ (figure 5.6 w arrow heads) embryos, but cells appeared to be disorganised as compared to their respective controls. However cellular organisation in *Ror2*$^{-/-}$ embryo section appears less affected when compared to *Wnt5a*$^{-/-}$ embryo.

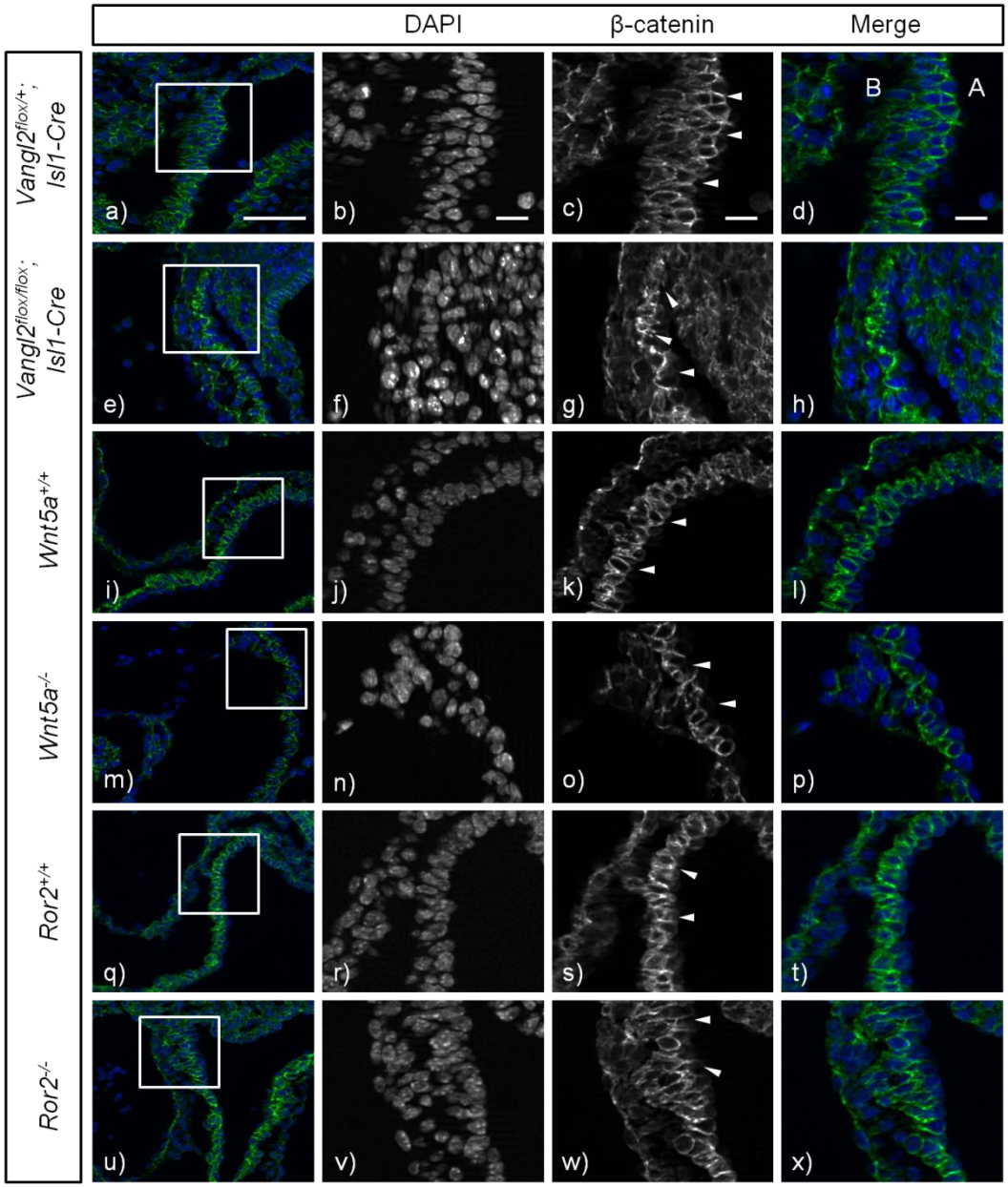

Figure 5.6: Disorganized expression of β-catenin in transition zone of *Vangl2$^{flox/flox}$;Isl1-Cre, Wnt5a-/-* and *Ror2-/-* mutants at E9.5

a-d) β-catenin expression (in green) in *Vangl2$^{flox/+}$;Isl1-Cre* control (a) showing membrane bound expression (arrow heads in c). **e-h)** β-catenin expression in *Vangl2$^{flox/flox}$;Isl1-Cre* mutant (e) with disorganized expression in some cells in the transition zone (arrow heads in g). **i-l)** β-catenin expression in *Wnt5a$^{+/-}$* control (i) showing membrane bound expression (arrow heads in k). **m-p)** β-catenin expression in *Wnt5a$^{-/-}$* mutant (m) with disorganized expression in some cells in the transition zone (arrow heads in o). **q-t)** β-catenin expression in *Ror2$^{+/-}$* control (q) showing membrane bound expression (arrow heads in s). **u-x)** β-catenin expression in *Ror2$^{-/-}$* mutant (u) with some cells in disorganized manner in the transition zone (arrow heads in w). A-apical, B-basal. Scale - 100µm.

Expression of these markers was looked at another region than transition zone in the distal outflow tract to check if it is a universal effect or just in the transition zone. E-cadherin and β-catenin expression was looked at dorsal wall of aortic sac as observed in *Vangl2;Isl1-Cre* embryos, and confirm disruption of expression only in the transition zone. It was observed that these adhesion proteins are expressed in a comparable manner in controls and mutants in regions other than transition zone (figure 5.7 a2-h2 arrow heads) and show different expression pattern in transition zone only.

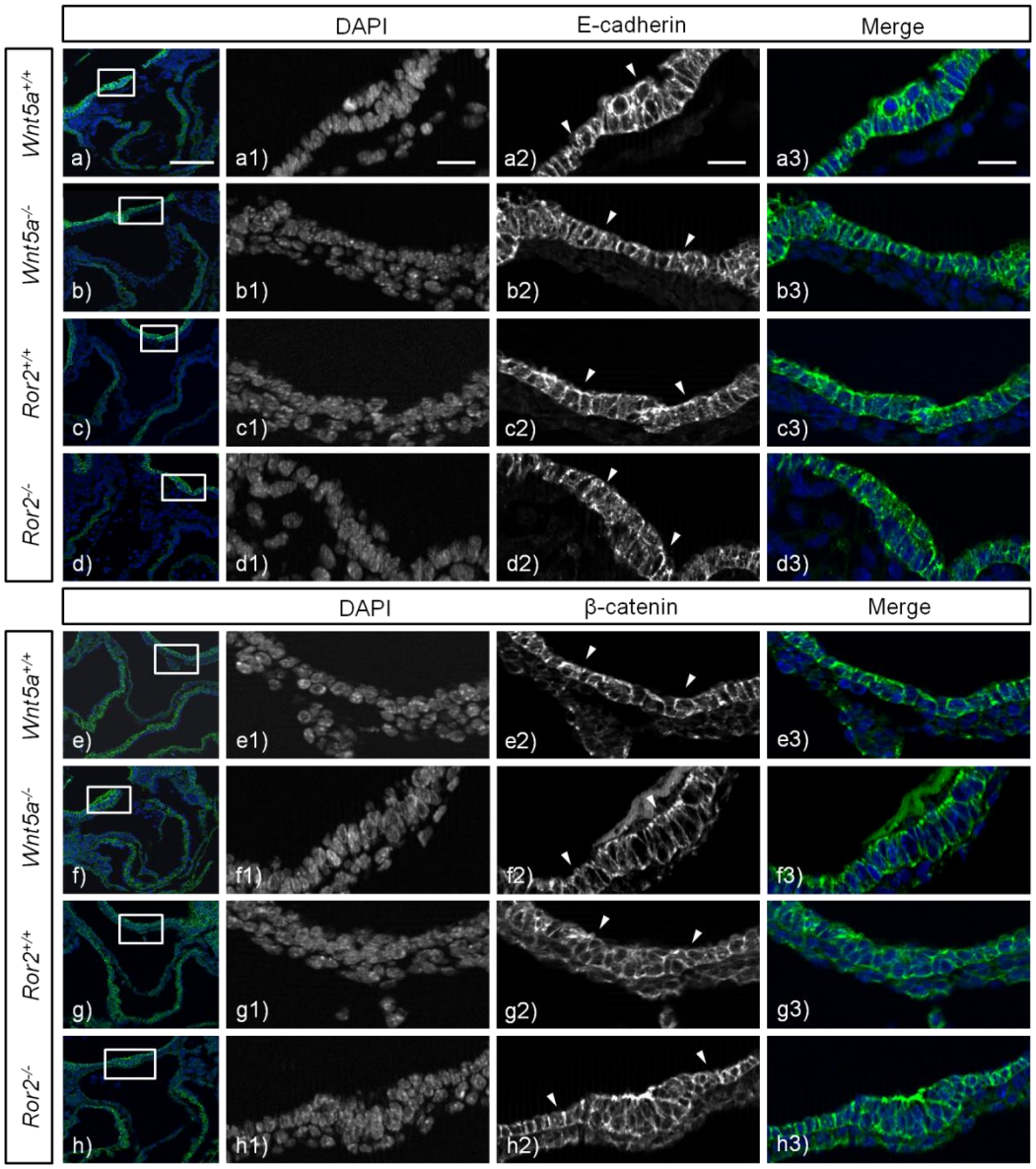

Figure 5.7: Comparable expression of E-cadherin and β-catenin in controls and mutants outside transition zone

a-d) E-cadherin expression (in green) in *Wnt5a*$^{+/-}$ control (a) and *Ror2*$^{+/-}$ control (c) showing apical–basal expression (arrow heads in a2,c2) and in *Wnt5a-/-* mutant (b) and *Ror2*$^{-/-}$ mutant (d) also with apical-basal expression in cells in the dorsal wall of aortic sac (arrow heads in b2,d2). **e-h)** β-catenin expression (in green) in *Wnt5a*$^{+/-}$ control (e) and *Ror2*$^{+/-}$ control (g) showing membrane bound expression (arrow heads in e2,g2) and in *Wnt5a*$^{-/-}$ mutant (f) and *Ror2*$^{-/-}$ mutant (h) also showing membrane bound expression in cells in the dorsal wall of aortic sac (arrow heads in f2,h2). Scale - 100µm.

Similar expression pattern of these markers was observed in *Vangl2*$^{flox/flox}$*;Isl1-Cre* mutants at E9.5 in the distal outflow tract, indicating disruption of AJ and loss of epithelial nature of the cells in the transition zone in *Wnt5a*$^{-/-}$ and *Ror2*$^{-/-}$ embryos, like in *Vangl2*$^{flox/flox}$*;Isl1-Cre* mutants. This similar phenotype in the absence of *Vangl2*, *Wnt5a* and *Ror2* suggested relation between them indicating disruption in one may lead of similar disruption in cell behaviour.

5.2.1.3 Disruption of tight junctions in Wnt5a$^{-/-}$ *and Ror2*$^{-/-}$ *embryos*

Another epithelial marker, PKCζ expression was looked at, which is present enriched in apical compartment of the cells at the point of tight junctions (TJ). In *Vangl2*$^{flox/flox}$*;Isl1-Cre* mutant embryos loss of apical enrichment of PKCζ expression in the distal outflow tract from cells was observed at E9.5 (figure 5.8 c,g arrow heads) indicating disruption in TJ. Figure 5.8 shows PKCζ expression localized at TJ (at the apical side of the cells) in *Wnt5a*$^{+/+}$ embryo (figure 5.8 k arrow heads) and *Ror2*$^{+/+}$ embryo (figure 5.8 s arrow heads). This expression can be seen in cells before entering the outflow tract and while in distal outflow tract. However, in *Wnt5a*$^{-/-}$ embryos PKCζ expression was mislocalised with no apical localization in cells in the dorsal pericardial wall and in the distal outflow tract (figure 5.8 o arrow heads). In *Ror2*$^{-/-}$ embryos, cells before entering outflow tract had this apical localization, while the cells in the distal outflow tract in the transition zone had mislocalised PKCζ expression with no apical localization (figure 5.8 w arrow heads) similar to *Vangl2*$^{flox/flox}$*;Isl1-Cre* phenotype. Mislocalization of PKCζ expression in TJ have role in polarity of cells and similar expression leading to disrupted cellular polarity was also seen in our *Vangl2*$^{flox/flox}$*;Isl1-Cre* mutants indicating a strong link between these genes.

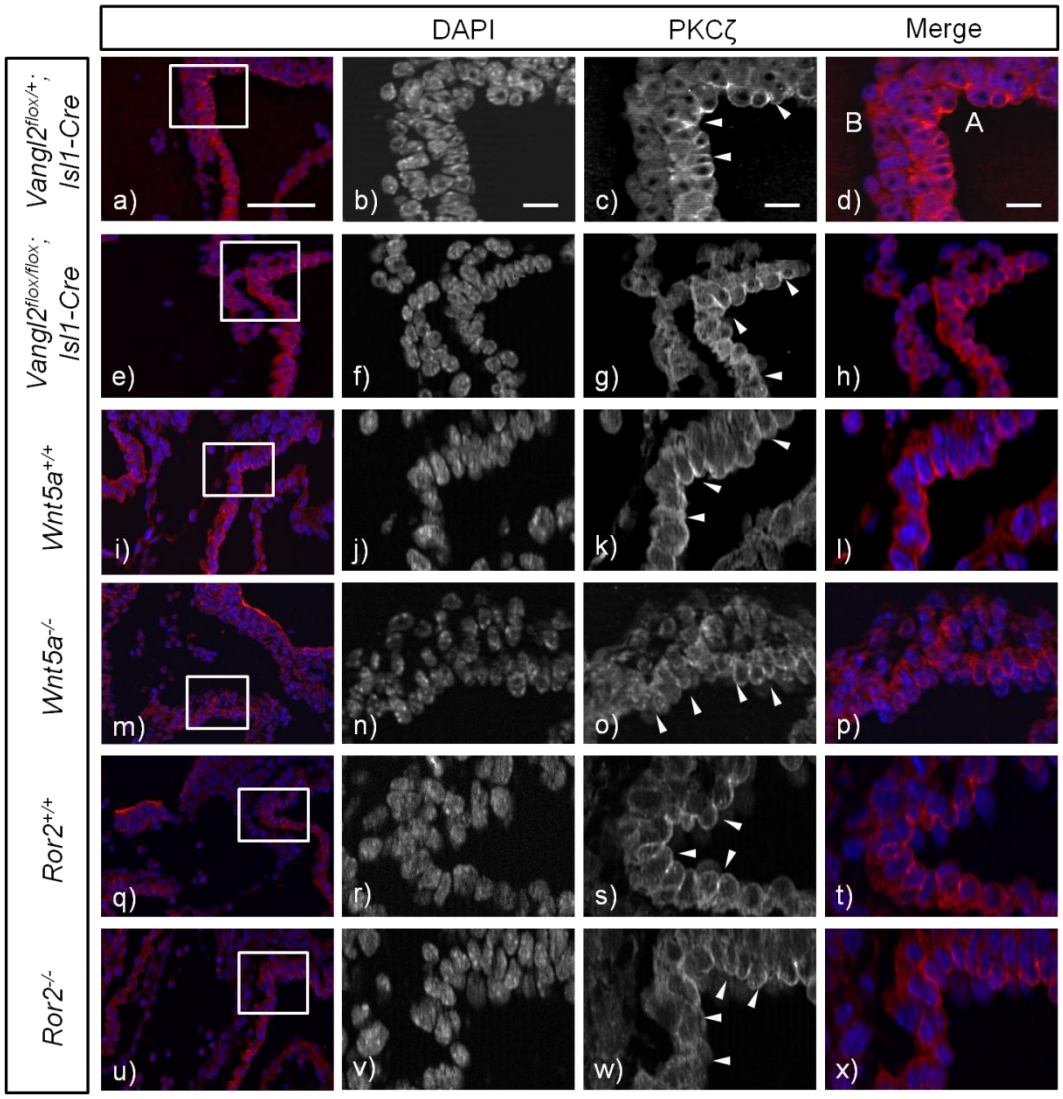

Figure 5.8: Mislocalization of PKCζ expression in transition zone of *Vangl2$^{flox/flox}$;Isl1-Cre, Wnt5a$^{-/-}$* and *Ror2$^{-/-}$* mutants at E9.5

a-d) PKCζ expression (in red) in *Vangl2$^{flox/+}$;Isl1-Cre* control (a) showing apical localization at tight junctions (arrow heads in c). **e-h** PKCζ expression in *Vangl2$^{flox/flox}$;Isl1-Cre* mutant (e) with mislocalized expression in cells in the transition zone but apically localized expression in dorsal pericardial wall (arrow heads in g). **i-l)** PKCζ expression in *Wnt5a$^{+/-}$* control (i) showing apical localization at tight junctions (arrow heads in k). **m-p)** PKCζ expression in *Wnt5a$^{-/-}$* mutant (m) with mislocalized expression in cells in the transition zone and in dorsal pericardial wall (arrow heads in o). **q-t)** PKCζ expression in *Ror2$^{+/-}$* control (q) showing apical localization at tight junctions (arrow heads in s). **u-x)** PKCζ expression in *Ror2$^{-/-}$* mutant (u) with mislocalized expression in cells in the transition zone but apically localized expression in dorsal pericardial wall (arrow heads in w). A-apical, B-basal. Scale - 100µm.

5.2.1.4 Loss of apical-basolateral polarity in Wnt5a$^{-/-}$ and Ror2$^{-/-}$ embryos

The extra-cellular marker laminin is found extra-cellularly at the basal side of the cell giving a clear representation of which is the apical side and which is the basal side. Laminin expression was disrupted in E9.5 *Vangl2$^{flox/flox}$;Isl1-Cre* mutant embryos in the transition zone in the distal outflow tract (figure 8c,d arrows) indicating abnormal compartmentalisation of cell into apical and basal sides in this region. Similar expression was seen in *Wnt5a* and *Ror2* embryos. There was uniform basal expression in *Wnt5a$^{+/+}$* (figure 8e arrows) and *Ror2$^{+/+}$* (figure 8g arrows) embryos, however abnormal expression pattern was observed in *Wnt5a$^{-/-}$* (figure 8f arrows) and *Ror2$^{-/-}$* (figure 8h arrows) embryos with laminin expression being irregular and not limited to the basal side of the cell. This similar pattern of disruption in ABP in cells in the transition zone showed mutation in *Vangl2*, *Wnt5a* or *Ror2* leads to similar phenotype, indicating their role in the same pathway and genetic relation between them.

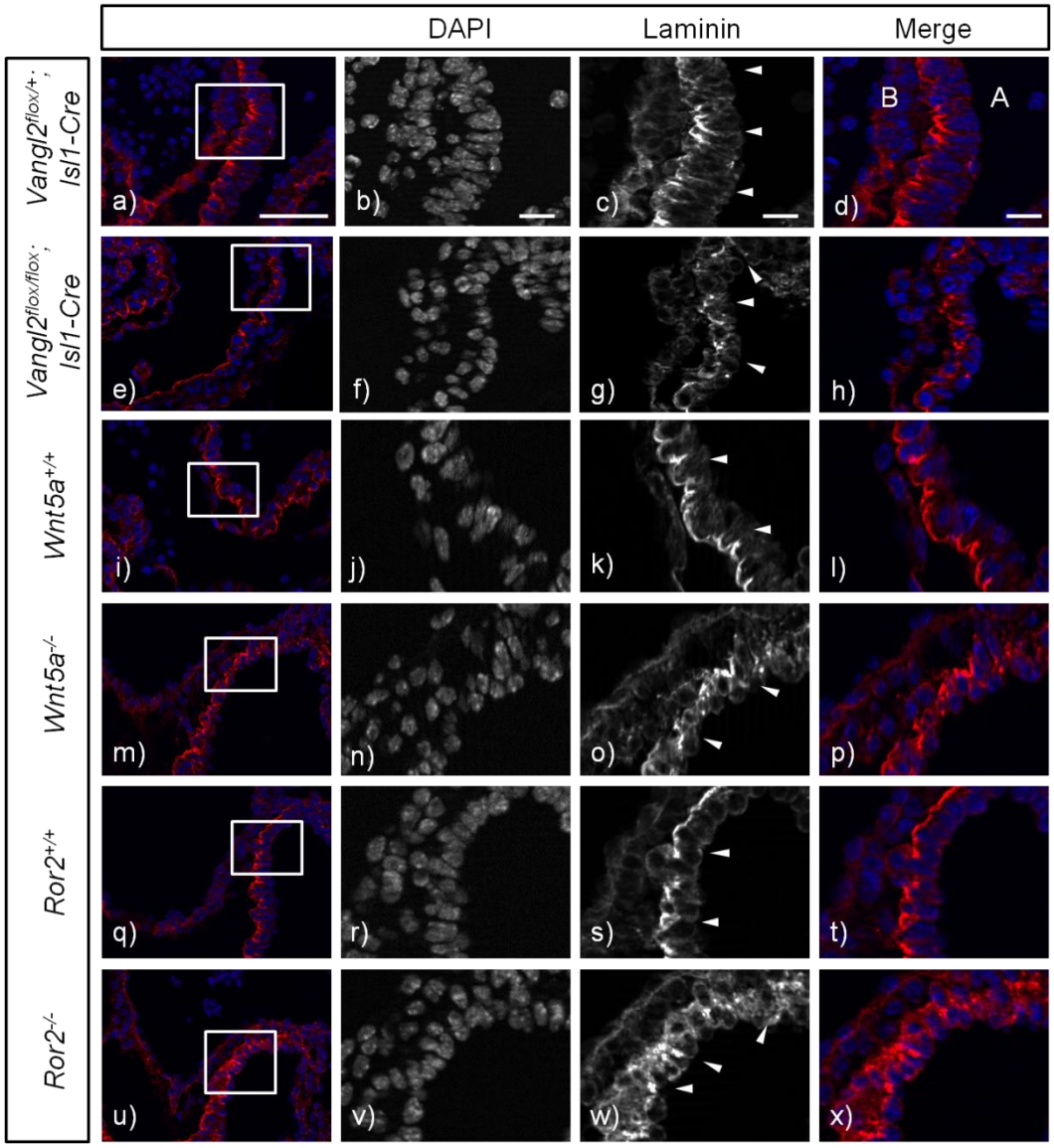

Figure 5.9: Disruption of laminin basal expression in transition zone of *Vangl2$^{flox/flox}$;Isl1-Cre*, *Wnt5a$^{-/-}$* and *Ror2$^{-/-}$* mutants at E9.5

a-d) Laminin expression (in red) in *Vangl2$^{flox/+}$;Isl1-Cre* control (a) showing uniform basal expression (arrow heads in c). **e-h)** Laminin expression in *Vangl2$^{flox/flox}$;Isl1-Cre* mutant (e) with disrupted expression with not being limited to basal side of the cells in the transition zone (arrow heads in g). **i-l)** Laminin expression in *Wnt5a$^{+/-}$* control (i) showing uniform basal expression (arrow heads in k). **m-p)** Laminin expression in *Wnt5a$^{-/-}$* mutant (m) with disrupted expression with not being limited to basal side of the cells in the transition zone (arrow heads in o). **q-t)** Laminin expression in *Ror2$^{+/-}$* control (q) showing uniform basal expression (arrow heads in s). **u-x)** Laminin expression in *Ror2$^{-/-}$* mutant (u) with disrupted expression with not being limited to basal side of the cells in the transition zone (arrow heads in w). A-apical, B-basal. Scale - 100µm.

However, when laminin expression was seen in the proximal outflow tract having differentiated cardiomyocytes it was observed that the expression was limited to the basal side and comparable in both *Wnt5a* and *Ror2* controls and mutants (figure 5.10 c,g,k,o arrow heads), showing that the expression is only disrupted in the transition zone.

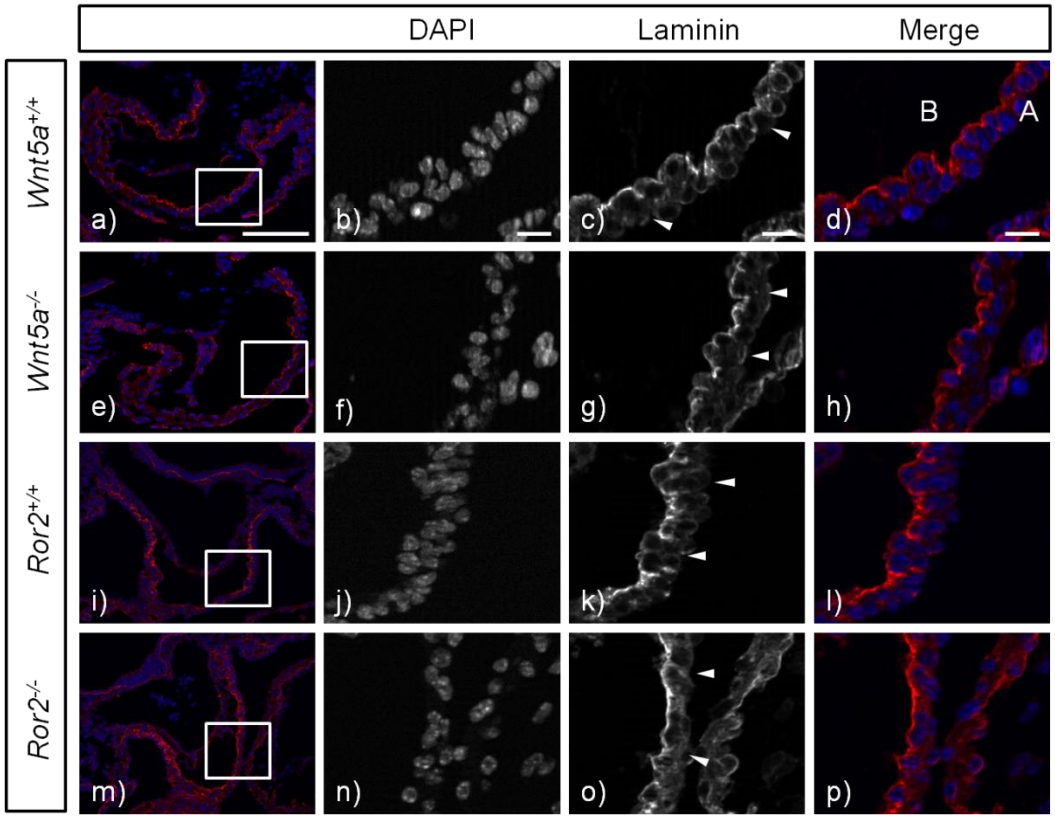

Figure 5.10: Basal expression of laminin in proximal outflow tract of *Wnt5a*$^{-/-}$ and *Ror2*$^{-/-}$ mutants at E9.5

a-d) Laminin expression (in red) in *Wnt5a*$^{+/-}$ control showing basal expression between the basement membrane and the cells (arrow heads in c). **e-h)** Laminin expression in *Wnt5a*$^{-/-}$ mutant showing basal expression similar to control (g arrow heads). **i-l)** Laminin expression (in red) in *Ror2*$^{+/-}$ control showing basal expression between the basement membrane and the cells (arrow heads in k). **e-h)** Laminin expression in *Ror2*$^{-/-}$ mutant showing basal expression similar to control (o arrow heads). A-apical, B-basal. Scale - 100µm.

These results suggested that the basal determinants of the cells in the transition zone are not limited to basal side in the absence of *Wnt5a* and *Ror2*, indicating loss of apical-basal identity of cells in the transition zone.

5.2.2 ROCK and Rac1 as downstream targets of PCP pathway

The PCP pathway as discussed before in chapter 1 requires different proteins to work together in a coordinated manner. Vangl2 is one of the core proteins in this pathway and is upstream of Rac1 and ROCK. Expression of Rac1 and ROCK was specifically deleted/knocked down in cells derived from SHF and phenotype was compared with *Vangl2*$^{flox/flox}$*;Isl1-Cre* mutants.

5.2.2.1 Role of ROCK in SHF cells

ROCKDN females, which were heterozygous for *ROCKDN* construct were incorporated with *YFP* and were crossed with *Isl1-Cre* males to get the mutant phenotype of *ROCKDN;Isl1-Cre* with *YFP* incorporated in the genome. Embryos which did not express ROCKDN, but were *Isl1-Cre* positive were used as controls (referred as *ROCK* Control). Figure 5.11 shows the cross to drive ROCKDN expression in SHF cells using *Isl1-Cre*.

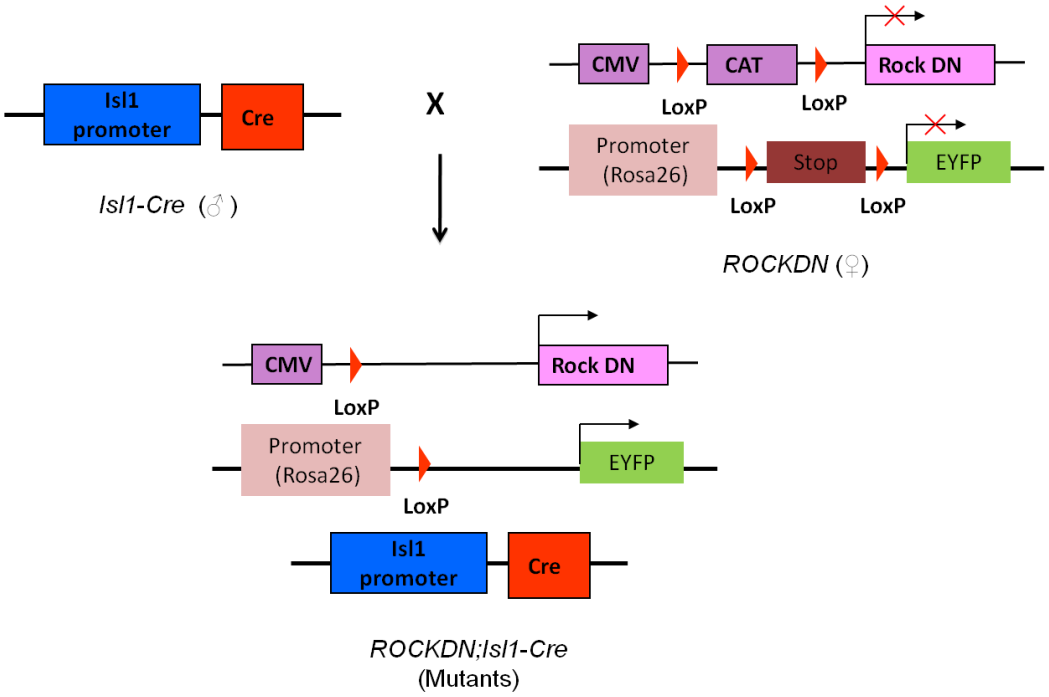

Figure 5.11: *ROCKDN* cross with *Isl1-Cre*

All *ROCKDN* females were incorporated with *eYFP* sequence. *Isl1-Cre* x *ROCKDN* cross to have expression of *ROCKDN* in *Isl1* expressing cells. *CAT* cassette ahead of *ROCKDN* and Stop cassette ahead of *eYFP* has *loxP* sites on either sides (shown in red), which gets removed with the expression of Cre. Resulting genotype would express *ROCKDN* and *eYFP* in all the cells which express *Cre* and leads to loss of function of ROCK as ROCKDN prevents function of ROCK1 and ROCK2 by binding to them and preventing them from binding with RhoA and hence blocks their function.

5.2.2.2 ROCKDN;Isl1-Cre embryos have cardiac outflow tract defects

To check the occurrence of cardiac defects in *ROCKDN;Isl1-Cre* mutants, embryos were collected at E14.5. Five out of seven mutants were processed by Dr Jonathan Peat in the Henderson Lab. External phenotype was therefore analysed of only 2 mutant embryos. One embryo out of these 2 mutants had haemorrhage (figure 5.12 b arrow); however the other was indistinguishable from their control littermates (figure 5.12 a,c). Genotyping was done to identify the mutants and were further examined for heart phenotype. Both mutant and control embryos wax embedded and were transversely sectioned through heart to look at the heart phenotype (figure 5.12 d). H&E staining was done on the sections, which revealed there was 100% penetrance of an outflow tract defect in *ROCKDN;Isl1-Cre* embryos, with 6/7 mutant embryos showing common arterial trunk (figure 5.12 f) and 1/7 had double outlet right ventricle. Control embryos had a normal outflow tract with septation between aorta and pulmonary trunk (figure 5.12 e). All 7 mutant embryos had ventricular septal defect (figure 5.12h) and 3/7 had atrio-ventricular septal defect and 1/7 embryo has atrial septal defect. Six out of seven mutant embryos also had aortic arch defect, retroesophageal subclavian artery (figure 5.12 h). These range of heart defects are summarized in table 5.2.

Table 5.2: Cardiac defects in *ROCKDN;Isl1-Cre* at E14.5

Cardiac defects		*ROCKDN;Isl1-Cre* (n=7)
Outflow tract defects	CAT	6 (86%)
	DORV	1 (14%)
VSD		7 (100%)
ASD		1 (14%)
AVSD		3 (43%)
RRESA		6 (86%)

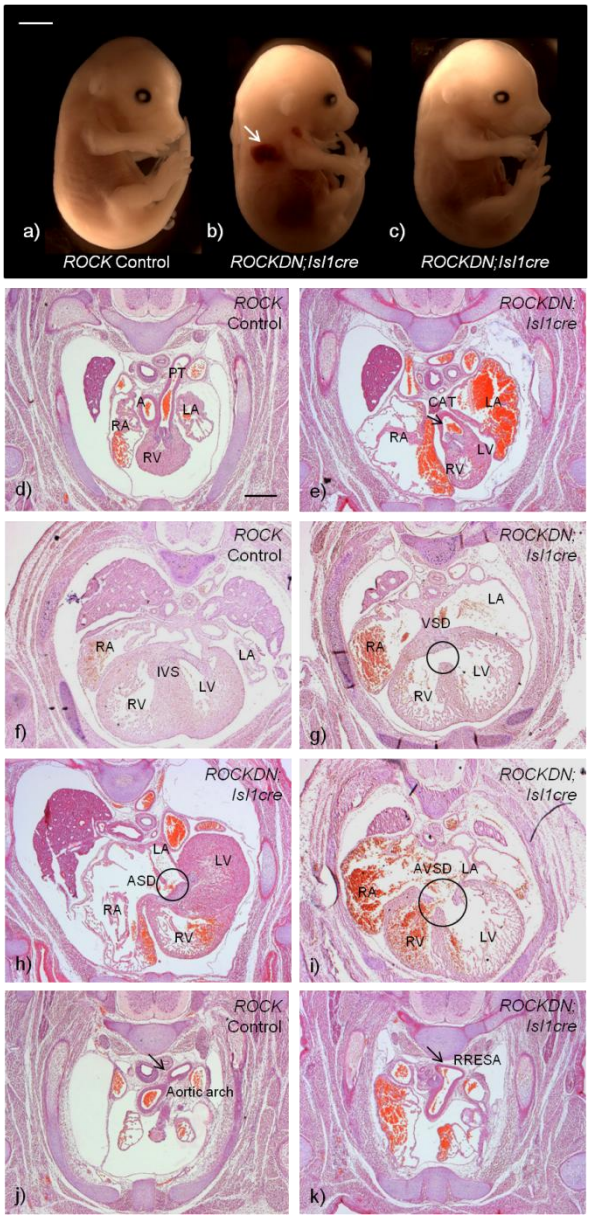

Figure 5.12: External phenotype and cardiovascular defects in *ROCKDN;Isl1-Cre* embryos at E14.5

a-c) Whole embryo at E14.5 with normal external phenotype of control embryo (**a**), mutant embryo with haemorrhage (**b**, arrow), and mutant embryo with normal phenotype (**c**). Scale - 2000µm. **d-k**) Transverse sections of heart from *ROCKDN* x *Isl1-Cre* litter. Transverse section through heart of *ROCK* control embryo showing normal heart development with separate aorta and pulmonary trunk (**d**), intra-ventricular septum (f) and normal left-sided aortic arch (**j**). Heart section from *ROCKDN;Isl1-Cre* embryo showing common arterial trunk (**e**), ventricular septal defect (g), atrial septal defect (h), atrio-ventricular septal defect (i) and retroesophageal subclavian artery (**k**). RA-right atria, LA-left atria, RV-right ventricle, LV-left ventricle, A-aorta, PT-pulmonary trunk, CAT- common arterial trunk, IVS- intra-ventricular septum, VSD-ventricular septal defect, ASD-atrial septal defect, AVSD-atrio-ventricular septal defect, RRESA-retroesophageal subclavian artery. Scale - 20µm.

5.2.2.3 Role of Rac1 in SHF cells

To look for cardiac defects caused by the absence of *Rac1* from SHF cells, $Rac1^{flox/+;}$*Isl1-Cre* and $Rac1^{flox/flox}$;$YFP^{flox/flox}$ mice were generated and then these parents were crossed together to get $Rac1^{flox/flox}$;*Isl1-Cre* embryos with *Rac1* deleted from all SHF derived cells and with *YFP* incorporated in the genome to label these SHF cells (figure 5.13). Embryos were collected to look at the external and heart phenotype. This was initially carried out by Dr Hong Jun Rhee and Dr Iain Keenan in the Henderson lab.

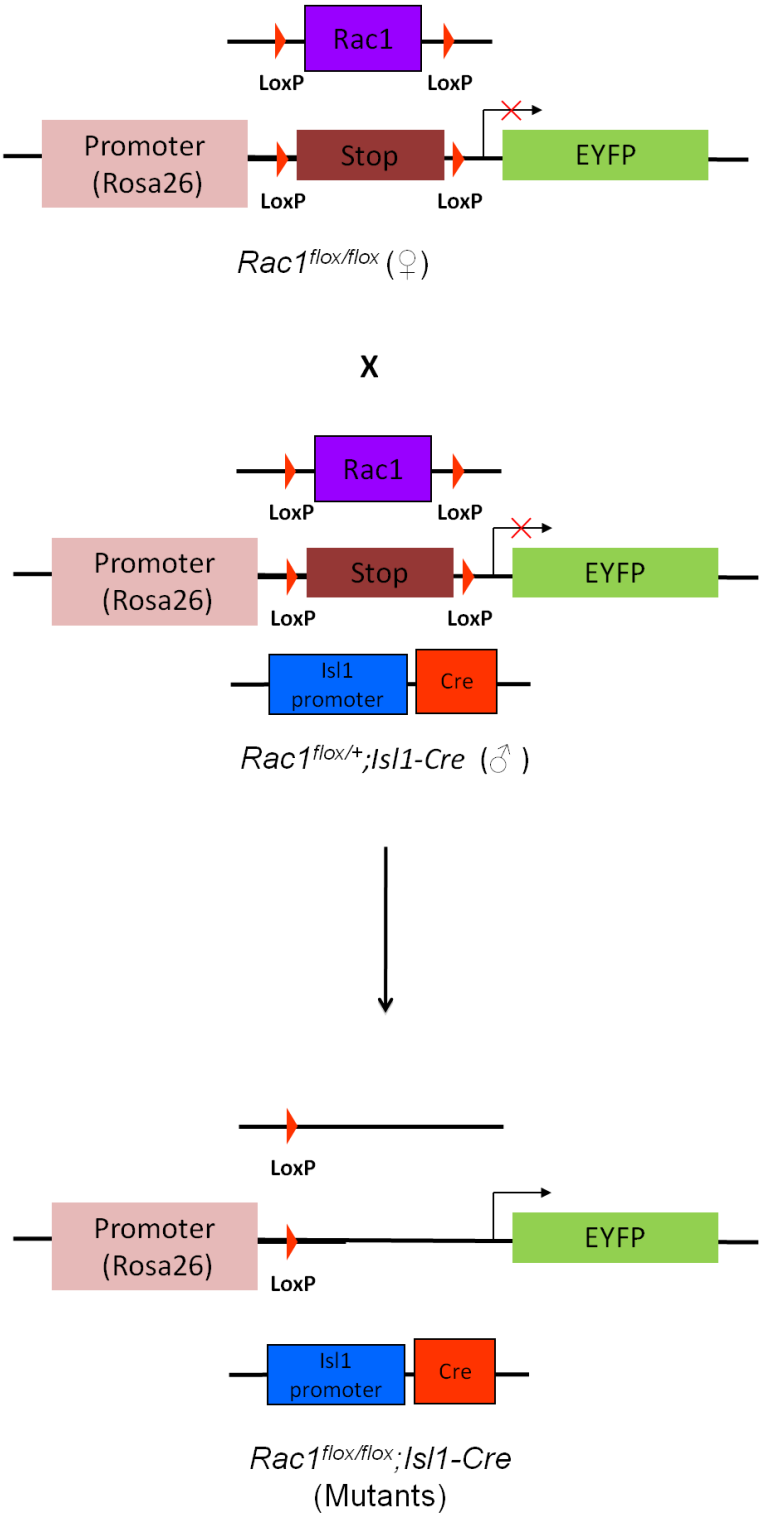

Figure 5.13: *Rac1*^{flox} cross specifically within SHF cells, using *Isl1-Cre*

All *Rac1*^{flox} mice were incorporated with *eYFP* sequence.. **c)** *Rac1*$^{flox/+}$;*Isl1-Cre* x *Rac1*$^{flox/flox}$;*YFP* $^{flox/flox}$ cross to have deletion of *Rac1* gene specifically in SHF cells using *Isl1Cre* (*Rac1*$^{flox/flox}$;*Isl1-Cre*).

5.2.2.4 Rac1$^{flox/flox}$;Isl1-Cre embryos have external and cardiac outflow tract defects

External and cardiac phenotype analysis on *Rac1;Isl1-Cre* embryos was initially done by Dr Hong Jun Rhee and Dr Iain Keenan in the Henderson lab (Keenan *et al.*, 2012). Embryos were collected at E14.5, and some of the *Rac1$^{flox/flox}$;Isl1-Cre* mutant embryos showed abnormal external phenotype, including haemorrhage (figure 5.14 b,c white arrows) and oedema (figure 5.14 b red arrow) (Keenan *et al.*, 2012). These embryos along with controls were further embedded in wax and sectioned. H&E staining was done to look at the heart morphology and it revealed that these mutants had 100% penetrance for outflow tract defects (4/5 had common arterial trunk and 1/5 had double outlet right ventricle) (figure 5.14 e) and ventricular septal defect (figure g), although only 2/5 showed atrial septal defect (figure g) and 1/5 embryos showed aortic defect, double sided aortic arch (figure 5.14 f). *Rac1$^{flox/flox}$;Isl1-Cre* mutants also have lymphatic defects, where the jugular veins and lymph sacs did not separate and had accumulation of large numbers of blood cells (Keenan *et al.*, 2012). These range of heart defects are summarized in table 5.3.

Table 5.3: Cardiac defects in *Rac1$^{flox/flox}$;Isl1-Cre* at E14.5

Cardiac defects		*Rac1$^{flox/flox}$;Isl1-Cre* (n=5)
Outflow tract defects	CAT	4 (80%)
	DORV	1 (20%)
VSD		5 (100%)
ASD		2 (40%)
DSAA		1 (20%)

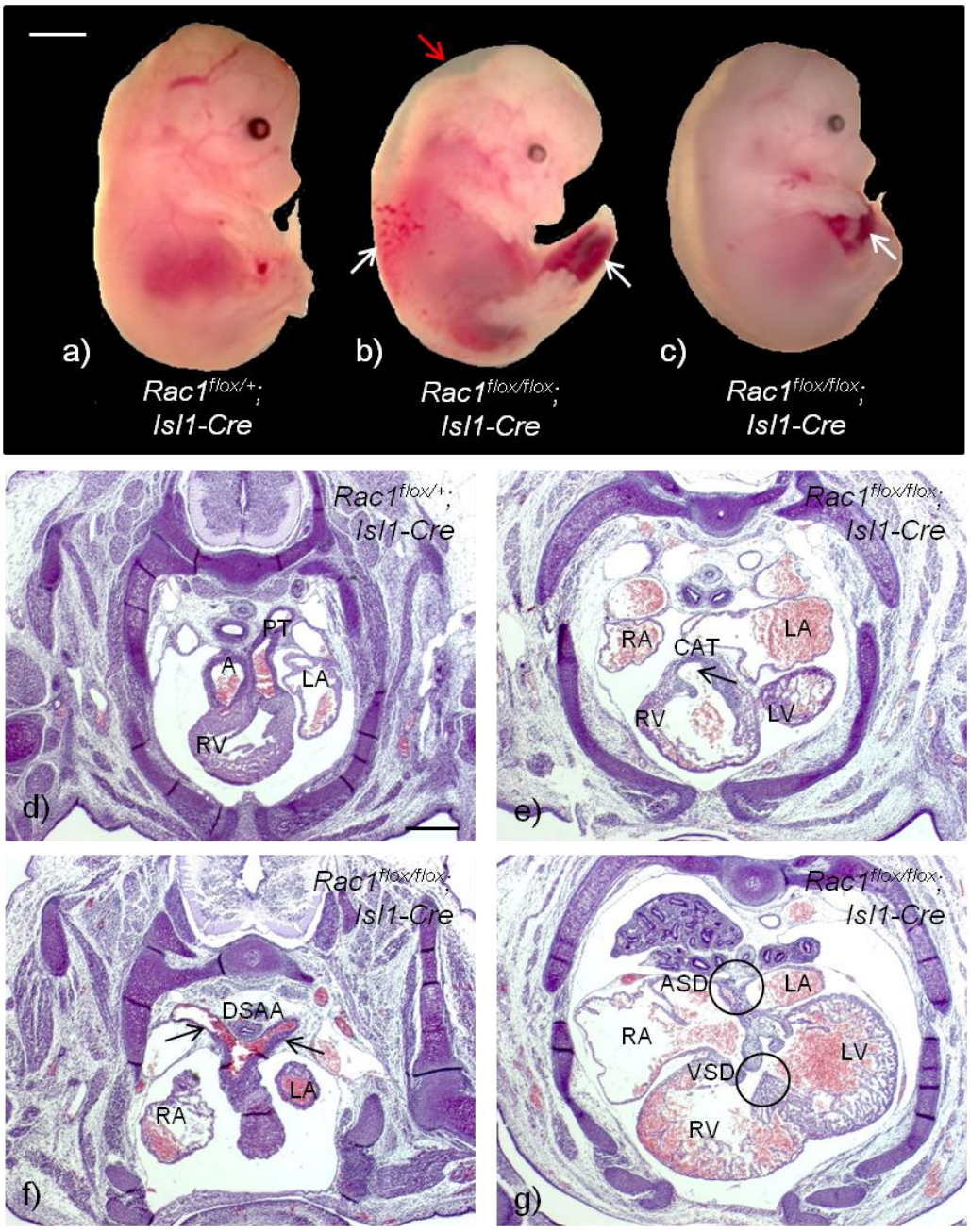

Figure 5.14: External phenotype and cardiovascular defects in *Rac1$^{flox/flox}$;Isl1-Cre* embryos at E14.5

a-c) Whole embryo at E14.5 with normal external phenotype of control embryo (**a**), mutant embryo with haemorrhage (b,c white arrows) and oedema (b red arrow). Scale - 2000µm. **d-g**) Transverse sections of heart from *Rac1$^{flox/+}$;Isl1-Cre* x *Rac1$^{flox/flox}$;YFP $^{flox/flox}$* litter. Transverse section through heart of control embryo showing normal heart development with separate aorta and pulmonary trunk (**d**). Heart section from *Rac1$^{flox/flox}$;Isl1-Cre* embryo showing common arterial trunk (**e**), double sided aortic arch (f) and ventricular septal defect (**g**). RA-right atria, LA-left atria, RV-right ventricle, LV-left ventricle, A-aorta, PT-pulmonary trunk, CAT- common arterial trunk, DSAA- double sided aortic arch, VSD-ventricular septal defect, ASD-atrial septal defect. Scale - 20µm.

Results confirm that both *Rac1* and *ROCK*, similarly to *Vangl2*, are regulating SHF cells in the outflow tract of the developing heart and are important for proper septation of the outflow tract during developmental stage. Hence it was considered important to do similar analysis as done on *Vangl2$^{flox/flox}$;Isl1-Cre* mutants to understand the behaviour of the cells in this distal outflow tract.

5.2.2.5 Disruption of adherens junctions in ROCKDN;Isl1-Cre and Rac1$^{flox/flox}$;Isl1-Cre mutants

To understand the mechanism behind the role *ROCK* and *Rac1* plays in development of the heart, a similar hypothesis as was proposed for the role of *Vangl2* was put forward. It was hypothesised that as both *ROCK* and *Rac1* are downstream effectors of the PCP pathway, of which Vangl2 is a key component; both may also play a role in cellular polarity of SHF cells whilst they are moving into the heart. Mutation of *ROCK* or *Rac1* will result in disrupted polarity, as in *Vangl2* mutants, and hence lead to cardiac defects.

Embryos were collected at E9.5 as previously, and genotyping was done to identify the mutants and total 3 control and 3 mutant embryos were used for analysis. As *ROCK* and *Rac1* like *Vangl2* are involved in morphogenesis of the outflow tract, the same markers were investigated in the transition zone of the outflow tract to look at the polarized nature of SHF cells. Embryos were embedded in wax and transverse sections were taken to label them with fluorescent antibodies, using immunohistochemistry method. AJ markers including E-cadherin and β-catenin were used. Both *ROCKDN;Isl1-Cre* mutants and *Rac1$^{flox/flox}$;Isl1-Cre* mutants showed abnormal expression for E-cadherin as compared to the respective controls. Figure 5.15 shows E-cadherin expression in *ROCK* control embryo with expression at the apical-basal boundary of the cells in the distal outflow tract as seen in *Vangl2$^{flox/+}$;Isl1-Cre* control (figure 5.15 c,k arrow heads). In contrast, expression was seen in basolateral compartment of some cells in the *ROCKDN;Isl1-Cre* mutant (figure 5.15 o arrow heads). This mislocalization of E-cadherin was also seen in *Vangl2$^{flox/flox}$;Isl1-Cre* mutant (figure 5.15 f arrow heads). Rac1 embryos also showed similar disturbance in E-

cadherin expression, with apical-basal expression in *Rac1$^{flox/+}$;Isl1-Cre* control (figure 5.15 s arrow heads) and disruption of this expression in *Rac1$^{flox/flox}$;Isl1-Cre* mutant (figure 5.15 w arrow heads).

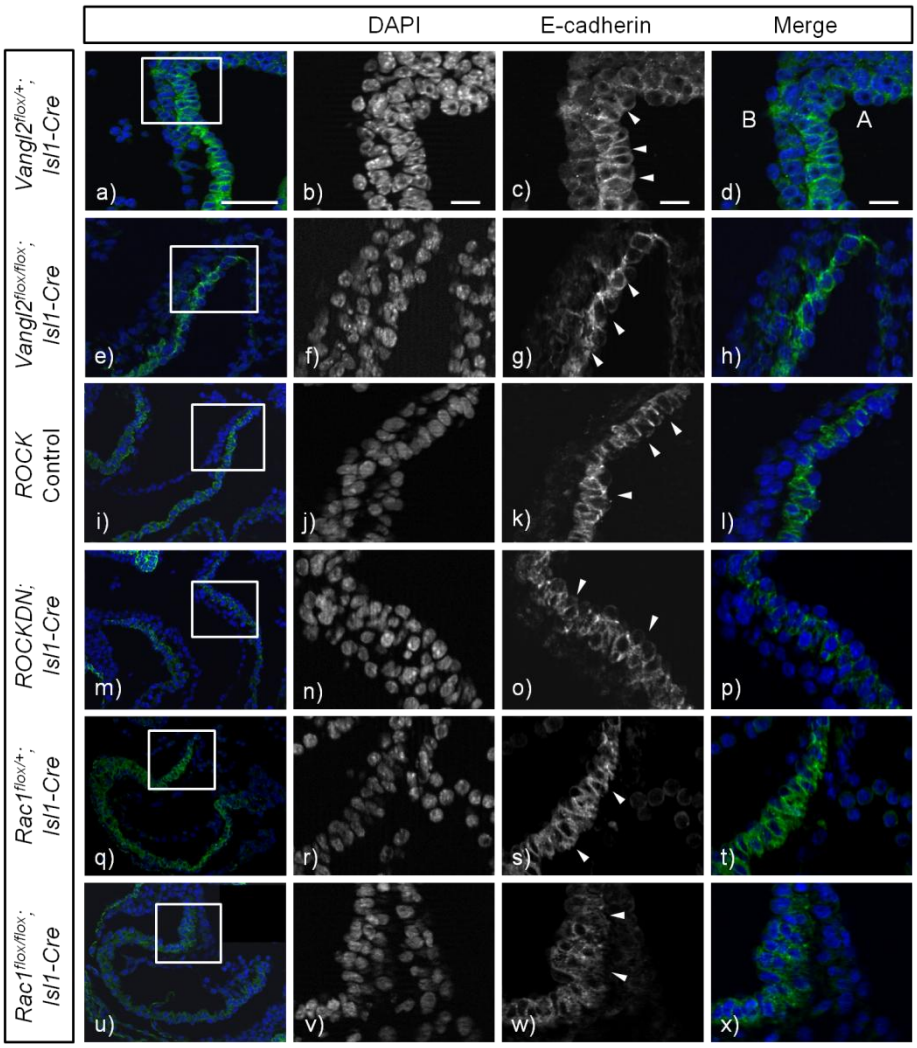

Figure 5.15: Loss of apical-basal localization of E-Cadherins expression in transition zone of *Vangl2$^{flox/flox}$;Isl1-Cre, ROCKDN;Isl1-Cre* and *Rac1$^{flox/flox}$;Isl1-Cre* mutants at E9.5

a-d) E-cadherin expression (in green) in *Vangl2$^{flox/+}$;Isl1-Cre* control (a) showing apical –basal expression (arrow heads in c). **e-h)** E-cadherin expression in *Vangl2$^{flox/flox}$;Isl1-Cre* mutant (e) with expression at basolateral compartment of some cells in the transition zone (arrow heads in g). **i-l)** E-cadherin expression in *ROCK* control (i) showing apical –basal expression (arrow heads in k). **m-p)** E-cadherin expression in *ROCKDN;Isl1-Cre* mutant (m) with disruption of expression in some cells in the transition zone (arrow heads in o). **q-t)** E-cadherin expression in *Rac1$^{flox/+}$;Isl1-Cre* control (q) showing apical –basal expression (arrow heads in s). **u-x)** E-cadherin expression in *Rac1$^{flox/flox}$;Isl1-Cre* mutant (u) with disrupted expression at cell boundary and expression at basolateral compartment of some cells in the transition zone (arrow heads in w). A-apical, B-basal. Scale - 100µm.

β-catenin expression was seen to mark the basolateral compartment of the epithelial SHF cells in the transition zone in *Vangl2*$^{flox/+}$*;Isl1-Cre* control embryo (figure 5.16 c arrow heads) and showed disorganisation of cells in the zone in *Vangl2*$^{flox/flox}$*;Isl1-Cre* (figure 5.16 g arrow heads). Similar expression pattern was seen in *ROCK* control (figure 5.16 k arrow heads) and *Rac1*$^{flox/+}$*;Isl1-Cre* control (figure 5.16 s arrow heads) with cells in the transition zone showing β-catenin expression in their basolateral compartments. However, expression in mutants was present, cells were slightly disorganized in *ROCKDN;Isl1-Cre* mutant (figure 5.16 o arrow heads) and much more disorganisation was seen in *Rac1*$^{flox/+}$*;Isl1-Cre* mutant (figure 5.16 w arrow heads) like in *Vangl2*$^{flox/flox}$*;Isl1-Cre*.

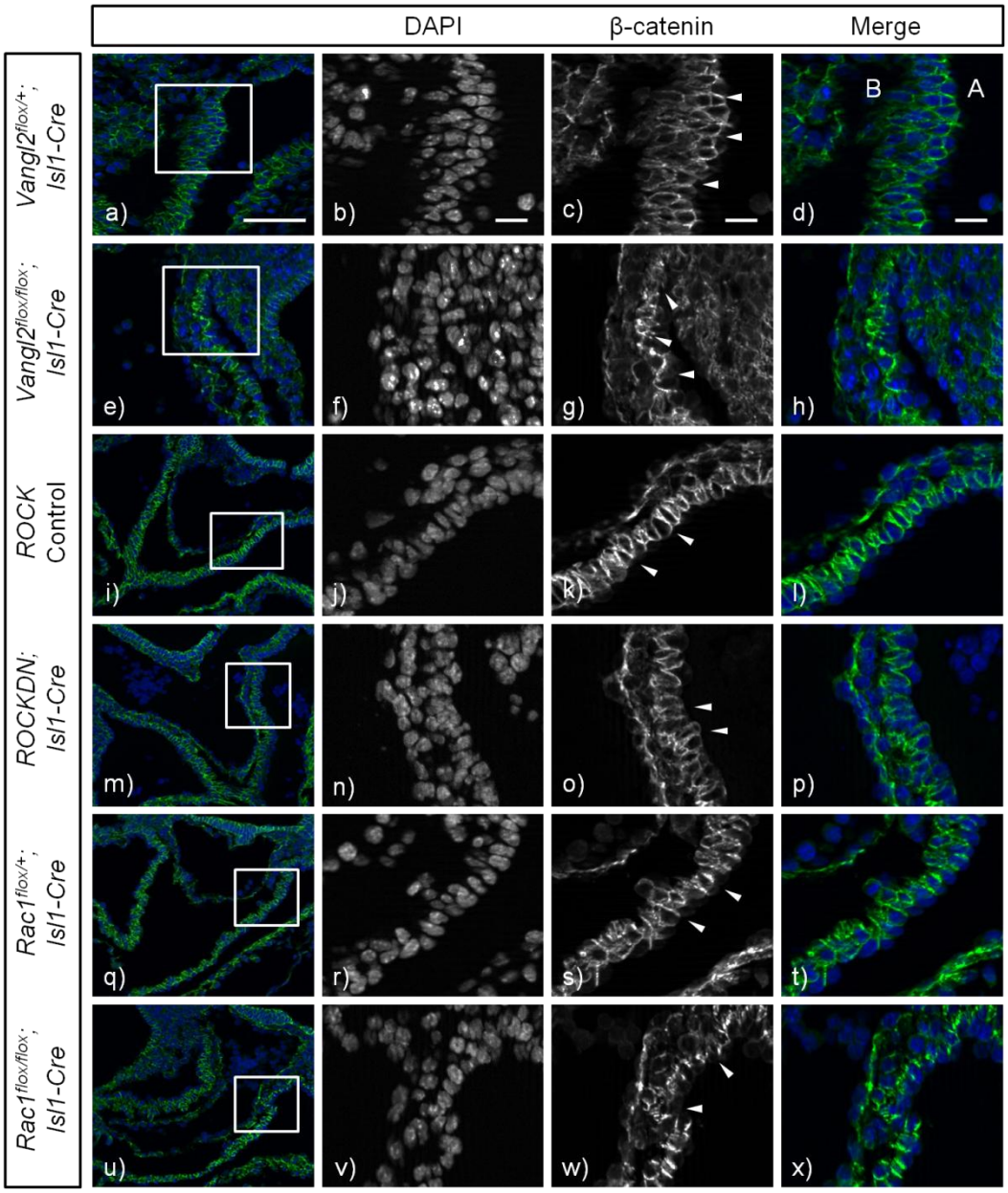

Figure 5.16: Disorganized expression of β-catenin in transition zone of *Vangl2$^{flox/flox}$;Isl1Cre*, *ROCKDN;Isl1Cre* and *Rac1$^{flox/flox}$;Isl1Cre* mutants at E9.5

a-d) β-catenin expression (in green) in *Vangl2$^{flox/+}$;Isl1-Cre* control (a) showing membrane bound expression (arrow heads in c). **e-h)** β-catenin expression in *Vangl2$^{flox/flox}$;Isl1-Cre* mutant (e) with disorganized expression in some cells in the transition zone (arrow heads in g). **i-l)** β-catenin expression in *ROCK* control (i) showing membrane bound expression (arrow heads in k). **m-p)** β-catenin expression in *ROCKDN;Isl1-Cre* mutant (m) with disorganized expression in some cells in the transition zone (arrow heads in o). **q-t)** β-catenin expression in *Rac1$^{flox/+}$;Isl1-Cre* control (q) showing membrane bound expression (arrow heads in s). **u-x)** β-catenin expression in *Rac1$^{flox/flox}$;Isl1-Cre* mutant (u) with some cells in disorganized manner in the transition zone (arrow heads in w). A-apical, B-basal. Scale - 100µm.

Expression of E-cadherin and β-catenin expression was looked at dorsal wall of aortic sac to check disruption of expression was limited only to the transition zone. It was observed that these adhesion proteins, E-cadherin and β-catenin are expressed in a comparable manner in controls and mutants in dorsal wall of aortic sac (figure 5.17 a2-h2 arrow heads) like in *Vangl2*$^{flox/+}$*;Isl1-Cre* controls, and show different expression pattern in transition zone only.

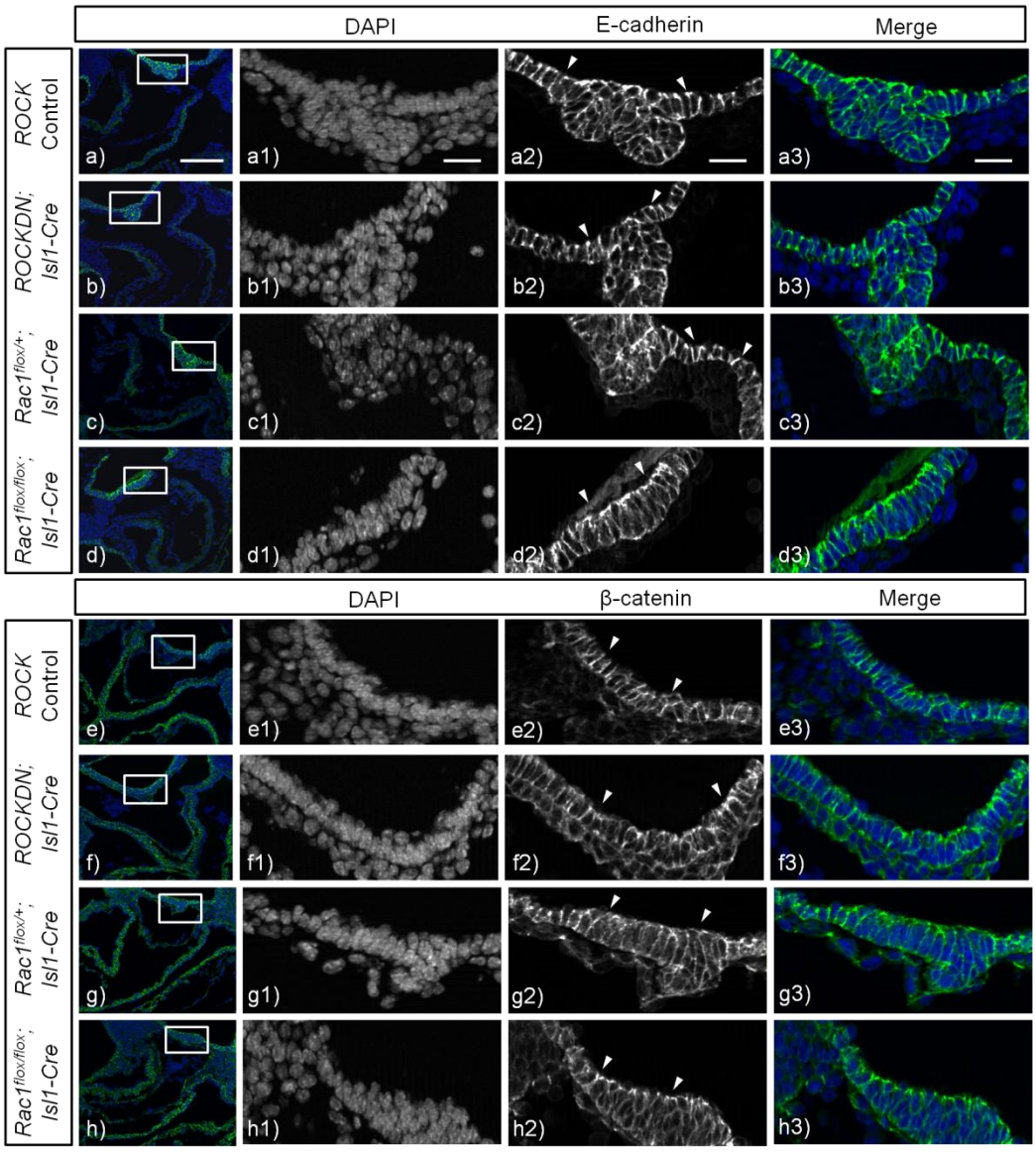

Figure 5.17: Comparable expression of E-cadherin and β-catenin in controls and mutants outside transition zone

a-d) E-cadherin expression (in green) in *ROCK* control (a) and *Rac1$^{flox/+}$;Isl1-Cre* control (c) showing apical–basal expression (arrow heads in a2,c2) and in *ROCKDN;Isl1-Cre* mutant (b) and *Rac1$^{flox/flox}$;Isl1-Cre* mutant (d) also with apical-basal expression in cells in the dorsal wall of aortic sac (arrow heads in b2,d2). **e-h)** β-catenin expression (in green) in *ROCK* control (e) and *Rac1$^{flox/+}$;Isl1-Cre* control (g) showing membrane bound expression (arrow heads in e2,g2) and in *ROCKDN;Isl1-Cre* mutant (f) and *Rac1$^{flox/flox}$;Isl1-Cre* mutant (h) also showing membrane bound expression in cells in the dorsal wall of aortic sac (arrow heads in f2,h2). Scale - 100µm.

5.2.2.6 Disruption of tight junctions in Rac1$^{flox/flox}$;Isl1-Cre and ROCKDN;Isl1-Cre mutants

Disruption of AJ indicate that absence of *Rac1* or *ROCK* in SHF cells could lead to disruption in compartmentalisation of cells into apical and basal domains like in the absence of *Vangl2*, to confirm this, PKCζ expression was looked at in the same region of the distal outflow tract at E9.5 embryos. Embryos were wax embedded and section transversally and immunostained with PKCζ antibody. As expected and seen in *Vangl2$^{flox/flox}$;Isl1-Cre* mutants, there was mislocalization of PKCζ in *Rac1$^{flox/flox}$;Isl1-Cre* and *ROCKDN;Isl1-Cre* mutants (n=3). Figure 5.18 compares PKCζ expression in *Vangl2, ROCK* and *Rac1* controls embryos with their respective mutants. *Vangl2$^{flox/+}$;Isl1-Cre* control shows apical enrichment of PKCζ in the SHF cells in the dorsal pericardial wall and as they move into the distal outflow tract in the transition zone (figure 5.18 c arrow heads). This apical enrichment was lost in *Vangl2$^{flox/flox}$;Isl1-Cre* mutant, however only in the transition zone as cells in the dorsal pericardial wall still had apical localization of PKCζ (figure 5.18 g arrow heads). *ROCK* control and *Rac1$^{flox/+}$;Isl1-Cre* control also show apical localization of PKCζ expression in the dorsal pericardial wall and the distal outflow tract (figure 5.18 k,s arrow heads), however in both *ROCKDN;Isl1-Cre* and *Rac1$^{flox/flox}$;Isl1-Cre* mutant embryo similar mislocalization of PKCζ expression was seen as observed in *Vangl2$^{flox/flox}$;Isl1-Cre* mutant embryo, that too only in transition zone and had apical localization of PKCζ expression in the dorsal pericardial wall in both mutants (figure 5.18 o,w arrow heads).

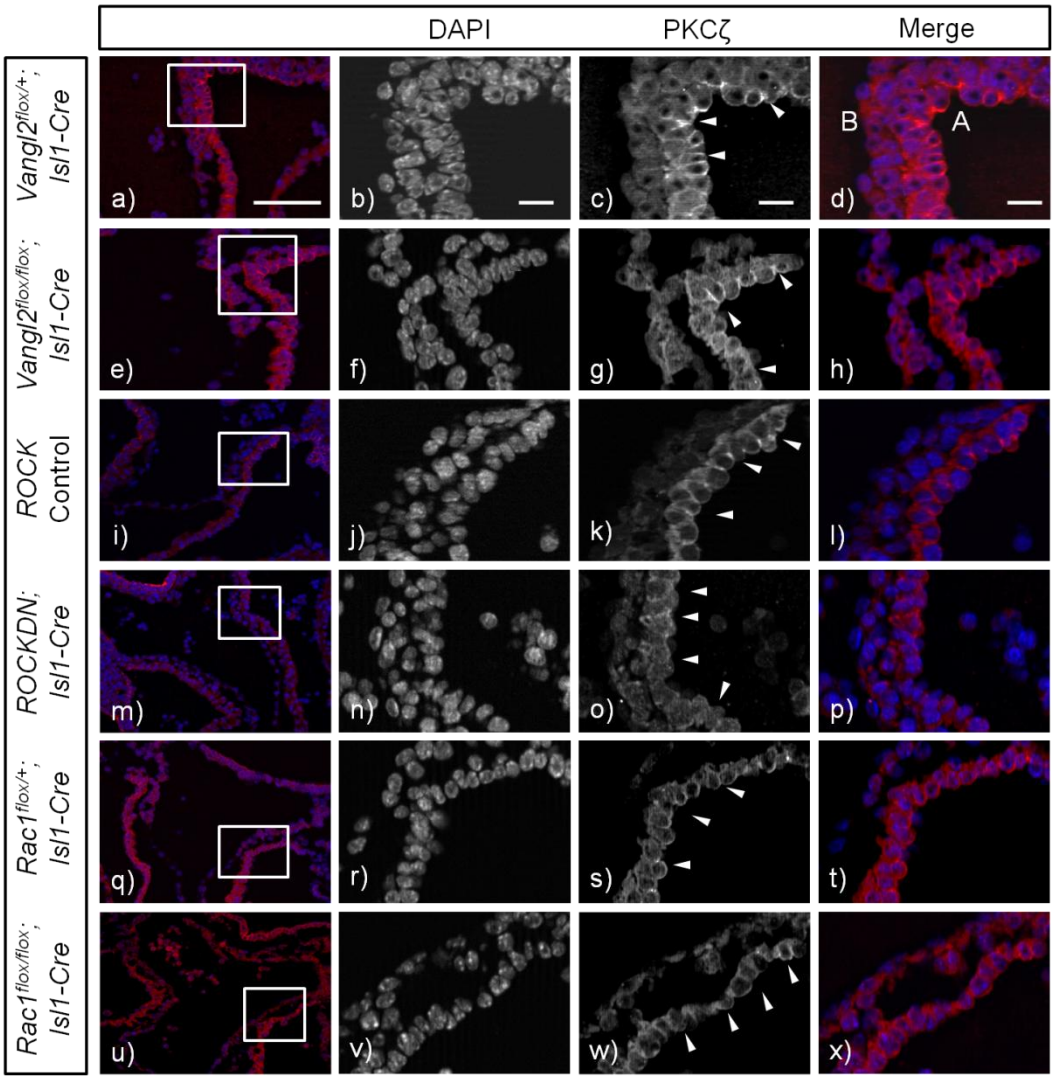

Figure 5.18: Mislocalization of PKCζ expression in transition zone of *Vangl2$^{flox/flox}$;Isl1Cre, ROCKDN;Isl1Cre* and *Rac1$^{flox/flox}$;Isl1Cre* mutants at E9.5

a-d) PKCζ expression (in red) in *Vangl2$^{flox/+}$;Isl1-Cre* control (a) showing apical localization at tight junctions (arrow heads in c). **e-h** PKCζ expression in *Vangl2$^{flox/flox}$;Isl1-Cre* mutant (e) with mislocalized expression in cells in the transition zone but apically localized expression in dorsal pericardial wall (arrow heads in g). **i-l)** PKCζ expression in *ROCK* control (i) showing apical localization at tight junctions (arrow heads in k). **m-p)** PKCζ expression in *ROCKDN;Isl1-Cre* mutant (m) with mislocalized expression in cells in the transition zone but apically localized expression in dorsal pericardial wall (arrow heads in o). **q-t)** PKCζ expression in *Rac1$^{flox/+}$;Isl1-Cre* control (q) showing apical localization at tight junctions (arrow heads in s). **u-x)** PKCζ expression in *Rac1$^{flox/flox}$;Isl1-Cre* mutant (u) with mislocalized expression in cells in the transition zone but apically localized expression in dorsal pericardial wall (arrow heads in w). A-apical, B-basal. Scale - 100µm.

5.2.2.7 Loss of apical-basolateral polarity in ROCKDN;Isl1Cre and Rac1$^{flox/flox}$;Isl1Cre embryos

Laminin is an extra-cellular marker and labels the basal side of the cells, which was observed in *Vangl2$^{flox/+}$;Isl1-Cre* control embryo at E9.5 (figure 5.19 c arrow heads). This basal localization was disrupted in stage-matched *Vangl2$^{flox/flox}$;Isl1-Cre* mutant and expression was observed to be not limiting to basal side of the cells and present at the apical side of some cells in the transition zone (figure 5.19 g arrow heads), indicating loss of apical-basal compartmentalization in *Vangl2$^{flox/flox}$;Isl1-Cre* mutants. *ROCK* and Rac1 embryos (3 controls and 3 mutants) were also collected at E9.5, wax embedded and sectioned transversally. *ROCK* control embryo showed basal localization of laminin in the transition zone (figure 5.19 k arrow heads), but this localization was disrupted in *ROCKDN;Isl1-Cre* mutant with irregular expression and some cells showing expression towards their apical side as well (figure 5.19 o arrow heads). Similar disruption was seen in *Rac1$^{flox/flox}$;Isl1-Cre* mutant (figure 5.19 s arrow heads) with expression throughout around the cells as compared to the uniform basal expression seen in *Rac1$^{flox/+}$;Isl1-Cre* control (figure 5.19 w arrow heads).

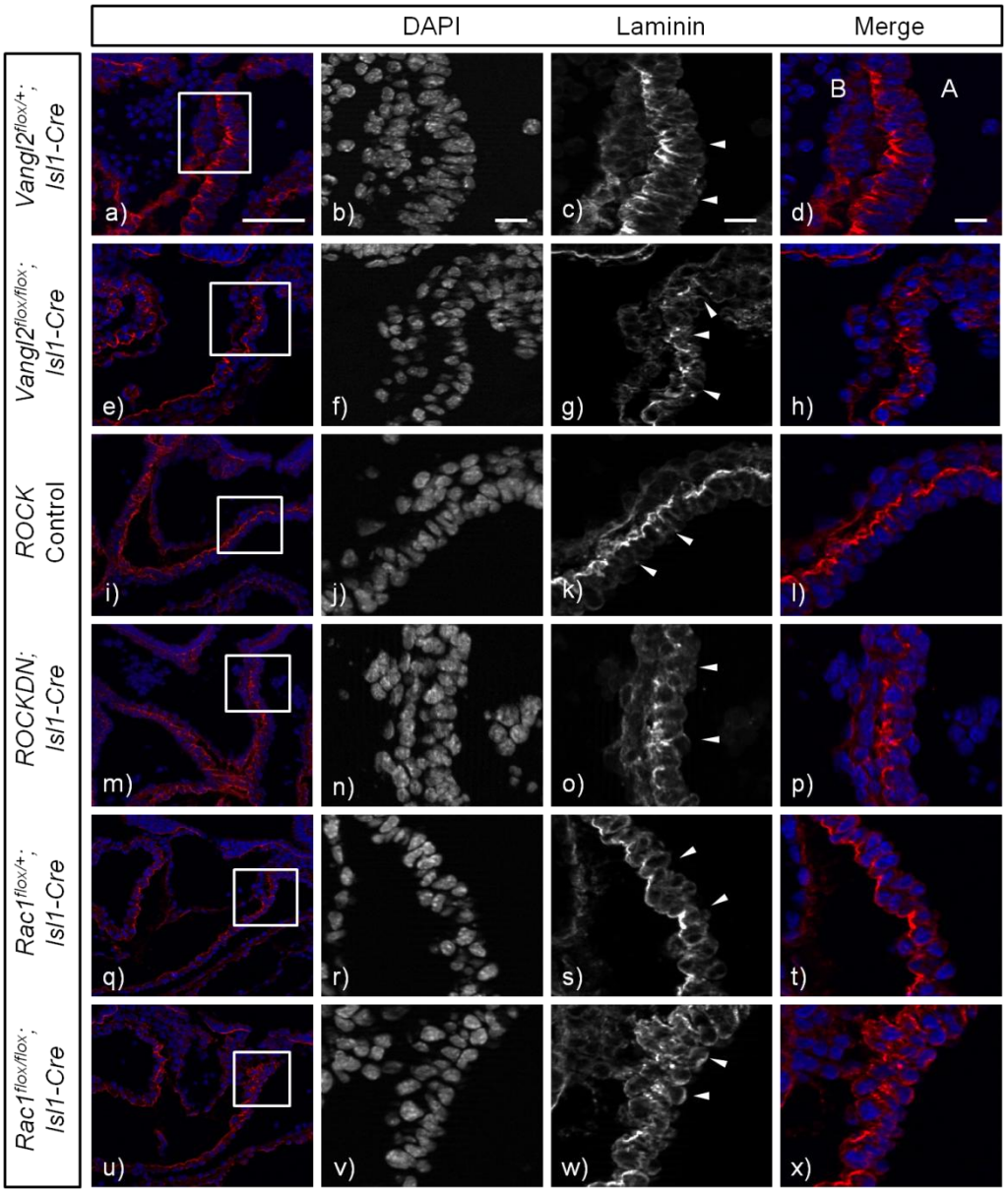

Figure 5.19: Disruption of laminin basal expression in transition zone of *Vangl2$^{flox/flox}$;Isl1-Cre, ROCKDN;Isl1-Cre* and *Rac1$^{flox/flox}$;Isl1-Cre* mutants at E9.5

a-d) Laminin expression (in red) in *Vangl2$^{flox/+}$;Isl1-Cre* control (a) showing uniform basal expression (arrow heads in c). **e-h)** Laminin expression in *Vangl2$^{flox/flox}$;Isl1-Cre* mutant (e) with disrupted expression with not being limited to basal side of the cells in the transition zone (arrow heads in g). **i-l)** Laminin expression in *ROCK* control (i) showing uniform basal expression (arrow heads in k). **m-p)** Laminin expression in *ROCKDN;Isl1-Cre* mutant (m) with disrupted expression with not being limited to basal side of the cells in the transition zone (arrow heads in o). **q-t)** Laminin expression in *Rac1$^{flox/+}$;Isl1-Cre* control (q) showing uniform basal expression (arrow heads in s). **u-x)** Laminin expression in *Rac1$^{flox/flox}$;Isl1-Cre* mutant (u) with disrupted expression with not being limited to basal side of the cells in the transition zone (arrow heads in w). A-apical, B-basal. Scale - 100µm.

To check if apical-basal compartmentalisation is disrupted on in the transition zone in the distal outflow tract, laminin expression was checked in the proximal outflow tract having differentiated cardiomyocytes. Expression was limited to the basal side and comparable in both controls and mutants (figure 5.20 c,g,k,o arrow heads), showing that the expression is only disrupted in the transition zone.

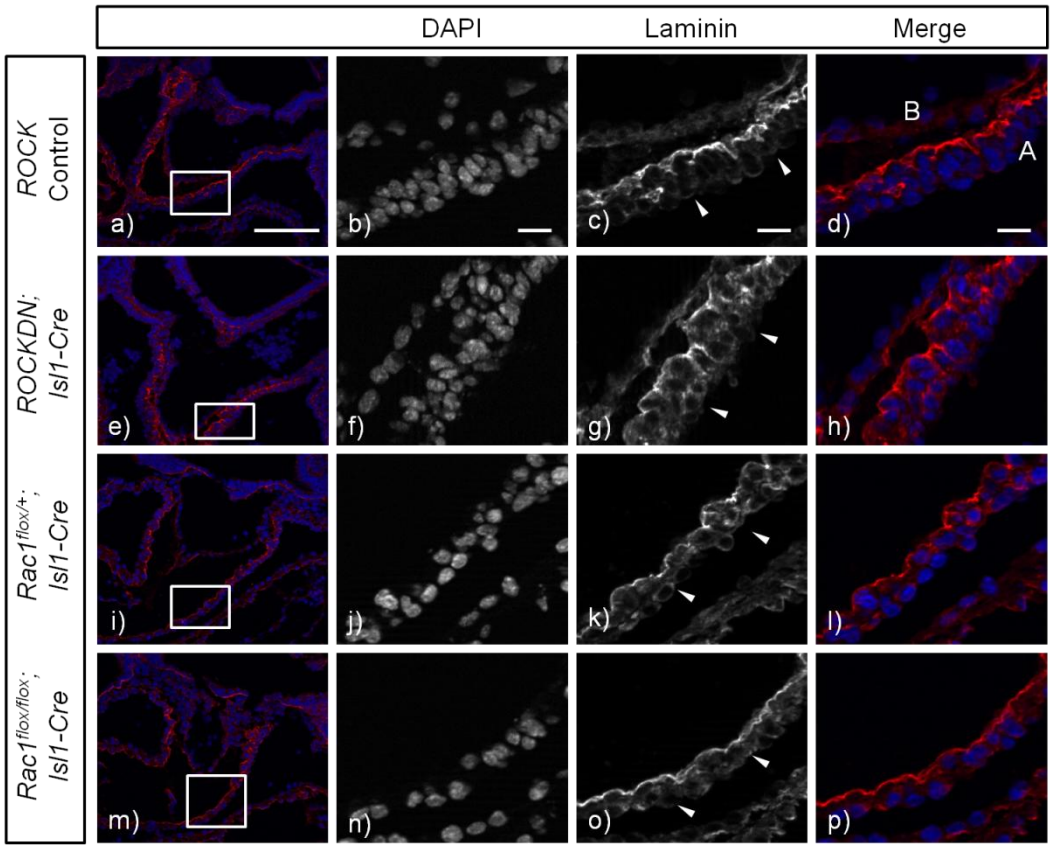

Figure 5.20: Basal expression of laminin in proximal outflow tract of *ROCKDN;Isl1-Cre* and *Rac1$^{flox/flox}$;Isl1-Cre* mutants at E9.5

a-d) Laminin expression (in red) in *ROCK* control showing basal expression between the basement membrane and the cells (arrow heads in c). **e-h)** Laminin expression in *ROCKDN;Isl1-Cre* mutant showing basal expression similar to control (g arrow heads). **i-l)** Laminin expression (in red) in *Rac1$^{flox/+}$;Isl1-Cre* control showing basal expression between the basement membrane and the cells (arrow heads in k). **e-h)** Laminin expression in *Rac1$^{flox/flox}$;Isl1-Cre* mutant showing basal expression similar to control (o arrow heads). A-apical, B-basal. Scale - 100µm.

5.3 Discussion

Vangl2 upstream receptors, Wnt5a and Ror2, and downstream effectors, Rac1 and ROCK, have been implicated in playing roles during heart development with their absence or loss of function resulting in defects affecting the outflow region of the heart. It was established in the previous chapter that *Vangl2* regulates undifferentiated SHF cells in the transition zone and helps in lengthening of the outflow tract, and absence of *Vangl2* disrupts this process leading to outflow tract defect. Outflow tract defects were also observed in *Wnt5a*$^{-/-}$, *ROCK* and *Rac1* SHF mutants (*ROCKDN;Isl1-Cre*, *Rac1*$^{flox/flox}$*;Isl1-Cre*) and to some extent in *Ror2*$^{-/-}$ (1 out of 4 embryos), therefore a similar hypothesis of disrupted cell organization and polarity was tested in these mutants.

Apart from cardiac defects, there were external defects seen in *Wnt5a*$^{-/-}$, *Ror2*$^{-/-}$, *ROCKDN;Isl1-Cre* and *Rac1*$^{flox/flox}$*;Isl1-Cre* mutant embryos. Neural tube defect in *Wnt5a*$^{-/-}$ and *Ror2*$^{-/-}$ embryos can be explained because of the global loss of these genes, similar to the global loss of *Vangl2* in *Lp* mutants. In *ROCKDN;Isl1-Cre* and *Rac1*$^{flox/flox}$*;Isl1-Cre* haemorrhage and oedema were observed, which were not seen in *Vangl2*$^{flox/flox}$*;Isl1-Cre* mutants. Oedema is defined as abnormal presence of fluid anywhere in the body and is considered as a good marker of heart problem because due to oedema heart loses its pumping ability. Jugular and umbilical haemorrhage were focussed because these are also markers of heart defects and second heart field progenitors are expressed in these regions (Keenan *et al.*, 2012). It is known that *Isl1* progenitors are also expressed in regions outside the heart (Keenan *et al.*, 2012), which may accounts for the high incidence of abnormal external phenotypes in the *ROCKDN;Isl1-Cre* and *Rac1*$^{flox/flox}$*;Isl1-Cre* mutants, apart from ROCK and Rac1 having other functions and having different response of other upstream pathways.

Wnt5a deletion leads to cardiac defects like common arterial trunk and ventricular septal defect (Schleiffarth *et al.*, 2007) and *Ror2* deletion results in a less severe phenotype, with just ventricular septal defect (Oishi *et al.*, 2003) and double outlet right ventricle (1/4 embryos). Although cardiac defects seen in *Wnt5a*$^{-/-}$ embryos are more severe than our *Vangl2*$^{flox/flox}$*;Isl1-Cre* mutants, it could be due

to the fact that Wnt5a acts upstream of Vangl2 and has more broader range of action. However, the results confirm the importance of both *Wnt5a* and *Ror2* during embryonic heart development; however the particular cell type which is regulated still needs to be established.

On the other hand, disruption of *ROCK* expression in NCC leads to double outlet right ventricle in 39% of mutant cases (Phillips *et al.*, 2013) and deletion of *Rac1* specifically in NCC also results in cardiac defects like common arterial trunk and aberrant remodelling of pharyngeal arch arteries (Thomas *et al.*, 2010). These studies have established the role of *ROCK* and *Rac1* in outflow tract development, but only in NCC. This chapter establishes the role of both *ROCK* and *Rac1* in regulating SHF cells during outflow tract development.

We investigated whether these components work in a similar way to polarize SHF cells. The data shows that all of these components of the PCP pathway play an important role in regulating SHF cells while they are entering the outflow tract during heart development. Disruption of epithelial markers, E-cadherin, β-catenin and PKCζ in *Wnt5a*$^{-/-}$, *Ror2*$^{-/-}$, *ROCKDN;Isl1-Cre* and *Rac1*$^{flox/flox}$*;Isl1-Cre* mutant embryos indicate loss of the epithelial nature of cells in the distal outflow tract along with abnormalities in adherens and tight junctions suggesting loss of ABP in the cells and misorientation of cells. Disruption of laminin expression in these affected cells and its expression being not limited to the basal side of the cells strengthens the possibility of loss of ABP and loss of orientation in the absence of *Wnt5a, Ror2, ROCK* and *Rac1,* as observed in the absence of *Vangl2*.

The mechanism through which *Wnt5a, Ror2, Rac1, ROCK* and *Vangl2* regulate SHF cells is similar and shares characteristics. Adherens junctions and tight junctions both are disrupted in the absence of any of these genes, indicating the loss of polarity in the cells. However, the phenotype of *Ror2-/-* embryos is less severe as compared to *Wnt5a*$^{-/-}$ embryos when looked at heart defects, which was reflected in the analysis of the polarity markers as well (β-catenin and PKCζ). This may be because *Ror2* absence leads to weakened Wnt signalling rather than complete loss of it (Gao *et al.*, 2011). Vangl2 protein is a trans-membrane protein and shows membrane localization in the cells while they are entering the outflow tract (figure 4.5). However, like in *Lp* mutants, Vangl2 protein fails to

reach the membrane in *Wnt5a*$^{-/-}$ embryos resulting in no membrane localization and reduced localization in *Ror2*$^{-/-}$ embryos as a result of weakened Wnt signalling (Gao *et al.*, 2011). This interaction between Wnt5a, Ror2 and Vangl2 could be the reason behind similar behaviour of cells in the distal outflow tract.

Relating the results and analysis with the mechanism suggested in *Vangl2*$^{flox/flox}$*;Isl1-Cre* mutants, it can be suggested that *ROCK* and *Rac1* is also playing a role in undifferentiated precursor SHF cells along with role in NCC, unlike *Vangl2*. It has been shown that absence of *Wnt5a* leads to migration defect of NCCs in the heart leading to loss of aorto-pulmonary septum (Schleiffarth *et al.*, 2007). Apart from the already established connection between *Wnt5a*, *ROCK* and *Rac1* with NCC, we have shown that *Wnt5a*, *Ror2*, *ROCK* and *Rac1* signalling could also be involved in the polarisation of SHF cells into the distal outflow tract.

It is clear that it is not just *Vangl2*, but the whole PCP signalling pathway which regulates SHF during outflow tract morphogenesis. As PCP signalling starts as one pathway from *Wnt5a*, *Ror2* to *Vangl2*, but is divided into two pathways, one with *Rac1* leading to *JNK* activation and one with *ROCK* which plays a role in gene transcription and cellular actin cytoskeleton formation, disruption at any of the level of the signalling, in any component of the pathway would cause abnormal behaviour in SHF cells. This highlights the importance of whole non-canonical wnt/PCP signalling pathway in proper functioning of SHF cells. These results give us an insight into how the SHF cells behave, which can be useful in finding alternate ways to bring SHF cells back to normal even while these proteins are not present.

Chapter 6

Discussion

Heart development is a very complex process which requires morphological and structural changes co-ordinated along with gene expression at the correction location and time. At early developmental stages of heart, SHF cells contribute as an extra-cardiac cell population and contribute to different parts of the heart. Genetic control of SHF cells has been studied using a range of gene knockout and tissue tracking experiments, which have shown the importance of several genes within the SHF. However, the exact function and regulation of these genes remain unclear to date. Also how SHF cells behave, move and polarise is still unanswered.

Over the years, genes which are required for establishing cell polarity and its maintenance have been identified and shown to regulate developmental processes in a range of species. These genes are members of a highly conserved signalling pathway known as the non-canonical Wnt signalling pathway or PCP pathway. More recently, studies have suggested a link between PCP and embryonic cardiac development with defects in the PCP genes resulting in abnormal cardiac morphogenesis leading to cardiovascular defects.

Vangl2 is a PCP gene, which is mutated in naturally occurring *Lp* mice, has a potential role in cardiac development. This is suggested because of the various cardiac abnormalities including cardiac alignment defects such as double outlet right ventricle, ventricular septal defect and pharyngeal arch artery remodelling defects seen in *Lp* mutants. Thus, this study was aimed to investigate a possible role for *Vangl2* during early cardiac development.

The *Vangl2 Lp* mutant has been used extensively to understand the role Vangl2 plays during mammalian embryonic development. *Lp* mice have gross morphological defects, including craniorachischisis and incomplete axial rotation, which are characteristic of this mutant. However, mutation in *Vangl2* in all body cells leading to neural tube defects limit the use of *Lp* mice in dissecting out the role of *Vangl2* gene during heart morphogenesis. *Lp* mutants display a spectrum

of cardiac defects which specifically affect the outflow region of the heart, including double outlet right ventricle, ventricular septal defect, and aortic arch abnormalities (Henderson *et al.*, 2001). But global loss of *Vangl2* in *Lp* mice makes it inadequate for the purpose of establishing the precise role of Vangl2 in heart development. It was suggested that these heart abnormalities could be secondary to the neural tube defects and axial turning defects (Henderson *et al.*, 2001). However, even if these cardiac defects are not secondary to other embryonic defects, the role of Vangl2 in embryonic heart development could still be complex, given the number of different cell populations that contribute to the developing outflow tract. Defects identified within the developing outflow tract of *Lp* mutants could arise from disruptions to either NCC or SHF derived cells, but the integration of cells from these two lineages into this region makes dissecting the causes of malformation extremely difficult. To answer this, a more specific conditional knockout of *Vangl2* was required to knock out *Vangl2* in particular cell types. Thus, a floxed allele of *Vangl2* was generated. The generation of mice that allowed for the conditional deletion of *Vangl2* in specific cell types within the heart has enabled us to establish the cardiac cell type that is critically dependent on *Vangl2* function – the SHF. In addition to this, immunofluorescence experiments have allowed us to study the cellular localisation of Vangl2 and the affect its loss has on polarity of SHF, further enabling us to attempt to unravel its role within the developing heart.

Vangl2 is a trans-membrane protein, with exon 4 of *Vangl2* gene containing its trans-membrane domains. These domains are essential for its activity; therefore *Vangl2flox* line was generated where loxP sites flank exon 4 of *Vangl2*, and remove the trans-membrane domain. A *neomycin* selection cassette was used within the targeting vector. $Vangl2^{floxneo/+}$ embryos were normal showing that Vangl2 gene is not haploinsufficient. However, $Vangl2^{floxneo/floxneo}$ embryos, which had the *neomycin* selection cassette on both alleles, were hypomorphic for *Vangl2*. They showed a more variable external phenotype (displayed craniorachischisis and spina bifida) as compared to the phenotype seen in *Lp/Lp* (displayed craniorachischisis only). This hypomorphic phenotype has previously been reported because of the presence of *neomycin*, for example *Fgf8neo* and *Pax9neo*

(Meyers *et al.*, 1998; Kist *et al.*, 2007), but it still needs to be established to what extend the function is Vangl2 is affected in its presence, which could be taken up in further studies. Vangl2 level can also be analysed in *Vangl2*$^{floxneo/floxneo}$ which would aid in understanding the level of expression in the presence of *neomycin*. Although heart abnormalities in both *Lp/Lp* and *Vangl2*$^{floxneo/floxneo}$ were the same, to eliminate any influence *neomycin* might have, the cassette was removed by crossing the *Vangl2fn* mice with *FLPe* mice.

To analyse whether this flox line is able to recapitulate the *Lp* phenotype, *Vangl2flox* mice was then crossed with globally expressing Cre, *PGK-Cre* (Lallemand *et al.*, 1998) and *Sox2-Cre (Hayashi et al., 2002)* and as expected, mutants from both the crosses recapitulated *Lp/Lp* phenotype, both external and cardiac, confirming our *flox* line was suitable to be used to genetically dissect the role of Vangl2 using cell specific *Cre*. Recombination due to the activity of the enzyme Cre deletes exon 4, creates a frame shift and a stop codon that truncates the protein at amino acid 78 and is predicted to give rise to a small 8KDa protein, which lacks the four trans-membrane domains required of Vangl2 activity and C-terminal PDZ-binding domain through which Vangl2 interacts with various other proteins (Torban *et al.*, 2004; Montcouquiol *et al.*, 2006). Recombination was confirmed by RT-PCR and western blotting. RT-PCR showed loss of *Vangl2* transcript; however, western blotting showed a faint Vangl2 band in the mutants although the developmental defects were present. Therefore, even if the truncated protein is stable, it is predicted to be non-functional and even if there is some protein left, the deletion is enough to cause the developmental abnormalities.

The genesis of outflow tract defects was originally hypothesised to be solely dependent upon the contribution of the neural crest to the outflow tract and pharyngeal arch arteries; which was confirmed by the spectrum of phenotypes seen in the neural crest ablated embryos. However, studies have shown that SHF cells are also involved in outflow tract development and in their absence outflow tract defects are observed (Cai *et al.*, 2003). Therefore, to look at the role Vangl2 plays during the outflow tract development; its expression was deleted specifically from cells involved during the process. When *Vangl2* was deleted only in NCC using *Wnt1-Cre (Danielian et al., 1998)* there were no neural tube or

cardiac abnormalities and mutants mice when born were healthy and indistinguishable from controls littermates and had normal heart analysed at P28. However, when Vangl2 was deleted specially from SHF cells using *Isl1-Cre* (Yang *et al.*, 2006) the mutant embryos showed same cardiac outflow defects as seen in *Lp/Lp* (double outlet right ventricle and ventricular septal defect), but the external phenotype was normal. Immunostaining confirmed the loss of Vangl2 specifically in Isl1 positive cells; however with Wnt1cre positive cells colocalization of Vangl2 was not observed, suggesting Vangl2 is not expressed in NCC. In the *Lp* mouse, there is disorganization of cardiomyocytes in the early stages of cardiac development which affects the integrity of the early heart tube and thus prevents it from looping correctly, resulting in alignment and septation defects of the heart (Phillips *et al.*, 2005). However, the observation that heart defects in *Vangl2*$^{flox/flox}$*;PGK-Cre*, *Vangl2*$^{flox/flox}$*;Sox2-Cre* and *Lp/Lp* embryos were only found in embryos with NTDs or gastroschisis, suggests that the cardiac alignment defects (double outlet right ventricle and peri-membranous ventricular septal defect) may be secondary to the axial rotation and changes in body plan caused by these gross abnormalities in body form and not primarily as a result of loss of *Vangl2*. Henderson et al (2001) originally suggested that the cardiac looping defects observed in the *Lp* mutant may be secondary to the neural tube closure and axial turning defects (Henderson *et al.*, 2001), as heart development is quite sensitive to disturbances in cervical flexure and axial rotation (Manner *et al.*, 1993; Melloy *et al.*, 1998). The body form abnormalities and axial rotation defects could affect cell movement and prevent the heart from looping correctly, both of which would ultimately prevent the correct remodelling of the heart and lead to the ventricular septation and alignment defects identified in the mice with NTDs and/or gastroschisis. However, loss of Vangl2 in SHF cells recapitulates the cardiac malformations seen in *Lp* mice with normal external phenotype, and looking at these results in addition to *Vangl2*^{floxneo} result, where double outlet right ventricle was observed in heart in the absence of craniorachischisis, shows that heart defects are not secondary to the neural tube defects and axial rotation defects as been suggested before. Moreover, it shows that *Vangl2* has an important role in SHF cells and deletion of *Vangl2* in only SHF cells is causing the cardiac defects seen in *Lp/Lp* mutants. It can also be stated that SHF do not

contribute to the neural tube defects but are responsible for heart morphogenesis. Although, the aortic arch abnormalities seen in *Lp* (Henderson *et al.*, 2001), and in the *Vangl2*$^{flox/flox}$*;PGK-Cre* and *Vangl2*$^{flox/flox}$*;Sox2-Cre* mutants, may be secondary to these abnormalities in body form, as they are only observed in the presence of craniorachischisis.

The results showed that loss of Vangl2 from SHF cells leads to outflow tract defect and colocalization between Vangl2 and SHF in different regions of heart concludes that cells derived from SHF express Vangl2 in respective regions of heart and validates the histological results observed showing heart defects when Vangl2 was deleted specifically in SHF. Loss of Vangl2 in differentiated SHF cells, in myocardium derived from SHF, using *Mlc2v-Cre* (Chen *et al.*, 1998), and endothelial cells, using *Tie2-Cre* (Kisanuki *et al.*, 2001) showed normal outflow tract development suggesting importance of Vangl2 in undifferentiated precursor SHF cells. However, Vangl2 can also be deleted in SHF cells at different stages of development to establish at which stage Vangl2 plays the critical role.

Undifferentiated precursor SHF cells enter the distal outflow tract from the dorsal pericardial wall and transitions to differentiated myocardium while moving proximally in the outflow tract. This zone where the transition is taking place is termed as transition zone and when Vangl2 expression was seen in this zone, it was observed to have membrane localized expression. However as cells move more proximally and differentiate into myocardium, Vangl2 expression becomes more cytoplasmic. It is known that loss of Vangl2 expression from the membrane causes *Lp* phenotype (Torban *et al.*, 2007) underlining the importance of membrane localization of Vangl2 in the outflow tract in the transition zone. When cells are entering the outflow tract, there is loss of nuclear *Isl1* expression in the *Vangl2*$^{flox/flox}$*;Isl1-Cre* mutants, indicating premature differentiation of cells into cardiomyocytes (Ramsbottom et al 2014), suggesting the role of Vangl2 in keeping SHF cells in undifferentiated progenitor state. This was validated by early onset of αSMA expression, marking smooth muscle cells in the mutants, meaning loss of Vangl2 leads to early differentiation. The particular region in the distal outflow tract where Vangl2 changes its expression and become membrane

localized and undifferentiated SHF precursor cells are moving into the outflow tract was hence used as the zone under observation for further experiments. Vangl2 is a polarity protein and after further analysis of transition zone, epithelial nature of the cells and loss of polarity was revealed in the cells. ABP was disrupted, with apical and basal determinants not being limited to their compartments along with abnormal orientation of cells. Similar affect has been observed with loss prickle, another PCP protein, in *Drosophila* leading to disturbances in ABP (Tao et al, 2009; 2012). In zebrafish, mislocalisation of ABP markers leads to cardiac malformations and similar phenotype is observed in mouse as well with disturbances in cellular polarity leading to cardiac malformations (Rohr *et al.*, 2006).

AJ and TJ are present forming a belt around the cell, dividing the cell into apical and basal compartments. They also keep a check that apical and basal determinants remain in their boundary and disruption in these junctions lead to loss of ABP (Kaplan *et al.*, 2009). Our results show change in expression pattern of cadherins (N and E) and PKCζ which are a part of AJ and TJ respectively, along with disruption in β-catenin expression which associates with cadherins in AJ. These markers apart from marking AJ and TJ are classic epithelial markers as well and therefore disruption in their expression in the transition zone leads to loss of ABP in the SHF cells along with loss of epithelial nature of the cells. This was confirmed by showing the position of MTOC, which should be present apically in epithelial cells, but in the *Vangl2*$^{flox/flox}$*;Isl1-Cre* mutants they were not restricted to the apical side of the cell, and by expression of extra-cellular markers, laminin and fibronectin, which marks the basolateral side of the cells, but were extended to apical part of the cells in the mutants only in the transition zone and had normal expression in the proximal outflow tract with differentiated myocardium cells. These SHF cells in the transition zone lack Vangl2, solidifying our finding that loss of Vangl2 leads to loss of ABP. However, apart from disruption of ABP, another possibility could be abnormal orientation of cells which makes these apical and basal determinants look misoriented. Mislocalisation of cellular component like MTOCs and an extra cellular marker, like laminin suggests it could be because of the abnormal orientation of cells and loss of ABP. Hence, it

could be a combination of both the factors. Apart from ABP, loss of Vangl2 also leads to loss of PCP. PCP pathway is a multi-protein complex, of which Vangl2 is one key component, but when 2 other proteins involved in the pathway, Dvl2 and Celsr1, were looked in *Vangl2$^{flox/flox}$;Isl1-Cre* mutants, there expression was also lost from the membrane similarly to Vangl2. A shortcoming of this study would be that the analysis of the loss of ABP, PCP and abnormal localisation of cells in the transition zone in the distal outflow tract as done at E9.5, but the cause behind this affect hasn't been checked. This could be done by looking at these markers at an earlier stage and analyse their expression along with quantification of cells showing abnormal expression.

Loss of Vangl2 globally (*Lp*, *Vangl2$^{flox/flox}$;PGK-Cre* and *Vangl2$^{flox/flox}$;Sox2-Cre*) and specifically from SHF cells (*Vangl2$^{flox/flox}$;Isl1-Cre*) leads to double outlet right ventricle suggesting the role cells derived from SHF play for proper orientation of the outflow vessels to the ventricles. SHF move as an epithelial sheet of cells (Van Den Berg *et al.*, 2009) with cohesion and organization between the cells. This is analogous to the movements of epithelial sheets in other organ systems (Muñoz-Soriano *et al.*, 2012; Guillot and Lecuit, 2013). This organization is disrupted by the loss of cellular polarity by the loss of Vangl2 in SHF cells leading to disorientation of the outflow vessel causing double outlet right ventricle. The possible explanation would be that loss of Vangl2 from SHF-derived cells results in loss polarity in SHF which leads to disorganization of the cells and their early differentiation. These disorganized cells fail to move into the outflow tract and thus a failure to form adequate length of the outflow tract and differentiate into myocardium leading to shortened outflow tract which hampers the rotation of the vessel, which is essential for correct orientation. Link between a shortened outflow tract and double outlet right ventricle is already known (Yelbuz *et al.*, 2002; Ward *et al.*, 2005). As the rotation doesn't happen, aorta and pulmonary trunk both comes out parallel from the right ventricle. Although it is suggested that Vangl2 plays a key role in SHF deployment and movement leading to outflow tract lengthening, this can be substantiated by looking at the actual movement of SHF cells. This can be done by 2 ways; firstly SHF cells can be labelled by injecting BrdU at E8.5 and then examining their position and

distribution at E9.5 which would help in determining the movement of SHF cells into the outflow tract in the absence of *Vangl2*. Another method could be using cell culture techniques. Outflow tract can be dissected out and cells grown using cell culture. Immunostaining using anti-GFP antibody would mark Isl1 positive cells and show their movement pattern in both controls and mutants. They could be colabelled with another antibody, like MTOC antibody which would determine the apical side and indicate the direction in which the cells would move. Therefore, it would be beneficial to obtain mutant embryos at earlier stages to investigate the movement and initial addition of SHF cells, and at later stages to define ultimate SHF cell distribution.

The role polarity plays in the cardiac development and malformations has been extensively studied before, but the thesis explains the role of *Vangl2* and the possible mechanism of the cardiac defect caused by its absence. *Wnt5a* is one of the main ligand implicated in activating PCP signalling, and Vangl2 works after phosphorylation by Wnt5a-Ror2 complex (Gao *et al.*, 2011) and activates downstream targets of the PCP pathway. *Wnt5a* and *Ror2* have been looked separately for cardiac defects and to check the polarity. Results showed that although loss of *Ror2* had a milder phenotype as compared to loss of *Wnt5a*, absence of both leads to cardiac defects and disruption of cellular polarity along with abnormal cell orientation confirmed by looking at the same markers as for *Vangl2;Isl1-Cre* embryos. Vangl2 acts via RhoA/ROCK1 in the non-canonical Wnt signalling pathway, therefore downstream PCP components (*ROCK* and *Rac1*) were looked at in SHF as well. Interestingly, outflow defects were observed in $Rac1^{flox/flox}$*;Isl1-Cre* and *ROCKDN;Isl1-Cre* mutant embryos because of the disruption in cellular polarity and abnormal cell orientation in the distal outflow tract. Thus, *Vangl2* may be acting with these other factors in a network that regulates the addition of SHF to the lengthening outflow tract. There is loss of Vangl2 membrane localisation in $Wnt5a^{-/-}$ and reduced localisation in $Ror2^{-/-}$ (Gao *et al.*, 2011), suggesting these upstream factors are involved in Vangl2 localisation. An additional experiment for future work can be looking at Rac1 and ROCK expression in *Vangl2* mutants. As these are downstream targets of *Vangl2*, loss of Rac1 and ROCK localisation would be expected when *Vangl2* is deleted. Whole PCP pathway is important for cardiac development, and mutation in different

components leads to defect in the outflow region, for example, in *Dvl 1-3* (Hamblet *et al.*, 2002; Etheridge *et al.*, 2008), *Celsr1* (Curtin *et al.*, 2003), *Wnt5a* (Schleiffarth *et al.*, 2007), *Wnt11* (Zhou *et al.*, 2007b; Nagy *et al.*, 2010), *Fz1/Fz2* (Yu *et al.*, 2010), *Scrib* (Phillips *et al.*, 2007) and *Ptk7* (Paudyal *et al.*, 2010), highlighting the importance of cellular polarity during outflow tract development. Our results provide more insight to it and solidify the conclusion that all components of the pathway are involved in outflow tract morphogenesis and absence of any component leads to loss of polarity and hence outflow defects.

We found that *Vangl2* is required for the correct localization for the junctional components of SHF and potentially accounting for the disrupted cell-cell adhesion and cardiomyocytes disorganization seen in the early heart of the *Lp*. The establishment of polarity within cardiomyocytes, and the correct formation of cell-cell junctions between them, is critical for their correct organization and ultimately the integrity, maturation and normal function of cardiac tissue. Our results indicate that *Vangl2* may be essential for both of these early processes, categorizing its role as crucial for correct cardiac morphogenesis. Thus, disruption of *Vangl2* in the undifferentiated precursor SHF cells leads to clinically relevant congenital heart defects at later stages of cardiogenesis. The findings of this study confirm the possible role of not only *Vangl2*, but also other components of non-canonical Wnt/PCP signalling pathway in the establishment of ABP and PCP, and in the development of the heart.

The results not only confirm the role of whole PCP pathway in SHF cells during heart development in the embryo, but also suggest a possible mechanism which hasn't been shown before. Studies have suggested NCC as the cell type which is regulated by PCP signalling, however we confirm that NCC are not dependednt on Vangl2. Role of other PCP components like ROCK and Rac1 have been reported in NCC, but their potential role in regulating SHF cells gives a new dimension of whole PCP pathway in SHF movement, differentiation as well as their nature. Recently Sinha et al studied the abnormalities in outflow tract morphogenesis in *Dvl2* mutants in more detail, concluding they resulted from abnormalities in the incorporation of SHF progenitors into the dorsal pericardial wall, prior to movement into the outflow vessel (Sinha *et al.*, 2012). The

mechanism by which a disruption of a key PCP protein disrupts SHF contributions to the outflow region appears to differ between the *Vangl2* and *Dvl2* mutants, perhaps reflecting multiple roles for PCP signalling in deployment of SHF cells to the heart.

Apart from the role of PCP signalling in regulating SHF cells, the thesis also gives an insight about the nature of the SHF cells. SHF cells haven't been described to have an epithelial nature before, and this novel finding makes the understanding of SHF behaviour during heart morphogenesis much easier and clearer. Therefore SHF cells can form continuous sheets attached to each other by adherens junctions and tight junctions, and also being polarised in nature. This would be helpful in understanding role of other genes in SHF cells, keeping their epithelial nature in consideration. Hence, the work provides a mechanistic insight with regards to outflow tract morphogenesis and these findings provide a framework for understand this process in humans, unravelling answers about etiology of congenital heart defects.

References

- Abu-Issa, R. and Kirby, M.L. 23 (2007) 'Heart field: From mesoderm to heart tube'. pp. 45-68. Available at: http://www.scopus.com/inward/record.url?eid=2-s2.0-38149048031&partnerID=40&md5=db5cd6f5708ee2215d395fbf5da7dca5.
- Abu-Issa, R., Smyth, G., Smoak, I., Yamamura, K.I. and Meyers, E.N. (2002) 'Fgf8 is required for pharyngeal arch and cardiovascular development in the mouse', *Development*, 129(19), pp. 4613-4625.
- Adler, P.N. (2002) 'Planar signaling and morphogenesis in Drosophila', *Developmental Cell*, 2(5), pp. 525-535.
- Aggarwal, V.S., Liao, J., Bondarev, A., Schimmang, T., Lewandoski, M., Locker, J., Shanske, A., Campione, M. and Morrow, B.E. (2006) 'Dissection of Tbx1 and Fgf interactions in mouse models of 22q11DS suggests functional redundancy', *Human Molecular Genetics*, 15(21), pp. 3219-3228.
- Amano, M., Nakayama, M. and Kaibuchi, K. (2010) 'Rho-kinase/ROCK: A key regulator of the cytoskeleton and cell polarity', *Cytoskeleton*, 67(9), pp. 545-554.
- Anderson, R.H., Chaudhry, B., Mohun, T.J., Bamforth, S.D., Hoyland, D., Phillips, H.M., Webb, S., Moorman, A.F.M., Brown, N.A. and Henderson, D.J. (2012) 'Normal and abnormal development of the intrapericardial arterial trunks in humans and mice', *Cardiovascular Research*, 95(1), pp. 108-115.
- Anderson, R.H., Webb, S., Brown, N.A., Lamers, W. and Moorman, A. (2003) 'Development of the heart: (3) Formation of the ventricular outflow tracts, arterial valves, and intrapericardial arterial trunks', *Heart*, 89(9), pp. 1110-1118.
- Andre, P., Wang, Q., Wang, N., Gao, B., Schilit, A., Halford, M.M., Stacker, S.A., Zhang, X. and Yang, Y. (2012) 'The Wnt coreceptor Ryk regulates Wnt/planar cell polarity by modulating the degradation of the core planar cell polarity component Vangl2', *Journal of Biological Chemistry*, 287(53), pp. 44518-44525.
- Armstrong, E.J. and Bischoff, J. (2004) 'Heart valve development: Endothelial cell signaling and differentiation', *Circulation Research*, 95(5), pp. 459-470.
- Auerbach, R. (1954) ' Analysis of the developmental effects of a lethal mutation in the house mouse', *Journal of Experimental Zoology*, 127, pp. 305–329.
- Bakre, M.M., Hoi, A., Mong, J.C.Y., Koh, Y.Y., Wong, K.Y. and Stanton, L.W. (2007) 'Generation of multipotential mesendodermal progenitors from mouse embryonic stem cells via sustained Wnt pathway activation', *Journal of Biological Chemistry*, 282(43), pp. 31703-31712.
- Baldini, A. (2005) 'Dissecting contiguous gene defects: TBX1', *Current Opinion in Genetics and Development*, 15(3 SPEC. ISS.), pp. 279-284.
- Banerjee, S., Gordon, L., Donn, T.M., Berti, C., Moens, C.B., Burden, S.J. and Granato, M. (2011) 'A novel role for MuSK and non-canonical wnt

signaling during segmental neural crest cell migration', *Development*, 138(15), pp. 3287-3296.

- Bartelings, M.M. and Gittenberger-de Groot, A.C. (1989) 'The outflow tract of the heart. Embryologic and morphologic correlations', *International Journal of Cardiology*, 22(3), pp. 289-300.
- Barth, J.L., Clark, C.D., Fresco, V.M., Knoll, E.P., Lee, B., Argraves, W.S. and Lee, K.H. (2010) 'Jarid2 is among a set of genes differentially regulated by Nkx2.5 during outflow tract morphogenesis', *Developmental Dynamics*, 239(7), pp. 2024-2033.
- Bastock, R., Strutt, H. and Strutt, D. (2003) 'Strabismus is asymmetrically localised and binds to Prickle and Dishevelled during Drosophila planar polarity patterning', *Development*, 130(13), pp. 3007-3014.
- Bi, W., Drake, C.J. and Schwarz, J.J. (1999) 'The transcription factor MEF2C-null mouse exhibits complex vascular malformations and reduced cardiac expression of angiopoietin 1 and VEGF', *Developmental Biology*, 211(2), pp. 255-267.
- Bockman, D.E. and Kirby, M.L. (1984) 'Dependence of thymus development on derivatives of the neural crest', *Science*, 223(4635), pp. 498-500.
- Bökenkamp, R., Gittenberger-De Groot, A.C., Van Munsteren, C.J., Grauss, R.W., Ottenkamp, J. and DeRuiter, M.C. (2006) 'Persistent ductus arteriosus in the Brown-Norway inbred rat strain', *Pediatric Research*, 60(4), pp. 407-412.
- Bondue, A., Tännler, S., Chiapparo, G., Chabab, S., Ramialison, M., Paulissen, C., Beck, B., Harvey, R. and Blanpain, C. (2011) 'Defining the earliest step of cardiovascular progenitor specification during embryonic stem cell differentiation', *Journal of Cell Biology*, 192(5), pp. 751-765.
- Bosco, E.E., Mulloy, J.C. and Zheng, Y. (2009) 'Rac1 GTPase: A "Rac" of all trades', *Cellular and Molecular Life Sciences*, 66(3), pp. 370-374.
- Brade, T., Männer, J. and Kühl, M. (2006) 'The role of Wnt signalling in cardiac development and tissue remodelling in the mature heart', *Cardiovascular Research*, 72(2), pp. 198-209.
- Bradshaw, L., Chaudhry, B., Hildreth, V., Webb, S. and Henderson, D.J. (2009) 'Dual role for neural crest cells during outflow tract septation in the neural crest-deficient mutant Splotch2H', *Journal of Anatomy*, 214(2), pp. 245-257.
- Brand, T. (2003) 'Heart development: Molecular insights into cardiac specification and early morphogenesis', *Developmental Biology*, 258(1), pp. 1-19.
- Brault, V., Moore, R., Kutsch, S., Ishibashi, M., Rowitch, D.H., McMahon, A.P., Sommer, L., Boussadia, O. and Kemler, R. (2001) 'Inactivation of the β-catenin gene by Wnt1-Cre-mediated deletion results in dramatic brain malformation and failure of craniofacial development', *Development*, 128(8), pp. 1253-1264.
- Brown, C.B., Feiner, L., Lu, M.M., Li, J., Ma, X., Webber, A.L., Jia, L., Raper, J.A. and Epstein, J.A. (2001) 'PlexinA2 and semaphorin signaling during cardiac neural crest development', *Development*, 128(16), pp. 3071-3080.

- Brown, C.B., Wenning, J.M., Lu, M.M., Epstein, D.J., Meyers, E.N. and Epstein, J.A. (2004) 'Cre-mediated excision of Fgf8 in the Tbx1 expression domain reveals a critical role for Fgf8 in cardiovascular development in the mouse', *Developmental Biology*, 267(1), pp. 190-202.
- Bruneau, B.G. (2002) 'Transcriptional regulation of vertebrate cardiac morphogenesis', *Circulation Research*, 90(5), pp. 509-519.
- Bruneau, B.G. (2008) 'The developmental genetics of congenital heart disease', *Nature*, 451(7181), pp. 943-948.
- Buckingham, M., Meilhac, S. and Zaffran, S. (2005) 'Building the mammalian heart from two sources of myocardial cells', *Nature Reviews Genetics*, 6(11), pp. 826-835.
- Cabrera, C.V., Alonso, M.C., Johnston, P., Phillips, R.G. and Lawrence, P.A. (1987) 'Phenocopies induced with antisense RNA identify the wingless gene', *Cell*, 50(4), pp. 659-663.
- Cadigan, K.M. and Nusse, R. (1997) 'Wnt signaling: A common theme in animal development', *Genes and Development*, 11(24), pp. 3286-3305.
- Cai, C.L., Liang, X., Shi, Y., Chu, P.H., Pfaff, S.L., Chen, J. and Evans, S. (2003) 'Isl1 identifies a cardiac progenitor population that proliferates prior to differentiation and contributes a majority of cells to the heart', *Developmental Cell*, 5(6), pp. 877-889.
- Carmeliet, P., Ferreira, V., Breier, G., Pollefeyt, S., Kieckens, L., Gertsenstein, M., Fahrig, M., Vandenhoeck, A., Harpal, K., Eberhardt, C., Declercq, C., Pawling, J., Moons, L., Collen, D., Risaut, W. and Nagy, A. (1996) 'Abnormal blood vessel development and lethality in embryos lacking a single VEGF allele', *Nature*, 380(6573), pp. 435-439.
- Carmona-Fontaine, C., Matthews, H. and Mayor, R. (2008a) 'Directional cell migration in vivo: Wnt at the crest', *Cell adhesion & migration*, 2(4), pp. 240-242.
- Carmona-Fontaine, C., Matthews, H.K., Kuriyama, S., Moreno, M., Dunn, G.A., Parsons, M., Stern, C.D. and Mayor, R. (2008b) 'Contact inhibition of locomotion in vivo controls neural crest directional migration', *Nature*, 456(7224), pp. 957-961.
- Chen, J., Kubalak, S.W., Minamisawa, S., Price, R.L., Becker, K.D., Hickey, R., Ross Jr, J. and Chien, K.R. (1998) 'Selective requirement of myosin light chain 2v in embryonic heart function', *Journal of Biological Chemistry*, 273(2), pp. 1252-1256.
- Chen, L., Fulcoli, F.G., Ferrentino, R., Martucciello, S., Illingworth, E.A. and Baldini, A. (2012) 'Transcriptional control in cardiac progenitors: Tbx1 interacts with the BAF chromatin remodeling complex and regulates Wnt5a', *PLoS Genetics*, 8(3).
- Chen, L., Fulcoli, F.G., Tang, S. and Baldini, A. (2009) 'Tbx1 regulates proliferation and differentiation of multipotent heart progenitors', *Circulation Research*, 105(9), pp. 842-851.
- Chen, Y.H., Ishii, M., Sun, J., Sucov, H.M. and Maxson Jr, R.E. (2007) 'Msx1 and Msx2 regulate survival of secondary heart field precursors and post-migratory proliferation of cardiac neural crest in the outflow tract', *Developmental Biology*, 308(2), pp. 421-437.

- Clouthier, D.E., Williams, S.C., Hammer, R.E., Richardson, J.A. and Yanagisawa, M. (2003) 'Cell-autonomous and nonautonomous actions of endothelin-A receptor signaling in craniofacial and cardiovascular development', *Developmental Biology*, 261(2), pp. 506-519.
- Cohen, E.D., Miller, M.F., Wang, Z., Moon, R.T. and Morrisey, E.E. (2012) 'Wnt5a and wnt11 are essential for second heart field progenitor development', *Development*, 139(11), pp. 1931-1940.
- Cohen, E.D., Wang, Z., Lepore, J.J., Min, M.L., Taketo, M.M., Epstein, D.J. and Morrisey, E.E. (2007) 'Wnt/β-catenin signaling promotes expansion of Isl-1-positive cardiac progenitor cells through regulation of FGF signaling', *Journal of Clinical Investigation*, 117(7), pp. 1794-1804.
- Colosimo, P.F., Liu, X., Kaplan, N.A. and Tolwinski, N.S. (2010) 'GSK3β affects apical-basal polarity and cell-cell adhesion by regulating aPKC levels', *Developmental Dynamics*, 239(1), pp. 115-125.
- Conway, S.J., Godt, R.E., Hatcher, C.J., Leatherbury, L., Zolotouchnikov, V.V., Brotto, M.A.P., Copp, A.J., Kirby, M.L. and Creazzo, T.L. (1997a) 'Neural crest is involved in development of abnormal myocardial function', *Journal of Molecular and Cellular Cardiology*, 29(10), pp. 2675-2685.
- Conway, S.J., Henderson, D.J. and Copp, A.J. (1997b) 'Pax3 is required for cardiac neural crest migration in the mouse: Evidence from the splotch (Sp(2H)) mutant', *Development*, 124(2), pp. 505-514.
- Conway, S.J., Henderson, D.J., Kirby, M.L., Anderson, R.H. and Copp, A.J. (1997c) 'Development of a lethal congenital heart defect in the splotch (Pax3) mutant mouse', *Cardiovascular Research*, 36(2), pp. 163-173.
- Cooper, W.O., Hernandez-Diaz, S., Arbogast, P.G., Dudley, J.A., Dyer, S., Gideon, P.S., Hall, K. and Ray, W.A. (2006) 'Major congenital malformations after first-trimester exposure to ACE inhibitors', *New England Journal of Medicine*, 354(23), pp. 2443-2451.
- Copp, A.J., Checiu, I. and Henson, J.N. (1994) 'Developmental basis of severe neural tube defects in the loop-tail (Lp) mutant mouse: Use of microsatellite DNA markers to identify embryonic genotype', *Developmental Biology*, 165(1), pp. 20-29.
- Creazzo, T.L., Godt, R.E., Leatherbury, L., Conway, S.J. and Kirby, M.L. 60 (1998) 'Role of cardiac neural crest cells in cardiovascular development'. pp. 267-286. Available at: http://www.scopus.com/inward/record.url?eid=2-s2.0-0031942931&partnerID=40&md5=16ce22d21e5d3d090a04abdbd1d628ee.
- Curtin, J.A., Quint, E., Tsipouri, V., Arkell, R.M., Cattanach, B., Copp, A.J., Henderson, D.J., Spurr, N., Stanier, P., Fisher, E.M., Nolan, P.M., Steel, K.P., Brown, S.D.M., Gray, I.C. and Murdoch, J.N. (2003) 'Mutation of Celsr1 disrupts planar polarity of inner ear hair cells and causes severe neural tube defects in the mouse', *Current Biology*, 13(13), pp. 1129-1133.
- D'Amico, G., Jones, D.T., Nye, E., Sapienza, K., Ramjuan, A.R., Reynolds, L.E., Robinson, S.D., Kostourou, V., Martinez, D., Aubyn, D., Grose, R., Thomas, G.J., Spencer-Dene, B., Zicha, D., Davies, D.,

Tybulewicz, V. and Hodivala-Dilke, K.M. (2009) 'Regulation of lymphatic-blood vessel separation by endothelial Rac1', *Development*, 136(23), pp. 4043-4053.

- Danielian, P.S., Muccino, D., Rowitch, D.H., Michael, S.K. and McMahon, A.P. (1998) 'Modification of gene activity in mouse embryos in utero by a tamoxifen-inducible form of Cre recombinase', *Current Biology*, 8(24), pp. 1323-1326.
- Das, G., Jenny, A., Klein, T.J., Eaton, S. and Mlodzik, M. (2004) 'Diego interacts with Prickle and Strabismus/Van Gogh to localize planar cell polarity complexes', *Development*, 131(18), pp. 4467-4476.
- de Boer, B.A., van den Berg, G., de Boer, P.A.J., Moorman, A.F.M. and Ruijter, J.M. (2012) 'Growth of the developing mouse heart: An interactive qualitative and quantitative 3D atlas', *Developmental Biology*, 368(2), pp. 203-213.
- De Calisto, J., Araya, C., Marchant, L., Riaz, C.F. and Mayor, R. (2005) 'Essential role of non-canonical Wnt signalling in neural crest migration', *Development*, 132(11), pp. 2587-2597.
- De La Cruz, M.V., Sanchez Gomez, C., Arteaga, M.M. and Arguello, C. (1977) 'Experimental study of the development of the truncus and the conus in the chick embryo', *Journal of Anatomy*, 123(3), pp. 661-686.
- DeChiara, T.M., Kimble, R.B., Poueymirou, W.T., Rojas, J., Masiakowski, P., Valenzuela, D.M. and Yancopoulos, G.D. (2000) 'Ror2, encoding a receptor-like tyrosine kinase, is required for cartilage and growth plate development', *Nature Genetics*, 24(3), pp. 271-274.
- DeRuiter, M.C., Poelmann, R.E., Van Der Plas-De Vries, I., Mentink, M.M.T. and Gittenberger-De Groot, A.C. (1992) 'The development of the myocardium and endocardium in mouse embryos. Fusion of two heart tubes?', *Anatomy and Embryology*, 185(5), pp. 461-473.
- Di Felice, V. and Zummo, G. (2009) 'Tetralogy of Fallot as a Model to Study Cardiac Progenitor Cell Migration and Differentiation During Heart Development', *Trends in Cardiovascular Medicine*, 19(4), pp. 130-135.
- Djiane, A., Yogev, S. and Mlodzik, M. (2005) 'The apical determinants aPKC and dPatj regulate frizzled-dependent planar cell polarity in the Drosophila eye', *Cell*, 121(4), pp. 621-631.
- Dodou, E., Verzi, M.P., Anderson, J.P., Xu, S.M. and Black, B.L. (2004) 'Mef2c is a direct transcriptional target of ISL1 and GATA factors in the anterior heart field during mouse embryonic development', *Development*, 131(16), pp. 3931-3942.
- Doudney, K., Moore, G.E., Stanier, P., Ybot-Gonzalez, P., Paternotte, C., Greene, N.D.E., Copp, A.J. and Stevenson, R.E. (2005) 'Analysis of the planar cell polarity gene Vangl2 and its co-expressed paralogue Vangl1 in neural tube defect patients [2]', *American Journal of Medical Genetics*, 136 A(1), pp. 90-92.
- Dyer, L.A. and Kirby, M.L. (2009) 'Sonic hedgehog maintains proliferation in secondary heart field progenitors and is required for normal arterial pole formation', *Developmental Biology*, 330(2), pp. 305-317.

- Dyer, L.A., Makadia, F.A., Scott, A., Pegram, K., Hutson, M.R. and Kirby, M.L. (2010) 'BMP signaling modulates hedgehog-induced secondary heart field proliferation', *Developmental Biology*, 348(2), pp. 167-176.
- Epstein, J.A. (1996) 'Pax3, neural crest and cardiovascular development', *Trends in Cardiovascular Medicine*, 6(8), pp. 255-261.
- Epstein, J.A., Li, J., Lang, D., Chen, F., Brown, C.B., Jin, F., Lu, M.M., Thomas, M., Liu, E.C.J., Wessels, A. and Lo, C.W. (2000) 'Migration of cardiac neural crest cells in Splotch embryos', *Development*, 127(9), pp. 1869-1878.
- Etheridge, S.L., Ray, S., Li, S., Hamblet, N.S., Lijam, N., Tsang, M., Greer, J., Kardos, N., Wang, J., Sussman, D.J., Chen, P. and Wynshaw-Boris, A. (2008) 'Murine dishevelled 3 functions in redundant pathways with dishevelled 1 and 2 in normal cardiac outflow tract, cochlea, and neural tube development', *PLoS Genetics*, 4(11).
- Etienne-Manneville, S. (2012) 'Adherens junctions during cell migration', *Sub-cellular biochemistry*, 60, pp. 225-249.
- Evans, S.M., Yelon, D., Conlon, F.L. and Kirby, M.L. (2010) 'Myocardial lineage development', *Circulation Research*, 107(12), pp. 1428-1444.
- Fanto, M. and McNeill, H. (2004) 'Planar polarity from flies to vertebrates', *Journal of Cell Science*, 117(4), pp. 527-533.
- Fedeles, S. and Gallagher, A.R. (2013) 'Cell polarity and cystic kidney disease', *Pediatric Nephrology*, 28(8), pp. 1161-1172.
- Fiedler, L.R. (2009) 'Rac1 regulates cardiovascular development and postnatal function of endothelium', *Cell Adhesion and Migration*, 3(2), pp. 143-145.
- Formstone, C.J. and Little, P.F.R. (2001) 'The flamingo-related mouse Celsr family (Celsr1-3) genes exhibit distinct patterns of expression during embryonic development', *Mechanisms of Development*, 109(1), pp. 91-94.
- Francou, A., Saint-Michel, E., Mesbah, K., Théveniau-Ruissy, M., Rana, M.S., Christoffels, V.M. and Kelly, R.G. (2013) 'Second heart field cardiac progenitor cells in the early mouse embryo', *Biochimica et Biophysica Acta - Molecular Cell Research*, 1833(4), pp. 795-798.
- Frank, D.U., Fotheringham, L.K., Brewer, J.A., Muglia, L.J., Tristani-Firouzi, M., Capecchi, M.R. and Moon, A.M. (2002) 'An Fgf8 mouse mutant phenocopies human 22q11 deletion syndrome', *Development*, 129(19), pp. 4591-4603.
- Franz, T. (1989) 'Persistent truncus arteriosus in the Splotch mutant mouse', *Anatomy and Embryology*, 180(5), pp. 457-464.
- Franz, T. and Kothary, R. (1993) 'Characterization of the neural crest defect in Splotch (Sp1H) mutant mice using a lacZ transgene', *Developmental Brain Research*, 72(1), pp. 99-105.
- Fulcoli, F.G., Huynh, T., Scambler, P.J. and Baldini, A. (2009) 'Tbx1 regulates the BMP-smad1 pathway in a transcription independent manner', *PLoS ONE*, 4(6).
- Galli, D., Domínguez, J.N., Zaffran, S., Munk, A., Brown, N.A. and Buckingham, M.E. (2008) 'Atrial myocardium derives from the posterior

region of the second heart field, which acquires left-right identity as Pitx2c is expressed', *Development*, 135(6), pp. 1157-1167.

- Gao, B., Song, H., Bishop, K., Elliot, G., Garrett, L., English, M.A., Andre, P., Robinson, J., Sood, R., Minami, Y., Economides, A.N. and Yang, Y. (2011) 'Wnt Signaling Gradients Establish Planar Cell Polarity by Inducing Vangl2 Phosphorylation through Ror2', *Developmental Cell*, 20(2), pp. 163-176.
- Garg, V., Muth, A.N., Ransom, J.F., Schluterman, M.K., Barnes, R., King, I.N., Grossfeld, P.D. and Srivastava, D. (2005) 'Mutations in NOTCH1 cause aortic valve disease', *Nature*, 437(7056), pp. 270-274.
- Garg, V., Yamagishi, C., Hu, T., Kathiriya, I.S., Yamagishi, H. and Srivastava, D. (2001) 'Tbx1, a DiGeorge syndrome candidate gene, is regulated by sonic hedgehog during pharyngeal arch development', *Developmental Biology*, 235(1), pp. 62-73.
- Gessert, S. and Kühl, M. (2010) 'The multiple phases and faces of Wnt signaling during cardiac differentiation and development', *Circulation Research*, 107(2), pp. 186-199.
- Gilbert, S. (2000) 'The Neural Crest', in *Developmental Biology*. 6th edn. Sunderland (MA): Sinauer Associates.
- Goddeeris, M.M., Schwartz, R., Klingensmith, J. and Meyers, E.N. (2007) 'Independent requirements for hedgehog signaling by both the anterior heart field and neural crest cells for outflow tract development', *Development*, 134(8), pp. 1593-1604.
- Goldmann, W.H. and Ingber, D.E. (2002) 'Intact vinculin protein is required for control of cell shape, cell mechanics, and rac-dependent lamellipodia formation', *Biochemical and Biophysical Research Communications*, 290(2), pp. 749-755.
- Goodrich, L.V. and Strutt, D. (2011) 'Principles of planar polarity in animal development', *Development*, 138(10), pp. 1877-1892.
- Gordon, M.D. and Nusse, R. (2006) 'Wnt signaling: Multiple pathways, multiple receptors, and multiple transcription factors', *Journal of Biological Chemistry*, 281(32), pp. 22429-22433.
- Goulding, M., Sterrer, S., Fleming, J., Balling, R., Nadeau, J., Moore, K.J., Brown, S.D.M., Steel, K.P. and Gruss, P. (1993) 'Analysis of the Pax-3 gene in the mouse mutant splotch', *Genomics*, 17(2), pp. 355-363.
- Gruber, P.J., Stevens, K.N., Hakonarson, H., Kim, C.E., Doevendans, P.A., Koeleman, B.P.C., Mital, S., Raue, J., Glessner, J.T., Coles, J.G., Moreno, V., Granger, A. and Gruber, S.B. (2010) 'Common Variation in ISL1Confers Genetic Susceptibility for Human Congenital Heart Disease', *PLoS ONE*, 5(5).
- Guillot, C. and Lecuit, T. (2013) 'Mechanics of epithelial tissue homeostasis and morphogenesis', *Science*, 340(6137), pp. 1185-1189.
- Guo, C., Sun, Y., Zhou, B., Adam, R.M., Li, X., Pu, W.T., Morrow, B.E. and Moon, A. (2011) 'A Tbx1-Six1/Eya1-Fgf8 genetic pathway controls mammalian cardiovascular and craniofacial morphogenesis', *Journal of Clinical Investigation*, 121(4), pp. 1585-1595.

- Guo, N., Hawkins, C. and Nathans, J. (2004) 'Frizzled6 controls hair patterning in mice', *Proceedings of the National Academy of Sciences of the United States of America*, 101(25), pp. 9277-9281.
- Guyot, M.C., Bosoi, C.M., Kharfallah, F., Reynolds, A., Drapeau, P., Justice, M., Gros, P. and Kibar, Z. (2011) 'A novel hypomorphic Looptail allele at the planar cell polarity Vangl2 gene', *Developmental Dynamics*, 240(4), pp. 839-849.
- Habas, R. and Dawid, I.B. (2005) 'Dishevelled and Wnt signaling: Is the nucleus the final frontier?', *Journal of Biology*, 4(1).
- Habas, R., Dawid, I.B. and He, X. (2003) 'Coactivation of Rac and Rho by Wnt/Frizzled signaling is required for vertebrate gastrulation', *Genes and Development*, 17(2), pp. 295-309.
- Habas, R. and He, X. 406 (2006) 'Activation of Rho and Rac by Wnt/Frizzled signaling'. pp. 500-511. Available at: http://www.scopus.com/inward/record.url?eid=2-s2.0-32144436083&partnerID=40&md5=301ba0fa062c6c9bf0302a6dd782aa5d.
- Habas, R., Kato, Y. and He, X. (2001) 'Wnt/Frizzled activation of Rho regulates vertebrate gastrulation and requires a novel formin homology protein Daam1', *Cell*, 107(7), pp. 843-854.
- Hamblet, N.S., Lijam, N., Ruiz-Lozano, P., Wang, J., Yang, Y., Luo, Z., Mei, L., Chien, K.R., Sussman, D.J. and Wynshaw-Boris, A. (2002) 'Dishevelled 2 is essential for cardiac outflow tract development, somite segmentation and neural tube closure', *Development*, 129(24), pp. 5827-5838.
- Hartsock, A. and Nelson, W.J. (2008) 'Adherens and tight junctions: Structure, function and connections to the actin cytoskeleton', *Biochimica et Biophysica Acta - Biomembranes*, 1778(3), pp. 660-669.
- Hayashi, S., Lewis, P., Pevny, L. and McMahon, A.P. (2002) 'Efficient gene modulation in mouse epiblast using a Sox2Cre transgenic mouse strain', *Gene Expression Patterns*, 2(1-2), pp. 93-97.
- He, X., Semenov, M., Tamai, K. and Zeng, X. (2004) 'LDL receptor-related proteins 5 and 6 in Wnt/β-catenin signaling: Arrows point the way', *Development*, 131(8), pp. 1663-1677.
- Heisenberg, C.P., Tada, M., Rauch, G.J., Saúde, L., Concha, M.L., Geisler, R., Stemple, D.L., Smith, J.C. and Wilson, S.W. (2000) 'Silberblick/Wnt11 mediates convergent extension movements during zebrafish gastrulation', *Nature*, 405(6782), pp. 76-81.
- Henderson, D.J. and Chaudhry, B. (2011) 'Getting to the heart of planar cell polarity signaling', *Birth Defects Research Part A - Clinical and Molecular Teratology*, 91(6), pp. 460-467.
- Henderson, D.J., Conway, S.J., Greene, N.D.E., Gerrelli, D., Murdoch, J.N., Anderson, R.H. and Copp, A.J. (2001) 'Cardiovascular defects associated with abnormalities in midline development in the Loop-tail mouse mutant', *Circulation Research*, 89(1), pp. 6-12.
- Henderson, D.J., Phillips, H.M. and Chaudhry, B. (2006) 'Vang-like 2 and noncanonical Wnt signaling in outflow tract development', *Trends in Cardiovascular Medicine*, 16(2), pp. 38-45.

- Henrich, V.C., Vogtli, M.E., Antoniewski, C., Spindler-Barth, M., Przibilla, S., Noureddine, M. and Lezzi, M. (2000) 'Widespread recombinase expression using FLPeR (flipper) mice', *Genesis*, 28(3-4), pp. 106-110.
- High, F.A., Jain, R., Stoller, J.Z., Antonucci, N.B., Min, M.L., Loomes, K.M., Kaestner, K.H., Pear, W.S. and Epstein, J.A. (2009) 'Murine Jagged1/Notch signaling in the second heart field orchestrates Fgf8 expression and tissue-tissue interactions during outflow tract development', *Journal of Clinical Investigation*, 119(7), pp. 1986-1996.
- Hildreth, V., Webb, S., Chaudhry, B., Peat, J.D., Phillips, H.M., Brown, N., Anderson, R.H. and Henderson, D.J. (2009) 'Left cardiac isomerism in the Sonic hedgehog null mouse', *Journal of Anatomy*, 214(6), pp. 894-904.
- Hiruma, T. and Nakajima, Y. (2002) 'Development of pharyngeal arch arteries in early mouse embryo', *Journal of Anatomy*, 201(1), pp. 15-29.
- Hu, T., Yamagishi, H., Maeda, J., McAnally, J., Yamagishi, C. and Srivastava, D. (2004) 'Tbx1 regulates fibroblast growth factors in the anterior heart field through reinforcing autoregulatory loop involving forkhead transcription factors', *Development*, 131(21), pp. 5491-5502.
- Huang, G.Y., Cooper, E.S., Waldo, K., Kirby, M.L., Gilula, N.B. and Lo, C.W. (1998) 'Gap junction-mediated cell-cell communication modulates mouse neural crest migration', *Journal of Cell Biology*, 143(6), pp. 1725-1734.
- Huang, X. and Saint-Jeannet, J.P. (2004) 'Induction of the neural crest and the opportunities of life on the edge', *Developmental Biology*, 275(1), pp. 1-11.
- Huh, S.H. and Ornitz, D.M. (2010) 'β-Catenin deficiency causes DiGeorge syndrome-like phenotypes through regulation of Tbx1', *Development*, 137(7), pp. 1137-1147.
- Hutson, M.R. and Kirby, M.L. (2003) 'Neural crest and cardiovascular development: A 20-year perspective', *Birth Defects Research Part C - Embryo Today: Reviews*, 69(1), pp. 2-13.
- Hutson, M.R. and Kirby, M.L. (2007) 'Model systems for the study of heart development and disease. Cardiac neural crest and conotruncal malformations', *Seminars in Cell and Developmental Biology*, 18(1), pp. 101-110.
- Hutson, M.R., Zhang, P., Stadt, H.A., Sato, A.K., Li, Y.X., Burch, J., Creazzo, T.L. and Kirby, M.L. (2006) 'Cardiac arterial pole alignment is sensitive to FGF8 signaling in the pharynx', *Developmental Biology*, 295(2), pp. 486-497.
- Huynh, T., Chen, L., Terrell, P. and Baldini, A. (2007) 'A fate map of Tbx1 expressing cells reveals heterogeneity in the second cardiac field', *Genesis*, 45(7), pp. 470-475.
- Ilagan, R., Abu-Issa, R., Brown, D., Yang, Y.P., Jiao, K., Schwartz, R.J., Klingensmith, J. and Meyers, E.N. (2006) 'Fgf8 is required for anterior heart field development', *Development*, 133(12), pp. 2435-2445.
- Inoki, K., Ouyang, H., Zhu, T., Lindvall, C., Wang, Y., Zhang, X., Yang, Q., Bennett, C., Harada, Y., Stankunas, K., Wang, C.y., He, X., MacDougald, O.A., You, M., Williams, B.O. and Guan, K.L. (2006)

'TSC2 Integrates Wnt and Energy Signals via a Coordinated Phosphorylation by AMPK and GSK3 to Regulate Cell Growth', *Cell*, 126(5), pp. 955-968.

- Jacks, T., Shih, T.S., Schmitt, E.M., Bronson, R.T., Bernards, A. and Weinberg, R.A. (1994) 'Tumour predisposition in mice heterozygous for a targeted mutation in Nf1', *Nature Genetics*, 7(3), pp. 353-361.
- James Nelson, W. 75 (2008) 'Regulation of cell-cell adhesion by the cadherin-catenin complex'. pp. 149-155. Available at: http://www.scopus.com/inward/record.url?eid=2-s2.0-84870311943&partnerID=40&md5=46074d9a637d60c22474cbc15f76d169.
- Jenkins, K.J., Correa, A., Feinstein, J.A., Botto, L., Britt, A.E., Daniels, S.R., Elixson, M., Warnes, C.A. and Webb, C.L. (2007) 'Noninherited risk factors and congenital cardiovascular defects: Current knowledge - A scientific statement from the American Heart Association Council on Cardiovascular Disease in the Young', *Circulation*, 115(23), pp. 2995-3014.
- Jerome, L.A. and Papaioannou, V.E. (2001) 'DiGeorge syndrome phenotype in mice mutant for the T-box gene, Tbx1', *Nature Genetics*, 27(3), pp. 286-291.
- Jessen, J.R. and Solnica-Krezel, L. (2004) 'Identification and developmental expression pattern of van gogh-like 1, a second zebrafish strabismus homologue', *Gene Expression Patterns*, 4(3), pp. 339-344.
- Jessen, J.R., Topczewski, J., Bingham, S., Sepich, D.S., Marlow, F., Chandrasekhar, A. and Solnica-Krezel, L. (2002) 'Zebrafish trilobite identifies new roles for Strabismus in gastrulation and neuronal movements', *Nature Cell Biology*, 4(8), pp. 610-615.
- Jiang, X., Rowitch, D.H., Soriano, P., McMahon, A.P. and Sucov, H.M. (2000) 'Fate of the mammalian cardiac neural crest', *Development*, 127(8), pp. 1607-1616.
- Joberty, G., Petersen, C., Gao, L. and Macara, I.G. (2000) 'The cell-polarity protein Par6 links Par3 and atypical protein kinase C to Cdc42', *Nature Cell Biology*, 2(8), pp. 531-539.
- Kagan, H.M. and Trackman, P.C. (1991) 'Properties and function of lysyl oxidase', *American journal of respiratory cell and molecular biology*, 5(3), pp. 206-210.
- Kaldis, P. and Pagano, M. (2009) 'Wnt Signaling in Mitosis', *Developmental Cell*, 17(6), pp. 749-750.
- Kallay, L.M., McNickle, A., Brennwald, P.J., Hubbard, A.L. and Braiterman, L.T. (2006) 'Scribble associates with two polarity proteins, Lgl2 and Vangl2, via distinct molecular domains', *Journal of Cellular Biochemistry*, 99(2), pp. 647-664.
- Kang, J., Nathan, E., Xu, S.M., Tzahor, E. and Black, B.L. (2009) 'Isl1 is a direct transcriptional target of Forkhead transcription factors in second heart field-derived mesoderm', *Developmental Biology*, 334(2), pp. 513-522.

- Kaplan, N.A., Liu, X. and Tolwinski, N.S. (2009) 'Epithelial polarity: Interactions between junctions and apical-basal machinery', *Genetics*, 183(3), pp. 897-904.
- Karnik, S.K., Brooke, B.S., Bayes-Genis, A., Sorensen, L., Wythe, J.D., Schwartz, R.S., Keating, M.T. and Li, D.Y. (2003) 'A critical role for elastin signaling in vascular morphogenesis and disease', *Development*, 130(2), pp. 411-423.
- Katoh, M. (2002) 'Strabismus (STB)/Vang-like (VANGL) gene family (Review)', *International journal of molecular medicine*, 10(1), pp. 11-15.
- Katoh, M. (2005) 'WNT/PCP signaling pathway and human cancer (Review)', *Oncology Reports*, 14(6), pp. 1583-1588.
- Keenan, I.D., Rhee, H.J., Chaudhry, B. and Henderson, D.J. (2012) 'Origin of non-cardiac endothelial cells from an Isl1+ lineage', *FEBS Letters*, 586(13), pp. 1790-1794.
- Keller, R. (2002) 'Shaping the vertebrate body plan by polarized embryonic cell movements', *Science*, 298(5600), pp. 1950-1954.
- Keller, R., Davidson, L.A. and Shook, D.R. (2003) 'How we are shaped: The biomechanics of gastrulation', *Differentiation*, 71(3), pp. 171-205.
- Kelly, R.G. 100 (2012) 'The Second Heart Field'. pp. 33-65. Available at: http://www.scopus.com/inward/record.url?eid=2-s2.0-84858782974&partnerID=40&md5=1a01dcb9982838cb51658ff5e3dad06b.
- Kelly, R.G., Brown, N.A. and Buckingham, M.E. (2001) 'The Arterial Pole of the Mouse Heart Forms from Fgf10-Expressing Cells in Pharyngeal Mesoderm', *Developmental Cell*, 1(3), pp. 435-440.
- Kelly, R.G. and Buckingham, M.E. (2002) 'The anterior heart-forming field: Voyage to the arterial pole of the heart', *Trends in Genetics*, 18(4), pp. 210-216.
- Kibar, Z., Vogan, K.J., Groulx, N., Justice, M.J., Underhill, D.A. and Gros, P. (2001) 'Ltap, a mammalian homolog of Drosophila Strabismus/Van Gogh, is altered in the mouse neural tube mutant Loop-tail', *Nature Genetics*, 28(3), pp. 251-255.
- Kirby, M.L. (1987) 'Cardiac morphogenesis - Recent research advances', *Pediatric Research*, 21(3), pp. 219-224.
- Kirby, M.L. (2007) *Cardiac Development*. Oxford University Press.
- Kirby, M.L. and Creazzo, T.L. (1995) 'Cardiovascular development. Neural crest and new perspectives', *Cardiology in Review*, 3(4), pp. 226-235.
- Kirby, M.L., Gale, T.F. and Stewart, D.E. (1983) 'Neural crest cells contribute to normal aorticopulmonary septation', *Science*, 220(4601), pp. 1059-1061.
- Kirby, M.L. and Hutson, M.R. (2010) 'Factors controlling cardiac neural crest cell migration', *Cell Adhesion and Migration*, 4(4), pp. 609-621.
- Kirby, M.L. and Waldo, K.L. (1990) 'Role of neural crest in congenital heart disease', *Circulation*, 82(2), pp. 332-340.
- Kirby, M.L. and Waldo, K.L. (1995) 'Neural crest and cardiovascular patterning', *Circulation Research*, 77(2), pp. 211-215.

- Kisanuki, Y.Y., Hammer, R.E., Miyazaki, J.I., Williams, S.C., Richardson, J.A. and Yanagisawa, M. (2001) 'Tie2-Cre transgenic mice: A new model for endothelial cell-lineage analysis in vivo', *Developmental Biology*, 230(2), pp. 230-242.
- Kist, R., Greally, E. and Peters, H. (2007) 'Derivation of a mouse model for conditional inactivation of Pax9', *Genesis*, 45(7), pp. 460-464.
- Klaus, A. and Birchmeier, W. (2008) 'Wnt signalling and its impact on development and cancer', *Nature Reviews Cancer*, 8(5), pp. 387-398.
- Klaus, A., Müller, M., Schulz, H., Saga, Y., Martin, J.F. and Birchmeier, W. (2012) 'Wnt/β-catenin and Bmp signals control distinct sets of transcription factors in cardiac progenitor cells', *Proceedings of the National Academy of Sciences of the United States of America*, 109(27), pp. 10921-10926.
- Klein, T.J., Jenny, A., Djiane, A. and Mlodzik, M. (2006) 'CKIε/discs overgrown Promotes Both Wnt-Fz/β-Catenin and Fz/PCP Signaling in Drosophila', *Current Biology*, 16(13), pp. 1337-1343.
- Klein, T.J. and Mlodzik, M. 21 (2005) 'Planar cell polarization: An emerging model points in the right direction'. pp. 155-176. Available at: http://www.scopus.com/inward/record.url?eid=2-s2.0-27744538492&partnerID=40&md5=d392f66a8bf017e126e27773e0b88456.
- Kobayashi, K., Takahashi, M., Matsushita, N., Miyazaki, J.I., Koike, M., Yaginuma, H., Osumi, N. and Kaibuchi, K. (2004) 'Survival of Developing Motor Neurons Mediated by Rho GTPase Signaling Pathway through Rho-Kinase', *Journal of Neuroscience*, 24(14), pp. 3480-3488.
- Komiya, Y. and Habas, R. (2008) 'Wnt signal transduction pathways', *Organogenesis*, 4(2), pp. 68-75.
- Kramer, K.L. and Yost, H.J. 67 (2002) 'Cardiac left-right development: Are the early steps conserved?'. pp. 37-43. Available at: http://www.scopus.com/inward/record.url?eid=2-s2.0-0038463781&partnerID=40&md5=a92b95498cd41b4ee3c506ab8139327d.
- Kruithof, B.P.T., Van den Hoff, M.J.B., Wessels, A. and Moorman, A.F.M. (2003) 'Cardiac muscle cell formation after development of the linear heart tube', *Developmental Dynamics*, 227(1), pp. 1-13.
- Kupfer, A., Dennert, G. and Singer, S.J. (1983) 'Polarization of the Golgi apparatus and the microtubule-organizing center within cloned natural killer cells bound to their targets', *Proceedings of the National Academy of Sciences of the United States of America*, 80(23 I), pp. 7224-7228.
- Kupfer, A., Louvard, D. and Singer, S.J. (1982) 'Polarization of the Golgi apparatus and the microtubule-organizing center in cultured fibroblasts at the edge of an experimental wound', *Proceedings of the National Academy of Sciences of the United States of America*, 79(8 I), pp. 2603-2607.
- Kuratani, S.C. and Kirby, M.L. (1991) 'Initial migration and distribution of the cardiac neural crest in the avian embryo: An introduction to the concept of the circumpharyngeal crest', *American Journal of Anatomy*, 191(3), pp. 215-227.

- Kuratani, S.C. and Kirby, M.L. (1992) 'Migration and distribution of circumpharyngeal crest cells in the chick embryo: Formation of the circumpharyngeal ridge and E/C8+ crest cells in the vertebrate head region', *Anatomical Record*, 234(2), pp. 263-280.
- Kurihara, Y., Kurihara, H., Oda, H., Maemura, K., Nagai, R., Ishikawa, T. and Yazaki, Y. (1995) 'Aortic arch malformations and ventricular septal defect in mice deficient in endothelin-1', *Journal of Clinical Investigation*, 96(1), pp. 293-300.
- Kwang, S.J., Brugger, S.M., Lazik, A., Merrill, A.E., Wu, L.Y., Liu, Y.H., Ishii, M., Sangiorgi, F.O., Rauchman, M., Sucov, H.M., Maas, R.L. and Maxson Jr, R.E. (2002) 'Msx2 is an immediate downstream effector of Pax3 in the development of the murine cardiac neural crest', *Development*, 129(2), pp. 527-538.
- Kwon, C., Qian, L., Cheng, P., Nigam, V., Arnold, J. and Srivastava, D. (2009) 'A regulatory pathway involving Notch1/β-catenin/Isl1 determines cardiac progenitor cell fate', *Nature Cell Biology*, 11(8), pp. 951-957.
- Lallemand, Y., Luria, V., Haffner-Krausz, R. and Lonai, P. (1998) 'Maternally expressed PGK-Cre transgene as a tool for early and uniform activation of the Cre site-specific recombinase', *Transgenic Research*, 7(2), pp. 105-112.
- Laugwitz, K.L., Moretti, A., Lam, J., Gruber, P., Chen, Y., Woodard, S., Lin, L.Z., Cai, C.L., Lu, M.M., Reth, M., Platoshyn, O., Yuan, J.X.J., Evans, S. and Chien, K.B. (2005) 'Postnatal isl1+ cardioblasts enter fully differentiated cardiomyocyte lineages', *Nature*, 433(7026), pp. 647-653.
- Lawrence, P.A. and Shelton, P.M.J. (1975) 'The determination of polarity in the developing insect retina', *Journal of Embryology and Experimental Morphology*, 33(2), pp. 471-486.
- Le Douarin, N.M. (1982) *The Neural Crest*. New York: Cambridge University Press.
- Le Lievre, C.S. and Le Douarin, N.M. (1975) 'Mesenchymal derivatives of the neural crest: analysis of chimaeric quail and chick embryos', *Journal of Embryology and Experimental Morphology*, 34(1), pp. 125-154.
- Leatherbury, L. and Kirby, M.L. (1996) 'Cardiac development and perinatal care of infants with neural crest- associated conotruncal defects', *Seminars in Perinatology*, 20(6), pp. 473-481.
- Lee, M.J., Brennan, A., Blanchard, A., Zoidl, G., Dong, Z., Tabernero, A., Zoidl, C., Dent, M.A.R., Jessen, K.R. and Mirsky, R. (1996) 'P0 is constitutively expressed in the rat neural crest and embryonic nerves and is negatively and positively regulated by axons to generate non- myelin-forming and myelin-forming Schwann cells, respectively', *Molecular and Cellular Neurosciences*, 8(5), pp. 336-350.
- Lefort, C.T., Wojciechowski, K. and Hocking, D.C. (2011) 'N-cadherin cell-cell adhesion complexes are regulated by fibronectin matrix assembly', *Journal of Biological Chemistry*, 286(4), pp. 3149-3160.
- Lewis, A.E., Vasudevan, H.N., O'Neill, A.K., Soriano, P. and Bush, J.O. (2013) 'The widely used Wnt1-Cre transgene causes developmental phenotypes by ectopic activation of Wnt signaling', *Developmental Biology*, 379(2), pp. 229-234.

- Li, C., Xiao, J., Hormi, K., Borok, Z. and Minoo, P. (2002) 'Wnt5a participates in distal lung morphogenesis', *Developmental Biology*, 248(1), pp. 68-81.
- Li, L., Yuan, H., Xie, W., Mao, J., Caruso, A.M., McMahon, A., Sussman, D.J. and Wu, D. (1999) 'Dishevelled proteins lead to two signaling pathways: Regulation of LEF- 1 and c-Jun N-terminal kinase in mammalian cells', *Journal of Biological Chemistry*, 274(1), pp. 129-134.
- Li, P., Pashmforoush, M. and Sucov, H.M. (2010) 'Retinoic acid regulates differentiation of the secondary heart field and TGFbeta-mediated outflow tract septation', *Developmental Cell*, 18(3), pp. 480-485.
- Lieschke, G.J. and Currie, P.D. (2007) 'Animal models of human disease: Zebrafish swim into view', *Nature Reviews Genetics*, 8(5), pp. 353-367.
- Lin, D., Edwards, A.S., Fawcett, J.P., Mbamalu, G., Scott, J.D. and Pawson, T. (2000) 'A mammalian PAR-3-PAR-6 complex implicated in Cdc42/Rac1 and aPKC signalling and cell polarity', *Nature Cell Biology*, 2(8), pp. 540-547.
- Lin, L., Cui, L., Zhou, W., Dufort, D., Zhang, X., Cai, C.L., Bu, L., Yang, L., Martin, J., Kemler, R., Rosenfeld, M.G., Chen, J. and Evans, S.M. (2007) 'β-Catenin directly regulates Islet1 expression in cardiovascular progenitors and is required for multiple aspects of cardiogenesis', *Proceedings of the National Academy of Sciences of the United States of America*, 104(22), pp. 9313-9318.
- Lin, Q., Lu, J., Yanagisawa, H., Webb, R., Lyons, G.E., Richardson, J.A. and Olson, E.N. (1998) 'Requirement of the MADS-box transcription factor MEF2C for vascular development', *Development*, 125(22), pp. 4565-4574.
- Lin, Q., Schwarz, J., Bucana, C. and Olson, E.N. (1997) 'Control of mouse cardiac morphogenesis and myogenesis by transcription factor MEF2C', *Science*, 276(5317), pp. 1404-1407.
- Lindqvist, M., Horn, Z., Bryja, V., Schulte, G., Papachristou, P., Ajima, R., Dyberg, C., Arenas, E., Yamaguchi, T.P., Lagercrantz, H. and Ringstedt, T. (2010) 'Vang-like protein 2 and Rac1 interact to regulate adherens junctions', *Journal of Cell Science*, 123(3), pp. 472-483.
- Lindsay, E.A., Vitelli, F., Su, H., Morishima, M., Huynh, T., Pramparo, T., Jurecic, V., Ogunrinu, G., Sutherland, H.F., Scambler, P.J., Bradley, A. and Baldini, A. (2001) 'Tbx1 haploinsufficiency in the DiGeorge syndrome region causes aortic arch defects in mice', *Nature*, 410(6824), pp. 97-101.
- Little, C.C. (1937) 'US science wars against an unknown enemy: cancer', *Life*, 2, pp. 11–17
- Liu, X., Zhao, Y., Gao, J., Pawlyk, B., Starcher, B., Spencer, J.A., Yanagisawa, H., Zuo, J. and Li, T. (2004) 'Elastic fiber homeostasis requires lysyl oxidase-like 1 protein', *Nature Genetics*, 36(2), pp. 178-182.
- Lo, C.W., Cohen, M. F., Huang, G.-Y., Lazatin, B. O., Patel, N., Sullivan, R., Pauken, C. and Park, S.M.J. (1997) 'Cx43 gap junction gene expression and gap junctional communication in mouse neural crest cells', *Dev. Genet.*, 20(2), pp. 119–132.

- Lo, C.W., Waldo, K.L. and Kirby, M.L. (1999) 'Gap junction communication and the modulation of cardiac neural crest cells', *Trends in Cardiovascular Medicine*, 9(3-4), pp. 63-69.
- Logan, C.Y. and Nusse, R. 20 (2004) 'The Wnt signaling pathway in development and disease'. pp. 781-810. Available at: http://www.scopus.com/inward/record.url?eid=2-s2.0-8444251784&partnerID=40&md5=bcb1d384ff231fe98a8a28845963a67c.
- Loirand, G., Guérin, P. and Pacaud, P. (2006) 'Rho kinases in cardiovascular physiology and pathophysiology', *Circulation Research*, 98(3), pp. 322-334.
- Lu, W., Yamamoto, V., Ortega, B. and Baltimore, D. (2004a) 'Mammalian Ryk is a Wnt coreceptor required for stimulation of neurite outgrowth', *Cell*, 119(1), pp. 97-108.
- Lu, X., Borchers, A.G.M., Jolicoeur, C., Rayburn, H., Baker, J.C. and Tessier-Lavigne, M. (2004b) 'PTK7/CCK-4 is a novel regulator of planar cell polarity in vertebrates', *Nature*, 430(6995), pp. 93-98.
- Maeda, J., Yamagishi, H., McAnally, J., Yamagishi, C. and Srivastava, D. (2006) 'Tbx1 is regulated by forkhead proteins in the secondary heart field', *Developmental Dynamics*, 235(3), pp. 701-710.
- Magdalena, J., Millard, T.H. and Machesky, L.M. (2003) 'Microtubule involvement in NIH 3T3 Golgi and MTOC polarity establishment', *Journal of Cell Science*, 116(4), pp. 743-756.
- Majumdar, A., Vainio, S., Kispert, A., McMahon, J. and McMahon, A.P. (2003) 'Wnt11 and Ret/Gdnf pathways cooperate in regulating ureteric branching during metanephric kidney development', *Development*, 130(14), pp. 3175-3185.
- Manner, J., Seidl, W. and Steding, G. (1993) 'Correlation between the embryonic head flexures and cardiac development. An experimental study in chick embryos', *Anatomy and Embryology*, 188(3), pp. 269-285.
- Marino, T.A. (2005) *Development of the Cardiovascular System*. Available at: http://isc.temple.edu/marino/embryo/cardiohand.htm.
- Marlow, F., Topczewski, J., Sepich, D. and Solnica-Krezel, L. (2002) 'Zebrafish Rho kinase 2 acts downstream of Wnt11 to mediate cell polarity and effective convergence and extension movements', *Current Biology*, 12(11), pp. 876-884.
- Matakatsu, H. and Blair, S.S. (2004) 'Interactions between Fat and Dachsous and the regulation of planar cell polarity in the Drosophila wing', *Development*, 131(15), pp. 3785-3794.
- Matthews, H.K., Marchant, L., Carmona-Fontaine, C., Kuriyama, S., Larraín, J., Holt, M.R., Parsons, M. and Mayor, R. (2008) 'Directional migration of neural crest cells in vivo is regulated by Syndecan-4/Rac1 and non-canonical Wnt signaling/RhoA', *Development*, 135(10), pp. 1771-1780.
- Mayor, R. and Theveneau, E. (2014) 'The role of the non-canonical Wnt-planar cell polarity pathway in neural crest migration', *Biochemical Journal*, 457(1), pp. 19-26.
- McBurney, M.W., Staines, W.A., Boekelheide, K., Parry, D., Jardine, K. and Pickavance, L. (1994) 'Murine Pgk-1 promoter drives widespread but

not uniform expression in transgenic mice', *Developmental Dynamics*, 200(4), pp. 278-293.

- Melloy, P.G., Ewart, J.L., Cohen, M.F., Desmond, M.E., Kuehn, M.R. and Lo, C.W. (1998) 'No turning, a mouse mutation causing left-right and axial patterning defects', *Developmental Biology*, 193(1), pp. 77-89.
- Mesbah, K., Rana, M.S., Francou, A., van duijvenboden, K., Papaioannou, V.E., Moorman, A.F., Kelly, R.G. and Christoffels, V.M. (2012) 'Identification of a Tbx1/Tbx2/Tbx3 genetic pathway governing pharyngeal and arterial pole morphogenesis', *Human Molecular Genetics*, 21(6), pp. 1217-1229.
- Meyers, E.N., Lewandoski, M. and Martin, G.R. (1998) 'An Fgf8 mutant allelic series generated by Cre-and Flp-mediated recombination', *Nature Genetics*, 18(2), pp. 136-141.
- Miquerol, L. and Kelly, R.G. (2013) 'Organogenesis of the vertebrate heart', *Wiley Interdisciplinary Reviews: Developmental Biology*, 2(1), pp. 17-29.
- Mjaatvedt, C.H., Nakaoka, T., Moreno-Rodriguez, R., Norris, R.A., Kern, M.J., Eisenberg, C.A., Turner, D. and Markwald, R.R. (2001) 'The outflow tract of the heart is recruited from a novel heart-forming field', *Developmental Biology*, 238(1), pp. 97-109.
- Mlodzik, M. (1999) 'Planar polarity in the Drosophila eye: A multifaceted view of signaling specificity and cross-talk', *EMBO Journal*, 18(24), pp. 6873-6879.
- Mlodzik, M. (2002) 'Planar cell polarization: Do the same mechanisms regulate Drosophila tissue polarity and vertebrate gastrulation?', *Trends in Genetics*, 18(11), pp. 564-571.
- Montcouquiol, M., Rachel, R.A., Lanford, P.J., Copeland, N.G., Jenkins, N.A. and Kelley, M.W. (2003) 'Identification of Vangl2 and Scrb1 as planar polarity genes in mammals', *Nature*, 423(6936), pp. 173-177.
- Montcouquiol, M., Sans, N., Huss, D., Kach, J., David Dickman, J., Forge, A., Rachel, R.A., Copeland, N.G., Jenkins, N.A., Bogani, D., Murdoch, J., Warchol, M.E., Wenthold, R.J. and Kelley, M.W. (2006) 'Asymmetric localization of Vangl2 and Fz3 indicate novel mechanisms for planar cell polarity in mammals', *Journal of Neuroscience*, 26(19), pp. 5265-5275.
- Moon, A. 84 (2008) 'Chapter 4 Mouse Models of Congenital Cardiovascular Disease'. pp. 171-248. Available at: http://www.scopus.com/inward/record.url?eid=2-s2.0-58749101736&partnerID=40&md5=8a7aba711a009ccefb6c23e73966775c.
- Moon, R.T., Campbell, R.M., Christian, J.L., McGrew, L.L., Shih, J. and Fraser, S. (1993) 'Xwnt-5A: A maternal Wnt that affects morphogenetic movements after overexpression in embryos of Xenopus laevis', *Development*, 119(1), pp. 96-111.
- Moorman, A.F.M., Christoffels, V.M., Anderson, R.H. and Van Den Hoff, M.J.B. (2007) 'The heart-forming fields: One or multiple?', *Philosophical Transactions of the Royal Society B: Biological Sciences*, 362(1484), pp. 1257-1265.

- Moretti, A., Caron, L., Nakano, A., Lam, J.T., Bernshausen, A., Chen, Y., Qyang, Y., Bu, L., Sasaki, M., Martin-Puig, S., Sun, Y., Evans, S.M., Laugwitz, K.L. and Chien, K.R. (2006) 'Multipotent Embryonic Isl1+ Progenitor Cells Lead to Cardiac, Smooth Muscle, and Endothelial Cell Diversification', *Cell*, 127(6), pp. 1151-1165.
- Morrison-Graham, K., Schatteman, G.C., Bork, T., Bowen-Pope, D.F. and Weston, J.A. (1992) 'A PDGF receptor mutation in the mouse (Patch) perturbs the development of a non-neuronal subset of neural crest-derived cells', *Development*, 115(1), pp. 133-142.
- Muller, H.J. (1932) 'Further Studies on the Nature and Causes of Gene Mutations', *Proceedings of the 6th International Congress of Genetics*, pp. 213–255.
- Müller, U. (1999) 'Ten years of gene targeting: Targeted mouse mutants, from vector design to phenotype analysis', *Mechanisms of Development*, 82(1-2), pp. 3-21.
- Muñoz-Soriano, V., Belacortu, Y. and Paricio, N. (2012) 'Planar cell polarity signaling in collective cell movements during morphogenesis and disease', *Current Genomics*, 13(8), pp. 609-622.
- Murdoch, J.N., Doudney, K., Paternotte, C., Copp, A.J. and Stanier, P. (2001a) 'Severe neural tube defects in the loop-tail mouse result from mutation of Lpp1, a novel gene involved in floor plate specification', *Human Molecular Genetics*, 10(22), pp. 2593-2601.
- Murdoch, J.N., Henderson, D.J., Doudney, K., Gaston-Massuet, C., Phillips, H.M., Paternotte, C., Arkell, R., Stanier, P. and Copp, A.J. (2003) 'Disruption of scribble (Scrb1) causes severe neural tube defects in the circletail mouse', *Human Molecular Genetics*, 12(2), pp. 87-98.
- Murdoch, J.N., Rachel, R.A., Shah, S., Beermann, F., Stanier, P., Mason, C.A. and Copp, A.J. (2001b) 'Circletail, a new mouse mutant with severe neural tube defects: Chromosomal localization and interaction with the loop-tail mutation', *Genomics*, 78(1-2), pp. 55-63.
- Myers, D.C., Sepich, D.S. and Solnica-Krezel, L. (2002) 'Convergence and extension in vertebrate gastrulae: Cell movements according to or in search of identity?', *Trends in Genetics*, 18(9), pp. 447-455.
- Nagy, I.I., Railo, A., Rapila, R., Hast, T., Sormunen, R., Tavi, P., Räsänen, J. and Vainio, S.J. (2010) 'Wnt-11 signalling controls ventricular myocardium development by patterning N-cadherin and β-catenin expression', *Cardiovascular Research*, 85(1), pp. 100-109.
- Niessen, C.M. (2007) 'Tight junctions/adherens junctions: Basic structure and function', *Journal of Investigative Dermatology*, 127(11), pp. 2525-2532.
- Niessen, K. and Karsan, A. (2008) 'Notch signaling in cardiac development', *Circulation Research*, 102(10), pp. 1169-1181.
- Nishita, M., Sa, K.Y., Nomachi, A., Kani, S., Sougawa, N., Ohta, Y., Takada, S., Kikuchi, A. and Minami, Y. (2006) 'Filopodia formation mediated by receptor tyrosine kinase Ror2 is required for Wnt5a-induced cell migration', *Journal of Cell Biology*, 175(4), pp. 555-562.
- Nusse, R. (2008) 'Wnt signaling and stem cell control', *Cell Research*, 18(5), pp. 523-527.

- Nusse, R., van Ooyen, A., Cox, D., Fung, Y.K. and Varmus, H. (1984) 'Mode of proviral activation of a putative mammary oncogene (int-1) on mouse chromosome 15', *Nature*, 307(5947), pp. 131-136.
- Nusse, R. and Varmus, H. (2012) 'Three decades of Wnts: A personal perspective on how a scientific field developed', *EMBO Journal*, 31(12), pp. 2670-2684.
- Nusslein-Volhard, C. and Wieschaus, E. (1980) 'Mutations affecting segment number and polarity in Drosophila', *Nature*, 287(5785), pp. 795-801.
- Nüsslein-Volhard, C., Wieschaus, E. and Kluding, H. (1984) 'Mutations affecting the pattern of the larval cuticle in Drosophila melanogaster - I. Zygotic loci on the second chromosome', *Wilhelm Roux's Archives of Developmental Biology*, 193(5), pp. 267-282.
- Ohno, S. (2001) 'Intercellular junctions and cellular polarity: The PAR-aPKC complex, a conserved core cassette playing fundamental roles in cell polarity', *Current Opinion in Cell Biology*, 13(5), pp. 641-648.
- Oishi, I., Suzuki, H., Onishi, N., Takada, R., Kani, S., Ohkawara, B., Koshida, I., Suzuki, K., Yamada, G., Schwabe, G.C., Mundlos, S., Shibuya, H., Takada, S. and Minami, Y. (2003) 'The receptor tyrosine kinase Ror2 is involved in non-canonical Wnt5a/JNK signalling pathway', *Genes to Cells*, 8(7), pp. 645-654.
- Panáková, D., Werdich, A.A. and MacRae, C.A. (2010) 'Wnt11 patterns a myocardial electrical gradient through regulation of the L-type Ca2+ channel', *Nature*, 466(7308), pp. 874-878.
- Pane, L.S., Zhang, Z., Ferrentino, R., Huynh, T., Cutillo, L. and Baldini, A. (2012) 'Tbx1 is a negative modulator of Mef2c', *Human Molecular Genetics*, 21(11), pp. 2485-2496.
- Park, E.J., Ogden, L.A., Talbot, A., Evans, S., Cai, C.L., Black, B.L., Frank, D.U. and Moon, A.M. (2006) 'Required, tissue-specific roles for Fgf8 in outflow tract formation and remodeling', *Development*, 133(12), pp. 2419-2433.
- Park, E.J., Watanabe, Y., Smyth, G., Miyagawa-Tomita, S., Meyers, E., Klingensmith, J., Camenisch, T., Buckingham, M. and Moon, A.M. (2008) 'An FGF autocrine loop initiated in second heart field mesoderm regulates morphogenesis at the arterial pole of the heart', *Development*, 135(21), pp. 3599-3610.
- Paudyal, A., Damrau, C., Patterson, V.L., Ermakov, A., Formstone, C., Lalanne, Z., Wells, S., Lu, X., Norris, D.P., Dean, C.H., Henderson, D.J. and Murdoch, J.N. (2010) 'The novel mouse mutant, chuzhoi, has disruption of Ptk7 protein and exhibits defects in neural tube, heart and lung development and abnormal planar cell polarity in the ear', *BMC Developmental Biology*, 10.
- Peters, L.L., Robledo, R.F., Bult, C.J., Churchill, G.A., Paigen, B.J. and Svenson, K.L. (2007) 'The mouse as a model for human biology: A resource guide for complex trait analysis', *Nature Reviews Genetics*, 8(1), pp. 58-69.
- Phillips, H.M., Hildreth, V., Peat, J.D., Murdoch, J.N., Kobayashi, K., Chaudhry, B. and Henderson, D.J. (2008) 'Non-cell-autonomous roles for

the planar cell polarity gene vangl2 in development of the coronary circulation', *Circulation Research*, 102(5), pp. 615-623.

- Phillips, H.M., Mahendran, P., Singh, E., Anderson, R.H., Chaudhry, B. and Henderson, D.J. (2013) 'Neural crest cells are required for correct positioning of the developing outflow cushions and pattern the arterial valve leaflets', *Cardiovascular Research*, 99(3), pp. 452-460.
- Phillips, H.M., Murdoch, J.N., Chaudhry, B., Copp, A.J. and Henderson, D.J. (2005) 'Vangl2 acts via RhoA signaling to regulate polarized cell movements during development of the proximal outflow tract', *Circulation Research*, 96(3), pp. 292-299.
- Phillips, H.M., Rhee, H.J., Murdoch, J.N., Hildreth, V., Peat, J.D., Anderson, R.H., Copp, A.J., Chaudhry, B. and Henderson, D.J. (2007) 'Disruption of planar cell polarity signaling results in congenital heart defects and cardiomyopathy attributable to early cardiomyocyte disorganization', *Circulation Research*, 101(2), pp. 137-145.
- Phillips, M.T., Kirby, M.L. and Forbes, G. (1987) 'Analysis of cranial neural crest distribution in the developing heart using quail-chick chimeras', *Circulation Research*, 60(1), pp. 27-30.
- Prall, O.W.J., Menon, M.K., Solloway, M.J., Watanabe, Y., Zaffran, S., Bajolle, F., Biben, C., McBride, J.J., Robertson, B.R., Chaulet, H., Stennard, F.A., Wise, N., Schaft, D., Wolstein, O., Furtado, M.B., Shiratori, H., Chien, K.R., Hamada, H., Black, B.L., Saga, Y., Robertson, E.J., Buckingham, M.E. and Harvey, R.P. (2007) 'An Nkx2-5/Bmp2/Smad1 Negative Feedback Loop Controls Heart Progenitor Specification and Proliferation', *Cell*, 128(5), pp. 947-959.
- Price, R.L., Thielen, T.E., Borg, T.K. and Terracio, L. (2001) 'Cardiac defects associated with the absence of the platelet-derived growth factor α receptor in the Patch mouse', *Microscopy and Microanalysis*, 7(1), pp. 56-65.
- Prosser, H. and Rastan, S. (2003) 'Manipulation of the mouse genome: A multiple impact resource for drug discovery and development', *Trends in Biotechnology*, 21(5), pp. 224-232.
- Qian, D., Jones, C., Rzadzinska, A., Mark, S., Zhang, X., Steel, K.P., Dai, X. and Chen, P. (2007) 'Wnt5a functions in planar cell polarity regulation in mice', *Developmental Biology*, 306(1), pp. 121-133.
- Raftopoulou, M. and Hall, A. (2004) 'Cell migration: Rho GTPases lead the way', *Developmental Biology*, 265(1), pp. 23-32.
- Rana, M.S., Horsten, N.C.A., Tesink-Taekema, S., Lamers, W.H., Moorman, A.F.M. and Van Den Hoff, M.J.B. (2007) 'Trabeculated right ventricular free wall in the chicken heart forms by ventricularization of the myocardium initially forming the outflow tract', *Circulation Research*, 100(7), pp. 1000-1007.
- Rao, T.P. and Kühl, M. (2010) 'An updated overview on wnt signaling pathways: A prelude for more', *Circulation Research*, 106(12), pp. 1798-1806.
- Reaume, A.G., De Sousa, P.A., Kulkarni, S., Langille, B.L., Zhu, D., Davies, T.C., Juneja, S.C., Kidder, G.M. and Rossant, J. (1995) 'Cardiac

malformation in neonatal mice lacking connexin43', *Science*, 267(5205), pp. 1831-1834.
- Ridley, A.J. (2001) 'Rho GTPases and cell migration', *Journal of Cell Science*, 114(15), pp. 2713-2722.
- Riento, K. and Ridley, A.J. (2003) 'Rocks: Multifunctional kinases in cell behaviour', *Nature Reviews Molecular Cell Biology*, 4(6), pp. 446-456.
- Rijsewijk, F., Schuermann, M., Wagenaar, E., Parren, P., Weigel, D. and Nusse, R. (1987) 'The Drosophila homology of the mouse mammary oncogene int-1 is identical to the segment polarity gene wingless', *Cell*, 50(4), pp. 649-657.
- Roberts, C., Ivins, S.M., James, C.T. and Scambler, P.J. (2005) 'Retinoic acid down-regulates Tbx1 expression in vivo and in vitro', *Developmental Dynamics*, 232(4), pp. 928-938.
- Rochais, F., Dandonneau, M., Mesbah, K., Jarry, T., Mattei, M.G. and Kelly, R.G. (2009a) 'Hes1 is expressed in the second heart field and is required for outflow tract development', *PLoS ONE*, 4(7).
- Rochais, F., Mesbah, K. and Kelly, R.G. (2009b) 'Signaling pathways controlling second heart field development', *Circulation Research*, 104(8), pp. 933-942.
- Rohr, S., Bit-Avragim, N. and Abdelilah-Seyfried, S. (2006) 'Heart and soul/PRKCi and nagie oko/Mpp5 regulate myocardial coherence and remodeling during cardiac morphogenesis', *Development*, 133(1), pp. 107-115.
- Rowe, A., Sarkar, S., Brickell, P.M. and Thorogood, P. (1994) 'Differential expression of RAR-β and RXR-γ transcripts in cultured cranial neural crest cells', *Roux's Archives of Developmental Biology*, 203(7-8), pp. 445-449.
- Sahai, E., Olson, M.F. and Marshall, C.J. (2001) 'Cross-talk between Ras and Rho signalling pathways in transformation favours proliferation and increased motility', *EMBO Journal*, 20(4), pp. 755-766.
- Sasai, N., Nakazawa, Y., Haraguchi, T. and Sasai, Y. (2004) 'The neurotrophin-receptor-related protein NRH1 is essential for convergent extension movements', *Nature Cell Biology*, 6(8), pp. 741-748.
- Satoda, M., Zhao, F., Diaz, G.A., Burn, J., Goodship, J., Davidson, H.R., Pierpont, M.E.M. and Gelb, B.D. (2000) 'Mutations in TFAP2B cause Char syndrome, a familial form of patent ductus arteriosus', *Nature Genetics*, 25(1), pp. 42-46.
- Satoh, K., Fukumoto, Y. and Shimokawa, H. (2011) 'Rho-kinase: Important new therapeutic target in cardiovascular diseases', *American Journal of Physiology - Heart and Circulatory Physiology*, 301(2), pp. H287-H296.
- Sawada, N., Li, Y. and Liao, J.K. (2010) 'Novel aspects of the roles of Rac1 GTPase in the cardiovascular system', *Current Opinion in Pharmacology*, 10(2), pp. 116-121.
- Schleiffarth, J.R., Person, A.D., Martinsen, B.J., Sukovich, D.J., Neumann, A., Baker, C.V.H., Lohr, J.L., Cornfield, D.N., Ekker, S.C. and Petryk, A. (2007) 'Wnt5a is required for cardiac outflow tract septation in mice', *Pediatric Research*, 61(4), pp. 386-391.

- Schott, J.J., Benson, D.W., Basson, C.T., Pease, W., Silberbach, G.M., Moak, J.P., Maron, B.J., Seidman, C.E. and Seidman, J.G. (1998) 'Congenital heart disease caused by mutations in the transcription factor NKX2-5', *Science*, 281(5373), pp. 108-111.
- Sebbagh, M., Renvoizé, C., Hamelin, J., Riché, N., Bertoglio, J. and Bréard, J. (2001) 'Caspase-3-mediated cleavage of ROCK I induces MLC phosphorylation and apoptotic membrane blebbing', *Nature Cell Biology*, 3(4), pp. 346-352.
- Shnitsar, I. and Borchers, A. (2008) 'PTK7 recruits dsh to regulate neural crest migration', *Development*, 135(24), pp. 4015-4024.
- Simon, M.A. (2004) 'Planar cell polarity in the Drosophila eye is directed by graded four-jointed and Dachsous expression', *Development*, 131(24), pp. 6175-6184.
- Simons, M. and Mlodzik, M. 42 (2008) 'Planar cell polarity signaling: From fly development to human disease'. pp. 517-540.
- Sinha, T., Wang, B., Evans, S., Wynshaw-Boris, A. and Wang, J. (2012) 'Disheveled mediated planar cell polarity signaling is required in the second heart field lineage for outflow tract morphogenesis', *Developmental Biology*, 370(1), pp. 135-144.
- Sisson, B.E. and Topczewski, J. (2009) 'Expression of five frizzleds during zebrafish craniofacial development', *Gene Expression Patterns*, 9(7), pp. 520-527.
- Sizarov, A., Lamers, W.H., Mohun, T.J., Brown, N.A., Anderson, R.H. and Moorman, A.F.M. (2012) 'Three-dimensional and molecular analysis of the arterial pole of the developing human heart', *Journal of Anatomy*, 220(4), pp. 336-349.
- Smith, E.A., Seldin, M.F., Martinez, L., Watson, M.L., Choudhury, G.G., Lalley, P.A., Pierce, J., Aaronson, S., Barker, J., Naylor, S.L. and Sakaguchi, A.Y. (1991) 'Mouse platelet-derived growth factor receptor α gene is deleted in W19H and patch mutations on chromosome 5', *Proceedings of the National Academy of Sciences of the United States of America*, 88(11), pp. 4811-4815.
- Snarr, B.S., O'Neal, J.L., Chintalapudi, M.R., Wirrig, E.E., Phelps, A.L., Kubalak, S.W. and Wessels, A. (2007) 'Isl1 expression at the venous pole identifies a novel role for the second heart field in cardiac development', *Circulation Research*, 101(10), pp. 971-974.
- Sokol, S. (2000) 'A role for Wnts in morphogenesis and tissue polarity', *Nature Cell Biology*, 2(7), pp. E124-E126.
- Sokol, S.Y. (1999) 'Wnt signaling and dorso-ventral axis specification in vertebrates', *Current Opinion in Genetics and Development*, 9(4), pp. 405-410.
- Song, H., Hu, J., Chen, W., Elliott, G., Andre, P., Gao, B. and Yang, Y. (2010) 'Planar cell polarity breaks bilateral symmetry by controlling ciliary positioning', *Nature*, 466(7304), pp. 378-382.
- Sordella, R., Classon, M., Hu, K.Q., Matheson, S.F., Brouns, M.R., Fine, B., Le, Z., Takami, H., Yamada, Y. and Settleman, J. (2002) 'Modulation of CREB activity by the Rho GTPase regulates cell and organism size

during mouse embryonic development', *Developmental Cell*, 2(5), pp. 553-565.

- Srinivas, S., Watanabe, T., Lin, C.S., William, C.M., Tanabe, Y., Jessell, T.M. and Costantini, F. (2001) 'Cre reporter strains produced by targeted insertion of EYFP and ECFP into the ROSA26 locus', *BMC Developmental Biology*, 1, pp. 1-8.
- Srivastava, D. and Olson, E.N. (2000) 'A genetic blueprint for cardiac development', *Nature*, 407(6801), pp. 221-226.
- Stalsberg, H. and DeHaan, R.L. (1969) 'The precardiac areas and formation of the tubular heart in the chick embryo', *Developmental Biology*, 19(2), pp. 128-159.
- Strong, L.C. and Hollander, W.F. (1949) 'Hereditary loop-tail in the house mouse: Accompanied by imperforate vagina and with lethal craniorachischisis when homozygous', *Journal of Heredity*, 40(12), pp. 329-334.
- Strutt, D. (2003) 'Frizzled signalling and cell polarisation in Drosophila and vertebrates', *Development*, 130(19), pp. 4501-4513.
- Strutt, H., Price, M.A. and Strutt, D. (2006) 'Planar Polarity Is Positively Regulated by Casein Kinase Iε in Drosophila', *Current Biology*, 16(13), pp. 1329-1336.
- Sugishita, Y., Watanabe, M. and Fisher, S.A. (2004) 'The development of the embryonic outflow tract provides novel insights into cardiac differentiation and remodeling', *Trends in Cardiovascular Medicine*, 14(6), pp. 235-241.
- Sun, Y., Liang, X., Najafi, N., Cass, M., Lin, L., Cai, C.L., Chen, J. and Evans, S.M. (2007) 'Islet 1 is expressed in distinct cardiovascular lineages, including pacemaker and coronary vascular cells', *Developmental Biology*, 304(1), pp. 286-296.
- Suzuki, A., Yamanaka, T., Hirose, T., Manabe, N., Mizuno, K., Shimizu, M., Akimoto, K., Izumi, Y., Ohnishi, T. and Ohno, S. (2001) 'Atypical protein kinase C is involved in the evolutionarily conserved PAR protein complex and plays a critical role in establishing epithelia-specific junctional structures', *Journal of Cell Biology*, 152(6), pp. 1183-1196.
- Tada, M. and Smith, J.C. (2000) 'Xwnt11 is a target of Xenopus Brachyury: Regulation of gastrulation movements via Dishevelled, but not through the canonical Wnt pathway', *Development*, 127(10), pp. 2227-2238.
- Takeuchi, J.K., Mileikovskaia, M., Koshiba-Takeuchi, K., Heidt, A.B., Mori, A.D., Arruda, E.P., Gertsenstein, M., Georges, R., Davidson, L., Mo, R., Hui, C.C., Henkelman, R.M., Nemer, M., Black, B.L., Nagy, A. and Bruneau, B.G. (2005) 'Tbx20 dose-dependently regulates transcription factor networks required for mouse heart and motoneuron development', *Development*, 132(10), pp. 2463-2474.
- Takeuchi, S., Takeda, K., Oishi, I., Nomi, M., Ikeya, M., Itoh, K., Tamura, S., Ueda, T., Hatta, T., Otani, H., Terashima, T., Takada, S., Yamamura, H., Akira, S. and Minami, Y. (2000) 'Mouse Ror2 receptor tyrosine kinase is required for the heart development and limb formation', *Genes to Cells*, 5(1), pp. 71-78.

- Tam, P.P.L., Parameswaran, M., Kinder, S.J. and Weinberger, R.P. (1997) 'The allocation of epiblast cells to the embryonic heart and other mesodermal lineages: The role of ingression and tissue movement during gastrulation', *Development*, 124(9), pp. 1631-1642.
- Tan, W., Palmby, T.R., Gavard, J., Amornphimoltham, P., Zheng, Y. and Gutkind, J.S. (2008) 'An essential role for Rac1 in endothelial cell function and vascular development', *FASEB Journal*, 22(6), pp. 1829-1838.
- Tao, H., Inoue, K.I., Kiyonari, H., Bassuk, A.G., Axelrod, J.D., Sasaki, H., Aizawa, S. and Ueno, N. (2012) 'Nuclear localization of Prickle2 is required to establish cell polarity during early mouse embryogenesis', *Developmental Biology*, 364(2), pp. 138-148.
- Tao, H., Suzuki, M., Kiyonari, H., Abe, T., Sasaoka, T. and Ueno, N. (2009) 'Mouse prickle1, the homolog of a PCP gene, is essential for epiblast apical-basal polarity', *Proceedings of the National Academy of Sciences of the United States of America*, 106(34), pp. 14426-14431.
- Taylor, J., Abramova, N., Charlton, J. and Adler, P.N. (1998) 'Van Gogh: A new Drosophila tissue polarity gene', *Genetics*, 150(1), pp. 199-210.
- Tepass, U. (2002) 'Adherens junctions: new insight into assemble, modulation and functions', *Bioessays*, 24, pp. 690–695.
- Theveneau, E., Steventon, B., Scarpa, E., Garcia, S., Trepat, X., Streit, A. and Mayor, R. (2013) 'Chase-and-run between adjacent cell populations promotes directional collective migration', *Nature Cell Biology*, 15(7), pp. 763-772.
- Thomas, P.S., Kim, J., Nunez, S., Glogauer, M. and Kaartinen, V. (2010) 'Neural crest cell-specific deletion of Rac1 results in defective cell-matrix interactions and severe craniofacial and cardiovascular malformations', *Developmental Biology*, 340(2), pp. 613-625.
- Thompson, R.P., Sumida, H., Abercrombie, V., Satow, Y., Fitzharris, T.P. and Okamoto, N. (1985) 'Morphogenesis of human cardiac outflow', *Anatomical Record*, 213(4), pp. 578-586.
- Thumkeo, D., Keel, J., Ishizaki, T., Hirose, M., Nonomura, K., Oshima, H., Oshima, M., Taketo, M.M. and Narumiya, S. (2003) 'Targeted disruption of the mouse Rho-associated kinase 2 gene results in intrauterine growth retardation and fetal death', *Molecular and Cellular Biology*, 23(14), pp. 5043-5055.
- Thumkeo, D., Shimizu, Y., Sakamoto, S., Yamada, S. and Narumiya, S. (2005) 'ROCK-I and ROCK-II cooperatively regulate closure of eyelid and ventral body wall in mouse embryo', *Genes to Cells*, 10(8), pp. 825-834.
- Timpl, R., Rohde, H., Robey, P.G., Rennard, S.I., Foidart, J.M. and Martin, G.R. (1979) 'Laminin - A glycoprotein from basement membranes', *Journal of Biological Chemistry*, 254(19), pp. 9933-9937.
- Tirosh-Finkel, L., Elhanany, H., Rinon, A. and Tzahor, E. (2006) 'Mesoderm progenitor cells of common origin contribute to the head musculature and the cardiac outflow tract', *Development*, 133(10), pp. 1943-1953.

- Tirosh-Finkel, L., Zeisel, A., Brodt-Ivenshitz, M., Shamai, A., Yao, Z., Seger, R., Domany, E. and Tzahor, E. (2010) 'BMP-mediated inhibition of FGF signaling promotes cardiomyocyte differentiation of anterior heart field progenitors', *Development*, 137(18), pp. 2989-3000.
- Tissir, F. and Goffinet, A.M. (2006) 'Expression of planar cell polarity genes during development of the mouse CNS', *European Journal of Neuroscience*, 23(3), pp. 597-607.
- Topczewski, J., Dale, R.M. and Sisson, B.E. (2011) 'Planar cell polarity signaling in craniofacial development', *Organogenesis*, 7(4), pp. 255-259.
- Torban, E., Kor, C. and Gros, P. (2004) 'Van Gogh-like2 (Strabismus) and its role in planar cell polarity and convergent extension in vertebrates', *Trends in Genetics*, 20(11), pp. 570-577.
- Torban, E., Patenaude, A.M., Leclerc, S., Rakowiecki, S., Gauthier, S., Andelfinger, G., Epstein, D.J. and Gros, P. (2008) 'Genetic interaction between members of the Vangl family causes neural tube defects in mice', *Proceedings of the National Academy of Sciences of the United States of America*, 105(9), pp. 3449-3454.
- Torban, E., Wang, H.J., Patenaude, A.M., Riccomagno, M., Daniels, E., Epstein, D. and Gros, P. (2007) 'Tissue, cellular and sub-cellular localization of the Vangl2 protein during embryonic development: Effect of the Lp mutation', *Gene Expression Patterns*, 7(3), pp. 346-354.
- Tsuchihashi, T., Maeda, J., Shin, C.H., Ivey, K.N., Black, B.L., Olson, E.N., Yamagishi, H. and Srivastava, D. (2011) 'Hand2 function in second heart field progenitors is essential for cardiogenesis', *Developmental Biology*, 351(1), pp. 62-69.
- Ulloa, F. and Martí, E. (2010) 'Wnt won the war: Antagonistic role of Wnt over Shh controls dorso-ventral patterning of the vertebrate neural tube', *Developmental Dynamics*, 239(1), pp. 69-76.
- Ulmer, B., Hagenlocher, C., Schmalholz, S., Kurz, S., Schweickert, A., Kohl, A., Roth, L., Sela-Donenfeld, D. and Blum, M. (2013) 'Calponin 2 Acts As an Effector of Noncanonical Wnt-Mediated Cell Polarization during Neural Crest Cell Migration', *Cell Reports*, 3(3), pp. 615-621.
- Urness, L.D., Bleyl, S.B., Wright, T.J., Moon, A.M. and Mansour, S.L. (2011) 'Redundant and dosage sensitive requirements for Fgf3 and Fgf10 in cardiovascular development', *Developmental Biology*, 356(2), pp. 383-397.
- Van Amerongen, R., Fuerer, C., Mizutani, M. and Nusse, R. (2012) 'Wnt5a can both activate and repress Wnt/B-catenin signaling during mouse embryonic development', *Developmental Biology*, 369(1), pp. 101-114.
- Van Bokhoven, H., Celli, J., Kayserili, H., Van Beusekom, E., Balci, S., Brussel, W., Skovby, F., Kerr, B., Percin, E.F., Akarsu, N. and Brunner, H.G. (2000) 'Mutation of the gene encoding the ROR2 tyrosine kinase causes autosomal recessive Robinow syndrome', *Nature Genetics*, 25(4), pp. 423-426.
- Van Den Berg, G., Abu-Issa, R., De Boer, B.A., Hutson, M.R., De Boer, P.A.J., Soufan, A.T., Ruijter, J.M., Kirby, M.L., Van Den Hoff, M.J.B. and Moorman, A.F.M. (2009) 'A caudal proliferating growth center

contributes to both poles of the forming heart tube', *Circulation Research*, 104(2), pp. 179-188.

- Van Den Hoff, M.J.B., Moorman, A.F.M., Ruijter, J.M., Lamers, W.H., Bennington, R.W., Markwald, R.R. and Wessels, A. (1999) 'Myocardialization of the cardiac outflow tract', *Developmental Biology*, 212(2), pp. 477-490.
- Van Praagh, R. (2009) 'The First Stella Van Praagh Memorial Lecture: The History and Anatomy of Tetralogy of Fallot', *Seminars in Thoracic and Cardiovascular Surgery: Pediatric Cardiac Surgery Annual*, 12(1), pp. 19-38.
- Van Weerd, J.H., Koshiba-Takeuchi, K., Kwon, C. and Takeuchi, J.K. (2011) 'Epigenetic factors and cardiac development', *Cardiovascular Research*, 91(2), pp. 203-211.
- Veeman, M.T., Axelrod, J.D. and Moon, R.T. (2003) 'A second canon: Functions and mechanisms of β-catenin-independent Wnt signaling', *Developmental Cell*, 5(3), pp. 367-377.
- Verzi, M.P., McCulley, D.J., De Val, S., Dodou, E. and Black, B.L. (2005) 'The right ventricle, outflow tract, and ventricular septum comprise a restricted expression domain within the secondary/anterior heart field', *Developmental Biology*, 287(1), pp. 134-145.
- Vinson, C.R. and Adler, P.N. (1987) 'Directional non-cell autonomy and the transmission of polarity information by the frizzled gene of Drosophila', *Nature*, 329(6139), pp. 549-551.
- Viragh, S. and Challice, C.E. (1977) 'The development of the conduction system in the mouse embryo heart. II. Histogenesis of the atrioventricular node and bundle', *Developmental Biology*, 56(2), pp. 397-411.
- Vitelli, F., Morishima, M., Taddei, I., Lindsay, E.A. and Baldini, A. (2002a) 'Tbx1 mutation causes multiple cardiovascular defects and disrupts neural crest and cranial nerve migratory pathways', *Human Molecular Genetics*, 11(8), pp. 915-922.
- Vitelli, F., Taddei, I., Morishima, M., Meyers, E.N., Lindsay, E.A. and Baldini, A. (2002b) 'A genetic link between Tbx1 and fibroblast growth factor signaling', *Development*, 129(19), pp. 4605-4611.
- von Both, I., Silvestri, C., Erdemir, T., Lickert, H., Walls, J.R., Henkelman, R.M., Rossant, J., Harvey, R.P., Attisano, L. and Wrana, J.L. (2004) 'Foxh1 is essential for development of the anterior heart field', *Developmental Cell*, 7(3), pp. 331-345.
- Waldo, K., Miyagawa-Tomita, S., Kumiski, D. and Kirby, M.L. (1998) 'Cardiac neural crest cells provide new insight into septation of the cardiac outflow tract: Aortic sac to ventricular septal closure', *Developmental Biology*, 196(2), pp. 129-144.
- Waldo, K.L., Hutson, M.R., Stadt, H.A., Zdanowicz, M., Zdanowicz, J. and Kirby, M.L. (2005a) 'Cardiac neural crest is necessary for normal addition of the myocardium to the arterial pole from the secondary heart field', *Developmental Biology*, 281(1), pp. 66-77.
- Waldo, K.L., Hutson, M.R., Ward, C.C., Zdanowicz, M., Stadt, H.A., Kumiski, D., Abu-Issa, R. and Kirby, M.L. (2005b) 'Secondary heart field

contributes myocardium and smooth muscle to the arterial pole of the developing heart', *Developmental Biology*, 281(1), pp. 78-90.

- Waldo, K.L., Kumiski, D.H., Wallis, K.T., Stadt, H.A., Hutson, M.R., Platt, D.H. and Kirby, M.L. (2001) 'Conotruncal myocardium arises from a secondary heart field', *Development*, 128(16), pp. 3179-3188.
- Wallingford, J.B., Fraser, S.E. and Harland, R.M. (2002) 'Convergent extension: The molecular control of polarized cell movement during embryonic development', *Developmental Cell*, 2(6), pp. 695-706.
- Wallingford, J.B. and Habas, R. (2005) 'The developmental biology of Dishevelled: An enigmatic protein governing cell fate and cell polarity', *Development*, 132(20), pp. 4421-4436.
- Wallingford, J.B., Rowning, B.A., Vogell, K.M., Rothbächer, U., Fraser, S.E. and Harland, R.M. (2000) 'Dishevelled controls cell polarity during Xenopus gastrulation', *Nature*, 405(6782), pp. 81-85.
- Walmsley, M.J., Ooi, S.K.T., Reynolds, L.F., Smith, S.H., Ruf, S., Mathiot, A., Vanes, L., Williams, D.A., Cancro, M.P. and Tybulewicz, V.L.J. (2003) 'Critical Roles for Rac1 and Rac2 GTPases in B Cell Development and Signaling', *Science*, 302(5644), pp. 459-462.
- Wang, J., Greene, S.B., Bonilla-Claudio, M., Tao, Y., Zhang, J., Bai, Y., Huang, Z., Black, B.L., Wang, F. and Martin, J.F. (2010) 'Bmp Signaling Regulates Myocardial Differentiation from Cardiac Progenitors Through a MicroRNA-Mediated Mechanism', *Developmental Cell*, 19(6), pp. 903-912.
- Wang, Y., Guo, N. and Nathans, J. (2006) 'The role of Frizzled3 and Frizzled6 in neural tube closure and in the planar polarity of inner-ear sensory hair cells', *Journal of Neuroscience*, 26(8), pp. 2147-2156.
- Wang, Y. and Nathans, J. (2007) 'Tissue/planar cell polarity in vertebrates: New insights and new questions', *Development*, 134(4), pp. 647-658.
- Ward, C., Stadt, H., Hutson, M. and Kirby, M.L. (2005) 'Ablation of the secondary heart field leads to tetralogy of Fallot and pulmonary atresia', *Developmental Biology*, 284(1), pp. 72-83.
- Watanabe, Y., Miyagawa-Tomita, S., Vincent, S.D., Kelly, R.G., Moon, A.M. and Buckingham, M.E. (2010) 'Role of mesodermal FGF8 and FGF10 overlaps in the development of the arterial pole of the heart and pharyngeal arch arteries', *Circulation Research*, 106(3), pp. 495-503.
- Waterston, R.H., Lindblad-Toh, K., Birney, E., Rogers, J., Abril, J.F., Agarwal, P., Agarwala, R., Ainscough, R., Alexandersson, M., An, P., Antonarakis, S.E., Attwood, J., Baertsch, R., Bailey, J., Barlow, K., Beck, S., Berry, E., Birren, B., Bloom, T., Bork, P., Botcherby, M., Bray, N., Brent, M.R., Brown, D.G., Brown, S.D., Bult, C., Burton, J., Butler, J., Campbell, R.D., Carninci, P., Cawley, S., Chiaromonte, F., Chinwalla, A.T., Church, D.M., Clamp, M., Clee, C., Collins, F.S., Cook, L.L., Copley, R.R., Coulson, A., Couronne, O., Cuff, J., Curwen, V., Cutts, T., Daly, M., David, R., Davies, J., Delehaunty, K.D., Deri, J., Dermitzakis, E.T., Dewey, C., Dickens, N.J., Diekhans, M., Dodge, S., Dubchak, I., Dunn, D.M., Eddy, S.R., Elnitski, L., Emes, R.D., Eswara, P., Eyras, E., Felsenfeld, A., Fewell, G.A., Flicek, P., Foley, K., Frankel, W.N., Fulton, L.A., Fulton, R.S., Furey, T.S., Gage, D., Gibbs, R.A., Glusman, G.,

Gnerre, S., Goldman, N., Goodstadt, L., Grafham, D., Graves, T.A., Green, E.D., Gregory, S., Guigó, R., Guyer, M., Hardison, R.C., Haussler, D., Hayashizaki, Y., LaHillier, D.W., Hinrichs, A., Hlavina, W., Holzer, T., Hsu, F., Hua, A., Hubbard, T., Hunt, A., Jackson, I., Jaffe, D.B., Johnson, L.S., Jones, M., Jones, T.A., Joy, A., Kamal, M., Karlsson, E.K., et al. (2002) 'Initial sequencing and comparative analysis of the mouse genome', *Nature*, 420(6915), pp. 520-562.

- Wei, L., Roberts, W., Wang, L., Yamada, M., Zhang, S., Zhao, Z., Rivkees, S.A., Schwartz, R.J. and Imanaka-Yoshida, K. (2001) 'Rho kinases play an obligatory role in vertebrate embryonic organogenesis', *Development*, 128(15), pp. 2953-2962.
- Wolff, T. and Rubin, G.M. (1998) 'strabismus, a novel gene that regulates tissue polarity and cell fate decisions in Drosophila', *Development*, 125(6), pp. 1149-1159.
- Woll, P.S., Morris, J.K., Painschab, M.S., Marcus, R.K., Kohn, A.D., Biechele, T.L., Moon, R.T. and Kaufman, D.S. (2008) 'Wnt signaling promotes hematoendothelial cell development from human embryonic stem cells', *Blood*, 111(1), pp. 122-131.
- Worthylake, R.A. and Burridge, K. (2003) 'RhoA and ROCK promote migration by limiting membrane protrusions', *Journal of Biological Chemistry*, 278(15), pp. 13578-13584.
- Wu, J., Klein, T.J. and Mlodzik, M. (2004) 'Subcellular localization of frizzled receptors, mediated by their cytoplasmic tails, regulates signaling pathway specificity', *PLoS Biology*, 2(7).
- Wu, M., Smith, C.L., Hall, J.A., Lee, I., Luby-Phelps, K. and Tallquist, M.D. (2010) 'Epicardial Spindle Orientation Controls Cell Entry into the Myocardium', *Developmental Cell*, 19(1), pp. 114-125.
- Xu, H., Morishima, M., Wylie, J.N., Schwartz, R.J., Bruneau, B.G., Lindsay, E.A. and Baldini, A. (2004) 'Tbx1 has a dual role in the morphogenesis of the cardiac outflow tract', *Development*, 131(13), pp. 3217-3227.
- Yamagishi, H., Maeda, J., Hu, T., McAnally, J., Conway, S.J., Kume, T., Meyers, E.N., Yamagishi, C. and Srivastava, D. (2003) 'Tbx1 is regulated by tissue-specific forkhead proteins through a common Sonic hedgehog-responsive enhancer', *Genes and Development*, 17(2), pp. 269-281.
- Yamagishi, H., Maeda, J., Uchida, K., Tsuchihashi, T., Nakazawa, M., Aramaki, M., Kodo, K. and Yamagishi, C. (2009) 'Molecular embryology for an understanding of congenital heart diseases', *Anatomical Science International*, 84(3), pp. 88-94.
- Yamaguchi, T.P., Bradley, A., McMahon, A.P. and Jones, S. (1999) 'A Wnt5a pathway underlies outgrowth of multiple structures in the vertebrate embryo', *Development*, 126(6), pp. 1211-1223.
- Yanagisawa, H., Hammer, R.E., Richardson, J.A., Williams, S.C., Clouthier, D.E. and Yanagisawa, M. (1998) 'Role of endothelin-1/endothelin-A receptor-mediated signaling pathway in the aortic arch patterning in mice', *Journal of Clinical Investigation*, 102(1), pp. 22-33.

- Yang, C.H., Axelrod, J.D. and Simon, M.A. (2002) 'Regulation of Frizzled by Fat-like cadherins during planar polarity signaling in the Drosophila compound eye', *Cell*, 108(5), pp. 675-688.
- Yang, L., Cai, C.L., Lin, L., Qyang, Y., Chung, C., Monteiro, R.M., Mummery, C.L., Fishman, G.I., Cogen, A. and Evans, S. (2006) 'Isl1 Cre reveals a common Bmp pathway in heart and limb development', *Development*, 133(8), pp. 1575-1585.
- Yang, Y.-P., Li, H.-R., Cao, X.-M., Wang, Q.-X., Qiao, C.-J. and Ya, J. (2013) 'Second heart field and the development of the outflow tract in human embryonic heart', *Development, Growth & Differentiation*, 55(3), pp. 359-367.
- Yao, R., Natsume, Y. and Noda, T. (2004) 'MAGI-3 is involved in the regulation of the JNK signaling pathway as a scaffold protein for frizzled and Ltap', *Oncogene*, 23(36), pp. 6023-6030.
- Ybot-Gonzalez, P., Savery, D., Gerrelli, D., Signore, M., Mitchell, C.E., Faux, C.H., Greene, N.D.E. and Copp, A.J. (2007) 'Convergent extension, planar-cell-polarity signaling and initiation of mouse neural tube closure', *Development*, 134(4), pp. 789-799.
- Yelbuz, T.M., Waldo, K.L., Kumiski, D.H., Stadt, H.A., Wolfe, R.R., Leatherbury, L. and Kirby, M.L. (2002) 'Shortened outflow tract leads to altered cardiac looping after neural crest ablation', *Circulation*, 106(4), pp. 504-510.
- Yin, H., Copley, C.O., Goodrich, L.V. and Deans, M.R. (2012) 'Comparison of phenotypes between different vangl2 mutants demonstrates dominant effects of the looptail mutation during hair cell development', *PLoS ONE*, 7(2).
- Yu, H., Smallwood, P.M., Wang, Y., Vidaltamayo, R., Reed, R. and Nathans, J. (2010) 'Frizzled 1 and frizzled 2 genes function in palate, ventricular septum and neural tube closure: General implications for tissue fusion processes', *Development*, 137(21), pp. 3707-3717.
- Zaffran, S. and Frasch, M. (2002) 'Early signals in cardiac development', *Circulation Research*, 91(6), pp. 457-469.
- Zaffran, S., Kelly, R.G., Meilhac, S.M., Buckingham, M.E. and Brown, N.A. (2004) 'Right ventricular myocardium derives from the anterior heart field', *Circulation Research*, 95(3), pp. 261-268.
- Zeidler, M.P., Perrimon, N. and Strutt, D.I. (1999) 'The four-jointed gene is required in the Drosophila eye for ommatidial polarity specification', *Current Biology*, 9(23), pp. 1363-1372.
- Zeidler, M.P., Perrimon, N. and Strutt, D.I. (2000) 'Multiple roles for four-jointed in planar polarity and limb patterning', *Developmental Biology*, 228(2), pp. 181-196.
- Zhang, Z., Huynh, T. and Baldini, A. (2006) 'Mesodermal expression of Tbx1 is necessary and sufficient for pharyngeal arch and cardiac outflow tract development', *Development*, 133(18), pp. 3587-3595.
- Zhao, Z. and Rivkees, S.A. (2003) 'Rho-associated kinases play an essential role in cardiac morphogenesis and cardiomyocyte proliferation', *Developmental Dynamics*, 226(1), pp. 24-32.

- Zhou, W., Lin, L., Majumdar, A., Li, X., Zhang, X., Liu, W., Etheridge, L., Shi, Y., Martin, J., Van de Ven, W., Kaartinen, V., Wynshaw-Boris, A., McMahon, A.P., Rosenfeld, M.G. and Evans, S.M. (2007a) 'Modulation of morphogenesis by noncanonical Wnt signaling requires ATF/CREB family-mediated transcriptional activation of TGF[beta]2', *Nat Genet*, 39(10), pp. 1225-1234.
- Zhou, W., Lin, L., Majumdar, A., Li, X., Zhang, X., Liu, W., Etheridge, L., Shi, Y., Martin, J., Van De Ven, W., Kaartinen, V., Wynshaw-Boris, A., McMahon, A.P., Rosenfeld, M.G. and Evans, S.M. (2007b) 'Modulation of morphogenesis by noncanonical Wnt signaling requires ATF/CREB family-mediated transcriptional activation of TGFβ2', *Nature Genetics*, 39(10), pp. 1225-1234.
- Zondag, G.C.M., Evers, E.E., Ten Klooster, J.P., Janssen, L., Van Der Kammen, R.A. and Collard, J.G. (2000) 'Oncogenic Ras downregulates Rac activity, which leads to increased Rho activity and epithelial-mesenchymal transition', *Journal of Cell Biology*, 149(4), pp. 775-781.